Development of artificial neural network models based on near-infrared spectroscopy for the grape skin composting evaluation

Sokač Cvetnić, Tea

Doctoral thesis / Disertacija

2024

University of Zagreb

Faculty of Food Technology and Biotechnology

Tea Sokač Cvetnić

DEVELOPMENT OF ARTIFICIAL NEURAL NETWORK MODELS BASED ON NEAR-INFRARED SPECTROSCOPY FOR THE GRAPE SKIN COMPOSTING EVALUATION

DOCTORAL DISSERTATION

Zagreb, 2024.

Faculty of Food Technology and Biotechnology

Tea Sokač Cvetnić

DEVELOPMENT OF ARTIFICIAL NEURAL NETWORK MODELS BASED ON NEAR-INFRARED SPECTROSCOPY FOR THE GRAPE SKIN COMPOSTING EVALUATION

DOCTORAL DISSERTATION

Supervisor:

Ana Jurinjak Tušek, Ph.D., Associate Professor

Zagreb, 2024.

Sveučilište u Zagrebu

Prehrambeno-biotehnološki fakultet

Tea Sokač Cvetnić

RAZVOJ MODELA UMJETNIH NEURONSKIH MREŽA TEMELJENIH NA BLISKOJ INFRACRVENOJ SPEKTROSKOPIJI ZA PROCJENU UČINKOVITOSTI KOMPOSTIRANJA POKOŽICE GROŽĐA

DOKTORSKI RAD

Mentor:

Izv. prof. dr. sc. Ana Jurinjak Tušek

Zagreb, 2024.

University of Zagreb
Faculty of Food Technology and Biotechnology
University Doctoral Study in Biotechnology and Bioprocess Engineering, Food Technology and Nutrition
UDK: **543.428.3:628.473:663.2:663.26(043.3)**
Scientific Area: Biotechnical Sciences
Scientific Field: Biotechnology

DEVELOPMENT OF ARTIFICIAL NEURAL NETWORK MODELS BASED ON NEAR-INFRARED SPECTROSCOPY FOR THE GRAPE SKIN COMPOSTING EVALUATION

Tea Sokač Cvetnić, *MSc*

Thesis performed at the Faculty of Food Technology and Biotechnology.

Supervisor: Ana Jurinjak Tušek, Ph.D., Associate professor

Abstract: During the vine production, huge amounts of waste (grape pomace) are generated. The grape pomace can be used as a substrate for the composting process. The composting process is an aerobic, biological process in which organic matter is degraded in the presence of water, oxygen, and microorganisms. The efficiency of the composting process can be monitored through a few variables (such as moisture and dry matter content, organic carbon content and ash, carbon-nitrogen ratio, pH value), but these analyses are time-consuming. In the last few years, the use of near-infrared spectroscopy has been noted as a fast, non-destructive method for on-line monitoring the composting process. The aim of this doctoral thesis is the development of artificial neural networks models using chemometric tools based on the near infrared data for the evaluation of the efficiency of the composting process in laboratory reactors.

Number of pages: 247
Number of figures: 44
Number of tables: 99
Number of references: 165
Number of supplements: 3
Original in: English

Key words: composting, grape pomace, near-infrared spectroscopy, artificial neural network.

Thesis defended: June 7th, 2024

Reviewers:
1. Ivana Radojčić Redovniković, Ph.D., Full professor
2. Tamara Jurina, Ph.D., Assistant professor
3. Tamara Jakovljević, Ph.D., Scientific advisor

Thesis deposited in the library of the Faculty of Food Technology and Biotechnology, Kačićeva 23, National and University Library, Hrvatske bratske zajednice bb and University of Zagreb, Trg Republike Hrvatske 14.

RAZVOJ MODELA UMJETNIH NEURONSKIH MREŽA TEMELJENIH NA BLISKOJ INFRACRVENOJ SPEKTROSKOPIJI ZA PROCJENU UČINKOVITOSTI KOMPOSTIRANJA POKOŽICE GROŽĐA

Tea Sokač Cvetnić, mag. ing. oecoing.

Rad je izrađen na Prehrambeno-biotehnološkom fakultetu.

Mentor: izv. prof. dr. sc. Ana Jurinjak Tušek

Sažetak: Prilikom proizvodnje vina nastaje velika količina otpada, odnosno komina grožđa koja se može procesom kompostiranja prevesti u stabilan produkt. Proces kompostiranja je aeroban biološki proces tijekom kojeg dolazi do razgradnje organskih tvari u prisustvu vode, kisika i mikroorganizama. S obzirom da se učinkovitost procesa kompostiranja prati putem nekoliko varijabli (poput udjela vlage i suhe tvari, udjela organskog ugljika i pepela, omjera ugljika i dušika, pH vrijednosti) čije analize zahtijevaju dosta vremena, u posljednje vrijeme često se spominje upotreba blisko infracrvene spektroskopije kao brze, nedestruktivne metode za on-line praćenje učinkovitosti procesa kompostiranja. Cilj predložene teme ove doktorske disertacije je razvoj modela umjetnih neuronskih mreža primjenom kemometrijskih alata na temelju podataka dobivenih blisko infracrvenom spektroskopijom za procjenu učinkovitosti procesa kompostiranja pokožice grožđa u laboratorijskim reaktorima.

The dissertation topic was accepted at the 1ˢᵗ regular session of the Faculty Council of the Faculty of Food Technology and Biotechnology, University of Zagreb in the academic year 2023/2024 held on October 18ᵗʰ 2023, and the University of Zagreb Senate approved the initiation of the procedure for obtaining a doctorate of science within the doctoral study on February 13ᵗʰ 2024 at the 5ᵗʰ regular session in the 355ᵗʰ academic year (2023/2024).

Extendend abstract

Grape production is an important agricultural sector in Mediterranean countries, and it is often used for wine production. During wine production, solid and liquid waste are generated. The solid waste is the grape pomace, and the liquid waste refers to wastewater. The generated waste is characterized by an acidic pH and a high amount of polyphenols. Improper disposal of grape pomace presents a risk to the environment and human health. As one option for the use of this waste, it is often mentioned that the composting process results in fertilizer and can be used in a vineyard as a source of organic matter, nitrogen, and minerals. The composting process is an aerobic microbial process of the transformation of organic matter into a stable product. The main goals of the composting process are the decrease in the amount of disposed waste, the sanitation of waste, and the production of fertilizer.

For an effective composting process that results in a stable and mature compost, it is necessary to monitor several variables, such as temperature, moisture, dry matter content, pH, and the C/N ratio. During the composting process, lots of physicochemical and microbiological analysis should be performed, and these methods are time-consuming, which can prevent exact compost quality. The spectrophotometric methods are considered the appropriate measurement system for online monitoring of the composting process. Near-infrared spectroscopy is a method that can be used to control the quality of compost. This method is based on the absorption of electromagnetic radiation in the wavelength range from 800 to 2500 nm and it provides fast analysis without pre-treatment of the sample; it doesn't require the use of chemicals, which makes it adequate for on-line analysis of a large number of samples in a short time.

The near-infrared spectra are complex, and for the selection of important information to define the relation between spectral information and sample characteristics, it is necessary to use chemometric methods. Often, regression methods are used to analyze the relationship between the near-infrared spectra and the physical or chemical characteristics of samples. However, the development of the model includes a larger number of predictors in comparison with the number of samples, which leads to an inappropriate solution by the least squares method. The alternative is the use of non-linear models, such as artificial neural networks that imitate the human brain for information processing. Ensuring the reliable and meaningful experimental data for training, testing and model validation, is important for the development of the artificial neural network model.

In this dissertation, the composting processes of grape skins were carried out in laboratory reactors under different initial moisture contents and air flow rates to find optimal conditions for the composting process. During the composting processes, the physicochemical properties of compost samples and compost extract samples were analyzed (moisture and dry matter content, organic matter and ash content, carbon and nitrogen content, C/N ratio, total color change of compost and extracts, pH, total dissolved soilds and conductivity) and NIR spectra was recoreded with different NIR instruments. Also, the kinetics of organic matter degradation and microbial growth has been investigated. The obtained experimental results were used for the multivariate analysis that includes the development of multiple linear regression models, piecewise linear regression models and artificial neural network models for the prediction of physicochemical properties of compost samples. Considering that polyphenols can impedes the composting process, the aqueous extraction of bioactive molecules from grape skin were carried out under different conditions of extraction time, temperature, solid-liquid ratio and mixing speed. After the extraction, the physicochemical properties of extracts were analyzed (pH, total dissolved solids, conductivity, color variables Chroma and Hue, total polyphenol content, and antioxidant activity determined by DPPH and FRAP method). The extraction conditions have been optimized using the response surface methodology. Finally, different pretreatments of grape skin on the efficiency of the composting process in laboratory reactors have been investigated. The pretreatments were with or without extraction of bioactive molecules and ground or not ground grape skin. During the processes, the physicochemical properties (moisture and dry matter content, organic matter and ash content, carbon and nitrogen content, C/N ratio, total color change of compost and extracts, pH, total dissolved soilds and conductivity) of compost samples and compost extract samples were analyzed and NIR spectra were recorded. In this set of experiments, the kinetics of organic matter degradation and microbial growth has been investigated too. The artificial neural network models for prediction of the physicochemical and microbiological properties of compost during the composting process were developed based on the near-infrared spectra and applying the chemometric methods.

Key words: composting, grape pomace, near infrared spectroscopy, artificial neural network.

Prošireni sažetak

Proizvodnja grožđa je važan agrikulturalni sektor u Mediteranskim zemljama, a najveći udio grožđa koristi se za proizvodnju vina. Prilikom proizvodnje vina neizbježno je nastajanje krutog otpada koji se odnosi na kominu grožđa, a također nastaju i otpadne vode. Navedeni otpad je karakterističnog sastava pri čemu se ističu pH vrijednosti u kiselom području te visoki udio polifenola. Nepropisno odlaganje komine grožđa na odlagališta, predstavlja rizik za okoliš i ljudsko zdravlje. Proces kompostiranja navodi se kao jedna od mogućnosti iskorištavanja komine grožđa pri čemu se dobiva prirodno gnojivo koje se može koristiti u vinogradima kao izvor organskih i mineralnih tvari te dušika. Kompostiranje je aeroban mikrobiološki proces pretvorbe organskih tvari u stabilan produkt, a kao glavni ciljevi kompostiranja mogu se navesti smanjenje volumena otpada na odlagalištima, sanitacija otpada te dobivanje korisnog proizvoda.

Za uspješno provođenje procesa kompostiranja te za nastajanje stabilnog i zrelog komposta, važno je praćenje nekoliko varijabli poput temperature, udjela vlage i suhe tvari, pH vrijednosti te omjera ugljika i dušika. Tijekom procesa kompostiranja provodi se veliki broj fizikalno-kemijskih i mikrobioloških analiza koje su vremenski zahtjevne i otežavaju točnu procjenu kvalitete komposta. U posljednje vrijeme, spektroskopske metode su od velikog interesa zbog brzog mjernog sustava za on-line mjerenja kvalitete komposta. Jedna takva metoda je i blisko infracrvena spektroskopija koja se temelji na apsorpciji elektromagnetskog zračenja valnih duljina u rasponu od 800 do 2500 nm. Ova metoda omogućuje brzu, beskontaktnu analizu bez predtretmana uzoraka, ne zahtjeva upotrebu kemikalija zbog čega je pogodna za on-line analizu velikog broja uzoraka u kratkom vremenu.

Zbog činjenice da su blisko infracrveni spektri često složeni, izdvajanje korisnih informacija iz skupa spektralnih podataka u svrhu definiranja odnosa između spektralnih informacija i svojstava uzorka zahtijeva korištenje kemometrijskih metoda. Često se primjenjuju metode kemometrijske regresije koje analiziraju odnos između blisko infracrvenih spektara (neobrađeni/sirovi spektri ili grupa odabranih valnih duljina) i fizikalno-kemijskih svojstava ispitivanih uzoraka. Međutim, kod razvoja modela koji uključuju veći broj prediktora u usporedbi s brojem uzoraka dolazi do nemogućnosti pronalaženja jedinstvenog rješenja metodom najmanjih kvadrata. Alternativa je korištenje nelinearnih modela, kao što su modeli umjetnih neuronskih mreža koji oponašaju rad ljudskog mozga za obradu informacija. Odnos između ulaza (nezavisne varijable) i izlaza (zavisne varijable) je nelinearan, stoga je za razvoj

modela umjetnih neuronskih mreža potrebno osigurati pouzdane i značajne eksperimentalne podatke za treniranje (učenje), testiranje i validaciju modela.

U ovom doktorskom radu provedeni su procesi kompostiranja pokožice grožđa u laboratorijskim reaktorima pri različitim uvjetima početnog udjela vlage i protoka zraka s ciljem optimiranja procesnih uvjeta. Tijekom procesa kompostiranja, praćene su fizikalno-kemijske varijable (udio vlage i suhe tvari, udio organske tvari i pepela, udio ugljika i dušika, C/N omjer, ukupna promjena boje komposta i ekstrakata komposta, pH vrijednost, ukupne otopljene tvari i vodljivost) te su snimani NIR spektri različitim NIR instrumentima. Za navedene eksperimente analizirana je i kinetika razgradnje organske tvari i rasta mikroorganizama. Nadalje, na temelju eksperimentalno dobivenih rezultata provedena je multivariantna analiza koja uključuje razvoj modela višestruke linearne regresije, modela lokalne linearne regresije te modela umjetnih neuronskih mreža za predviđanje fizikalno-kemijskih svojstava komposta tijekom procesa kompostiranja. Uzevši u obzir da polifenoli mogu utjecati na uspješnost procesa kompostiranja pokožice grožđa, u drugom djelu ovog istraživanja provedena je vodena ekstrakcija bioaktivnih molekula iz pokožice grožđa pri različitim vremenima ekstrakcije, temperature, omjera kruto-tekuće i brzini miješanja. Nakon provedenih ekstrakcija, analizirane su fizikalno-kemijske karakteristike ekstrakata koje uključuju pH vrijednost, ukupne otopljene tvari, vodljivost, varijable boje Chroma i Hue, ukupni sadržaj polifenola, te antioksidativnu aktivnost određenu DPPH i FRAP metodom. Za optimiranje uvjeta ekstrakcije primijenjena je metoda odzivnih površina. Na kraju ovog istraživanja ispitan je utjecaj različitih predtretmana pokožice grožđa na uspješnost procesa kompostiranja, a predtretmani su uključivali ekstrahiranu i neekstrahiranu pokožicu grožđa, te usitnjenu i neusitnjenu pokožicu. Tijekom ovih procesa kompostiranja, praćene su fizikalno-kemijske varijable kao i u prvom setu eksperimenata, te su snimani NIR spektri. Također, analizirana je kinetika razgradnje organske tvari i rasta mikroorganizama. Na temelju podataka blisko infracrvenih spektara te primjenom kemometrijskih alata razvijeni su modeli umjetnih neuronskih mreža za predviđanje fizikalno-kemijskih i mikrobioloških svojstava komposta tijekom procesa kompostiranja.

Ključne riječi: kompostiranje, komina grožđa, bliska infracrvena spektroskopija, umjetne neuronske mreže.

Information about the supervisor – Ana Jurinjak Tušek, Ph.D., Associate Professor

Ana Jurinjak Tušek, PhD, Associate Professor, was born on June 2, 1984, in Zagreb. She is married and the mother of two children. She finished elementary school and general high school in Krapina. She graduated in 2007 at the Faculty of Food Technology and Biotechnology, University of Zagreb. She got her PhD in the field of biotechnology in 2013 after defending the thesis entitled "*Development of the biotransformation process of catechol in a microreactor.*".

In 2016, she also completed her education as a project manager for EU funds at the Experta Business School in Zagreb. She has been employed in the Laboratory for Measurement, Control and Automatisation of the Department of Process Engineering of the Faculty of Food Technology and Biotechnology University of Zagreb since 2008 as a researcher assistant, since 2017 as an assistant professor, and since 2022 as an associate professor. She trained scientifically and professionally at the Faculty of Chemistry and Chemical Technology, University of Maribor, Slovenia (December 2012–March 2013) and at numerous workshops.

From 2008 until today, she has participated in the teaching of the subjects Measurement and Process Management, Measurement and Process Management in the Food Industry, Modeling and Optimization in Nutrition, Modeling of Biotechnological Processes, Reactor Engineering, Basics of Measurement Methods in Nutrition Science, and Modeling in Food Engineering. She also introduced a new course called Computer Tools for Modeling Human Nutrition, which was accepted by the competent professional body of the higher education institution and is taught at the graduate study of nutrition at the Faculty of Food Technology and Biotechnology University of Zagreb. Under her mentorship, from 2018 until today, 2 undergraduate and 16 graduate theses were defended, as well as a research paper awarded the Rector's Prize in the academic year 2023-2024. The awarded work was chosen as the best work in the biotechnical field.

During her previous work, she published a total of 103 original scientific papers (74 indexed in Wos Journal, 10 indexed in secondary dana bases, and 20 complete scientific papers form international scientific conferences). As a co-author, she also published 10 book chapters. With more than 120 abstracts, she participated in international and domestic scientific meetings. She is also the co-author of two invited lectures at international scientific congresses. In her previous work, she was a member of three organizing committees of international scientific meetings (IMTB 2017, IMTB 2019, and IMTB 2022) and editor of three collections of papers from international meetings. Since 2022, she has been a member of the editorial board of the journal

"Chemistry in Industry." Also in 2022, she was chosen as a guest editor of the Special Issue of the magazine "Catalysts" under the title "Microflow (Bio)Catalysis." In her previous work, she has reviewed over 190 papers for international scientific journals.

As an associate, she participated in the implementation of 14 scientific projects. She was the project leader of a project financed by the European Social Fund with the support of the University of Zagreb. Her scientific research work includes research related to the application of mathematical and statistical modeling methodologies in biotechnology, with a special emphasis on the application of microflow systems. She is part of the first scientific group in the Republic of Croatia under the leadership of Bruno Zelić, Ph.D., Full Professor, who is intensively engaged in the application of microreactor technology in the field of biotechnology. She participated in research on separation and biotransformation processes in microreactor systems. Lately, she has also been intensively engaged in the application of mathematical modeling and optimization of the isolation process of biologically active components, chemometric analysis of spectroscopic data, and the application of systems biology methodology in the analysis of metabolic processes. She is the winner of the Annual Award of the Society of University Teachers and Other Teachers in Zagreb for 2018; silver medals at the Innovation Fair, 14th International Exhibition of Innovations, ARCA, 2016; and scholarships for "For Women in Science," L'Oreal and Unesco in 2013. She is a member of the Croatian Society of Chemical Engineers and Technologists and the Croatian Society for Biotechnology.

Table of contents

1. GENERAL INTRODUCTION

The world population is increasing daily, and the improvement in living conditions has led to an increasing demand for food production. The negative impact of increasing food production is the production of huge amounts of agricultural waste, which not only causes pollution and damage to the environment but also poses a potential health hazard to people. Globally, 140 billion tons of lignocellulose-related organic agricultural waste are generated each year (Xu et al., 2023). Enforcement of policies and laws encourages waste reduction, recycling, and conversion to usable products. Agricultural waste has the potential to become a sustainable resource for value addition and a major contributor to ecological sustainability (Awogbemi and Kallon, 2022).

Composting is one of the most effective methods to promote the recycling of organic waste, improve soil fertility and promote crop growth. This process not only reduces agricultural waste but also environmental pollution (Xu et al., 2023). Composting is a process of decomposition of organic matter by biological processes, and it is considered a natural way of recycling. The composting process must be suitably managed, and the progressive changes in the physicochemical properties of composts must be controlled to give a final product with optimum qualities. The analysis of physicochemical properties can be time-consuming and/or expensive, and consequently, more reliable methods are necessary for the management and traceability of the composting process (Vergnoux et al., 2009). Near-infrared spectroscopy has been considered a fast, cheap and reliable method for the determination of variables that are important for composting processes. It is a non-destructive technique with no sample preparation and no reagents required (Galvez-Sola et al., 2010a).

The aim of this dissertation was to develop artificial neural network models based on near-infrared spectroscopy using chemometric techniques to predict the physicochemical properties of grape skin compost obtained in laboratory reactors under different conditions of initial moisture content of grape skin and air flow rate, and using the different pretreated grape skin. The pretretment included fresh grape skin (not extracted and not ground) and extracted or ground grape skin. Also, in this research, the optimal conditions of tenperature, time of extraction, solid-liquid ratio and mixing speed for the extraction of bioactive molecules from grape skin were investigated.

2. THEORETICAL BACKGROUND

2.1. Winery by-products

The production of wine has become very important in agriculture and agribusiness worldwide (Ahmad et al., 2020; Ilyas et al., 2021). Grapes (*Vitis vinifera* L.) is one of the most cultivated and valued conventional fruit crops, and its annual production in Mediterranean Europe is around 29 milion tonnes out of which around 70-75% is used for wine production (Antonić et al., 2020; Chowdhary et al., 2021; Ilyas et al., 2021). During the wine production, the generation of solid waste (related to grape pomace) and liquid waste (related to wastewater) is unavoidable (Mirabella et al., 2014). After the pressing and fermentation process, 15-25% of grape pomace is generated and it is consisted of stalks, seeds and skins (Beres et al., 2017; Chowdhary et al., 2021). As shown in Figure 1, after the harvest, the grapes passes through some stages to the final product and also, there are the by-products which are produced in appropriate amount. According to Spinei and Oroian (2021), 1000 kg of grape pomace consists of 425 kg grape skins, 225 kg grape seeds and 249 kg grape stalks (Figure 2).
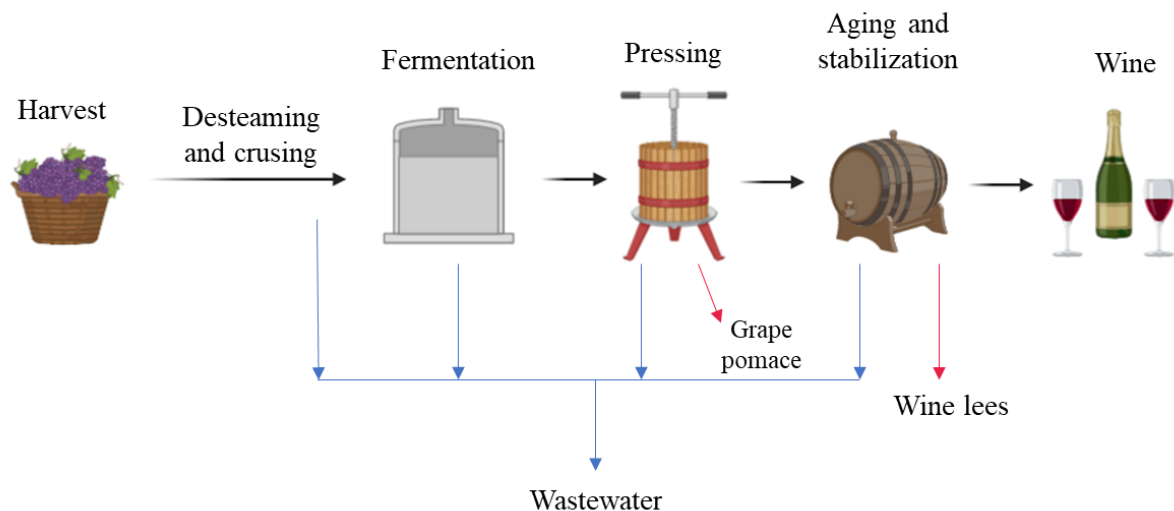
Figure 1. Schematic presentation of wine production (*adapted* from Rodrigues et al., 2022)

Figure 2. The average composition of grape pomace (*adapted* from Spinei and Oroian, 2021)

Furthermore, winery wastewater is generated by the different activities during the winemaking process, mainly from washing and rinsing operations of fermentation tanks, barrels and other equipment (Ioannou et al., 2013). The generated amounts depend on winemaking process (red, wine or special wines) and wineries scale (Lofrano and Meric, 2016). According to the available literature (Ioannou et al., 2013; Lofrano and Meric, 2016; Rodrigues et al., 2022), the wine industry produce 1-4 L of wastewater per liter of wine. The winery wastewater is characterized by pH values from 2.5-6, high amount of organic contaminants such as organic acids (tartaric, lactic and acetic acid), sugars (glucose and fructose), alcohols (ethanol and glycerol) and high-molecular weight compounds like polyphenols, tannins and lignins (Lofrano and Meric, 2016; Moreira et al., 2015). Due to mentioned characteristics, the wastewater needs pretreatment before discharging to enviroment, and the effective treatments include physicochemical treatments (coagulation, flocculation and decantation), membrane processes, advanced oxidation processes (ozonation, Fenton process) and biological treatments combined with advanced oxidation processes (Ioannou et al., 2013; Jorge et al., 2021; Rodrigues et al., 2022).

Due to a significant amount of compounds that can be considered beneficial to health, grape pomace has been recognized as important source and it finds the application in food industry, cosmetics, animal feed, bakery and pharmaceutical industry (Ahmad et al., 2020; Sokač et al., 2022a). In general, the grape pomace composition depends on climate conditions,

viticultural practices, maturity and winemaking process (García-Lomillo and González-SanJosé, 2017). The proximate composition of grape pomace is presented in Table 1.

Table 1. Proximate composition of grape pomace based on dry matter (Antonić et al., 2020; Moreno et al., 2020; Rodrigues et al., 2022; Spinei and Oroian, 2021)

Parameter	Value on dry matter (%)	Parameter	Quantity (g/kg)
Physicochemical variables		*Mineral substances*	
Moisture content	50-75	Na	0.87-2.44
Organic matter	50-72	K	11.84-37.90
Ash content	80-95	Mg	0.70-6.44
Lipids	14-19	Ca	0.91-20.60
Proteins	2-15	Mn	0.0002-0.10
Total carbohydrates	12-40	Fe	0.05-0.28
Dietary fibers	43-75	Zn	0.01-0.04
Lignin	16-24	Cu	0.01-0.28
Cellulose	27-37	P	0.04-2.70

Due to presence of different organic compounds in grape pomace, the disposal of this waste on landfills or open areas can have toxic environmental impacts and can lead to pollution of air, water or soil (Ahmad et al., 2020; Ilyas et al., 2021; Pinto et al., 2023). Thus, it is required to develop the adequate management approaches based on the sustainability and circular economy (Perra et al., 2022).

2.2. Composting

In a view of environmental concerns and referring to the principles of the circular economy, a rational method of organic waste utilization is composting (Jakubus and Spychalski, 2022). The composting process has been recognized as an alternative method for recycling organic waste to obtain a products which can be used in agriculture (Jakubus and Spychalski, 2022; Oviedo-Ocaña et al., 2023; Sokač Cvetnić et al., 2023).

The composting is biological process of transformation of organic waste in a homogenous and plant available material. Also, composting can be interpreted as the sum of complex metabolic processes performed by different microorganisms that in presence or in

absence of oxygen use the organic matter and produce their own biomass (Ayilara et al., 2020; Hemidat et al., 2018). Xie et al. (2023) explained that the composting process includes the processes which result with a stable humus products and that are:

- The effect of alienation – the process by which microorganisms convert large molecules in the body into small molecules and release energy;
- The effect of assimilation – the process by which microorganisms absorb external components and transform them into their own components.
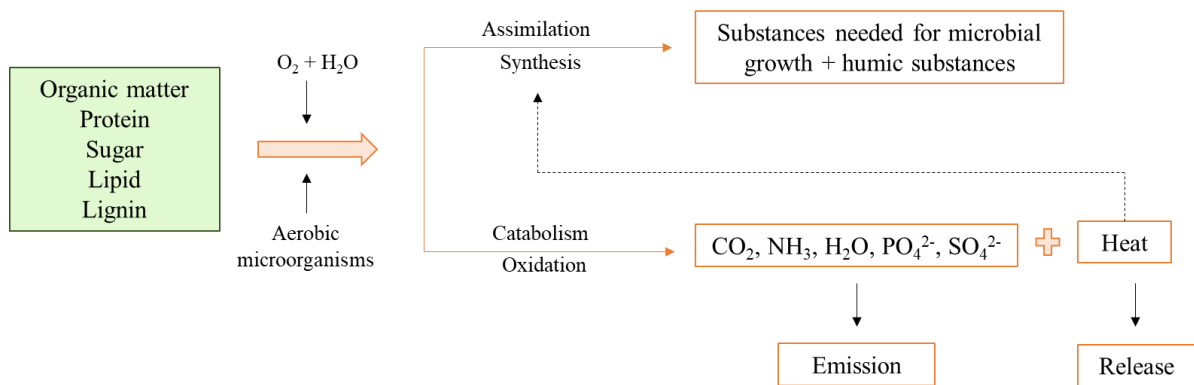
Figure 3. The principle of composting (*adapted* from Xie et al., 2023)

Considering the nature of microorganisms that are involved in the degradation of organic matter, composting can be divided into aerobic and anaerobic process (anaerobic digestion) (Meena et al., 2021) and both treatments are widely used for organic wastes treatment (Lin et al., 2019). Composting is an aerobic process in which microbes require oxygen and water to decompose organic matter to solid product (compost), heat, water, carbon dioxide and ammonia (Eq. 1) (Lin et al., 2019):

$$C_aH_bO_cN_d + \left(\frac{4a+b-2c+3d}{4}\right)O_2 \rightarrow aCO_2 + \left(\frac{b-3d}{2}\right)H_2O + dNH_3 \qquad (1)$$
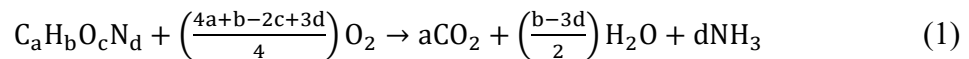
Furthermore, anaerobic digestion converts organic matter to biogas in the absence of oxygen and in this process the anaerobic microorganisms are involved (Lin et al., 2019). During the anaerobic digestion, the organic waste passes through four phases based on the major functional groups of microorganisms: hydrolysis, acidogenesis, acetogenesis and methanogenesis (Lin et al., 2019; Zieliński et al., 2023). Except biogas (methane) as the final product, carbon dioxide, ammonia, and other gases and organic acids in traces can be produced (Eq. 2) (Shah et al., 2017; Lin et al., 2019):

$$C_aH_bO_cN_d + \left(\frac{4a-b-2c+3d}{4}\right)H_2O \rightarrow \left(\frac{4a+b-2c-3d}{8}\right)CH_4 + \left(\frac{4a-b+2c+3d}{8}\right)CO_2 + dNH_3 \qquad (2)$$
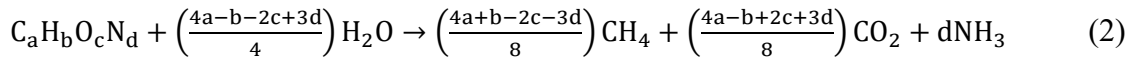
Figure 4 presents the scheme of the aerobic composting (a) and the anaerobic digestion (b) and in Table 2 are summarized the general advantages and disadvantages of both treatments.
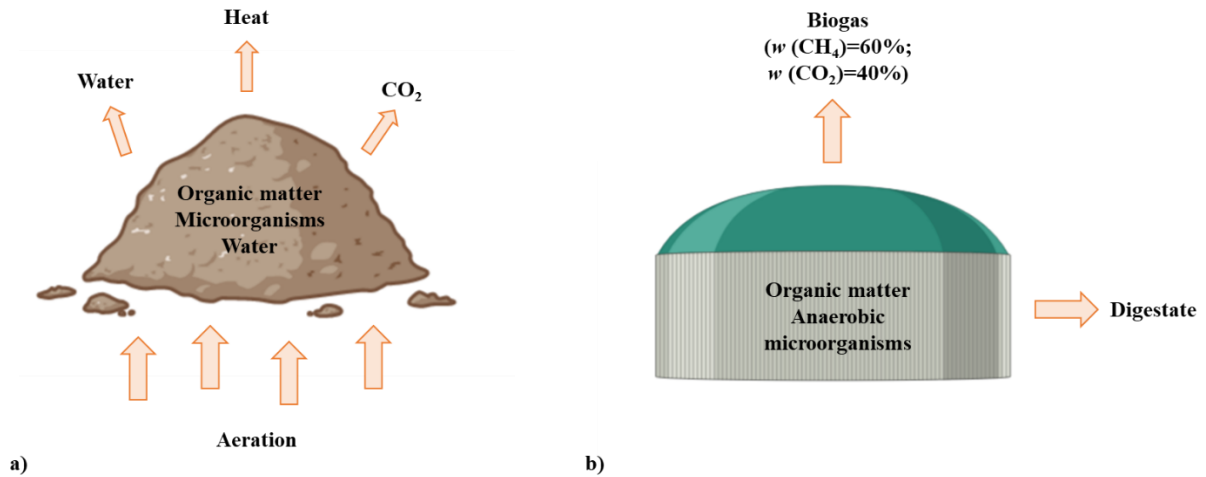
Figure 4. Scheme of (a) aerobic composting and (b) anaerobic composting (*adapted* from Lin et al., 2019)

Table 2. The advantages and disadvantages of composting and anaerobic digestion (Lin et al., 2019; Cucina, 2023)

	Advantages	**Disadvantages**
Composting	Fast degradation	Large area
	Small investment	Odor pollution
	Net energy producer	Leachate production
	Final product - compost	Greenhouse gas emission
Anaerobic digestion	Small area	Slow degradation
	Reduced odor	Posttreatment of digestate
	Final product – biogas	Large investment
	Energy producer	System instability

2.2.1. Composting variables

2.2.1.1. Temperature

A temperature plays an important role in the composting process (Turan, 2008; Onwosi et al., 2017; Azim et al., 2018). If the process is performed under favorable conditions, it proceeds through the main phases in which different communities of microorganisms predominate (Martínez Salgado et al., 2019; Sayara et al., 2020). These phases include:

1. Mezophilic phase

   This phase is also called „active" or „heating up" phase. In this phase, the energy rich and easily degradable organic compounds like sugars and proteins are degraded by mezophilic fungi, actinobacteria and bacteria. As the result of microbial activity and degradation, the heat is generated and the temperature increases passing from mezophilic phase (25-45°C) to thermophilic phase (45-65°C) (Diaz and Savage, 2007; Sayara et al., 2020; Xie et al., 2023).

2. Thermophilic phase

   In this phase thermophile bacteria and fungi continue to degrade organic matter and the temperature still increases up to 65°C (Diaz and Savage, 2007). The thermophile phase is considered as the important phase due to higher temperatures that kill phatogens, weed seeds and fly larvae (Azim et al., 2018; Sayara et al., 2020). Higher temperatures should be avoided, since they slow a biological activity and cause undesirable chemical modifications of organic matter (Azim et al., 2018). Also, temperatures higher than 55°C inhibit the fungal growth (Diaz and Savage, 2007). During the process, a supply of organic compounds becomes exhausted, biological activity and the temperature decrease, mesophilic microorganisms dominate again (Sayara et al., 2020; Waqas et al., 2023).

3. Second mesophilic phase

   This phase is also called „cooling" phase and it is characterized by mesophile microorganisms (fungi and bacteria) that degrade a starch and a cellulose (Diaz and Savage, 2007).

4. Maturation phase

   This phase takes place at lower temperatures and still many reactions are occuring (Sayara et al., 2020). The main characteristic of this phase is material huminification what gives an interesting value to the produced compost. Furthermore, the compounds

that are undegradable such as lignin-humus complexes, are formed and become predominant (Diaz and Savage, 2007).
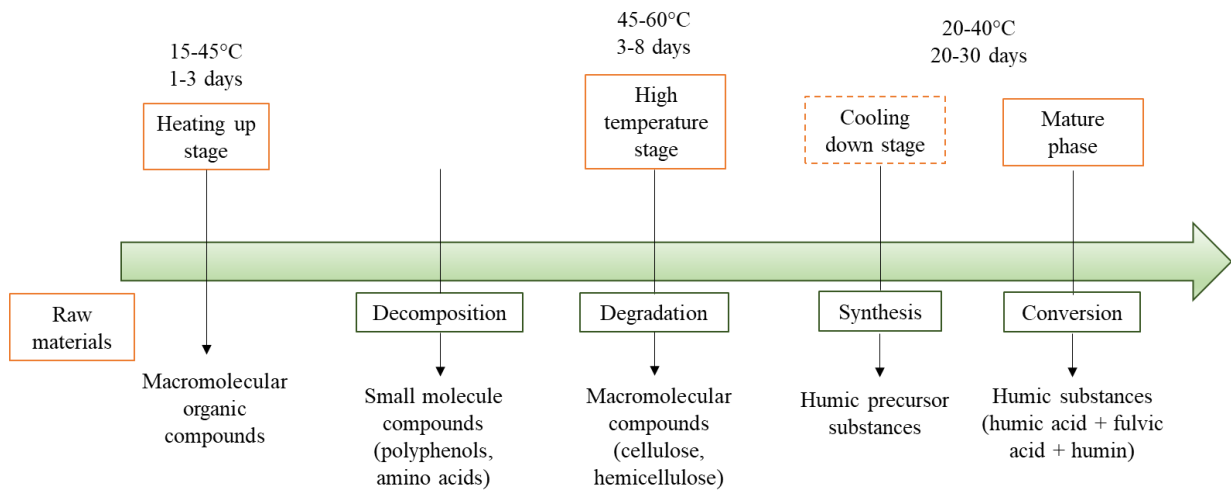
Figure 5. Stages during composting process (*adapted* from Xie et al., 2023)

2.2.1.2. Moisture content

A moisture content is another important parameter for the composting process, related to microbial activity (Onwosi et al., 2017; Azim et al., 2018). Also, it influences the oxygen uptake rate, a free air space and the temperature of the process. Microorganisms use water to transport nutrients and energy elements through the cell membrane (Azim et al., 2018). According to the authors (Diaz and Savage, 2007; Onwosi et al., 2017; Azim et al., 2018), an optimal value of the moisture content for the effective composting process is in the range 50-65%, but it can depend on organic waste type or a form. Lower values of moisture can cause a dehydration of substrate and it can decelerate microbial activity, and a higher values of moisture can plug the pores, impede gas exchange and it can lead to anaerobic conditions (Diaz and Savage, 2007).

2.2.1.3. C/N ratio

During the composting process, microorganisms break down organic compounds to obtain an energy for metabolism and they acquire nutrients (such as nitrogen, potassium and phosphorus) to keep the population. Carbon and nitrogen are important constituents: carbon is used as energy source and nitrogen is used for building cell structure (Onwosi et al., 2017; Xie et al., 2023). Furthermore, carbon nitrogen ratio is a major constituent parameter of organic matter and it is important for microbial life. It is necesarry to maintain a certain proportion of these elements to keep a microbial activity to obtain a high quality compost (Xie et al., 2023). According to the literature, a different ratios are acceptable for the composting process. As

stated by Diaz and Savage (2007) and Onwosi et al. (2017) an optimal C/N ratio for the composting process is 25-30:1. Petric et al. (2015) stated that the values between 25-40:1 are also suitable for the composting. The ratio decreases during the composting process due to the biological mineralization of carbon compounds and loss as carbon dioxide (Diaz and Savage, 2007). Finally, C/N ratio is an indicator of the degree of the decomposition of an organic matter (Onwosi et al., 2017). Table 3 presents the C/N ratio of various organic waste.

Table 3. C/N ratio in various organic waste (Diaz and Savage, 2007; Guo et al., 2012; Waqas et al., 2023)

Raw material	C/N
Activated sludge	6
Corn stalks	59-74
Fruit wastes	20-49
Grass clippings	12-15
Green waste and food waste	19.6
Household waste	17
Sawdust	200-500
Vegetable wastes	10-17

2.2.1.4. pH level

The pH level is another important variable of the composting process and it affects microbial activities (Onwosi et al., 2017). Diaz and Savage (2007) and Onwosi et al. (2017) stated that the optimal pH for composting is in a range from 5.5-8. Lower and higer values of pH may have an inhibitory effect on the microbial activity (Li et al., 2013). Also, the bacteria prefer a nearly neutral pH, and fungi prefer fairly acidic environment (Diaz and Savage, 2007).

A food waste is characterized by low pH due to presence of short chain organic acids (Yu and Huang, 2009). According to Turan (2008), changes in pH are considered as an indicator of microbial activity. In early stages of the composting process, the pH decreases and later increases. The decrease in pH can be due to the microbial degradation of the organic matter and formation of organic and inorganic acids (Diaz and Savage, 2007; Onwosi et al., 2017). Furthermore, in later stages these acids are mineralized and pH increases and at the end of the process is around 8-8.5 (Diaz and Savage, 2007).

pH changes several times during the composting process and there are four phases (Azim et al., 2018):

1. Acid-genesis phase – the pH decreases due to organic acids formed by microorganisms;

2. Alkalization phase – the bacterial hydrolysis of protein occurs and ammonia is produced, and as consequense pH increases;

3. pH stabilization phase – the C/N ratio decreases and reactions are slower. Ammonia is lost by volatilization, and microorganisms use nitrogen to form humic compounds;

4. Stable phase – pH is in neutral to lightly alkali area, and the compost is mature and stable.

2.2.1.5. Aeration

Considering that composting is an aerobic process, it is necessary to ensure the appropriate aeration rates for the effective process. Aeration is important for microbial growth and for compost quality (Li et al., 2013; Onwosi et al., 2017). The aeration ensures sufficient oxygen needed for the oxidation of organic matter and evaporates excess moisture from the substrate (Petric and Selimbašić, 2008). Gao et al. (2010) explained that too little aeration can lead to anaerobic conditions and slower degradation. On the other hand, the excessive aeration can lead to drying of the compost and preventing the thermophilic conditions (Gao et al., 2010; Qasim et al., 2019).

Gao et al. (2010) investigated the effect of different aeration rates (0.3, 0.5 and 0.7 L/min kg OM) on the forced-aeration composting of chicken manure and sawdust. Comparing the analyzed variables such as organic matter content, C/N ratio and germination index, the air flow rate of 0.5 L/min kg OM was favourable for the composting process. A similar results were reported by Rasapoor et al. (2009) who investigated different aeration rates on the composting of municipal solid wastes during 130 days. The results showed that medium aeration rate had the higher impacts in achieving optimal temperature and C/N ratio (Rasapoor et al., 2009). Furthermore, Qasim et al. (2019) carried out the composting processes of poultry manure and sawdust in different shapes of reactor and at different aeration rates. The experiments were performed in cylindrical and rectangular reactors (both had a volume of 60 L) at air flow rates of 0.3, 0.6 and 0.9 L/min kg DM. The airflows were intermittent, 45 min with aeration followed by 15 minutes without aeration. The results showed that high aeration rates in both reactor types

was not suitable for the composting due to rapid heat loss. Moreover, the aeration rate of 0.3 L/min kg DM in a cylindrical reactor provided better condition for maturation of compost.

2.2.1.6. Particle size

Another important parameter for efficient degradation is a particle size (Mishra and Yadav, 2022). The particle size of the organic waste for composting should not be too large because the degradation will be slowly. Also, the particle size should not be too small due to forming compast mass and reduction of oxygen intake (Onwosi et al., 2017). Otherwise, smaller particle size leads to larger surface area and makes it available for microorganisms and degradation (Mishra and Yadav, 2022).

Mishra and Yadav (2022) investigated the effect of particle size of garden waste on the selected physico-chemical parameters (such as moisture content, pH, C/N ratio etc.) during the composting process. The study was conducted with different particle sizes: 0.5-1.5 cm; 1.5-3.0 cm; 3.0-4.5 cm; 4.5-7.5 cm diameter. The greatest change in total carbon and C/N ratio comparing the initial and final values was obtained in the second experiment where the particle size was in the range from 1.5-3.0 cm diameter. Considering the obtained results, Mishra and Yadav (2022) concluded that particle size 1.5-3.0 cm diameter was an optimal for the efficient composting of garden waste.

Haynes et al. (2015) investigated the influence of different particle size of green waste aimed for the composting process on the carbon content, the C/N ratio, the ash content and the nutrient content. In general, they noticed with a decreasing particle size, the carbon content and the C/N ratio decreased, and the ash and the nutrient content increased. They explained that the larger particle sizes consist of hard lignified wood while smaller sizes were composed mainly of green material and some soil.

2.2.1.7. Pretreatment of substrate

Agricultural waste is rich in lignocellulosic biomass that consists of cellulose, hemicellulose, lignin, pectin and protein. The composition varies by origin and climate conditions. Due to a strong molecular structure, it is difficult to directly biodegrade lignocellulose by aerobic microorganisms during composting, which presents an obstacle to the large-scale industrial application of biological composting. The pretreatment is an essential way to destroy the structure of lignocellulose and then depolymerize lignin. However, the pretreatments which include the use of hydrogen peroxide or organic solvents should be

avoided due to reduction of microbial activity and inhibition of the composting process (Wu et al., 2022). As described by Wu et al. (2022) and Xu et al. (2023), the pretreatments for lignocellulose are as follows:

1. Physical pretreatment such as mechanical crushing and microwave processing. During this pretreatment, the lignocellulose structure is destroyed;
2. Chemical pretreatment includes the use of reagents (acids, alkali, hydrogen peroxide, Fenton process);
3. Microbial agent pretreatment which includes bacteria and fungi that secrete hydrolytic enzymes for the degradation;
4. Combined pretreatment – the combination of physical and chemical pretreatment.

2.3. Compost quality

A composting process that is well-performed results with a high-quality compost. Its quality is related to a stability and maturity. The stability is related to the resistance of the organic matter in compost against further microbial decomposition, and the maturity describes the ability of a product to be used effectively in the agriculture for plant growth (Sayara et al., 2020; Siles-Castellano et al., 2020).

Many researchers confirmed that the application of mature compost could improve physicochemical and biological characteristics of soil and provide various additional benefits to enhance the soil quality (Sayara et al., 2020; Gong et al., 2021; G. Wang et al., 2022). The addition of compost to a soil can ensure the organic matter and nutrient elements, boost soilwith microbial community, reduce soil bulk density, and also reduce the risk of erosion, reduce water evaporation, regulate moisture content and it can improve drainage (Sayara et al., 2020; Gong et al., 2021). Otherwise, the application of immature and unstable compost can be a threat to the soil health and environmental safety due to heavy metals and pathogenic microorganisms (Wang et al., 2020).

Phytotoxicity tests are often used to describe the degree of compost maturity. The tests are divided in four categories: germination tests (include root assessments), growth tests (assessment of top-growth and sometimes root mass), combinations of germination and growth and other biological methods such as enzyme activities. The germination tests could provide an instant picture of phytotoxicity, whereas growing tests would be affected by continuing changes in the stability or maturity of the tested compost (Cesaro et al., 2015).

Furthermore, germination index is widely used biological indicator for evaluating the compost maturity and phytotoxicity (Siles-Castellano et al., 2020; Wang et al., 2020; Gong et al., 2021). The use of simple tool such as germination index for monitoring the performance of the composting process and compost in industrial facilities would help to address operational weakness and improve the processing in order to obtain a high quality product (Siles-Castellano et al., 2020). Cesaro et al. (2015) reported that germination index was listed in the quality assessment regulation of compost for commercialization in most European countries. Also, the authors (Kong et al., 2022; G. Wang et al., 2022) reported that germination index changed during the composting process and it is due to the concentration of salts, organic acids, metals and ammonium ions.

As explained by Wang et al. (2020) and Xie et al. (2023) the maturity indicators of the compost could be divided in three categories: physical, chemical and biological. Table 4 presents the maturity indicators and compost characteristics.

Table 4. The maturity indicators, their determination method and the compost maturity characteristics (*adapted* from Wang et al. (2020) and Xie et al. (2023))

	Indicator	Method	Compost maturity characteristics
Physical indicators	Temperature	Continuously monitored	The temperature of compost substrate drops to ambient temperature and there is no obvious change
	Smell	Perceived by human nose	A damp earthly smell
	Color	Perceived by human eye	A dark brown color
	Moisture content	Determined by standard drying method	The moisture content of compost is significantly reduced
Chemical indicators	C/N	C, N contents determined by elemental analyzer	(15-20):1
	pH	Measured by pH meter	8-9
	Electrical conductivity	Measured by conductivity meter	Less than 9.0 mS cm^{-1}
Biological indicator	Germination index	Analyzed by seed germination culture test	GI > 80%

2.4. Composting systems

According to the literature (Miguel et al., 2022; Sokač Cvetnić et al., 2023) there are two main types of facilities for the performance of the composting process:

1. Open systems such as windrows and piles;
2. Closed systems such as reactors and composters.

Closed systems have some advantages compared to open ones: they require less space, provide better control of the process and consequently, high process efficiency can be achieved (Sokač Cvetnić et al., 2023). Furthermore, composting can be performed manually or automatically. Manual technology is a natural process and it requires a relatively long time to degrade organic matter to produce the compost. Also, it requires an isolated area to prevent the odor. The process should be monitored regularly to ensure the optimum composting conditions. On the other hand, an automatic systems attempt to automate some of the phases of the composting process. These systems have some advantages: the system requires less monitoring and less space, but it also requires electricity to speed up the process what makes it more expensive (Azis et al., 2022).

2.4.1. Manual technology

In manual composting, the process is operated by hands and there are five common types of manual composting (Figure 6): windrow, passively aerated windrow, bin, in vessel composting and vermicomposting.
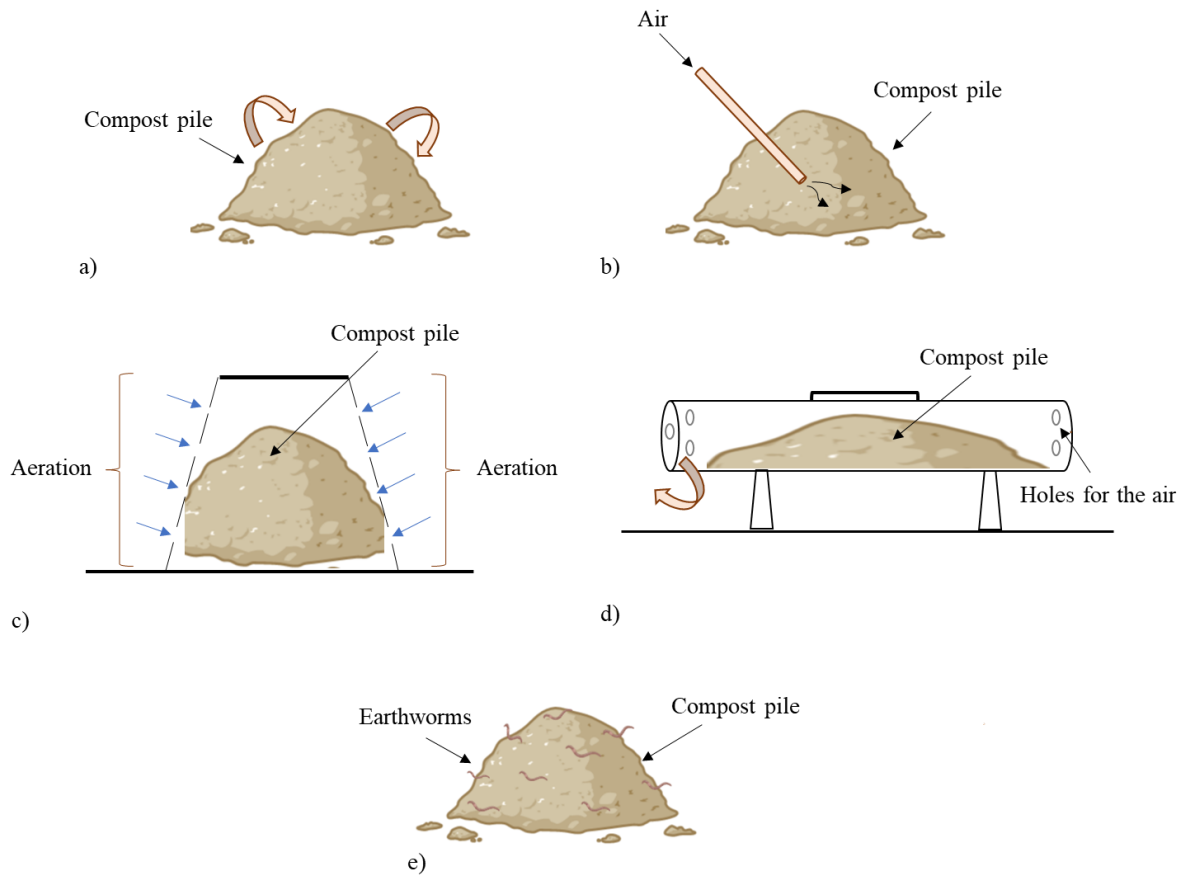
Figure 6. Different types of manual composting: a) Windrow; b) Passively aerated windrow composting; c) Bin composting; d) In vessel composting; e) Vermicomposting (*adapted* from Azis et al., 2022)

Windrow composting system, known as the most basic composting method, consists of linear piles of compost material which are turned to improve the aeration and to mix the compost constituents (Vigneswaran et al., 2016; Azis et al., 2022). There are some advantages of windrow composting compared to in-vessel ones (Vigneswaran et al., 2016):

- Easy to implement and operate;
- In this system a large volumes of organic waste can be composted what reduces the amount of waste disposed on landfills;
- Low capital costs;
- The minimal equipment is required;
- The system can be easily scaled from a small-scale to a large-scale;
- High quality compost can be produced.

Also, the windrow system has some drawbacks such as producing the odor during the composting process, requirements for relatively large open space and the process is affected by climate (high temperatures, wind, rain) (Vigneswaran et al., 2016).

As shown in Figure 6b, passively aerated windrow composting is an improvement over simple windrow composting by implementation of pipes at the center of the pile to ensure convective aeration throughout the pile (Manyapu et al., 2018). The main benefit of this technology is that it does not require any turning which allows the pile to retain the heat and consequently, makes the composting time shorter than in conventional windrow composting (Azis et al., 2022).

The bin composting is often used in households due to limited space. A limited amount of organic waste can be treated and it can result with a compost for self-consumption. This system is often made of perforated walls to retain the heat. Also, in this system turning is not required but the process is longer than in windrow systems (Azis et al., 2022).

„In-vessel" or „reactor" system is novel technology which is gaining interest due to easier monitoring of composting parameters (Manyapu et al., 2018; Azis et al., 2022). The aeration is provided either by rotation of the container which has holes or through aeration pumps. The main advantages of these systems are effective organic waste management and an improved environmental protection (no odor) (Manyapu et al., 2018).

The vermicomposting is a composting method which utilizes microorganisms and macroorganims, such as earthworm species, for degradation of organic matter (Azis et al., 2022; Sokač Cvetnić et al., 2023). The earthworms engulf the organic matter and mix up with the enzymes in their gut, and excrete the form that contains nutrients for the plants. The main disadvantage is that the earthworms are sensitive to heat and moisture, and the turning of the piles is necesarry. Due to temperature sensitivity, often the thermophile phase is not achieved, but anyway the pathogenic microorganisms can be destroyed (Vigneswaran et al., 2016).

2.4.2. Automatic technology

Mentioned manual composting technologies require some time to produce the compost, it is obligatory to monitor the process what makes it more complicated and some methods require more space. An automatization of the process should solve these problems and improve the process efficiency (Azis et al., 2022).
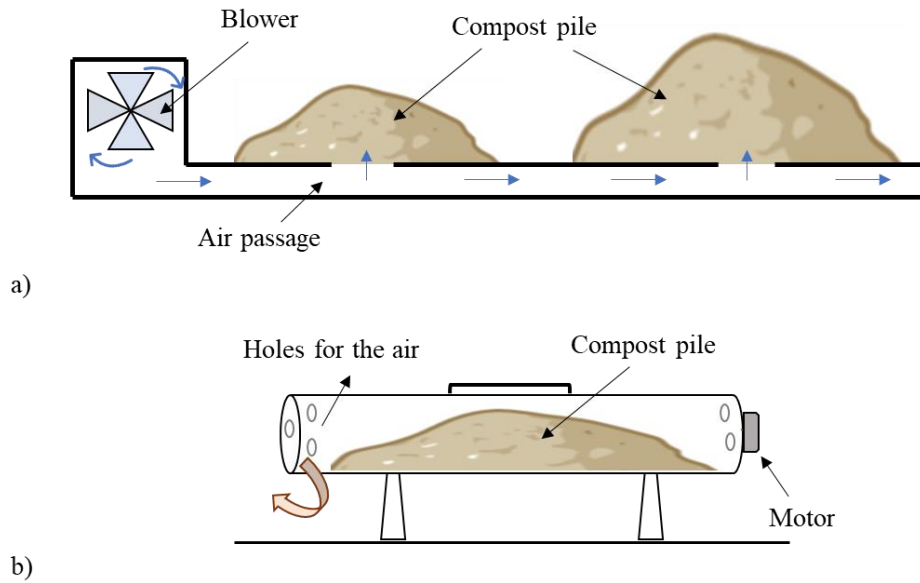
Figure 7. Automatic composting technologies: a) Forced aerated windrow composting; b) Automatic turning in-vessel composting (*adapted* from Azis et al., 2022)

In Figure 7 the automatic composting technologies are presented. In the forced aerated windrow system, blowers are installed to inject the air into compost piles to ensure an oxygen for microbial activity and to enhance degradation of organic matter. The airflow can be adjusted by changing the frequency or period of blowing the air. The compost piles are insulated due to retention of the heat and to allow the thermophilic temperature through the piles which can result in a shorter composting time. Furthermore, this method requires high investment for blower and aeration channels, and high maintenance (Azis et al., 2022).

The automatic in-vessel technology is similar to the manual in-vessel composting, but it has the automatic turining for the aeration of the composting piles powered by motor. The turning of the in-vessel reactor can be scheduled to rotate at desired times and frequency. Also, there are in-vessel reactors that have sensors for temperature and moisture content. The main advantages of this technology are space-efficient and requirement of a low amount of labor, but on the other hand the investment and maintenance costs are high (Azis et al., 2022).

The electric composter is an indoor compost bin that uses aeration, heat and pulverziation to minimize volume, emissions and odor of food waste. The electrical composter (food recycler) uses four-phases cycle to break down food waste: drying, grinding, cooling and curing. The main disadvantage of composter is high initial investment of the machine and high maintenance. Also, due to fast process, low space requirements and very low labor requirement, the electric composter is an attractive alternative to the conventional composting (Azis et al., 2022).

Table 5. The summary of manual and automatic composting technologies (*adapted* from Lim et al., 2017; Azis et al., 2022)

Method of composting	Cost	Maintenance	Space requirement	Composting duration	Labor requirement
Manual composting technologies					
Windrow	− −	− −	+ +	+/−	+ +
Passively aerated windrow	−	−	+ +	+/−	−
In-vessel	+ +	+ +	+/−	+	−
Bin	+/−	−	+/−	−	−
Vermicomposting	− −	−	−	+	− −
Automatic composting technologies					
Forced aerated windrow	+	+	+	+	−
Automatic turning in-vessel	+ +	+ +	+/−	+	− −
Electric composter	+	+	−	+ +	− −

* − − very low or very slow; − low or slow; +/− moderate; + high or fast; + + very high or very fast.

2.5. Near Infrared Spectroscopy (NIR)

2.5.1. The basics of Near Infrared Spectroscopy

The protocols and standardized methods are currently available for the testing and evaluating compost quality through physicochemical properties, but their determination can be time consuming, and require expensive equipment or numerous reagents (Huang et al., 2008; Soriano-Disla et al., 2010; Toledo et al., 2017). Furthermore, near infrared spectroscopy (NIR) has been reported as a useful alternative to monitor composting processes and to evaluate the compost quality (Huang et al., 2020; Kavdir et al., 2020; Rueda et al., 2023).

It is assumed that NIR spectroscopy started in the 1880s, when Abney and Festing measured the spectra of some simple organic compounds in the range from 700-1200 nm and in the 1950s, NIR spectroscopy received considerable interest for hydrogen bonding and anharmonicity studies (Ozaki et al., 2018). Over the last decades, this method is one of the fastest-growing and widely used for rapid and non-destructive analysis in industries such as agriculture, food, pharmaceuticals, textile, cosmetics and polymer production (Albrecht et al., 2011; Huang et al., 2020). Near-infrared (NIR) spectroscopy is a commonly used spectroscopic technique dealing with the absorption, emission and reflection of electromagnetic radiation in a wavelength range from 800 to 2500 nm (12 500 - 4000 1/cm) (Ozaki et al., 2018; Sokač Cvetnić et al., 2023). In other words, the NIR region lies between the visible and microwave region in electromagnetic spectrum as shown in Figure 8.
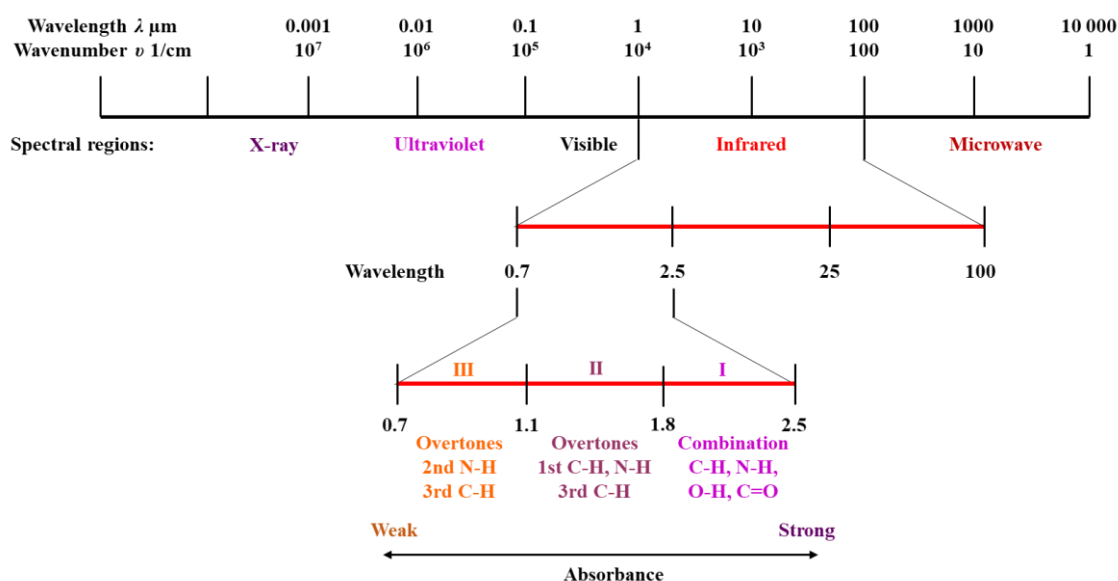
Figure 8. Electromagnetic spectrum with NIR regions (*adapted* from Raypah et al., 2022)

NIR spectroscopy is based on the principle that different chemical bonds in organic matter absorb or emit light of different wavelenghts when the sample is irradiated. Organic matter in samples has different spectral fingerprints owing to the specific vibrational frequencies of chemical bonds which are determined by the shape of molecule, the mass of constituent atoms, the stiffness of the bonds and the periods of the associated vibrational coupling. The most prominent absorption bands are associated with molecular overtone and combination vibrations of some hydrogen based functional groups such as O–H, C–H, C–O, and N–H (Zareef et al., 2020). Furthermore, the intensity of NIR bands depends on the change in dipole moment and the anharmonicity of the bond. Due to the hydrogen atom is the lightest, and exhibits the largest vibrations and the greatest deviations from harmonic behavior, the main bands typically observed in the NIR region correspond to bonds containing this and other light atoms (namely C–H, N–H, O–H and S–H); by contrast, the bands for bonds such as C=O, C–C and C–Cl are much weaker or even absent (Blanco and Villarroya, 2002). The main components of NIR spectroscopy and its principe of operation is shown in Figure 9.
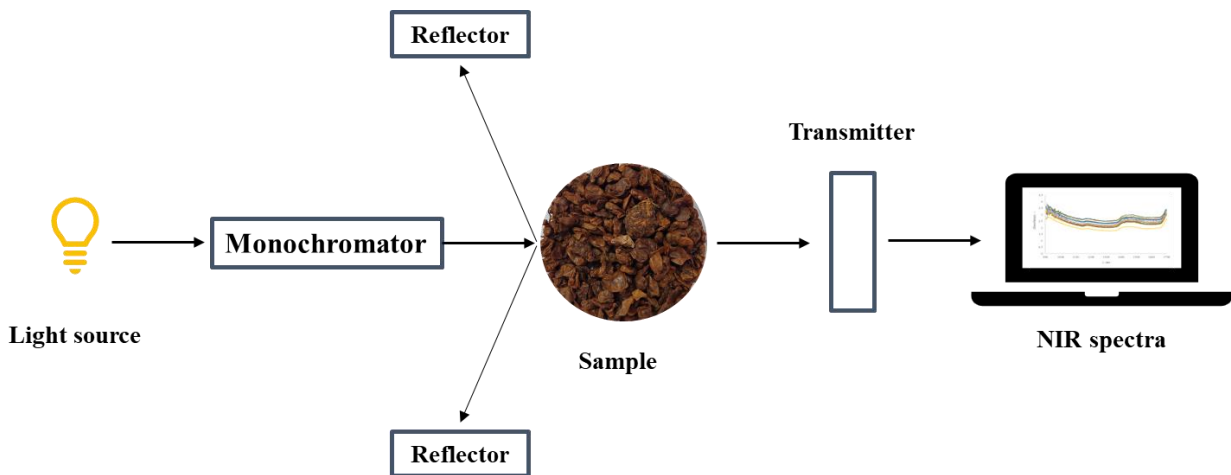
Figure 9. The main NIR components (*adapted* from Reich, 2005)

Moreover, the NIR wavelength has been divided into three regions (Sokač Cvetnić et al., 2023):

1. The first covers the wavelength range from 800-1200 nm, forming a visible near-infrared region. The main characteristic of this region is high permeability, enabling its application in medicine and agricultural industries. It is also specific due to the appearance of bands, which are consequences of electronic transitions, higher-order overtones, and combinations of fundamental vibrations of the XH bonds (X = C, N, O, S);

2. The second region covers the wavelength range from 1200-2000 nm containing a number of bands arising from the first and second overtones and combination modes. This wavelength range can be used for qualitative and quantitative analyses, but the permeability of the second region is low;

3. The third region (2000–2500 nm) deals with the combination modes and can be used for various purposes, such as investigations about the structure of proteins; however, the third region is characterized by relatively low permeability.
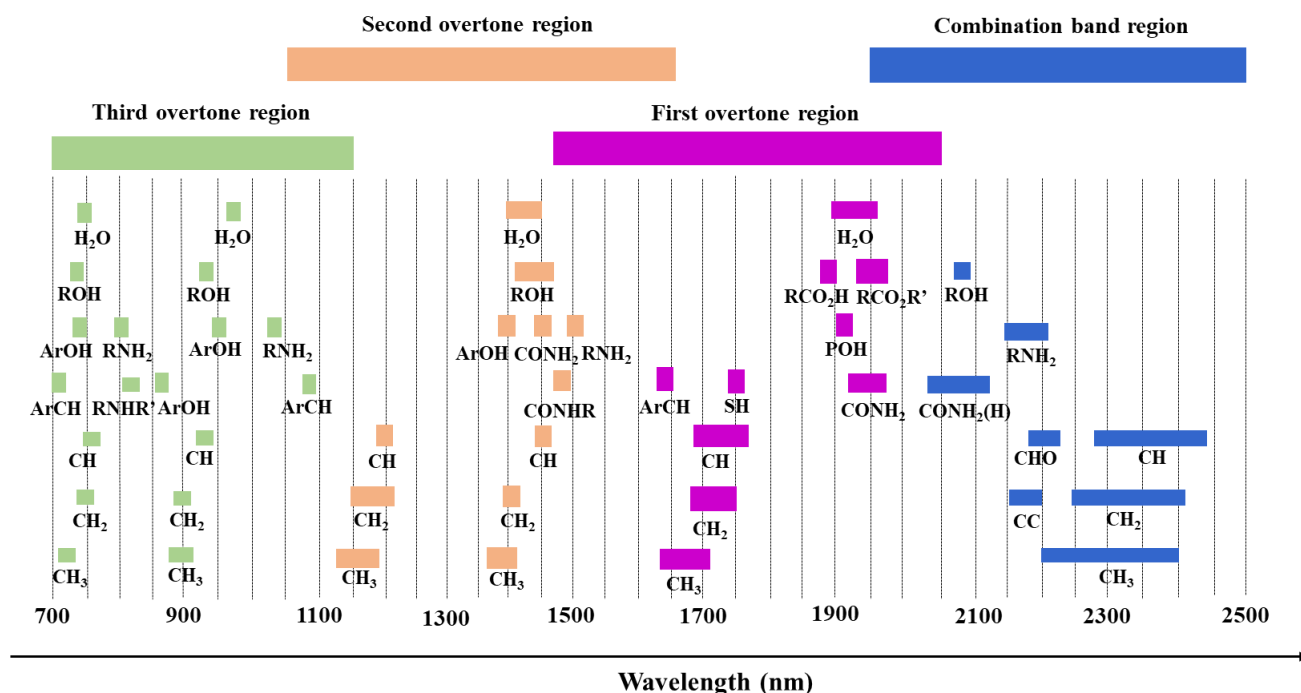
Figure 10. Overtones and combinations of NIR band assignments (*adapted* from Raypah et al., 2022)

2.5.2. Chemometrics

Considering the fact that NIR spectra are often complex and possess broad overlapping absorption bands, the extraction of useful information from the NIR data set requires the use of chemometrics (Blanco and Villarroya, 2002; Sokač Cvetnić et al., 2023). Chemometrics is a tool that relates spectral information to properties of samples. Also, chemometrics includes mathematical and statistical methods that separate irrelevant information from relevant (Reich, 2005; Iannucci, 2021). The chemometrics techniques include simultaneous analysis of more than one variable at a time, while considering the correlation among the data set variables (Kumar, 2021).

Chemometric method can be divided into three groups: (i) mathematical pretreatments or preprocessing (ii) classification methods and (iii) regression methods. The first chemometric step in NIR spectra analysis is data preprocessing in order to obtain more accurate, reliable and stable calibration model using non-linear algorithm (Zareef et al., 2020). There are many preprocessing techniques often used for the spectral data to remove the useless information and to obtain a quality spectral data (Zareef et al., 2020; Sokač Cvetnić et al., 2023):

- Baseline correction (or de-trending) - NIR spectra frequently display a curvilinear trend and baseline offset due to variations in illumination angle or optical path length, among other factors. Resetting all spectra to a common baseline is the goal of baseline removal. Most baseline correction techniques are straightforward and frequently maintain the primary spectral shape (Sandak et al., 2016).

- Standard normal variate transformation (SNV) - The SNV transformation is employed to minimize variations in the global intensities of the signals as well as the multiplicative effects of particle size and scattering. NIR diffuse reflectance spectra may be more challenging to interpret spectrally and linearly calibrate due to light scattering caused by interactions between IR radiation and sample particles. Path-length variations caused by light scattering produce a background signal level that varies with wavelength, resulting in baseline shift and curvature. This background signal level can differ significantly within and between samples (Zeaiter and Rutledge, 2009).

- Multiplicative scatter corrections (MSCs) - Usually, MSC is employed to account for variations in path length and light scattering effects. By applying the linear least squares method to fit a linear model between a reference spectrum and other spectra of the dataset, MSC reduces these deviations. The average of all the spectra in the dataset is frequently used to select the reference spectrum (Watanabe et al., 2018).

- Smoothing (SMTH) - Reducing high frequency noise, or "spikes" in the spectrum, is the goal of spectral smoothing. But when smoothing a spectrum, care must be taken to ensure that high frequency components containing valuable information are not eliminated.

- Savitzky-Golay (SG) - Reducing or eliminating the effects of multiplicative and additive effects in the spectra is the goal of this approach. Prior to computing the derivative (1st order, 2nd order, etc.), this strategy includes a spectrum smoothing step to lessen the detrimental impact on the signal-to-noise ratio that would result from using a traditional finite difference derivative (Amirvaresi and Parastar, 2023).

- Wavelet transforms (WT) - One effective technique for enhancing NIR spectral resolution and resolving overlapping spectra is the wavelet transform (WT). A spectrum is transformed into the trends of individual peaks with varying widths by the WT (Wang et al., 2023).

- Orthogonal signal correction (OSC) - A pre-processing method called orthogonal signal correction (OSC) is used to correct for instrument drift, bias, and scatter in near-infrared spectra. The variation is divided by OSC into orthogonal factors, which include the variation that is not correlated with the analyte vector data but is present in the spectral data matrix (Blanco et al., 2001).

2.5.2.1. Principal component analysis (PCA)

Since NIR spectral data contains a huge number of correlated variables, there is a need for reduction of variables. The best known and most widely used variable-reduction method is principal component analysis (Reich, 2005; Abdi and Williams, 2010). The main idea of this method is reducing the dimensionality of a dataset, while preserving as much variability as possible (Jollife and Cadima, 2016). This method analyzes the data representing observations described by several dependent variables which are intercorrelated. Its goal is to extract the important information from the data and to express this information as a set of new orthogonal variables called principal components. And finally, the relevant information for the system is contained in a reduced number of variables (Blanco and Villarroya, 2002; Abdi and Williams, 2010). PCA is used as the NIR spectra classification method.

2.5.2.2. Partial Least Square regression (PLS)

Interference and overlapping of the spectral information may be overcome using multicomponent analysis such as partial least square regression. This method allows a statistical approach using the full spectral region rather than unique and isolated absorption bands. The algorithm is based on the ability to mathematically correlate spectral data to a physicochemical variables, while simultaneously accounting for all other significant spectral factors that perturb the spectrum. Samples of known modifications are used as calibration samples and then the modifications of an unknown sample are directly calculated using the resulting equation under the same conditions (Vergnoux et al., 2009).

Table 6. Examples of application of NIR spectroscopy in the composting process

Type of composting	Composting material	Spectroscopic method and Chemomerics	Results	Reference
Windrow composting	Crushed green waste (1/3 volume), pine barks (1/3 volume) and local municipal sewage sludge (1/3 volume)	NIR spectroscopy in the wavelength range 400–2500 nm coupled with partial least squares regression.	The NIR spectroscopy can predict the carbon content ($R^2 = 0.95$), nitrogen content ($R^2 = 0.96$), C/N ratio ($R^2 = 0.96$) and age of compost ($R^2 = 0.96$).	Albrecht et al., 2008
In pile composting	Mixture of grape stalk, grape marc, exhausted grape marc, sewage sludge, cow manure, poultry manure	NIR spectroscopy in the wavelength range from 830-2630 nm coupled with a penalized signal regression and partial linear square regression	The combination of NIR analysis and statistical tools was used to estimate total phosphorus content. The coefficient of determination (R^2) was 0.99 for penalized signal regression and 0.93 for partial linear square regression.	Galvez-Sola et al., 2010
Comercial composter with natural aeration and static piles with forced aeration	Agroindustrial waste (grape stalk, exhausted grape marc, grape marc, cattle manure, poultry manure, sheep manure sewage sludge, tomato soup waste…)	NIR spectroscopy in the wavelength range from 830-2600 nm coupled with partial least square regression	The authors obtained excellent prediction results for total organic matter and total organic carbon, and successful calibrations for pH, conductivity, Fe and Mn.	Galvez-Sola et al., 2010a
Composting in adiabatic reactor, $V = 24$ L	The four substrates were composted: organic fraction of municipal solid waste (OFMSW), mixture of OFMSW with organge peel, sewage sludge with bulking agent, mixture of strawberry extrudate, fish waste, sewage sludge and bulking agent	NIR spectroscopy inthe wavelength range400–2500 nm coupledwith PCA andmultivariate regression.	The chemical composition of each substrate determined by NIR spectroscopy could be related to odor emissions. For all four substrates, correlations between experimental and multiple linear regression model estimated odor emission rate based on the NIR spectra were in the range from 0.74 to 0.88.	Toledo et al., 2017

Table 6. (*continuing*) Examples of application of NIR spectroscopy in the composting process

In pile composting	The rawmaterials were mixed with cow manure and corn stalksin a mass ratio of 10:1.	Handheld NIR sensor range of reflectance spectra were recorded from 950 to 1650 nm coupled with PCA and PLS modeling	The results showed that the handheld NIR could accurately detect moisture content (MC), totalnitrogen (TN), total carbon (TC), the carbon/nitrogen (C/N) ratio, organic matter (OM) and electrical conductivity (EC) during the trough composting process, with excellent predictions for MC, good predictions for TN and OM, approximate predictions for TC, C/N ratio and EC.	Huang et al., 2020
In pile composting	Olive oil solid waste	FT-NIR spectroscopy in the wavelength range from 780-2500 nm coupled with PLS regression	The highest prediction was obtained for the NO_3^- constituent, which was followed by pH value, NH_4^+, total inorganic N, total N, C/N ratio, total C and electrical conductivity with R^2 0.86, 0.82, 0.81, 0.81, 0.77, 0.75, 0.65, 0.51	Kavdir et al., 2020
The open composting system and semi-enclosed composting	Agricultural waste (rice straw and pig manure)	NIR spectroscopy in the wavelength range from 450-1650 nm coupled with partial least square regression	The results show that using different spectral pretreatment methods presents better predictions for OM content, TN content and C/N ratio with lower errors in relation to the full band original spectrum.	Shen et al., 2023
In pile composting	Olive mill pomace	Combination of FT-NIR and FT-MIR spectroscopy and principal component analysis	Information contained in FT-NIR and FT-MIR spectra allowed for understanding the structural changes occurring in compost organic matter	Rueda et al., 2023

2.5.2.3. Artificial neural network (ANN)

In the recent years, a rapid development and application of artificial inteligence techniques can be noticed in almost all fields such as medicine, engineering, finance, agriculture, education and meteorology. The artificial inteligence simulates the human brain and consequently, it serves for problem solving, learning, perception, understanding, reasoning and awareness of surroundings. ANNs have gained a great interest due to its capacity to handle a large amounts of data, mapping their non-linear relationships and predicting the results (Xu et al., 2021). The first neural network model describing how human neurons might work was proposed by Warren McCulloch and Walter Pitts in 1943 and their idea of simulation of human thinking provoked a huge amount of reasearch in the ensuing two decades (Huang et al., 2007; Xu et al., 2021).

Artificial neural network consist of groups of interconnected processing elements called neurons that are organized in layers producing "architecture" (Heberger, 2008). The type of layers are (Montesinos López et al., 2022):

1. Input layer – a set of neurons that receive information from the external sources of the network. The number of neurons in input layer is often the same as the number of the input variables provided to the network. Input layers are followed by at least one hidden layer;

2. Hidden layers are consisted of internal neurons that do not have direct contact with the outside. The number of hidden layers can be 0, 1 or more. They are called the hidden layers because the neurons of each hidden layer share the same type of information. It is important to mention that hidden layers are key components for capturing complex nonlinear behaviors of data more efficiently;

3. Output layer is consisted of neurons that transfer the information that the network has processed to the outside. The final output can be continuous, binary, ordinal, or count depending on the setup of the ANN which is controlled by the activation (or inverse link in the statistical domain) function we specified on the neurons in the output layer.
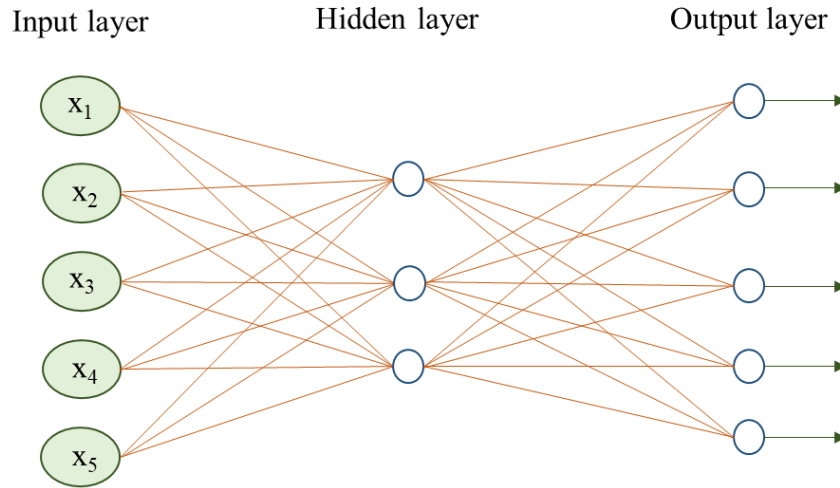
Figure 11. A scheme of artificial neural network (*adapted* from Huang et al., 2007)

Considering the mutual combination relationship between neurons, the artificial neural networks can be divided to (Sarker, 2021; Wang et al., 2022):

1. Multilayer perceptron (MLP);
2. Convolutional neural network (CNN);
3. Recurrent neural network (RNN).

Multilayer Perceptron Neural Network (MLP)

A typical multilayer is a fully connected network and it contains an input layer, several hidden layers and output layer (Wang et al., 2022). Input layer receives the information from an input data or from electrical sensors in an on-line application and forwards this information to the next layer of neurons. The output layer processes the input information from the previous layer and transfers the information out from the network (Huang et al., 2007; Sarker, 2021). The output of an MLP network is determined using a variety of activation functions such as ReLU (Rectified Linear Unit), Tanh, Sigmoid and Softmax (Sarker, 2021). Furthermore, a MLP is trained/learned to minimize the errors between the desired target values and the values computed from the model. If the network gives the wrong infromation, or if the errors are greater than a given threshold, the weights are updated to minimize them. Thus, errors are reduced and, as a result, future responses of the network are likely to be correct (Park and Lek, 2016). According to Park and Lek (2016), the MLP have some advantages such as:

- MLPs can be applied in a wide range of fields to find the solution;
- MLPs often provide more efficient results that conventional statistical methods;

- The learning process is adaptive and MLP can learn how to find the solution directly from the data being modeled;

- MLPs create the required decision function directly through the learning process with a given data set;

- MLPs are used for discrimination, pattern recognition, empirical modeling, and many other tasks.

Convolutional Neural Network (CNN)

Convolutional Neural Network (CNN) is a well-known deep learning architecture inspired by the natural visual perception mechanism of the living creatures (Gu et al., 2018; Sarker, 2021). CNNs are specifically intended to deal with a variety of 2D shapes and, consequently they are widely employed in visual recognition, medical image analysis, image segmentation, natural language processing and other (Sarker, 2021).

Recurrent neural network (RNN)

The recurrent neural network (RNN) is another popular neural network which employees sequential or time-series data and feeds the output from the previous step as input to the current stage (Sarker, 2021). This type of neural network is often recommended in voice recognition, language translation, natural language understanding and music synthesis. Also, this is a network with „memory" that plays a pivotal role in the modeling of sequential data (Wang et al., 2022).

2.5.2.4. Application of artificial neural network (ANN) for the composting process

The use of artificial neural networks has been described by Liang et al. (2003). Based on data obtained by composting process, the authors developed the artificial neural network models for estimation of microbial activity during the biosolids composting using moisture content and temperature as inputs. They concluded that in the future, these models can be incorporated into a decision support system for composting management to optimize the process and reduce operation costs.

Furthermore, Boniecki et al. (2012) investigated the options of applying artificial neural network models for the modeling of ammonia emissions released during composting of sewage sludge. The results show that the predictive neural models are well suited for assessing ammonia emissions (for all models the correlation coefficient reached values between 0.972 and 0.981), and the models have been found as a proper way to support sewage sludge management decisions.

Soto-Paz et al. (2020) investigated the optimization of the composting process of biowaste mixed with sugarcane filter cake using the artificial neural network and the particle swarm optimization algorithm. The developed artificial neural network models for the prediction of temperature, pH, oxygen content, total organic carbon, total nitrogen and total phosphorus resulted with a high coefficient of determination, it was between 0.93 and 0.97.

Dragoi et al. (2021) used neuro-evolutive methodology based on artificial neural network (ANN) and differential evolution for the prediction of petroleum hydrocarbons and organic carbon removal during the oily sludge composting process. Actually, the ANN represented the model and differential evolution was the optimizer applied to determine the characteristics of the model. The better prediction using the ANN models was achieved for the total petroleum hydrocarbons (the relative error was 5.96%) than for the organic carbon (the relative error was 12.7%).

Also, Sharma et al. (2021) applied central composite design and artificial neural network models for the optimizing amount of floral waste and cattle dung for the vermicomposting process using the earthworm *Eisenia fetida*. In particular, the obtained results showed that ANN models are in advantage over the central composite design for the optimization of waste amounts. Coefficients of determination obtained for ANN models were 0.92 for C/N ratio and 0.99 for germination indeks, and in a case of central composite design, the coefficients were 0.86 and 0.98, respectively.

Abdi et al. (2023) performed in-vessel composting process of vegetable and food waste with additives (coco peat and biochar obtained from coco peat), and they investigated the application of artificial neural network models for the prediction compost indicators such as electrical conductivity, pH, C/N ratio and germination index. The obtained coefficients of determination (R^2) were 0.92, 0.98, 0.96 and 0.99, respectively, which indicates the use of ANN models for the prediction of compost variables during the composting process.

2.6. Mathematical modeling and optimization of the composting process

2.6.1. Mathematical modeling

Mathematical modeling has been widely used for the interpretation of the complex dynamic interactions, exploring theoretical concepts and predicting the system performance. In other words, mathematical models provide a potential to reduce or even replace the need for physical experimentation during the investigation of new materia (Mason, 2006; Sokač et al., 2022c). The motivation of modeling is to develop mathematical tools to intergrate the knowledge with the phenomena, determine the direction of experimental design, evaluate experimental results, test hypotheses, reveal relatioships between variables, predict the system development and design the process and management strategies (Yang et al., 2021). Also, mathematical modeling provides a great opportunity for simulation and optimization of the processes (Papračanin and Petric, 2017).

As explained before, a number of biological and physical processes are involved in the composting process. These interrelated and often highly non-linear processes produce a variety of phenomena that are difficult to study experimentally and analytically. Thus, the reactions that occur during composting process may be approximated by mathematical models (Sokač et al., 2022c). Mathematical models of the composting process often include the heat and mass balance equations in time and microorganisms growth as well (Mason, 2006). By the literature review, several mathematical models are available to describe a composting process. The most of models rely on the assumption that the composting substrate is perfectly mixed and variables such as temperature, moisture content, oxygen concentration, organic matter content etc. are changing during the time (Vidriales-Escobar et al., 2017).

The examples of mathematical models used for the composting process are shown in Table 7.

Table 7. Application of mathematical models used for description of composting process

Composting system	Model formulation	Model description	Reference
Composting of organic fraction of municipal solid waste and polutry manure in laboratory reactors	Exponential equations describing decomposition rate	For modeling the decomposition rate, 9 models were applied. The models include important composting variables (such as moisture content, temperature, pH). The model with more measured variables is the most suitable model.	Petric et al., 2012
Static pile composting of wood chips	Mathematical model of vertical moisture content movement	The differential equations describe the dynamic of the moisture content change in a static composting pile. The amount of water in different composting layer depends on input water flux and output water flux by evaporation, diffusion and percolation.	Seng et al., 2012
Leachate produced during the tobacco waste composting	Mass balance for substrate and biomass	Mathematical model in form of differential equations for description of biodegradation of organic matter from leachate produced during composting of tobacco waste. The microbial growth was described using Monod model, modified Monod model, Haldane model and expanded Haldane model.	Ćosić et al., 2012
In-vessel composting of chicken manure, sawdust and wheat straw	Exponential equations describing decomposition rate	Model 1 is a function of process temperature, model 2 was a function of initial moisture content of the material and the heat values, model 3 was a function of process heat value and moisture content of the material.	Kulcu, 2016
In-vessel composting of sewage sludge and agricultural waste	Exponential equation describing the biodegradable organic matter loss	The equation includes correction factors for temperature, moisture content, oxygen content and porosity.	Malamis et al., 2016

In order to monitor the composting process and its efficiency, it is essential to investigate the biodegradation of the substrate and to maximise the decomposition rate (Malamis et al., 2016). The kinetic models are based on the decomposition of organic matter because it provides free energy required to drive the process and should be able to predict the processing rate (Aviezer and Lahav, 2022). The organic matter models, in which the amount or concentration of residual substrate serves as the independent variable, are most widely used techniques for

simulating the kinetics of the composting process (Abu Qdais and Al-Widyan, 2016). The decomposition rate during composting can be described using a zero-order (Ebrahimzadeh et al., 2017) (Eq. 3), first-order (Abu Qdais and Al-Widyan, 2016) (Eq. 4), second-order (Ezemagu et al., 2021) (Eq. 5) and n-order differential equations (Ebrahimzadeh et al., 2017; Ugak et al., 2022) (Eq. 6):

$$\frac{dOM}{dt} = -k \cdot OM^0 \tag{3}$$

$$\frac{dOM}{dt} = -k \cdot OM^1 \tag{4}$$

$$\frac{dOM}{dt} = -k \cdot OM^2 \tag{5}$$

$$\frac{dOM}{dt} = -k \cdot OM^n \tag{6}$$

where *OM* is an amount of biodegradable solids (%) at time *t* (day) of composting process, *k* is degradation rate (1/day) and *n* is exponent in defining reaction order.

2.6.2. Optimization of composting process

In order to achieve the maximum efficiency of the composting process and to obtain a high quality compost, all the mentioned variables and their interactions must be considered and the working conditions must be optimized. Optimization is very important to ensure good quality of the final product by performing the process under most favorable conditions (Sokač et al., 2022c).

There are several methods used for optimizing the composting process in the literature (Echarrafi et al., 2018). The single-factor optimization method has been used for the composting processes due to its simplicity. On the other hand, this method has the main disadvantage – it ignores the interactions between variables under the investigation. As an alternative, multivariate statistical and mathematical tools such as Response Surface Methods (RSMs) coupled with design of experiments (DOEs), have been developed. This method examines the response of several variables at once, which is the main advantage (Sokač Cvetnić et al., 2024). The application of RSM includes several stages: screening of independent process variables and their ranges, selection of experimental design and performance of real experiments, generation of regression model equations, verification of model adequacy, graphical

representation of obtained model and determination of optimal process conditions (Brzezińska et al., 2023).

Response Surface Methods coupled with design of experiments have been applied for the optimization of composting processes. Asadu et al. (2019) used the central composite design and RSM for the optimization of composting process of sawdust, sewage sludge and vegetable wastes. They optimized the variables such as composting time, moisture content and dosage ratio on the response factors (nitrogen, phosphorus and potassium content). Sharma et al. (2018) investigated the composting process of flower waste, cow dung and sawdust and they used the central composite design to evaluate the proportion of waste. After the performance of experiments and analysis of physicochemical variables, the response surface methodology was applied for the optimization of combinations of flower waste, cow dung and sawdust.

3. MATERIALS AND METHODS

3.1. Materials

3.1.1. Grape skin

The skin of the white grape pomace, *Vitis vinifera* cv. Graševina, harvested in 2021 (Kutjevo, Croatia), was used as a raw material for composting and extraction processes. The grape pomace was stored in a freezer at -18 °C. Before performing the experiments, the seeds and stalks were separated from the skins by sieving, and the grape skins were left at room temperature overnight. The physicochemical properties of the grape skin are shown in Table 8.

Table 8. Physicochemical properties of grape skins used in composting processes

Physicochemical variables	Value
Moisture content (%)	65.07
Dry matter content (%)	34.93
pH (-)	4.60
C/N (-)	32.16
Polyphenol content (g/g DM)	4.21

3.1.2. Chemicals

The sodium hydrogencarbonate was purchased from Kemika (Zagreb, Croatia), and the urea was from Gram-Mol (Zagreb, Croatia). Sodium chloride was purchased from Sigma Aldrich (St. Louis, Missouri, USA). The incubation media for the isolation of fungi was Sabouraud dextrose agar purchased from Liofilchem (Roseto degli Abruzzi, Italy), and for the isolation of bacteria, tryptic glucose yeast agar was purchased from Biolife Italiana (Monza, Italy).

Quartz sand, iron (II) cloride hexahydrate, and sodium acetate trihydrate were purchased from Gram-Mol (Zagreb, Croatia). Folin-Ciocalteu reagent was purchased from Kemika d.d. (Zagreb, Croatia), and gallic acid was purchased from Acros Organics (Geel, Belgium). 2,2-diphenyl-1-picrylhydrazyl (DPPH), 6-hydroxy-2,5,7,8-tetramethylchromane-2-carboxylic acid (Trolox), iron (II) sulfate heptahydrate, and 2,4,6-Tris(2-pyridyl)-s-triazine (TPTZ) were purchased from Sigma-Aldrich (Burlington, USA). Methanol was purchased from VWR Chemicals BDH (Lutterworth, United Kingdom). Acetic acid was purchased from T.T.T. (Sveta Nedjelja, Croatia), and hydrochloric acid was purchased from Fisher Chemical (Pittsburg, SAD).

3.1.3. Equipment

During this research the following equipment was used: analytical balance (Sartorius TE214-S0CE, Göttingen, Germany), desiccator (Normax, Marinha Grande, Portugal), colorimeter (PCE-CSM3, PCE Instruments, Meschede, Germany), conductometer (SevenCompact, MettlerToledo, Greifensee, Switzerland), laboratory dryer (ST60T, InkoLab, Zagreb, Croatia), muffle oven (B410, Nabertherm, Lilienthal, Germany), pH meter (914, Metrohm, Herisau, Switzerland), thermometer (WT-1, Chemland, Stargard, Poland), oil bath with stirer (HBR 4 digital, IKA-Werke, Staufen, Germany), NIR spectrometer (NIR-128-1.7-USB/6.25/50 μm, Control Development inc., Nashua, USA), NIR spectrometer (AvaSpec-NIR256-2.5-HSC-EVO, Avantes, Lafayette, USA), portable NIR spectrometer (NIR-S-G1, InnoSpectra, Hsinchu, Taiwan), portable NIR spectrometer (NIR-M-R2, InnoSpectra, Hsinchu, Taiwan), spectrophotometer (Libra S11, Biochrom, Holliston, SAD), magnetic stirrer with heating (Sb 162-3, Stuart, Chelmsford, United Kingdom), thermostat (561-08/2, InkoLab, Zagreb, Croatia), vortex (MS2, IKA-Werke, Staufen, Germany), water bath for cell culture media (WNB 14, Memmert, Schwabach, Germany), autoclave (AV 300 ART, InkoLab, Zagreb, Croatia), shaker (685/2, Lab Medical, Loos, France), mill (Tube Mill control, IKA-Werke, Staufen, Germany), air pumps (Oxyboost 300 Plus, Aquael, Dubovo Drugie, Poland), flowmeter (1-800-323-4340, Cole-Parmer, Vernon Hills, USA), laboratory reactors (own production), volumeter (own production), elemental analyzer (Leco CNS 2000, Leco instruments, St. Joseph, USA) with a spectrophotometer (LaboMed UV-VIS, Los Angeles, CA, USA).

3.1.4. Software

During this research the following software were used: Microsoft Excel 2010 (Microsoft Corporation, Redmond, USA), Unscrambler X 10.1 (CAMO AS, Oslo, Norway), Statistica 14.0 (TIBCO® Statistica, Palo Alto, USA) and WR Mathematica 10.0 (Wolfram, Champaign, USA). The NIR spectra were analyzed using the software: Control Development Spec 32 (Control Development inc., South Bend, USA), AvaSoft (Avantes, Lafayette, USA) and ISC-NIRScan (InnoSpectra, Hsinchu City, Taiwan).

3.2. Methods

3.2.1. The effect of initial moisture content and air flow rate on the efficiency of the composting process

As mentioned in theoretical background, moisture content and air flow rate are important variables for the composting process due to their impact on microbial activity and finally, on the rate of degradation. In order to investigate the optimal conditions, nine composting processes of grape skin were performed in laboratory reactors under different conditions of initial moisture content of substrate (50-65%) and air flow rate (0.35-2.00 L/min). The conditions of performed composting process are shown in Table 9.

Table 9. Experimental conditions for grape skin composting process according to full-factorial experimental design

Experiment	Moisture content (%)	Air flow rate (L/min)
1.	50	0.50
2.	50	1.25
3.	65	0.88
4.	65	1.40
5.	65	0.35
6.	50	2.00
7.	57.5	1.70
8.	57.5	0.43
9.	57.5	1.06

Except moisture content, another important variable for microbial activity is the pH value. As presented in Table 8, the pH of grape skin is in acidic range (around 4.60) and with that values it is unacceptable for performing composting process, because the optimal pH value for the process is 5.5-8. According to Yu and Huang (2009) the pH value can be adjusted using the sodium hydrogencarbonate solution. In this purpose, 10% sodium hydrogencarbonate solution was prepared and added to the grape skin to adjust the pH value and consequently the moisture content.

The composting processes of grape skin ($m = 1.9$ kg) were performed in laboratory batch reactors in a total volume of $V = 5$ L. The dimensions of the reactors were: diameter, $d = 16$ cm and the height, $h = 25$ cm. The reactors were isolated with a wall thickness of 5 cm. During the

30 days of the composting processes, the reactors were aerated with a constant air flow rate to ensure aerobic conditions during the process. Also, during the 30 days, processes were monitored through physicochemical and microbiological properties. The sheme of reactor system is shown in Figure 12.
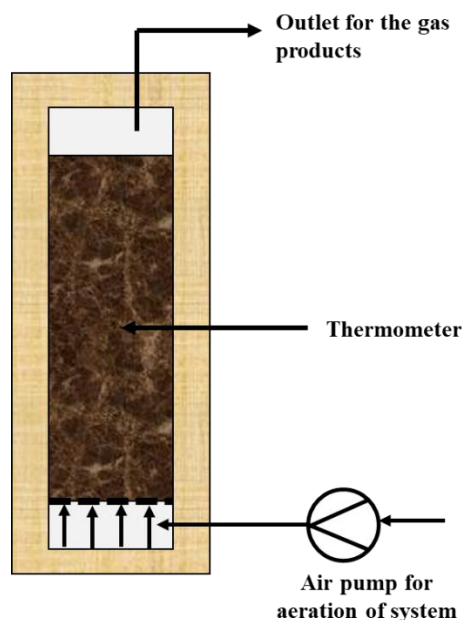
Figure 12. Scheme of reactor for the composting processes

3.2.2. Extraction of bioactive molecules from grape skins

The prepared extraction mixture (water:grape skin in appropiate solid-liquid ratio) was thermostated at a defined temperature in an oil bath (IKA-Werk GmbH & Co. KG, Staufen, Germany) at a certain mixing speed for a given time (Jurinjak Tušek et al., 2018). The extraction experiments were performed according to the conditions defined by the Box–Behnken experimental design (Table 10). The effects of extraction time (t = 60, 75 and 90 min), extraction temperature (T = 40, 60 and 80°C), solid–liquid phase ratio (S/L = 10, 20 and 30 g/L) and mixing speed (rpm = 250, 500 and 750 1/min) on the proportion of polyphenols in the extracts were tested. The independent variable scales were selected based on data concerning bioactive extraction conditions for grape residues obtained from the available literature (Bucić-Kojić et al., 2007; Librán et al., 2013; Chañi-Paucar et al., 2021). After extraction, the sample was filtered through a 100% cellulose paper filter (pore size d = 5–13 μm, LLG Labware, Meckenheim, Germany) to separate the aqueous extract from the solid phase. The physical and chemical properties of the extracts were then determined.

Table 10. The defined extraction conditions by Box-Behnken experimental design

Experiment	t (min)	T (ºC)	S/L (g/L)	Mixing speed (1/min)
1.	60	40	20	500
2.	90	40	20	500
3.	60	80	20	500
4.	90	80	20	500
5.	75	60	10	250
6.	75	60	30	250
7.	75	60	10	750
8.	75	60	30	750
9.	75	60	20	500
10.	60	60	20	250
11.	90	60	20	250
12.	60	60	20	750
13.	90	60	20	750
14.	75	40	10	500
15.	75	80	10	500
16.	75	40	30	500
17.	75	80	30	500
18.	75	60	20	500
19.	60	60	10	500
20.	90	60	10	500
21.	60	60	30	500
22.	90	60	30	500
23.	75	40	20	250
24.	75	80	20	250
25.	75	40	20	750
26.	75	80	20	750
27.	75	60	20	500
28.	75	60	20	500
29.	75	60	20	500
30.	75	60	20	500

3.2.3. The effect of different pretreatment of grape skins on the efficiency of the composting process

Besides the initial moisture content of grape skin and air flow rate, the different pretreatment of grape skins on the efficiency of the composting process was also investigated. The pretreatments included the extraction of bioactive molecules from grape skin and grinding. The extraction was performed under the appropiate conditions using the water as a solvent, and the grinding was performed using the mill (Tube Mill control, IKA-Werke, Staufen, Germany) at mixing speed *rpm* = 15000 1/min for t = 5 minutes.

The five composting processes were carried out:

1. Grape skin without pretreatment;
2. Ground grape skin without pretreatment;
3. Grape skin pretreated to extract bioactive molecules at T = 40°C during the t = 90 minutes;
4. Ground grape skin pretreated to extract bioactive molecules at T = 40 °C during the t = 90 minutes;
5. The mixture of grape skin consisted of: grape skin without pretreatment (w/w = 43.93 %), ground grape skin without pretreatment (w/w = 8.11 %), grape skin pretreated to extract bioactive molecules at T = 40 °C during the t = 90 minutes (w/w = 14.25 %) and ground grape skin pretreated to extract bioactive molecules at T = 40 °C during the t = 90 minutes (w/w = 33.66 %).

The pH level was adjusted using 10% sodium hydrogencarbonate solution (Section 3.2.1.). The composting processes of grape skin were performed in laboratory batch reactors as described in Section 3.2.1. During the 30 days of the composting processes, the reactors were aerated with a constant air flow rate (q = 2 L/min) to ensure the aerobic conditions, and the physicochemical and microbiological properties of grape skin compost and compost extracts were monitored.

3.2.4. Physicochemical and microbiological properties of compost samples and compost extract samples during the analysis of the effect of initial moisture content of grape skin and air flow rate and the pretreatment of grape skins on the efficiency of the composting process

3.2.4.1. Moisture and dry matter content of compost samples

The moisture and dry matter content were determined by drying the samples for $t = 24$ hours at $T = 105$ °C in a dryer (Inkolab ST60T, Zagreb, Croatia) (Chan et al., 2016). A certain mass of the sample ($m = 2$ g $\pm$ 0.001 g) was weighed into metal containers and after drying the containers were placed in a desiccator where they were cooled at room temperature. The difference between the mass before and after drying is the proportion of moisture content. Measurements were performed with three repetitions, and the results are presented as mean value $\pm$ standard deviation.

3.2.4.2. Total organic matter and ash content of compost samples

Total organic matter and ash content were determined by heating the samples after drying at $T = 550$ °C for $t = 5$ hours in a muffle oven (B410, Nabertherm, Njemačka). The percentage of loss of volatile substances was expressed as a share of total organic matter (Diaz et al., 2002), while the mass remaining after burning was expressed as the ash fraction (Waqas et al., 2018). Measurements were performed with three repetitions, and the results are presented as mean value $\pm$ standard deviation.

3.2.4.3. Carbon and nitrogen content and C/N ratio of compost samples

Total carbon and nitrogen content were determined by elemental analyzer (Leco CNS 2000, Leco instruments, St. Joseph, USA) with a spectrophotometer (LaboMed UV-VIS, Los Angeles, CA, USA) according to the method described by Lovreškov et al. (2022). The compost samples were burnt in elemental analyzer at $T = 1350$ °C in the oxygen presence. During the oxidation, nitrogen oxides are produced and transformed to molecular nitrogen which amount is determined based on thermal conductivity. The carbon and nitrogen content are expressed as mass percentage $\pm$ standard deviation. From the obtained values of carbon and nitrogen content, the C/N ratio was calculated.

3.2.4.4. pH, conductivity and total dissolved solids of compost samples

In order to perform pH, conductivity and total dissolved solids measurements, compost exctract samples were prepared. The extracts of compost samples were obtained by mixing the compost and distilled water in ratio 1:10 (w/v) and the extraction was carried out on a magnetic stirrer at $rpm = 150$ 1/min for $t = 1$ hour. After the extraction, the mixture was filtered (Waqas

et al., 2018). In the filtrate, the pH value was determined using a pH meter (914, Metrohm, Switzerland) and conductivity and total dissolved solids using conductometer (SevenCompact, MettlerToledo, Switzerland). Measurements were performed with three repetitions and the results are presented as mean value ± standard deviation.

3.2.4.5. Color change of the compost samples and compost extracts

The color of all composts and compost extracts was determined using a PCE-CSM3 colorimeter (PCE Instruments, Germany). The total colour change of the compost and corresponding compost extracts (ΔE) was determined according to the Eq.7:

$$\Delta E = \sqrt{(L^* - L_0^*)^2 + (a^* - a_0^*)^2 + (b^* - b_0^*)^2} \tag{7}$$

where L_0, a_0, and b_0 are the values of the Hunter coordinates of the samples/extracts of the initial substrate samples, and L, a and b are the values of the Hunter coordinates of the compost/compost extracts during the composting process. Measurements were performed with three repetitions and the results are presented as mean value ± standard deviation.

3.2.4.6. Microbiological analysis of the composting process

The viable count of the bacteria and fungi during the composting process was determined as described by (Sokač et al., 2022b) with some modification. Microorganisms were monitored every $t = 96$ hours. Mass of $m = 5$ g of milled compost sample was added to $V = 100$ mL of sterile saline solution and the suspension was mixed on a shaker at $rpm = 100$ 1/min (685/2, Nahita, Blue, France) for 1 hour. After the extraction time, the suspension was filtered through 100% cellulose filter paper (pore size $d = 5$–13µm, LLG Labware, Meckenheim, Germany) to separate the aqueous extract from the solid phase. The filtrate was used to prepare the appropriate decimal dilution. The viable plate count was determined by inoculation $V = 1$ mL of dilution on a media for growth bacteria or fungi. The Petri dishes were incubated in thermostat (561-08/2, InkoLab, Hrvatska) at $T = 28$ °C for fungi and at $T = 37$ °C for bacteria for 5 days. The results were expressed as CFU/g of dry matter.

3.2.4.7. Analysis of seed germination index (GI)

The germination test was performed during five days with salad seeds as described by Hashemi et al. (2019). Firstly, the compost extracts were prepared by adding $m = 1$ g of grape skin compost and $V = 10$ mL of distilled water and mixed at mixing speed $rpm = 150$ 1/min on a magnetic stirrer for an hour. After the extraction, the mixture was filtered through a 100%

cellulose paper filter (pore size d = 5–13 μm, LLG Labware, Meckenheim, Germany) to separate the extract from solid phase.

Furthermore, filter papers were placed in Petri dishes with V = 5 mL of compost extracts and one set was prepared with distilled water as a control. Twenty salad seeds were distributed to each set and incubated at T = 25 °C for five days. The number of germinating seeds and the root elongation for the samples were measured every four days until the end of the composting process. Finally, the GI was calculated using Eq.8:

$$GI = \frac{G_S \cdot L_S}{G_C \cdot L_C} \cdot 100 \qquad (8)$$

where G_S is the seed germination (%) and L_S is the root elongation (mm) for the compost sample and G_C and L_C correspond to control values (Hashemi et al., 2019; Kong et al., 2022). Measurements were performed with three repetitions and the results are presented as mean value ± standard deviation.

3.2.4.8. Bulk density and porosity of the final compost samples

Bulk density of a final compost sample was determined according to a method described by Buljat et al. (2019). Volumeter works on a principle of compressing the material by vibrations which cause squeeze the air between the particles and as the consequence, the volume decreases and bulk density increases. The final compost sample was poured in a graduated plastic container of predetermined tare weight, and the mass and volume of compost sample were recorded. Analysis was done in triplicate and the results are expressed as mean value ± standard deviation.

Compost porosity (ε) was determined using the known density of water (ρ_w = 1000 kg/m^3) and estimated densities of organic matter (ρ_{OM} = 1600 kg/m^3) and ash (ρ_{ash} = 2500 kg/m^3). If the moisture content (MC), dry matter (DM), organic matter (OM) and wet bulk density (ρ_{wb}) of the samples are known, the porosity can be calculated using the following equation (Eq.9) (Khater, 2015):

$$\varepsilon\,(\%) = 1 - \rho_{wb} \left[\frac{MC}{\rho_w} + \frac{DM \cdot OM}{\rho_{OM}} + \frac{DM \cdot (1-OM)}{\rho_{ash}} \right] \cdot 100 \qquad (9)$$

The moisture content, dry matter and organic matter content should be expressed as decimal numbers.

3.2.5. Physicochemical properties of grape skin aqueous extracts

3.2.5.1. pH, conductivity and total dissolved solids of extracts

The pH value of the extracts was determined using a pH meter (914, Metrohm, Switzerland). Conductivity and total dissolved solids of extracts were determined using conductometer (SevenCompact, MettlerToledo, Switzerland). Measurements were performed with three repetitions and the results are presented as mean value ± standard deviation.

3.2.5.2. Dry matter content of extracts

The total dry matter of grape skin extracts was determined using the standardized drying method at 105 °C (AOAC, 1995). The quartz sand was placed into a metal container to cover the bottom and the sand was dried at temperature $T = 105$ °C for $t = 1$ hour. After drying, the containers were placed to desiccator and after cooling at room temperature were weighed. Then, around 3 mL of grape skin extract was added to the container with sand, weighed and dried at $T = 105$ °C for 4 hours. After drying the samples, the containers were cooled at room temperature in desiccator and weighed again. Measurements were performed in duplicate and the results are presented as mean value ± standard deviation.

The moisture content (MC) in samples can be calculated from the mass loss (Eq.10):

$$MC = \frac{(A-B)}{m} \cdot 100 \qquad (10)$$

where *A* is the mass of container with the sample before drying (g), *B* is the mass of container with the sample after drying (g) and m is mass of the sample (g).

The dry matter content (DM) of samples was calculated using the Eq.11:

$$DM = 100 - MC \qquad (11)$$

3.2.5.3. Color of the extracts

The color of all extracts was determined using a PCE-CSM3 colorimeter (PCE Instruments, Germany). The total colour change of the extracts (ΔE) was determined according to the Eq.3. Measurements were performed with three repetitions and the results are presented as mean value ± standard deviation.

3.2.5.4. Total phenolic content

The total polyphenols content (TPC) in the grape skins extract were determined spectrophotometrically, according to Singleton et al. (1999), based on the colorimetric reaction of phenol with the Folin-Ciocalteu reagent. The Folin-Ciocalteu chemical process stresses in

redox reactions, accomplished by electron transfer from phenolic groups to phosphomolybdic and phosphotungstic acid compounds in an alkaline medium. Sodim carbonate is the alkali that extents an optimum pH for this reaction. During the reaction, phenolate ion groups are oxidized leading to the reduction of the acidic components in the FC reagent. The reacting acids change from an initial light yellow to a blue color (reduced state) of different intensity based on the number of reacting phenolic groups (Carmona-Hernandez et al., 2021).

Briefly, $V = 7.9$ mL of distilled water was mixed with $V = 500$ µL of Folin–Ciocalteu reagent (Folin–Ciocalteu reagent: water at ratio 1:2) and $V = 100$ µL sample. The reaction was started with addition of $V = 1.5$ mL of 20% Na_2CO_3 solution. After $t = 2$ h of incubation in a dark place, the absorbance of the reaction mixture was measured at $\lambda = 765$ nm using spectrophotometer (Biochrom Libra S11, Cambridge, UK). The polyphenol content was determined using a calibration curve for gallic acid presented in Supplementary (8.1.) and the results were expressed as mg GA equivalents (GAE)/g dry matter (DM). Measurements were performed in duplicates and the results are presented as mean value ± standard deviation.

3.2.5.5. Determination of antioxidant activity by DPPH method

In order to evaluate the antioxidative activity of specific compounds or extracts, the latter are allowed to react with a stable radical, 2,2-diphenyil-picrylhydrazyl (DPPH) in a methanol solution. The reduction of DPPH is followed by monitoring the decrease in its absorbance at a characteristic wavelength during the reaction. In its radical form, DPPH absorbs at 515 nm, but upon reduction by an antioxidant or a radical species, the absorption disappears (Brand-Williams et al., 1995).

The reaction mixture consisted of $V = 100$ µL of extract sample and $V = 3.9$ mL of DPPH radical ($c = 0.094$ mmol/L) dissolved in methanol. The mixture was homogenized and after 30 min of incubation, the absorbance of the reaction mixture was measured at $\lambda = 515$ nm. The results were derived from a calibration curve presented in Supplementary (8.2.) and they are expressed as mmol Trolox equivalents/g dry matter (DM). Measurements were performed in duplicate and the results are presented as mean value ± standard deviation.

3.2.5.6. Determination of antioxidant activity by FRAP method

The FRAP (Ferric ion reducing antioxidant power) method was carried out according to Benzie and Strain (1996). The method is based on the reduction of iron (III) tripyridyltriazine (Fe^{3+}-TPTZ) complex to ferrous form (Fe^{2+}), an intense blue color with an absorption maximum at 593 nm.

Firstly, the FRAP reagent was prepared and it consisted of $V = 25$ mL of the acetate buffer ($c = 300$ mmol/L), $V = 2.5$ mL TPTZ solution ($c = 10$ mmol/L) and $V = 2.5$ mL iron (II) cloride hexahidrate solution ($c = 20$ mmol/L). The reaction mixture consisted of $V = 50$ µL and $V = 950$ µL FRAP reagent and after the incubation for $t = 4$ minutes the apsorbance was measured at $\lambda = 593$ nm. The antioxidant capacity was calculated from the calibration curve (presented in Supplementary 8.3.) and the results were expressed as mmol $FeSO_4 \cdot 7H_2O$ equivalents per g dry matter plant material. Measurements were performed in duplicates and the results are presented as mean value ± standard deviation.

3.2.6. NIR spectroscopy

For all compost samples and compost extract samples obtained during composting proceses, NIR spectra were recorded using the different NIR instruments:

1. NIR spectrometer (NIR-128-1.7-USB/6.25/50 µm, Control Development Inc., USA) which records the absorbance in wavelength range from $\lambda = 904$ - 1699 nm for all samples. The spectra were analyzed using the software Control Development Spec 32 (Control Development Inc., USA);
2. NIR spectrometer (AvaSpec-NIR256-2.5-HSC-EVO, Avantes, USA) which records the absorbance in wavelength range from $\lambda = 1000$ - 2500 nm for all samples. The spectra were analyzed using the software AvaSoft (Avantes, USA);
3. Portable NIR spectrometer (NIR-S-G1, InnoSpectra, Taiwan) which records absorbance in wavelength range from $\lambda = 900$ - 1700 nm for compost samples obtained by composting processes with different pretreatment of grape skin. The spectra were analyzed using the software ISC-NIRScan (InnoSpectra, Taiwan);
4. Portable NIR spectrometer (NIR-M-R2, InnoSpectra, Taiwan) which records absorbance in wavelength range from $\lambda = 900$ - 1700 nm for compost extracts samples obtained by composting processes with different pretreatment of grape skin and grape skin extracts obtained by extractions under different conditions. The spectra were analyzed using the software ISC-NIRScan (InnoSpectra, Taiwan).

For the recording of the NIR spectra of compost samples and compost extract samples obtained in the first set of composting processes (where has been investigated the effect of initial moisture content of grape skin and air flow rate on the efficiency of the composting), the NIR spectrometer (NIR-128-1.7-USB/6.25/50 µm, Control Development Inc., USA) and NIR

spectrometer (AvaSpec-NIR256-2.5-HSC-EVO, Avantes, USA) were used. And, in the another set of composting experiments (where different pretreatments of grape skin on the efficiency of the composting were investigated), the four NIR spectrometers were used. The spectra for all samples were recorded using the mentioned above NIR instruments in five repetitions.

3.2.7. Statistical analysis and mathematical modelling

3.2.7.1. Basic statistical analysis

All the measurements of the physicochemical properties of compost samples and their extracts, and the physicochemical properties of prepared grape skin extracts in this work were performed in triplicates and a basic statistical analysis (mean values and standard deviation) was performed using the Statistica 14.0 software package (TIBCO® Statistica, Palo Alto, CA, USA). The correlations or associations between the physicochemical properties of the compost samples, and the correlations between physicochemical properties of grape skin extracts and the extraction conditions were analyzed using Principal Component Analysis (PCA) in the Statistica 14.0 software package. In addition, the mean values of the compost properties and grape skin extracts properties were compared using analysis of variance (ANOVA) in the Statistica 14.0 software package, and Tukey's test was used to compare significant differences ($p < 0.05$) between the physicochemical properties of the compost samples.

3.2.7.2. Optimization of initial moisture content of grape skin and air flow rate for the performance improvement of composting process

In order to achieve a high efficiency of the process and to obtain a stabilized compost, it is necessary to optimize process conditions which play an important role in the composting process performance (Iqbal et al., 2015). As mentioned before, composting is a complex process including numerous related physical, chemical and biological phenomena that are non-linear (Iqbal et al., 2015; Sokač et al., 2022c).

In this research, the response surface methodology (RSM) was used for the optimization of initial moisture content of grape skin and air flow rate for the composting process. The relationship between initial moisture content (X_1), air flow rate (X_2) and compost organic matter amount (Y) after 30 days of composting was analyzed. Second-order polynomial equation (Eq.12) was used to fit the experimental data:

$$Y = \beta_0 + \beta_1 \cdot X_1 + \beta_2 \cdot X_2 + \beta_{11} \cdot X_1^2 + \beta_{22} \cdot X_2^2 + \beta_{12} \cdot X_1 \cdot X_2 \qquad (12)$$

where Y is the predicted response, β_0 is the constant, β_1 and β_2 are the linear coefficients, β_{11} and β_{22} are quadratic coefficients, and β_{12} are the cross-product coefficients. Response surface

methodology was performed using Statistica 14.0 software package (TIBCO® Statistica, Palo Alto, USA).

3.2.7.3. Optimization of conditions for extraction of bioactive molecules from grape skin

The effects of four independent variables (extraction time (X_1), extraction temperature (X_2), solid–liquid ratio (X_3), and mixing speed (X_4)) were evaluated using a Box–Behnken design implemented in the Statistica 14.0 software package. The simultaneous optimization of three chemical properties (TPC, antioxidant activity determined by DPPH and FRAP method) of the aqueous grape skin extracts was performed. The effect of each parameter was analyzed at three levels (−1, 0, 1), and according to the experimental design, 30 experiments were performed randomly (Table 10). Second-order polynomial equations were used to fit the experimental data. Response surface modeling was performed using the Statistica 14.0 software package (TIBCO® Statistica, Palo Alto, CA, USA). The optimal extraction conditions were estimated based on the proposed RSM models.

3.2.7.4. Kinetics of organic matter degradation and microbial growth

The first-order kinetics is the most widely used equation for the description of the aerobic degradation of organic substrate and it is followed by the degradation of organic matter as a function of time (Eq.13) (Sangamithirai et al., 2015; Kulcu, 2016; Malamis et al., 2016):

$$\frac{dOM}{dt} = -k \cdot OM \tag{13}$$

where *OM* is an amount of biodegradable solids (%) at time *t* (day) of composting process and *k* is degradation rate (1/day).

The bacterial growth rate was also expressed as a function of time following the first order kinetic (Eq.14):

$$\frac{dX_{\text{bacteria}}}{dt} = \mu_{bacteria} \cdot X_{\text{bacteria}} \tag{14}$$

where X_{bacteria} is number of bacterial cells (logCFU/g_{DM}) at time *t* (day) of composting process and μ_b is specific bacterial growth rate (1/day). The fungal growth rate was expressed as a function of time following the logistic growth model of Verhulst-Pearl (Eq.15) (Robles-Morales et al., 2021):

$$\frac{dX_{\text{fungi}}}{dt} = \mu_{\text{fungi}} \cdot \left(1 - \frac{X_{\text{fungi}}}{X_{\text{max}}}\right) \cdot X_{\text{fungi}} \tag{15}$$

where X_{fungi} is number of fungal cells ($logCFU/g_{DM.}$) at time t (day) of composting process, μ_{fungi} is specific fungal growth rate (1/day) and X_{max} maximum level of fungal biomass.

Kinetic parameters were estimated by fitting the experimental data directly to the differential equation using the Parametric NDSolve algorithm implemented in WR Mathematica 10.0. The goodness of fit of the developed models was assessed using the Root Mean Square Value (RMSE), the Reduced Chi-square Value (χ^2) and modelling efficiency (EF) (Eq. 16-18) :

$$RMSE = \sqrt{\sum_{i=1}^{n} \frac{\left(OM_{pred,i} - OM_{exp,i}\right)^2}{N}} \tag{16}$$

$$\chi^2 = \frac{\sum_{i=1}^{N}\left(OM_{exp,i} - OM_{pred,i}\right)^2}{N-n} \tag{17}$$

$$EF = \frac{\sum_{i=1}^{n}\left(OM_{exp,i} - OM_{exp,mean}\right)^2 - \sum_{i=1}^{n}\left(OM_{pred,i} - OM_{exp,i}\right)^2}{\sum_{i=1}^{n}\left(OM_{exp,i} - OM_{exp,mean}\right)^2} \tag{18}$$

where OM_{exp} is the experimental organic matter amount, $OM_{exp,mean}$ is the mean value of the experimental organic matter amount, the OM_{pred} kinetic model predicts the organic matter amount, N is the number of experimental data points and n is the number of model parameters.

3.2.7.5. Multiple linear regression modelling (MLR), piecewise linear regression (PLR) modelling and artificial neural network (ANN) modelling for prediction of physicochemical properties of compost samples

It was assumed that the measured physicochemical properties of the compost samples ($i = 1, \ldots, 12$: moisture content (Y_1), dry matter content (Y_2), organic matter content (Y_3), ash content (Y_4), carbon content (Y_5), nitrogen content (Y_6), C/N ratio (Y_7), total color change of compost samples (Y_8), pH (Y_9), total dissolved solids (Y_{10}), conductivity (Y_{11}) and total color change of compost extract samples (Y_{12})) gathered through 9 independent experiments can be described as a function of initial moisture content (X_1), air flow (X_2) and sampling day (X_3) according to equation 19:

$$Y_i = f\left(X_1, X_2, X_3\right) \tag{19}$$

Multiple linear regression (MLR) (Eq.20), piecewise linear regression (PLR) (Eq.21) and artificial neural network (ANN) models were used to evaluate the relationship between input and output variables.

$$Y_i = b_0 + b_1 \cdot X_1 + b_2 \cdot X_2 + b_3 \cdot X_3 \tag{20}$$

$$Y_i = (b_{01} + b_{11} \cdot X_1 + b_{21} \cdot X_2 + b_{31} \cdot X_3) \ (for \ Y_i \leq b_n)$$
$$+(b_{02} + b_{12} \cdot X_1 + b_{22} \cdot X_2 + b_{32} \cdot X_3) \ (for \ Y_i > b_n) \qquad (21)$$

The MLR model parameters (Eq.20) and PLR model parameters (Eq.21) were calculated using the Levenberg-Marquardt algorithm implemented in Statistica 14.0 (Tibco Software Inc, Palo Alto, USA). Using the least squares method, the programme searches for optimal solutions in the parameter space of the function. The calculations were repeated 50 times with a convergence level of 10^{-6} and a confidence interval of 95% (Jurinjak Tušek et al., 2020). The data set (432 data points for each output variable = 16 sampling days x 3 repetitions x 9 reactors) for MLR and PLR modelling was randomly split into a calibration and a prediction data set (70:30). The applicability of the developed calibration models was estimated using the coefficient of determination for calibration (R_{cal}^2), the adjusted coefficient of determination for calibration ($R_{cal\,adj}^2$), the root mean square error for calibration (*RMSE*) and the F-value of the model. Predictive performance of the models was estimated using the coefficient of determination for prediction (R_{pred}^2), the adjusted coefficient of determination for calibration ($R_{pred\,adj}^2$), the root mean square error of prediction (*RMSEP*), the standard error of prediction (*SEP*), the ratio of prediction to deviation (*RPD*) and the ratio of the error range (*RER*) (Fearn, 2002).

In addition, multilayer perceptron (MLP) ANNs were used to predict physicochemical properties of the compost samples. ANN models were developed separately for each analysed output process variable. The ANN models contained an input layer, a hidden layer and an output layer. The input layer had three neurons representing the conditions of the composting process (moisture content, air flow and day of sampling), the output layer had one neuron (moisture content, dry matter content, organic matter content, ash content, carbon content, nitrogen content, C/N ratio, total colour change of compost samples, pH value, conductivity, total amount of dissolved solids, or total colour change of compost extract samples), and the number of neurons in the hidden layer varied between 4 and 13 and was selected by the algorithm. For the activation functions of the hidden layer and the output layer, the identity, logistic, hyperbolic tangent and exponential activation functions were randomly selected. For ANN modelling, the data set was split 70:30 into a calibration and a prediction data set. In addition, the calibration dataset was split into 70% for network training, 15% for network testing and 15% for model validation. The backpropagation algorithm was used for model training. The applicability of the developed calibration models was estimated using the coefficient of determination for

calibration (R_{cal}^2), the adjusted coefficient of determination for calibration ($R_{cal}{}^2_{adj}$), and the root mean square error for calibration (*RMSE*). Prediction performance of the models was estimated based on coefficient of determination for prediction (R_{pred}^2), the adjusted coefficient of determination for calibration ($R_{pred}{}^2_{adj}$), the root mean square error for prediction (*RMSEP*), the standard error of prediction (*SEP*), the ratio of prediction to deviation (*RPD*) and the ratio of the error range (*RER*) (Fearn, 2002).

3.2.7.6. NIR data pre-processing

The efficiency of the preprocessing methods for NIR spectra on sample grouping was analyzed using the Unscrambler X software (Version 10.1. CAMO AS, Oslo, Norway). The following preprocessing methods were tested:

(i)   raw spectra,

(ii)   smoothing,

(iii)   first-order Savitzky-Golay derivative (SG1D),

(iv)   second-order Savitzky-Golay derivative (SG2D),

(v)   standard normal variate (SNV),

(vi)   multiplicative scatter corrections (MSC),

(vii)   smoothing followed by standard normal variate (smooth+SNV),

(viii) smoothing followed by multiplicative scatter corrections (smooth+MSC),

(ix)   first-order Savitzky-Golay derivative (SG1D) followed by standard normal variate (SG1D+SNV),

(x)   first-order Savitzky-Golay derivative (SG1D) followed by multiplicative scatter corrections (SG1D+MSC),

(xi)   second-order Savitzky-Golay derivative (SG2D) followed by standard normal variate (SG2D+SNV), and

(xii)   second-order Savitzky-Golay derivative (SG2D) followed by multiplicative scatter corrections (SG2D+MSC).

Raw and preprocessed spectra were further used for principal component analysis (PCA). PCA was performed using the software Statistica 14.0. (TIBCO® Sta-istica, Palo Alto, CA, USA).

3.2.7.7. Artificial neural network modelling for prediction of physicochemical and microbiological properties of compost samples and compost extracts based on NIR spectra

Artificial Neural Networks (ANNs) modeling was used for prediction of physicochemical properties of the compost samples and compost extracts (moisture content (Y_1), dry matter content (Y_2), organic matter content (Y_3), ash content (Y_4), carbon content (Y_5), nitrogen content (Y_6), C/N ratio (Y_7), total color change of compost samples (Y_8), pH (Y_9), total dissolved solids (Y_{10}), conductivity (Y_{11}) and total color change of compost extract samples (Y_{12})) and microbiological properties (number of bacteria (Y_{13}), number of fungi (Y_{14}) and total number of microorganisms (Y_{15}) gathered during the 9 independent composting experiments which were carried out under different conditions of initial moisture content of grape skin and air flow rate, and also during the 5 independent composting experiments in which were investigated the different pretreatments of grape skin.

Multiple Layer Perceptron (MLP) ANNs were developed using the software Statistica 14.0. (TIBCO® Statistica, Palo Alto, CA, USA). ANNs consist of three layers: input, hidden, and output. The input layer consisted of 5 neurons that represent the coordinates of the first five factors obtained from PCA analysis. The first five principal components contributed to more than 99.99% of the data variability, and they were selected as the inputs. The number of neurons in the hidden layer varied between 4 and 13 and was randomly selected by the algorithm. The hidden activation function and output activation function were selected randomly from the following set: Identity, Logistic, Hyperbolic tangent, and exponential. For the sake of simplification in the analysis, each of the measured of physicochemical properties of the compost samples was individually tested as an output.

The dimension of the data set for ANNs development describing the 9 experiments was 144 x 17 (144 rows represent total number of gathered compost samples, 5 columns refer to 5 PCA coordinates (factors), and 12 columns represents measured physicochemical properties of the compost samples specifically moisture content, dry matter content, organic matter content, ash content, carbon content, nitrogen content, C/N ratio, total color change of compost samples, pH, total dissolved solids, conductivity, total color change of compost extract samples). The dimension of the data set for ANNs development describing the 5 experiments was 80 x 17 (80 rows represent total number of gathered compost samples, 5 columns refer to 5 PCA coordinates (factors), and 12 columns represents measured physicochemical properties of the compost samples specifically moisture content, dry matter content, organic matter content, ash content,

carbon content, nitrogen content, C/N ratio, total color change of compost samples, pH, total dissolved solids, conductivity and total color change of compost extract samples).

The number of generated networks for each output was set to 2000. Model training was carried out using back error propagation algorithm, and the error function was the sum of squares. For ANN modelling the data set was split 70:30 into a calibration and a prediction data set. In addition, the calibration data set was split into 70% for network training, 15% for network testing and 15% for model validation. The back propagation algorithm was used for model training. The applicability of the developed calibration models was estimated using the coefficient of determination for calibration (R_{cal}^2), the adjusted coefficient of determination for calibration ($R_{cal}{}^2_{adj}$), and the root mean square error for calibration (*RMSE*). Prediction performance of the models was estimated based on coefficient of determination for prediction (R_{pred}^2), the adjusted coefficient of determination for calibration ($R_{pred}{}^2_{adj}$), the root mean square error for prediction (*RMSEP*), the standard error of prediction (*SEP*), the ratio of prediction to deviation (*RPD*) and the ratio of the error range (*RER*) (Fearn, 2002).

4. RESULTS

4.1. Performance of grape skin composting processes under different conditions of initial moisture content of grape skin and air flow rate

In this chapter, the results obtained during grape skin composting processes under the different conditions of initial moisture content annd air flow rate are presented. This chapter includes the physicochemical properties (moisture and dry matter content, organic matter content, ash content, carbon and nitrogen content, C/N ratio, total color change of compost samples, pH, total dissolved solids, conductivity, total color change of compost extract samples) and microbiological properties of compost samples and compost extracts samples, optimization of composting conditions, kinetics of organic matter degradation and microbial growth and multivariate analysis. The NIR spectra recorded with different NIR instruments for all compost samples and compost extracts will be presented. Finally, the artificial neural network models for the prediction of compost characteristics including the different spectra pretretment will be presented too.

4.1.1. Physicochemical and microbiological properties of compost samples and compost extracts during composting processes

To investigate the optimal conditions of initial moisture content and air flow rate, 9 independet composting processes of grape skin were carried out in laboratory reactors under different conditions as shown in Table 9. One of the important variables for the composting process is temperature, and the changes of temperature in reactors during the 30 days of composting are shown in Figure 13.
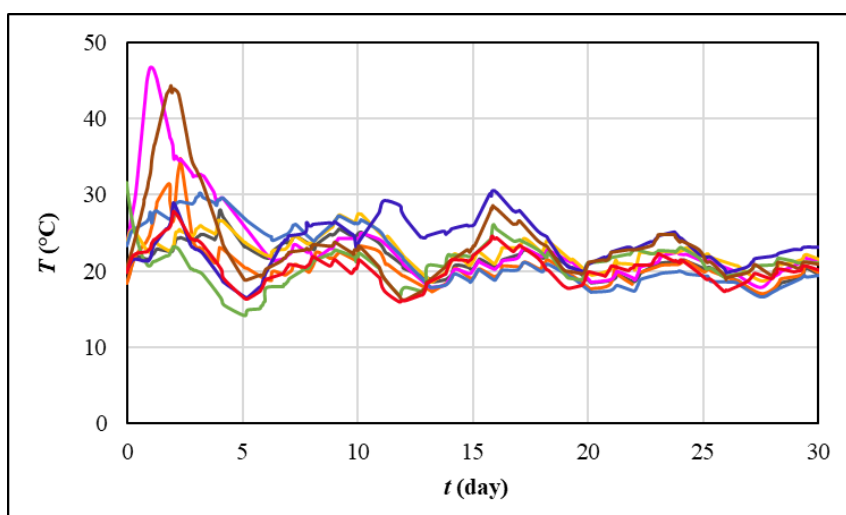
Figure 13. Temperature changes during the 30 days of the grape skin composting process (• experiment 1; • experiment 2; • experiment 3; • experiment 4; • experiment 5; • experiment 6; • experiment 7; • experiment 8; • experiment 9)

Figure 14 presents the apperance of grape skin before composting and after 30 days of the process in reactors. Besides temperature, the processes were monitored through important variables such as moisture and dry matter content, organic matter and ash content, carbon and nitrogen content, C/N ratio, total color change of compost samples, pH value, total dissolved solids (TDS), conductivity (*S*) and total color change of compost extract samples, and the results are shown in Figure 15.

a)　　　　　MC = 50 %　　　　　　MC = 57.5 %　　　　　　MC = 65 %

Exp. 1　　　Exp. 2　　　Exp. 3　　　Exp. 4　　　Exp. 5

b)　Exp. 6　　　Exp. 7　　　Exp. 8　　　Exp. 9
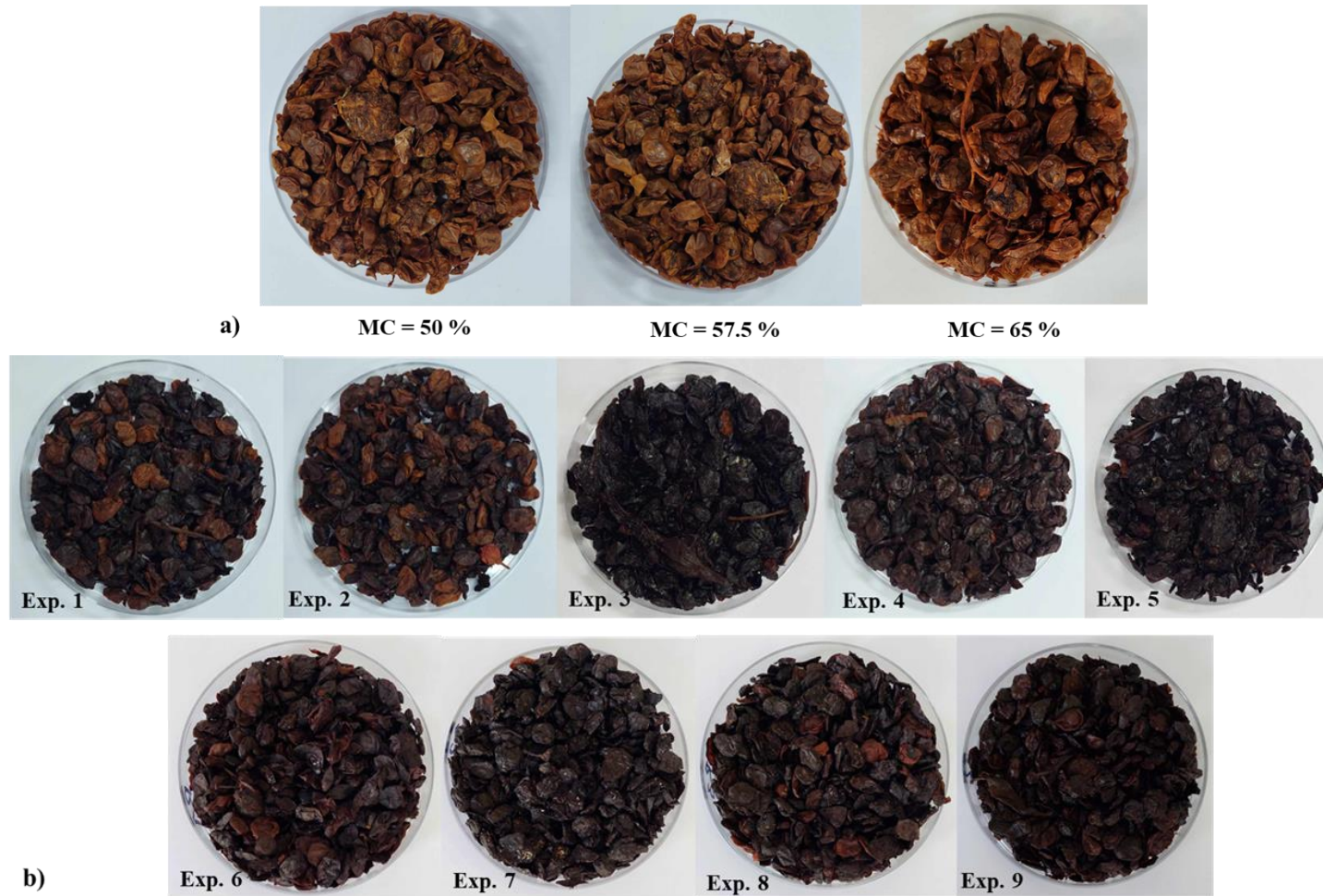
Figure 14. a) Fresh grape skin before composting and b) Grape skin compost after 30 days of composting under different experimental conditions
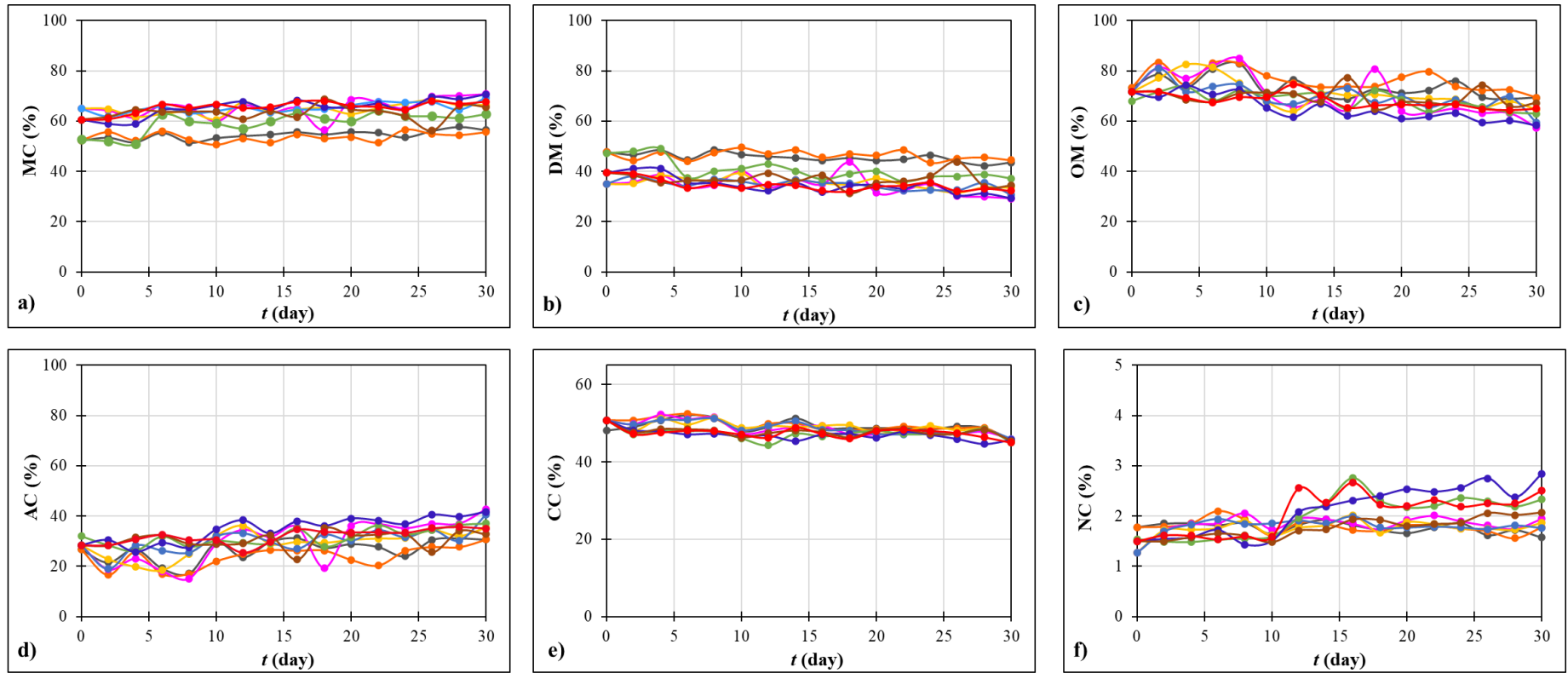
Figure 15. Changes in a) MC; b) DM; c) OM; d) AC; e) CC and f) NC during the 30 days of grape skin composting process (• experiment 1; • experiment 2; • experiment 3; • experiment 4; • experiment 5; • experiment 6; • experiment 7; • experiment 8; • experiment 9) (MC=moisture content; DM=dry matter content; OM= organic matter content; AC= ash content; CC=carbon content; NC= nitrogen content)
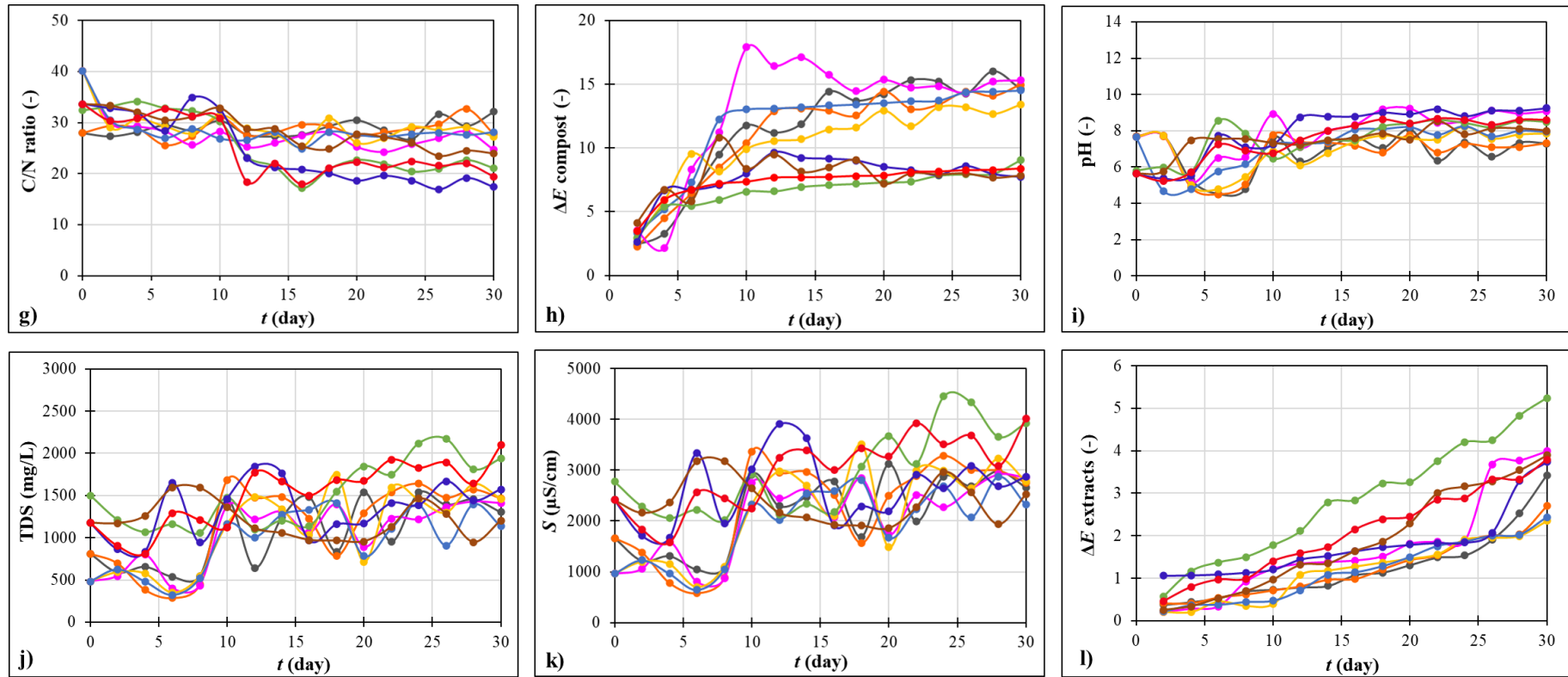
Figure 15. (*continuing)* Changes in g) C/N ratio; h) ΔE compost; i) pH; j) TDS; k) S and l) ΔE extracts during the 30 days of grape skin composting process (• experiment 1; • experiment 2; • experiment 3; • experiment 4; • experiment 5; • experiment 6; • experiment 7; • experiment 8; • experiment 9) (ΔE compost=total color change of compost samples; TDS=total dissolved solids; S=conductivity; ΔE extracts=total color change of compost extracts)

The results of microbiological analysis during the nine composting processes at different conditions are shown in Figure 16. The microbial growth was monitored every 96 hours.
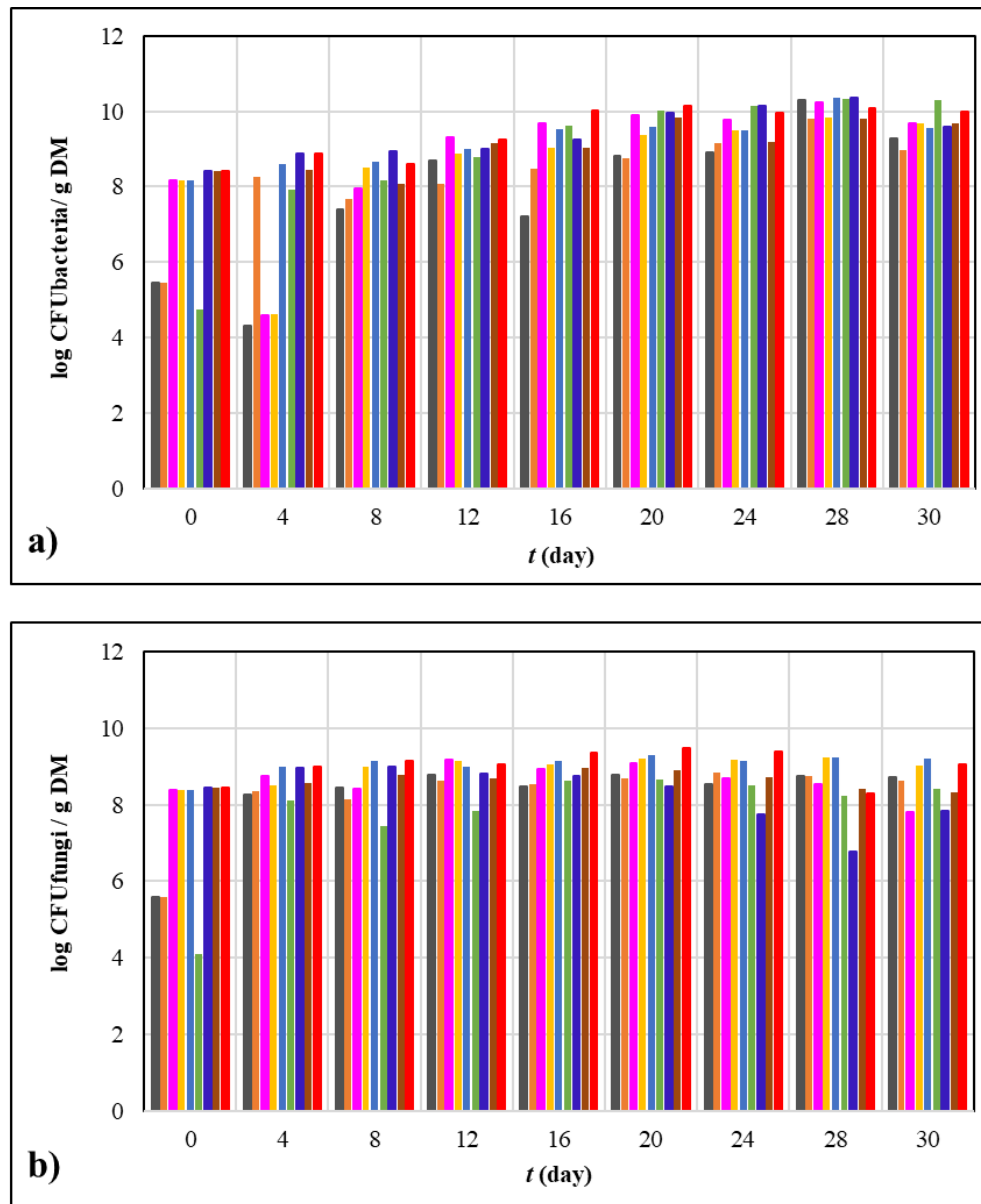
Figure 16. Microbial growth during the 30 days of the grape skin composting process: a) Bacterial growth and b) Growth of fungi (• experiment 1; • experiment 2; • experiment 3; • experiment 4; • experiment 5; • experiment 6; • experiment 7; • experiment 8; • experiment 9)

The changes in germination index in reactors during the 30 days of composting processes are shown in Figure 17, and Figure 18 presents the bulk density and porosity of final composts.
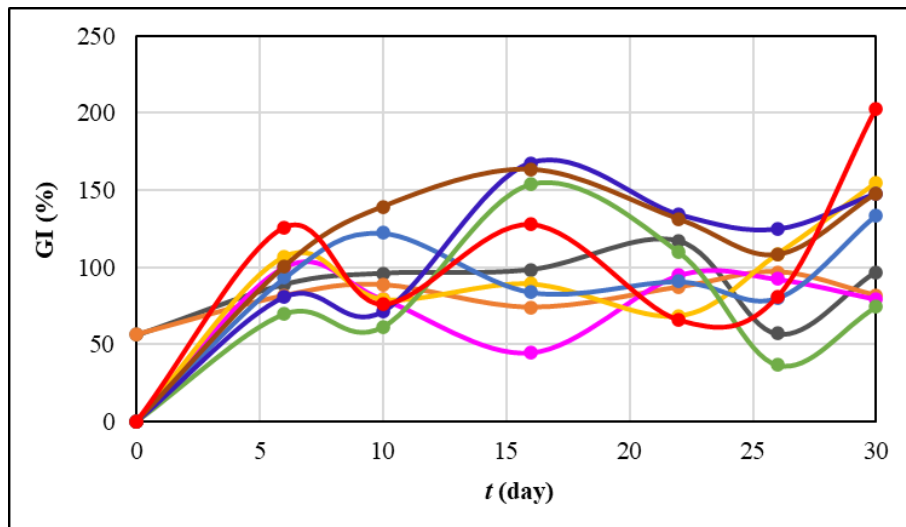
Figure 17. Changes in germination index during the 30 days of the grape skin composting process (• experiment 1; • experiment 2; • experiment 3; • experiment 4; • experiment 5; • experiment 6; • experiment 7; • experiment 8; • experiment 9)
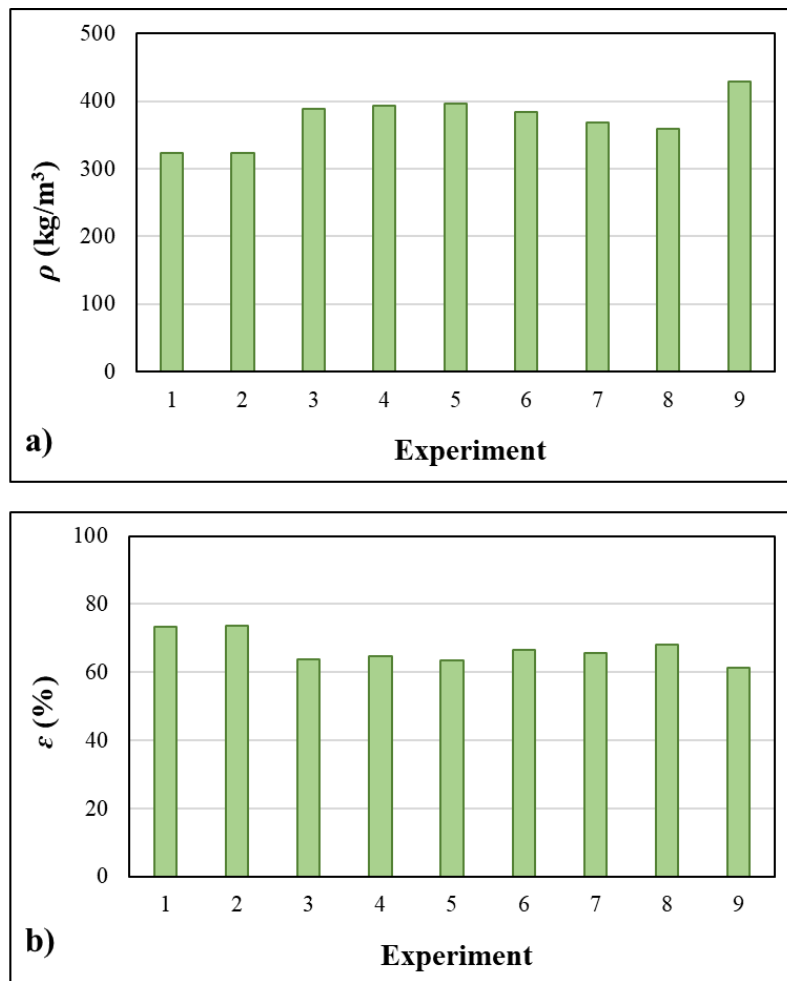
Figure 18. a) Bulk density (ρ) and b) Porosity (ε) of final composts obtained in grape skin composting processes under different conditions

4.1.2. Optimization of composting conditions

In this study, the response surface methodology was applied for the optimization of composting conditions. A second-order polynomial was used to describe the experimental data and the regression coefficients and analysis of variance (ANOVA) for RSM are shown in Table 11 (a significant coefficients ($p<0.05$) are marked in bold) (the regression coefficient for initial moisture content is β_1, and for air flow rate β_2). Furthermore, the optimal conditions of initial moisture content and air flow rate for the grape skin composting process are shown in Figure 19.

Table 11. Regression coefficients and analysis of variance for response surface model used for organic matter degradation description (a significant coefficients are marked in bold, $p < 0.05$)

	Coefficients ± standard error	Sum of squares (SS)	Degrees of freedom (df)	Mean squares (MS)	F value	p
β_0	73.749 ± 4.747					
β_1	**-8.445 ± 1.941**	266.279	1	266.279	39.4026	<0.0001
β_2	**-7.466 ± 2.592**	42.870	1	42.870	6.3438	0.0215
β_{11}	**-17.411 ± 9.971**	116.637	1	116.637	17.2593	0.0006
β_{22}	**-8.370 ± 4.713**	44.350	1	44.350	6.5626	0.0196
β_{12}	**0.544 ± 0.294**	0.481	1	0.481	0.0711	0.0427
Lack-of-fit		173.625	3	57.875	8.5640	0.0961
Pure error		121.642	18	6.758		
Total SS		624.234	26			
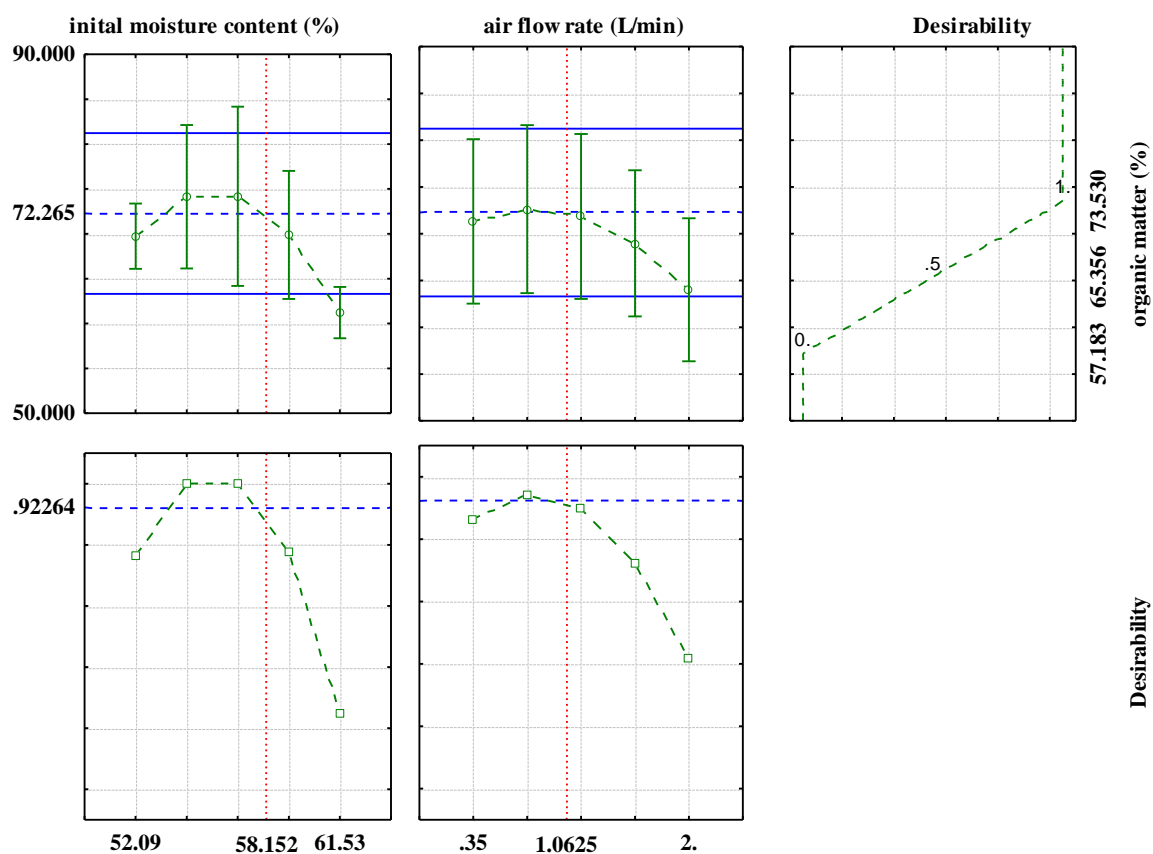
Figure 19. Profiles for predicted value of organic matter content at the end of the composting process and estimated optimal process conditions of initial moisture content and air flow rate

4.1.3. Kinetics of organic matter degradation and microbial growth during composting

Organic matter degradation in this work was described by first-order kinetic model, and the kinetic parameters and corresponding statistical analysis are shown in Table 12. Furthermore, the bacterial growth was also described by first-order kinetic model, and the fungal growth was described by logistic model. The results of the kinetic parameters are shown in Table 12.

Table 12. Kinetic parameters and corresponding statistical analysis for description on organic matter degradation and bacterial and fungal growth (k=degradation rate; OM_0=degraded organic matter content; μ=specific growth rate of bacteria or fungi; X=the number of bacterial/fungal cells; R^2 = coefficient of determination; R_{adj}^2= adjusted coefficient of determination; RMSE=root mean square error; χ^2= Chi-square; EF=modelling efficiency)

	Exp.	k (1/day)	OM_0 (%)	R^2	R^2_{adj}	RMSE	χ^2	EF
Organic matter degradation	1.	0.0035 ± 0.0014 (p<0.0001)	77.2451 ± 1.8158 (p<0.0001)	0.8148	0.7686	1.4083	2.4412	0.7908
	2.	0.0032 ± 0.0013 (p<0.0001)	79.7421 ± 1.8338 (p<0.0001)	0.8281	0.7852	1.5169	2.8323	0.7834
	3.	0.0093 ± 0.0023 (p<0.0001)	80.4016 ± 2.9808 (p<0.0001)	0.7798	0.7248	3.2285	2.8286	0.7668
	4.	0.0056 ± 0.0016 (p<0.0001)	77.1831 ± 2.0334 (p<0.0001)	0.7352	0.6691	2.3197	6.6231	0.7042
	5.	0.0052 ± 0.0013 (p<0.0001)	75.3750 ± 1.7064 (p<0.0001)	0.7256	0.6570	2.2491	6.2260	0.8364
	6.	0.0037 ± 0.0010 (p<0.0001)	72.2391 ± 1.2717 (p<0.0001)	0.6826	0.6032	1.3768	2.3332	0.6439
	7.	0.0073 ± 0.0010 (p<0.0001)	72.5545 ± 1.2172 (p<0.0001)	0.7887	0.7358	2.2731	6.3592	0.7887
	8.	0.0014 ± 0.0013 (p<0.0001)	70.9778 ± 1.5802 (p<0.0001)	0.7680	0.7100	1.3753	2.3279	0.5688
	9.	0.0034 ± 0.0008 (p<0.0001)	71.5794 ± 0.9761 (p<0.0001)	0.7976	0.7470	1.0316	1.3099	0.7919
	Exp.	μ (1/day)	X (logCFU/g$_{DM}$)	R^2	R^2_{adj}	RMSE	χ^2	EF
Bacterial growth	1.	0.0197 ± 0.0047 (p<0.0001)	5.6238 ± 0.5768 (p<0.0001)	0.7344	0.6751	0.7015	1.3125	0.7341
	2.	0.0115 ± 0.0031 (p<0.0001)	6.8753 ± 0.4308 (p<0.0001)	0.6829	0.5926	0.4933	0.6492	0.6827
	3.	0.0132 ± 0.0052 (p<0.0001)	7.0963 ± 0.7601 (p<0.0001)	0.6909	0.6198	0.8806	1.0682	0.6988
	4.	0.0120 ± 0.0049 (p<0.0001)	7.0797 ± 0.7077 (p<0.0001)	0.6801	0.6168	0.8135	1.7651	0.6801
	5.	0.0062 ± 0.0011 (p<0.0001)	8.3412 ± 0.1786 (p<0.0001)	0.8247	0.8196	0.1973	0.1038	0.8247
	6.	0.0161 ± 0.0038 (p<0.0001)	6.8255 ± 0.5522 (p<0.0001)	0.7378	0.6805	0.6534	1.1379	0.7369

Table 12. (*continuing*) Kinetic parameters and corresponding statistical analysis for description of organic matter degradation and bacterial and fungal growth (k=degradation rate; OM_0=degraded organic matter content; μ=specific growth rate of bacteria or fungi; X=the number of bacterial/fungal cells; R^2 = coefficient of determination; R_{adj}^2= adjusted coefficient of determination; RMSE=root mean square error; χ^{22}= Chi-square; EF=modelling efficiency)

	7.	0.0059 ± 0.0012 (p<0.0001)	8.5464 ± 0.1976 (p<0.0001)	0.7825	0.7521	0.2178	0.1265	0.7825
	8.	0.0058 ± 0.0013 (p<0.0001)	8.2618 ± 0.2155 (p<0.0001)	0.7337	0.6741	0.2377	0.1507	0.7338
	9.	0.0061 ± 0.0012 (p<0.0001)	8.5937 ± 0.2103 (p<0.0001)	0.7793	0.7468	0.2321	0.1437	0.7792
	Exp.	**μ (1/day)**	**X (logCFU/g_{DM})**	**R^2**	**R_{adj}^2**	**RMSE**	**χ^2**	**EF**
Fungal growth	1.	0.5879 ± 0.0181 (p<0.0001)	8.6482 ± 0.5768 (p<0.0001)	0.9868	0.9788	0.0851	0.0193	0.9859
	2.	0.6542 ± 0.0434 (p<0.0001)	8.6102 ± 0.6275 (p<0.0001)	0.9659	0.9456	0.1332	0.0473	0.9656
	3.	0.0625 ± 0.0038 (p<0.0001)	9.4025 ± 0.3320 (p<0.0001)	0.9372	0.8995	0.0826	0.0182	0.9211
	4.	0.1414 ± 0.0030 (p<0.0001)	9.1885 ± 0.5774 (p<0.0001)	0.8895	0.8233	0.0734	0.0144	0.8850
	5.	0.1404 ± 0.0041 (p<0.0001)	9.1855 ± 0.5724 (p<0.0001)	0.8333	0.7336	0.1040	0.0289	0.7111
	6.	0.9415 ± 0.0185 (p<0.0001)	8.2506 ± 0.6402 (p<0.0001)	0.9244	0.8789	0.2782	0.0207	0.9244
	7.	0.1174 ± 0.0338 (p<0.0001)	9.0259 ± 0.7977 (p<0.0001)	0.9714	0.9543	0.0892	0.0213	0.9699
	8.	0.0362 ± 0.0059 (p<0.0001)	9.0959 ± 0.2559 (p<0.0001)	0.9196	0.8714	0.0811	0.0175	0.7298
	9.	0.2462 ± 0.0221 (p<0.0001)	9.2894 ± 0.5399 (p<0.0001)	0.8045	0.6872	0.0979	0.0255	0.8043

4.1.4. Basic statistical analysis

The results of statistical analysis of physicochemical properties of compost samples and compost extracts at the beginning of the composting process and at the end of the process for all reactors are shown in Table 13.

Table 13. Mean values of physicochemical properties of compost at the beginning and end of the composting process. [A-I] The same superscript capital letters within a row denote no significant differences ($p > 0.05$) between the values obtained for the different composting processes according to Tukey's ANOVA. [a-i] The same superscript lowercase letters within a column denote no significant differences ($p > 0.05$) between values obtained for different days of composting process according to Tukey's ANOVA. (MC=moisture content; DM=dry matter content; OM=organic matter content; AC=ash content; CC=carbon content; NC=nitrogen content; TDS=total dissolved solids; S=conductivity)

	Day	Exp. 1	Exp. 2	Exp. 3	Exp. 4	Exp. 5	Exp. 6	Exp. 7	Exp. 8	Exp. 9
MC (%)	0.	$52.321\pm0.309^{A,a}$	$52.321\pm0.309^{A,a}$	$64.920\pm0.418^{B,a}$	$64.920\pm0.418^{B,a}$	$64.920\pm0.418^{B,a}$	$52.807\pm1.402^{A,a}$	$60.607\pm1.929^{B,a}$	$60.607\pm1.929^{B,a}$	$60.607\pm1.929^{B,a}$
	30.	$56.457\pm0.412^{A,a}$	$55.580\pm0.237^{A,a}$	$70.776\pm0.028^{B,b}$	$68.412\pm0.717^{B,a}$	$69.332\pm0.096^{B,a}$	$62.922\pm0.208^{C,b}$	$70.671\pm0.507^{B,b}$	$65.630\pm2.874^{B,a}$	$67.763\pm1.646^{B,b}$
DM (%)	0.	$47.679\pm0.309^{A,a}$	$47.679\pm0.309^{A,a}$	$35.080\pm0.419^{B,a}$	$35.080\pm0.419^{B,a}$	$35.080\pm0.419^{B,a}$	$47.197\pm1.402^{A,a}$	$39.393\pm1.929^{B,a}$	$39.393\pm1.929^{B,a}$	$39.393\pm1.929^{B,a}$
	30.	$43.512\pm0.412^{A,a}$	$44.419\pm0.237^{A,a}$	$29.226\pm0.023^{B,a}$	$33.588\pm0.717^{B,a}$	$30.668\pm0.097^{B,a}$	$37.077\pm0.208^{B,b}$	$29.329\pm0.508^{B,b}$	$34.369\pm2.874^{B,a}$	$32.237\pm1.646^{B,b}$
OM (%)	0.	$73.179\pm0.576^{A,a}$	$73.179\pm0.576^{A,a}$	$71.570\pm0.219^{A,a}$	$71.570\pm0.219^{A,a}$	$71.570\pm0.219^{A,a}$	$67.964\pm1.084^{A,a}$	$71.568\pm2.483^{A,a}$	$71.568\pm2.483^{A,a}$	$71.568\pm2.483^{A,a}$
	30.	$68.785\pm2.176^{A,a}$	$69.273\pm0.824^{A,a}$	$57.319\pm0.129^{B,c}$	$64.576\pm0.886^{B,b}$	$59.316\pm0.509^{B,b}$	$62.924\pm0.576^{A,a}$	$58.263\pm0.293^{B,b}$	$67.221\pm6.309^{A,a}$	$64.944\pm3.706^{A,b}$
AC (%)	0.	$26.821\pm0.576^{A,a}$	$26.821\pm0.576^{A,a}$	$28.429\pm0.219^{A,b}$	$28.429\pm0.219^{A,a}$	$28.429\pm0.219^{A,a}$	$32.035\pm1.084^{A,a}$	$28.431\pm2.482^{A,a}$	$28.431\pm2.482^{A,a}$	$28.431\pm2.482^{A,a}$
	30.	$30.682\pm2.176^{A,a}$	$30.726\pm0.824^{A,a}$	$42.688\pm0.129^{B,a}$	$35.423\pm0.886^{A,a}$	$40.684\pm0.509^{B,a}$	$37.078\pm0.848^{A,a}$	$41.736\pm0.293^{B,b}$	$32.779\pm6.309^{A,a}$	$35.056\pm3.706^{A,a}$
CC (%)	0.	$48.100\pm0.004^{B,b}$	$48.100\pm0.004^{B,b}$	$49.600\pm0.004^{A,b}$	$49.600\pm0.004^{A,b}$	$49.600\pm0.004^{A,b}$	$47.700\pm0.004^{B,b}$	$48.100\pm0.004^{B,a}$	$48.100\pm0.004^{B,a}$	$48.100\pm0.004^{B,a}$
	30.	$48.300\pm0.004^{A,b}$	$47.700\pm0.004^{A,b}$	$46.800\pm0.004^{B,c}$	$47.300\pm0.004^{A,b}$	$47.300\pm0.004^{A,c}$	$47.100\pm0.004^{A,b}$	$44.700\pm0.004^{A,b}$	$47.300\pm0.004^{A,a}$	$47.300\pm0.004^{A,a}$
NC (%)	0.	$1.780\pm0.004^{A,a}$	$1.780\pm0.004^{A,a}$	$1.270\pm0.004^{A,a}$	$1.270\pm0.004^{A,a}$	$1.270\pm0.004^{A,a}$	$1.540\pm0.004^{A,a}$	$1.500\pm0.004^{A,a}$	$1.500\pm0.004^{A,a}$	$1.500\pm0.004^{A,a}$
	30.	$1.570\pm0.004^{A,a}$	$1.670\pm0.004^{A,a}$	$1.900\pm0.004^{A,a}$	$1.870\pm0.004^{A,a}$	$1.760\pm0.004^{A,a}$	$2.330\pm0.004^{A,a}$	$2.840\pm0.004^{A,a}$	$2.070\pm0.004^{A,a}$	$2.510\pm0.004^{A,a}$
C/N ratio	0.	$27.947\pm6.210^{A,a}$	$27.947\pm6.210^{A,a}$	$40.074\pm7.347^{B,a}$	$40.074\pm7.347^{B,a}$	$40.074\pm7.347^{B,a}$	$32.419\pm8.442^{A,a}$	$33.652\pm9.023^{A,a}$	$33.652\pm9.023^{A,a}$	$33.652\pm9.023^{A,a}$
	30.	$26.142\pm8.169^{A,a}$	$27.125\pm6.156^{A,a}$	$24.673\pm4.959^{A,b}$	$27.174\pm5.729^{A,b}$	$28.168\pm6.336^{A,b}$	$21.041\pm3.491^{A,b}$	$17.365\pm2.328^{B,b}$	$23.960\pm4.521^{A,b}$	$19.438\pm2.975^{A,b}$
pH	0.	$7.683\pm0.005^{A,a}$	$7.683\pm0.005^{A,a}$	$7.647\pm0.006^{A,a}$	$7.647\pm0.006^{A,a}$	$7.647\pm0.006^{A,a}$	$5.803\pm0.006^{B,a}$	$5.623\pm0.006^{B,a}$	$5.623\pm0.006^{B,a}$	$5.623\pm0.006^{B,a}$
	30.	$7.297\pm0.006^{A,f}$	$7.303\pm0.006^{B,d}$	$9.080\pm0.010^{C,e}$	$7.833\pm0.015^{D,g}$	$7.943\pm0.015^{E,g}$	$8.483\pm0.035^{F,h}$	$9.243\pm0.021^{G,g}$	$8.003\pm0.012^{H,f}$	$8.587\pm0.006^{I,g}$
TDS	0.	$812.333\pm15.307^{A,b}$	$812.333\pm15.307^{A,c}$	$484.000\pm2.000^{B,d}$	$484.000\pm2.000^{B,a}$	$484.000\pm2.000^{B,a}$	$1502.333\pm38.397^{C,a}$	$1177.667\pm19.008^{C,a}$	$1177.667\pm19.008^{C,a}$	$1177.667\pm19.008^{C,a}$
	30.	$1303.667\pm24.906^{A,a}$	$1466.000\pm3.000^{A,b}$	$1409.000\pm17.578^{A,a}$	$1458.333\pm5.033^{A,b}$	$1134.333\pm10.263^{A,b}$	$1936.000\pm2.645^{B,c}$	$1574.333\pm23.544^{A,a}$	$1204.333\pm35.529^{A,c}$	$2097.000\pm15.716^{B,c}$
S	0.	$1666.667\pm5.507^{A,b}$	$1666.667\pm5.507^{A,c}$	$966.333\pm15.044^{B,d}$	$966.333\pm15.044^{B,a}$	$966.333\pm15.044^{B,a}$	$2780.000\pm80.000^{C,a}$	$2413.333\pm5.774^{C,a}$	$2413.333\pm5.773^{C,a}$	$2413.333\pm5.774^{C,a}$
	30.	$2663.333\pm5.773^{A,a}$	$2756.667\pm222.336^{A,b}$	$2860.000\pm10.000^{A,a}$	$2783.333\pm136.137^{A,b}$	$2320.000\pm10.000^{A,b}$	$3930.000\pm53.000^{B,c}$	$2876.667\pm70.946^{A,a}$	$2530.000\pm10.000^{A,c}$	$4013.333\pm96.090^{B,d}$

4.1.5. Multivariate analysis

4.1.5.1. Principal Component Analysis (PCA)

The effects of initial moisture content, air flow rate and sampling day on physicochemical properties of compost samples and compost extract samples during the composting process were analysed, and in this purpose the principal component analysis was used. The results are shown in Figure 20.
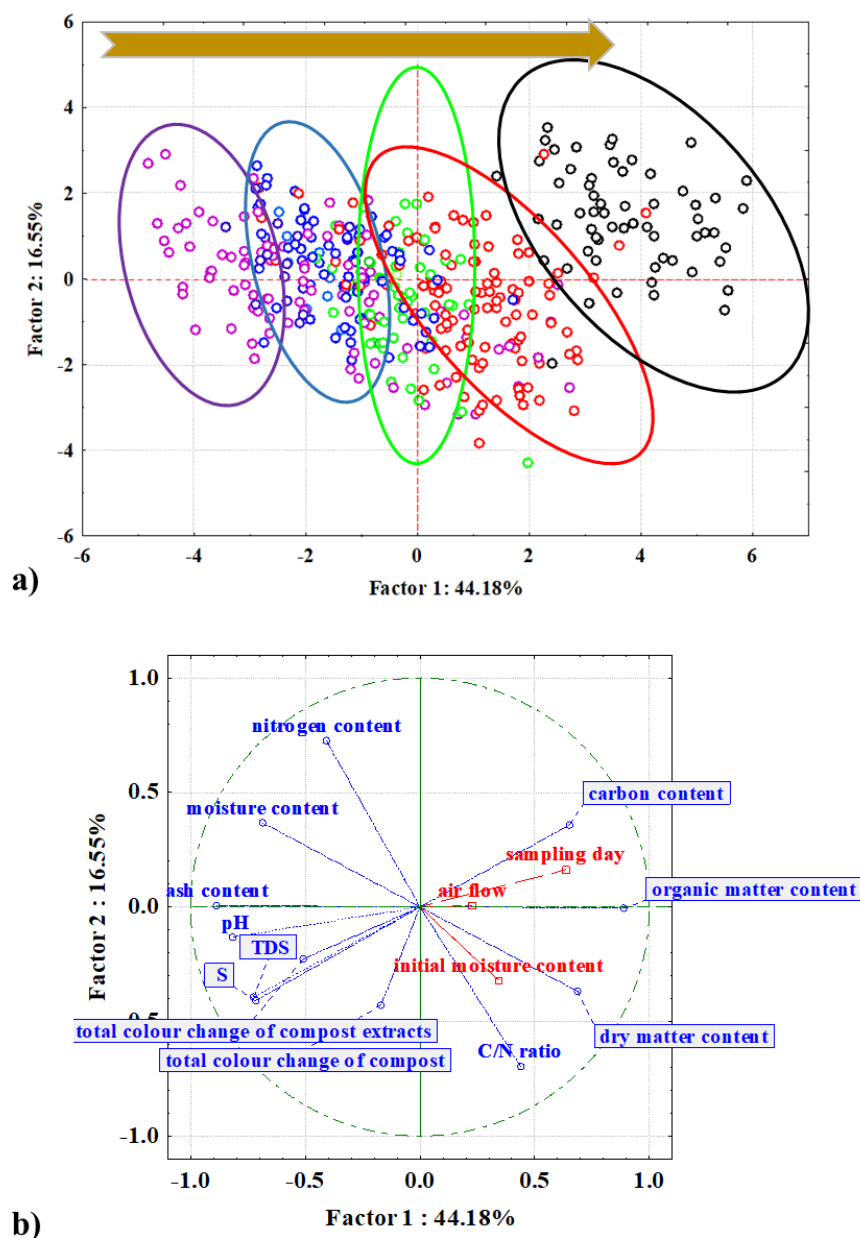
Figure 20. Principal c0omponent analysis (PCA): a) score plot and b) loading plot showing the relationship between initial moisture content, air flow, sampling day and physicochemical properties of compost during the composting process. Samples grouping according to total dissolved solids (TDS). (○) TDS = 286 - 664.8 mg/L, (○) TDS = 664.8 - 1044 mg/L, (○) TDS = 1044 - 1422 mg/L, (○) TDS = 1422 - 1801 mg/L, (○) TDS = 1801 - 2180 mg/L

4.1.5.2. Multiple linear regression (MLR) models for the prediction of physicochemical properties of compost and compost extracts

Hereafter, the multiple linear regression models were developed for predicting the physicochemical properties of grape skin compost and compost extracts. The equations with coefficients of MLR models are shown in Table 14 and the comparison between experimental data and MLR models predicted data of physicochemical properties of compost samples and compost extract samples are shown in Figure 21.

Table 14. The equations of multiple linear regression models for prediction of physicochemical properties of compost and compost extracts during the composting process based on initial moisture content (X_1), air flow rate (X_2) and sampling day (X_3) (significant coefficients are marked bold)

Output variable	Equation
Moisture content	$MC = -\mathbf{5.787} + \mathbf{1.086} \cdot X_1 + \mathbf{1.577} \cdot X_2 + \mathbf{0.182} \cdot X_3$
Dry matter content	$DM = \mathbf{105.787} - \mathbf{1.086} \cdot X_1 - \mathbf{1.577} \cdot X_2 - \mathbf{0.182} \cdot X_3$
Organic matter content	$OM = \mathbf{103.767} - \mathbf{0.452} \cdot X_1 - \mathbf{2.251} \cdot X_2 - \mathbf{0.327} \cdot X_3$
Ash content	$AC = -3.767 + \mathbf{0.452} \cdot X_1 + \mathbf{2.251} \cdot X_2 + \mathbf{0.327} \cdot X_3$
Carbon content	$CC = \mathbf{53.562} - \mathbf{0.065} \cdot X_1 - \mathbf{0.729} \cdot X_2 - \mathbf{0.041} \cdot X_3$
Nitrogen content	$NC = 1.409 + \mathbf{0.001} \cdot X_1 + \mathbf{0.150} \cdot X_2 + \mathbf{0.016} \cdot X_3$
C/N ratio	$C/N = 34.162 - \mathbf{0.016} \cdot X_1 - \mathbf{1.952} \cdot X_2 - \mathbf{0.272} \cdot X_3$
ΔE compost	$\Delta E\ compost = 12.170 - \mathbf{0.059} \cdot X_1 - \mathbf{2.182} \cdot X_2 + \mathbf{0.208} \cdot X_3$
pH	$pH = 2.\mathbf{713} + \mathbf{0.054} \cdot X_1 + \mathbf{0.289} \cdot X_2 + \mathbf{0.081} \cdot X_3$
TDS	$TDS = 523.463 + \mathbf{1.231} \cdot X_1 + \mathbf{223.603} \cdot X_2 + \mathbf{25.896} \cdot X_3$
S	$S = 1460.037 - \mathbf{3.969} \cdot X_1 + \mathbf{372.793} \cdot X_2 + \mathbf{53.389} \cdot X_3$
ΔE extract	$\Delta E\ extract = -0.042 + \mathbf{0.009} \cdot X_1 + \mathbf{0.399} \cdot X_2 + \mathbf{0.048} \cdot X_3$

Figure 21. Comparison between experimental data and multiple linear regression (MLR) models predicted data of physicochemical properties of compost and compost extracts during the composting process: a) MC; b) DM; c) OM; d) AC; e) CC and f) NC (○ calibration data set and ○ prediction data set) (MC=moisture content; DM=dry matter content; OM= organic matter content; AC= ash content; CC=carbon content; NC= nitrogen content) (R_{cal}^2=coefficient of determination for calibration; $R_{cal}^2{}_{adj}$=adjusted coefficient of determination for calibration; $RMSE$=root mean square error; F-value of the model; R_{pred}^2=coefficient of determination for prediction; $R_{pred}^2{}_{adj}$=adjusted coefficient of determination for prediction; $RMSEP$=root mean square of prediction; SEP=standard error of prediction; RPD=ratio of prediction to deviation; RER=ratio of the error range)

Figure 21. (*continuing*) Comparison between experimental data and multiple linear regression (MLR) models predicted data of physicochemical properties of compost and compost extracts during the composting process: g) C/N ratio; h) ΔE of compost; i) pH; j) TDS; k) S and l) ΔE of extract (○ calibration data set and ○ prediction data set) (ΔE compost=total color change of compost samples; TDS=total dissolved solids; S=conductivity; ΔE extracts=total color change of compost extracts) (R_{cal}^2=coefficient of determination for calibration; $R_{cal}^2{}_{adj}$=adjusted coefficient of determination for calibration; $RMSE$=root mean square error; F-value of the model; R_{pred}^2=coefficient of determination for prediction; $R_{pred}^2{}_{adj}$=adjusted coefficient of determination for prediction; $RMSEP$=root mean square of prediction; SEP=standard error of prediction; RPD=ratio of prediction to deviation; RER=ratio of the error range)

4.1.5.3. Piecewise linear regression (PLR) models for the prediction of physicochemical properties of compost and compost extracts

Also, the piecewise linear regression models were developed for predicting the physicochemical properties of grape skin compost and their extracts. The equations with coefficients of PLR models are shown in Table 15 and the comparison between experimental data and PLR models predicted data of physicochemical properties are shown in Figure 22.

Table 15. The coefficients of piecewise linear regression models for prediction of physicochemical properties of compost and compost extracts during the composting process based on initial moisture content (X_1), air flow rate (X_2) and sampling day (X_3) (significant coefficients are marked bold)

Output variable	Equation
Moisture content	$MC = (\mathbf{19.059} + \mathbf{0.609} \cdot X_1 + \mathbf{1.867} \cdot X_2 + \mathbf{0.136} \cdot X_3) + (\mathbf{32.022} + \mathbf{0.511} \cdot X_1 + \mathbf{0.571} \cdot X_2 + \mathbf{0.119} \cdot X_3)$
Dry matter content	$DM = (\mathbf{67.979} - \mathbf{0.511} \cdot X_1 - \mathbf{0.576} \cdot X_2 - \mathbf{0.121} \cdot X_3) + (\mathbf{80.940} - \mathbf{0.609} \cdot X_1 - \mathbf{1.867} \cdot X_2 - \mathbf{0.136} \cdot X_3)$
Organic matter content	$OM = (\mathbf{85.588} - \mathbf{0.319} \cdot X_1 - \mathbf{1.823} \cdot X_2 - \mathbf{0.157} \cdot X_3) + (\mathbf{83.851} - \mathbf{0.125} \cdot X_1 - \mathbf{1.124} \cdot X_2 - \mathbf{0.077} \cdot X_3)$
Ash content	$AC = (\mathbf{16.149} + \mathbf{0.124} \cdot X_1 + \mathbf{1.124} \cdot X_2 + \mathbf{0.078} \cdot X_3) + (\mathbf{10.412} + \mathbf{0.319} \cdot X_1 + \mathbf{1.823} \cdot X_2 + \mathbf{0.157} \cdot X_3)$
Carbon content	$CC = (\mathbf{51.269} - \mathbf{0.054} \cdot X_1 - \mathbf{0.543} \cdot X_2 - \mathbf{0.006} \cdot X_3) + (\mathbf{52.427} - \mathbf{0.033} \cdot X_1 - \mathbf{0.033} \cdot X_2 - \mathbf{0.103} \cdot X_3)$
Nitrogen content	$NC = (1.765 - \mathbf{0.005} \cdot X_1 - \mathbf{0.041} \cdot X_2 + \mathbf{0.006} \cdot X_3) + (1.657 + \mathbf{0.005} \cdot X_1 + \mathbf{0.097} \cdot X_2 + \mathbf{0.009} \cdot X_3)$
C/N ratio	$C/N = (31.328 - \mathbf{0.099} \cdot X_1 - \mathbf{1.484} \cdot X_2 - \mathbf{0.074} \cdot X_3) + (33.811 - \mathbf{0.006} \cdot X_1 + \mathbf{0.791} \cdot X_2 - \mathbf{0.121} \cdot X_3)$
ΔE compost	$\Delta E \text{ compost} = (0.133 + \mathbf{0.086} \cdot X_1 + \mathbf{0.114} \cdot X_2 + \mathbf{0.107} \cdot X_3) + (15.436 - \mathbf{0.029} \cdot X_1 - \mathbf{0.836} \cdot X_2 + \mathbf{0.026} \cdot X_3)$
pH	$\text{pH} = (\mathbf{1.014} + \mathbf{0.069} \cdot X_1 + \mathbf{0.270} \cdot X_2 + \mathbf{0.098} \cdot X_3) + (\mathbf{5.611} + \mathbf{0.029} \cdot X_1 + \mathbf{0.297} \cdot X_2 + \mathbf{0.024} \cdot X_3)$
TDS	$\text{TDS} = (179.145 + \mathbf{10.017} \cdot X_1 + \mathbf{145.035} \cdot X_2 + \mathbf{14.178} \cdot X_3)$ $+ (1424.494 + \mathbf{4.324} \cdot X_1 + \mathbf{207.526} \cdot X_2 + \mathbf{5.907} \cdot X_3)$
S	$S = (1135.893 + \mathbf{1.699} \cdot X_1 + \mathbf{142.480} \cdot X_2 + \mathbf{133.278} \cdot X_3)$ $+ (2900.114 + \mathbf{10.306} \cdot X_1 + \mathbf{421.914} \cdot X_2 + \mathbf{12.474} \cdot X_3)$
ΔE extract	$\Delta E \text{ extract} = (0.310 + \mathbf{0.004} \cdot X_1 + \mathbf{0.027} \cdot X_2 + \mathbf{0.024} \cdot X_3) + (2.353 + \mathbf{0.007} \cdot X_1 + \mathbf{0.363} \cdot X_2 + \mathbf{0.019} \cdot X_3)$
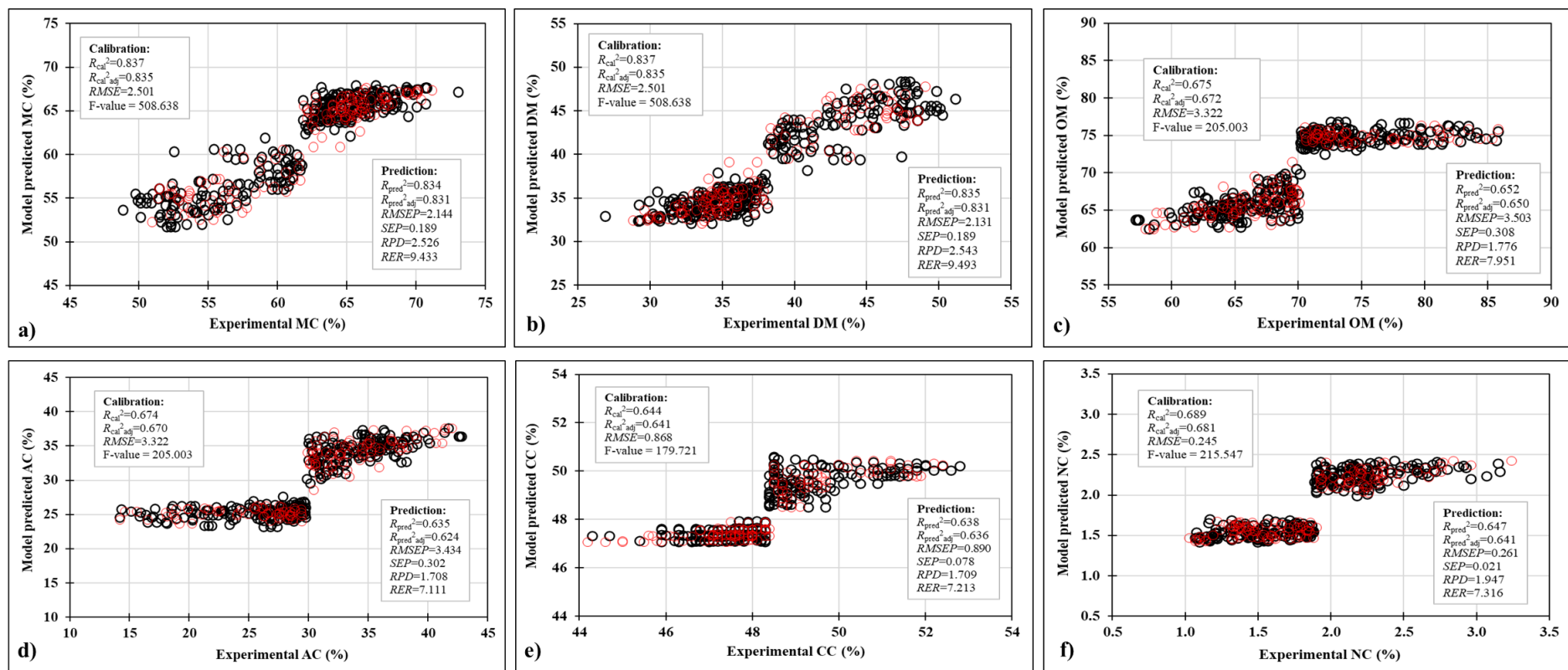
Figure 22. Comparison between experimental data and piecewise linear regression (PLR) models predicted data of physicochemical properties of compost and compost extracts during the composting process: a) MC; b) DM; c) OM; d) AC; e) CC and f) NC (○ calibration data set and ○ prediction data set) (MC=moisture content; DM=dry matter content; OM= organic matter content; AC= ash content; CC=carbon content; NC= nitrogen content) (R_{cal}^2=coefficient of determination for calibration; $R_{cal\,adj}^2$=adjusted coefficient of determination for calibration; $RMSE$=root mean square error; F-value of the model; R_{pred}^2=coefficient of determination for prediction; $R_{pred\,adj}^2$=adjusted coefficient of determination for prediction; $RMSEP$=root mean square of prediction; SEP=standard error of prediction; RPD=ratio of prediction to deviation; RER=ratio of the error range)
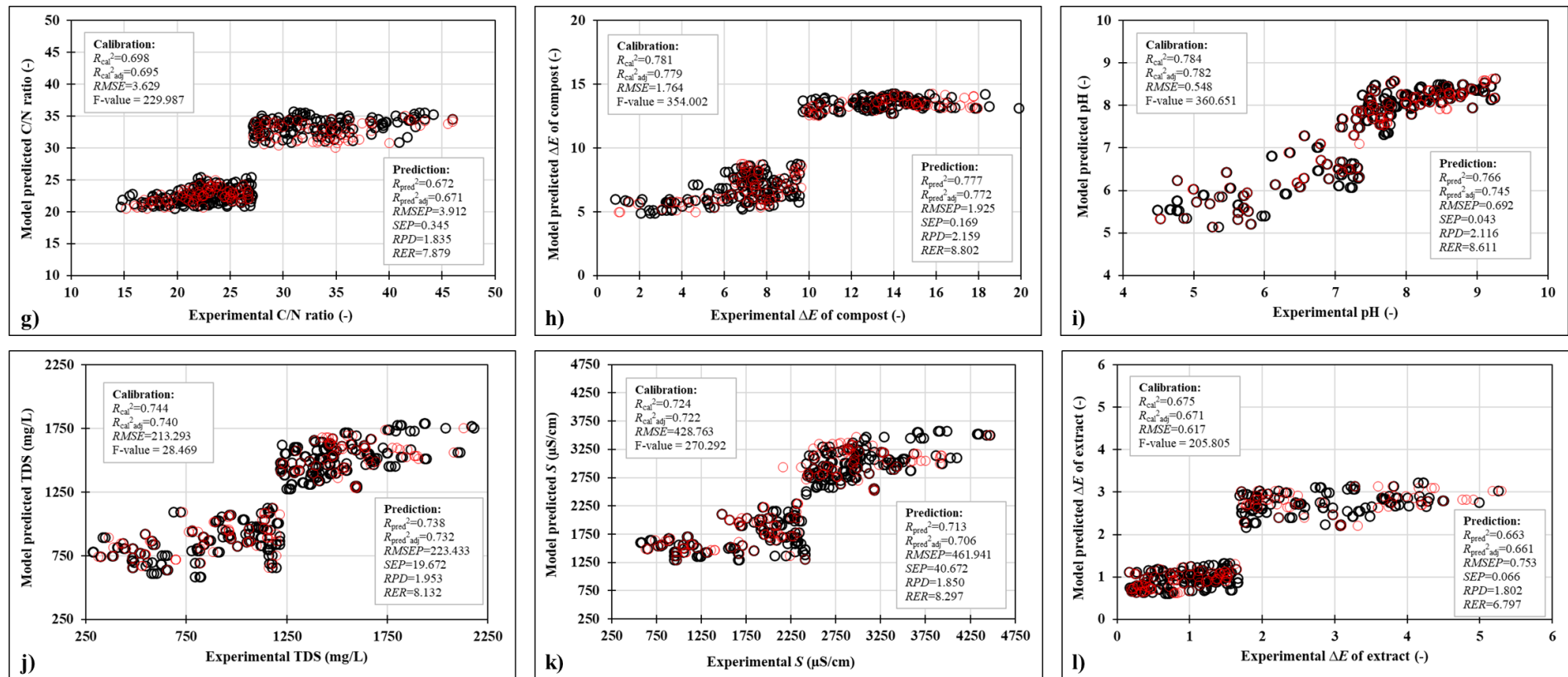
Figure 22. (*continuing*) Comparison between experimental data and piecewise linear regression (PLR) models predicted data of physicochemical properties of compost and compost extracts during the composting process: g) C/N ratio; h) ΔE of compost; i) pH; j) TDS; k) S and l) ΔE of extracts ($\circ$ calibration data set and $\circ$ prediction data set) (ΔE compost=total color change of compost samples; TDS=total dissolved solids; S=conductivity; ΔE extracts=total color change of compost extracts) (R_{cal}^2=coefficient of determination for calibration; $R_{cal}^2{}_{adj}$=adjusted coefficient of determination for calibration; $RMSE$=root mean square error; F-value of the model; R_{pred}^2=coefficient of determination for prediction; $R_{pred}^2{}_{adj}$=adjusted coefficient of determination for prediction; $RMSEP$=root mean square of prediction; SEP=standard error of prediction; RPD=ratio of prediction to deviation; RER=ratio of the error range)

4.1.5.4. Artificial neural network (ANN) models for the prediction of physicochemical properties of compost and compost extracts

Multilayer perceptron (MLP) neural network models were developed to improve the prediction of physicochemical properties of grape skin compost and compost extracts during the composting process. ANN models were developed individually for each of selected physicochemical property and the results are shown in Table 16 and in Figure 23.

Table 16. The artificial neural network (ANN) models for the prediction of physicochemical properties of grape skin compost

Output variable	Network name	Calibration			Hidden activation	Output activation
		Training perf. Training error	Test perf. Test error	Validation perf. Validation error		
Moisture content	MLP 3-6-1	0.9262 1.1201	0.9248 1.1335	0.9137 1.5458	Tanh	Logistic
Dry matter	MLP 3-10-1	0.9248 1.1222	0.9117 1.1258	0.9107 1.4933	Tanh	Logistic
Organic matter	MLP 3-9-1	0.7978 2.2311	0.7677 2.4293	0.7594 2.8152	Tanh	Tanh
Ash	MLP 3-10-1	0.8359 1.6794	0.8344 1.8354	0.8057 2.0836	Tanh	Tanh
Carbon content	MLP 3-8-1	0.8623 0.5664	0.8613 0.6265	0.8522 0.7596	Logistic	Identity
Nitrogen content	MLP 3-4-1	0.7556 0.0605	0.7554 0.0625	0.7236 0.0639	Logistic	Exponential
C/N ratio	MLP 3-10-1	0.7367 0.2016	0.6826 0.2683	0.6672 0.3913	Tanh	Exponential
ΔE (compost)	MLP 3-5-1	0.9219 1.3085	0.9177 1.3384	0.9056 1.3718	Logistic	Exponential
pH	MLP 3-10-1	0.9137 0.1148	0.8961 0.1569	0.8674 0.1640	Tanh	Identity
TDS	MLP 3-8-1	0.9231 83.3771	0.8961 134.5269	0.8334 163.2544	Tanh	Tanh
S	MLP 3-10-1	0.8670 87.4412	0.8965 151.1360	0.8076 182.1221	Tanh	Logistic
ΔE (compost extracts)	MLP 3-7-1	0.8055 0.3691	0.7936 0.6189	0.7853 0.6371	Logistic	Logistic

Figure 23. Comparison between experimental data and artificial neural network (ANN) models predicted data of physicochemical properties of compost and compost extracts during the composting process: a) MC; b) DM; c) OM; d) AC; e) CC and f) NC (○ training; △ test; ◇ validation and ○ prediction data set) (MC=moisture content; DM=dry matter content; OM= organic matter content; AC= ash content; CC=carbon content; NC= nitrogen content) (R_pred^2=coefficient of determination for prediction; $R_\text{pred}^2{}_\text{adj}$=adjusted coefficient of determination for prediction; *RMSEP*=root mean square of prediction; *SEP*=standard error of prediction; *RPD*=ratio of prediction to deviation; *RER*=ratio of the error range)
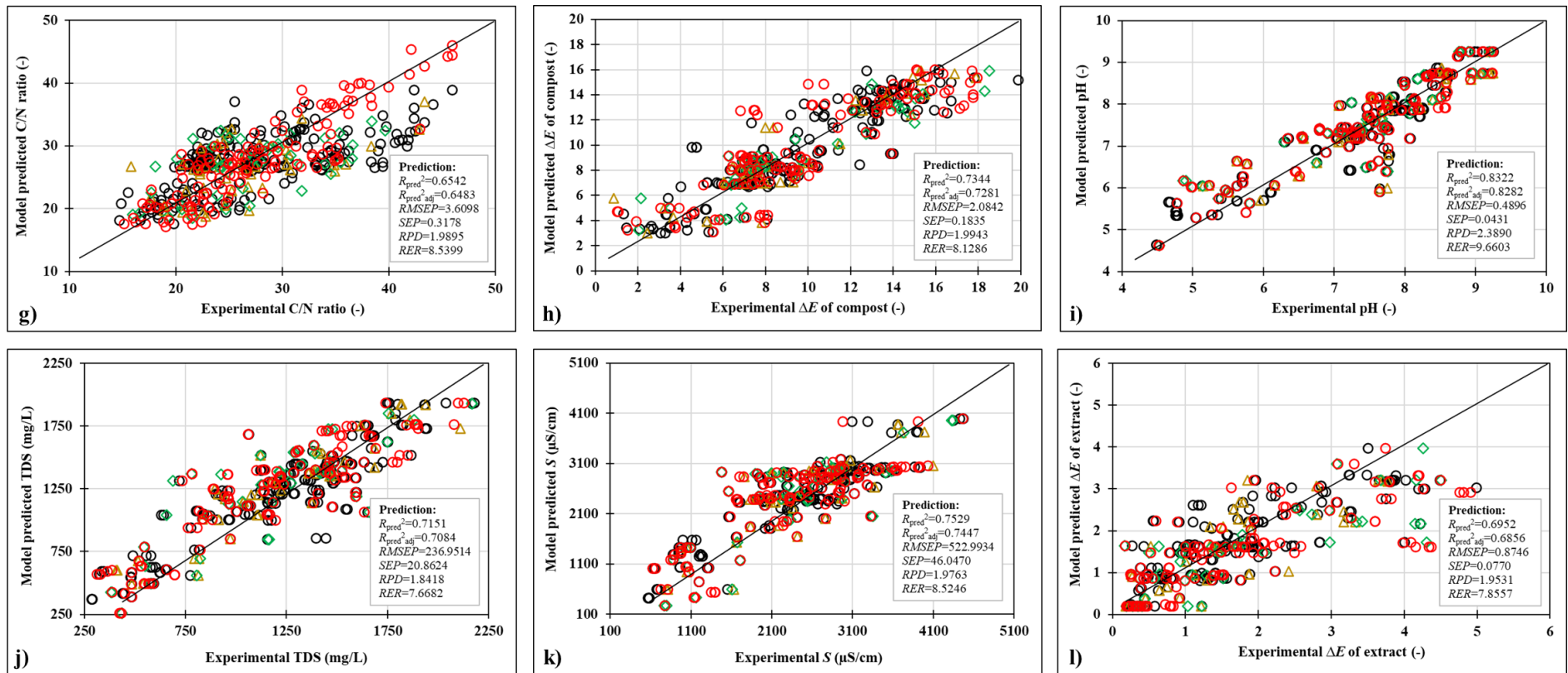
Figure 23. (*continuing*) Comparison between experimental data and artificial neural network (ANN) models predicted data of physicochemical properties of compost and compost extracts during the composting process: g) C/N ratio; h) ΔE of compost; i) pH; j) TDS; k) S and l) ΔE of extract (○ training; △ test; ◇ validation and ○ prediction data set) (ΔE compost=total color change of compost samples; TDS=total dissolved solids; S=conductivity; ΔE extracts=total color change of compost extracts) (R_{pred}^2=coefficient of determination for prediction; $R_{pred}^2{}_{adj}$=adjusted coefficient of determination for prediction; RMSEP=root mean square of prediction; SEP=standard error of prediction; RPD=ratio of prediction to deviation; RER=ratio of the error range)

4.1.6. NIR spectra of compost samples and compost extracts

During the composting processes, the NIR spectra were recorded for all compost samples and compost extracts with different NIR instruments. The recorded spectra are shown in Figures 24 and 25.
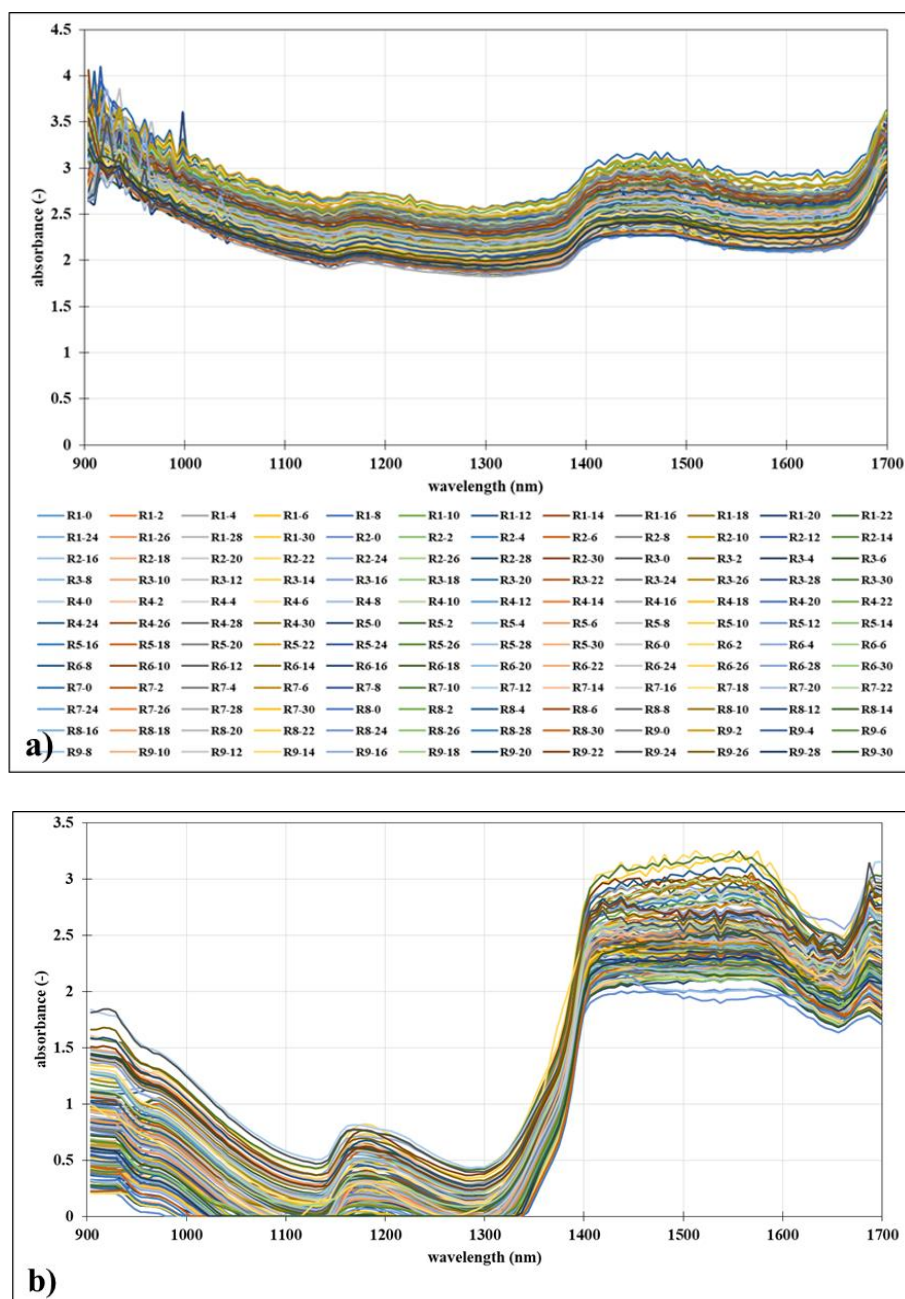
Figure 24. Average NIR spectra of a) compost samples and b) compost extract samples during the analysis of the effect of initial moisture content and air flow rate on the efficiency of the composting process gathered using NIR spectrometer (NIR-128-1.7-USB/6.25/50 μm, Control Development Inc., USA) (the legend from figure a) is applicable for figure b))
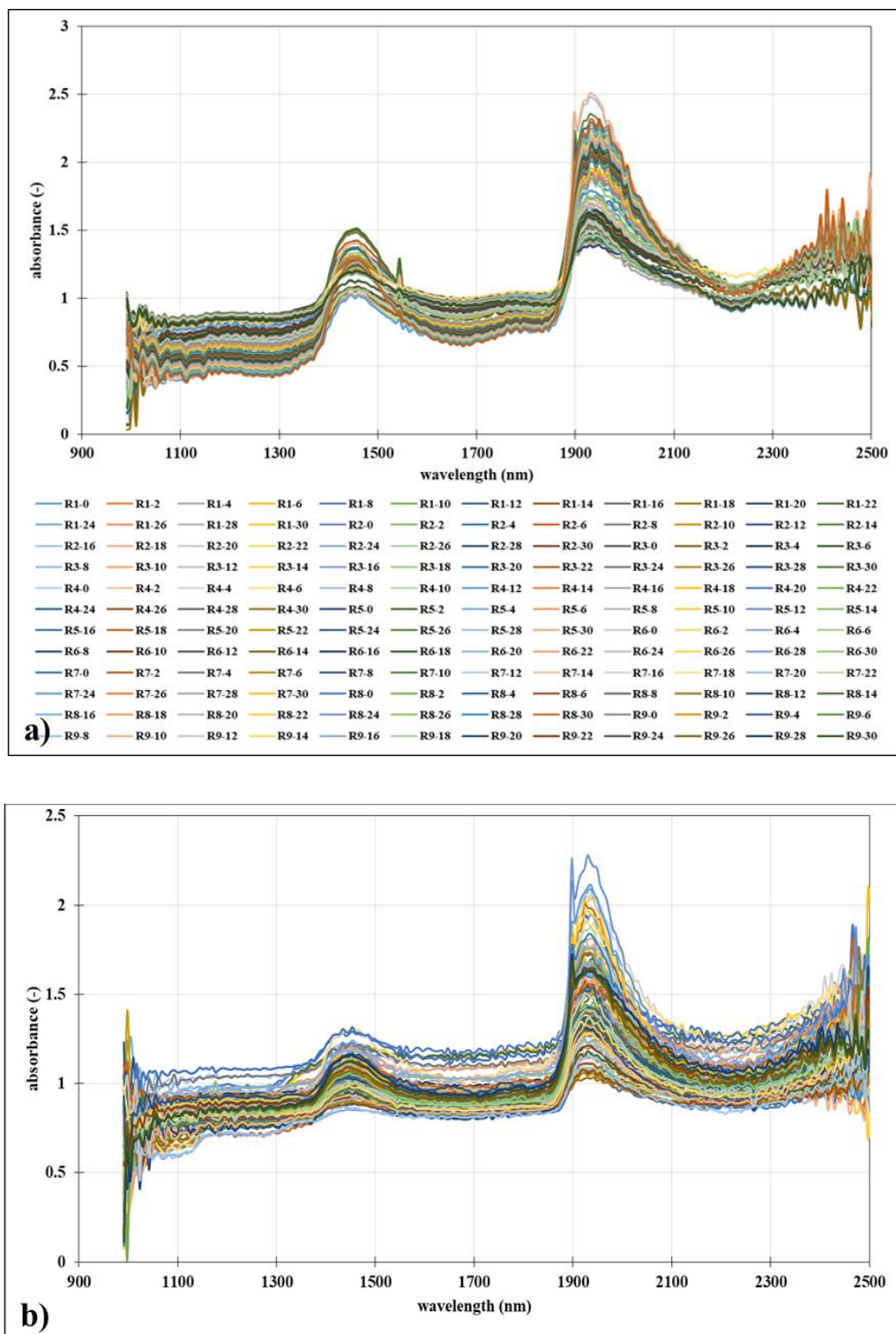
Figure 25. Average NIR spectra of a) compost samples and b) compost extract samples during the analysis of the effect of initial moisture content and air flow rate on the efficiency of the composting process gathered using NIR spectrometer (AvaSpec-NIR256-2.5-HSC-EVO, Avantes, USA) (the legend from figure a) is applicable for figure b))

4.1.7. Principal component analysis (PCA) of preprocessed NIR spectra of compost samples and compost extracts

The PCA analysis was performed for the preprocessing methods of average NIR spectra of compost samples and compost extracts recorded with different NIR instruments and the results are shown in figures below (Figures 26-29).
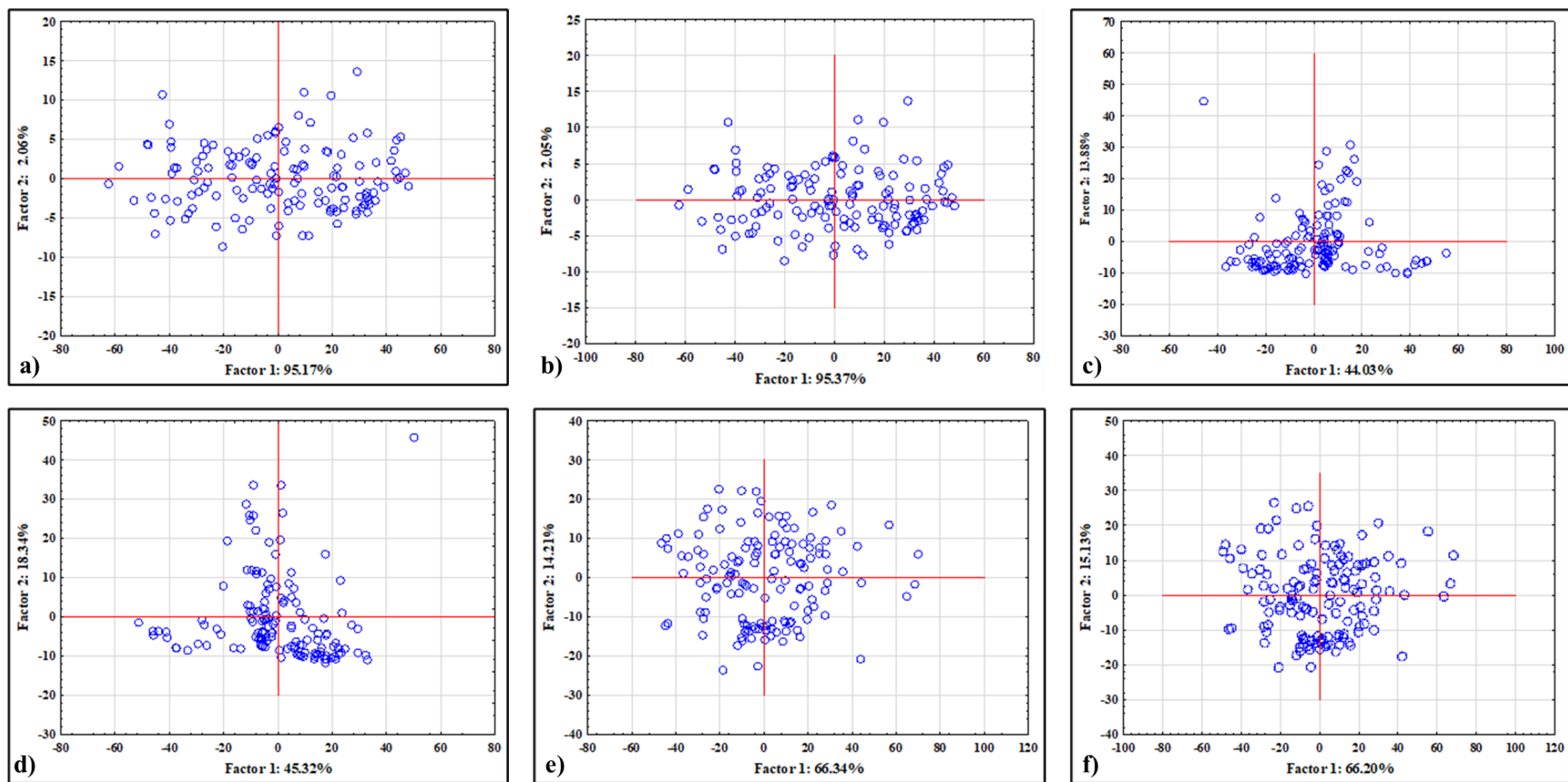
Figure 26. Principal component analysis (PCA) of a) raw and preprocessed: b) smoothing; c) SG1D; d) SG2D; e) SNV and f) MSC average NIR spectra of compost samples gathered using NIR spectrometer (NIR-128-1.7-USB/6.25/50 μm, Control Development Inc., USA) (SG1D= first-order Savitzky-Golay derivative; SG2D= second-order Savitzky-Golay derivative; SNV= standard normal variate; MSC= multiplicative scatter corrections)
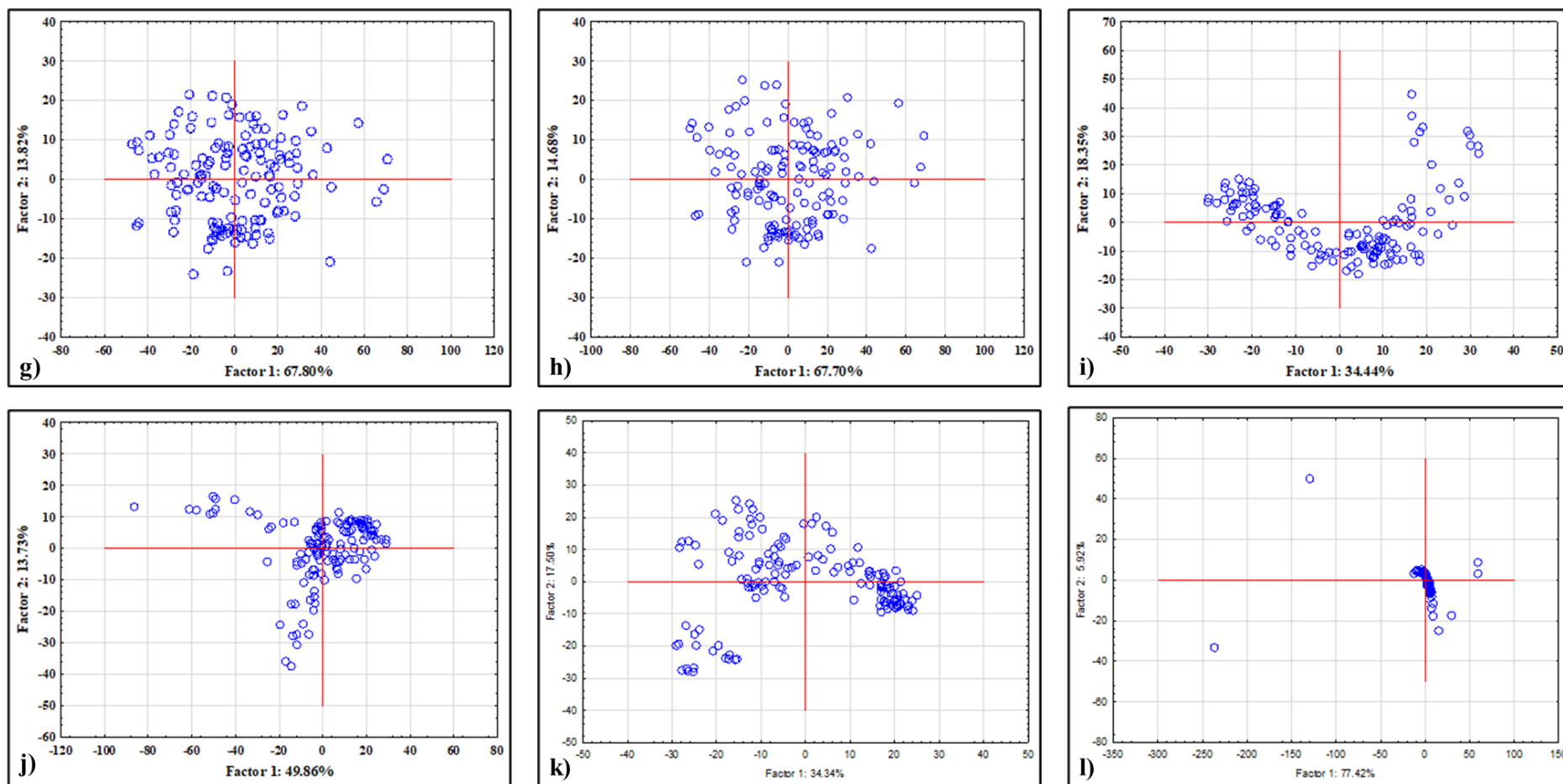
Figure 26. (*continuing*) Principal component analysis (PCA) of g) smoothing+SNV; h) smoothing+MSC; i) SG1D+SNV; j) SG1D+MSC; k) SG2D+SNV; l) SG2D+MSC average NIR spectra of compost samples gathered using NIR spectrometer (NIR-128-1.7-USB/6.25/50 μm, Control Development Inc., USA) (smoothing+SNV= smoothing followed by standard normal variate; smoothing+MSC= smoothing followed by multiplicative scatter corrections; SG1D+SNV=first-order Savitzky-Golay derivative followed by standard normal variate; SG1D+MSC= smoothing followed by multiplicative scatter corrections; SG2D+SNV= second-order Savitzky-Golay derivative followed by standard normal variate; SG2D+MSC= second-order Savitzky-Golay derivative followed by multiplicative scatter corrections)

Figure 27. Principal component analysis (PCA) of a) raw and preprocessed b) smoothing; c) SG1D; d) SG2D; e) SNV; f) MSC average NIR spectra of compost extracts samples gathered using NIR spectrometer (NIR-128-1.7-USB/6.25/50 μm, Control Development Inc., USA) (SG1D= first-order Savitzky-Golay derivative; SG2D= second-order Savitzky-Golay derivative; SNV= standard normal variate; MSC= multiplicative scatter corrections)
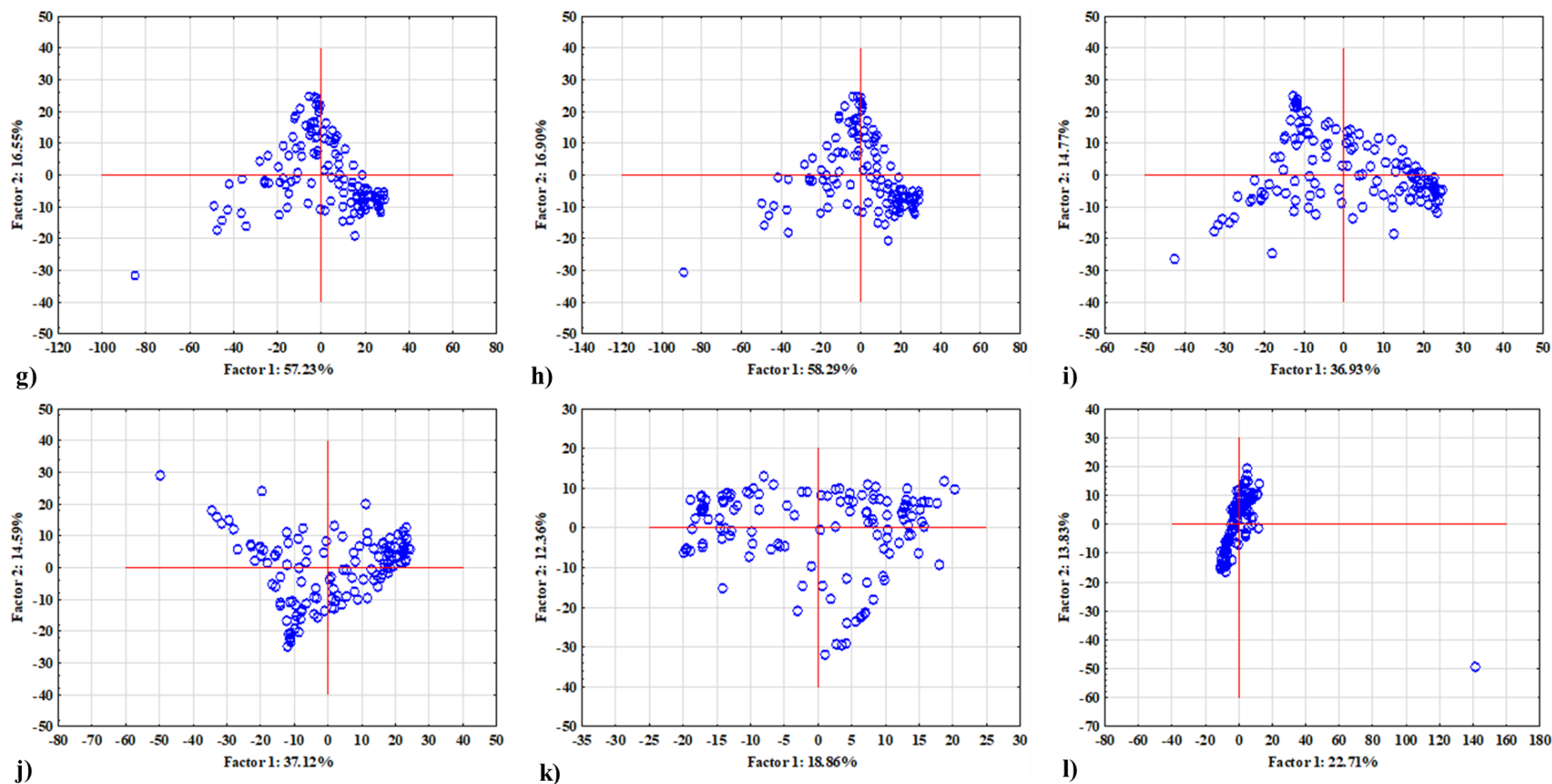
Figure 27. (*continuing*) Principal component analysis (PCA) of preprocessed g) smoothing+SNV; h) smoothing+MSC; i) SG1D+SNV; j) SG1D+MSC; k) SG2D+SNV; l) SG2D+MSC average NIR spectra of compost extracts samples gathered using NIR spectrometer (NIR-128-1.7-USB/6.25/50 μm, Control Development Inc., USA) (smoothing+SNV= smoothing followed by standard normal variate; smoothing+MSC= smoothing followed by multiplicative scatter corrections; SG1D+SNV=first-order Savitzky-Golay derivative followed by standard normal variate; SG1D+MSC= smoothing followed by multiplicative scatter corrections; SG2D+SNV= second-order Savitzky-Golay derivative followed by standard normal variate; SG2D+MSC= second-order Savitzky-Golay derivative followed by multiplicative scatter corrections)

Figure 28. Principal component analysis (PCA) of a) raw and preprocessed b) smoothing; c) SG1D; d) SG2D; e) SNV and f) MSC average NIR spectra of compost samples gathered using NIR spectrometer (AvaSpec-NIR256-2.5-HSC-EVO, Avantes, USA) (SG1D= first-order Savitzky-Golay derivative; SG2D= second-order Savitzky-Golay derivative; SNV= standard normal variate; MSC= multiplicative scatter corrections)
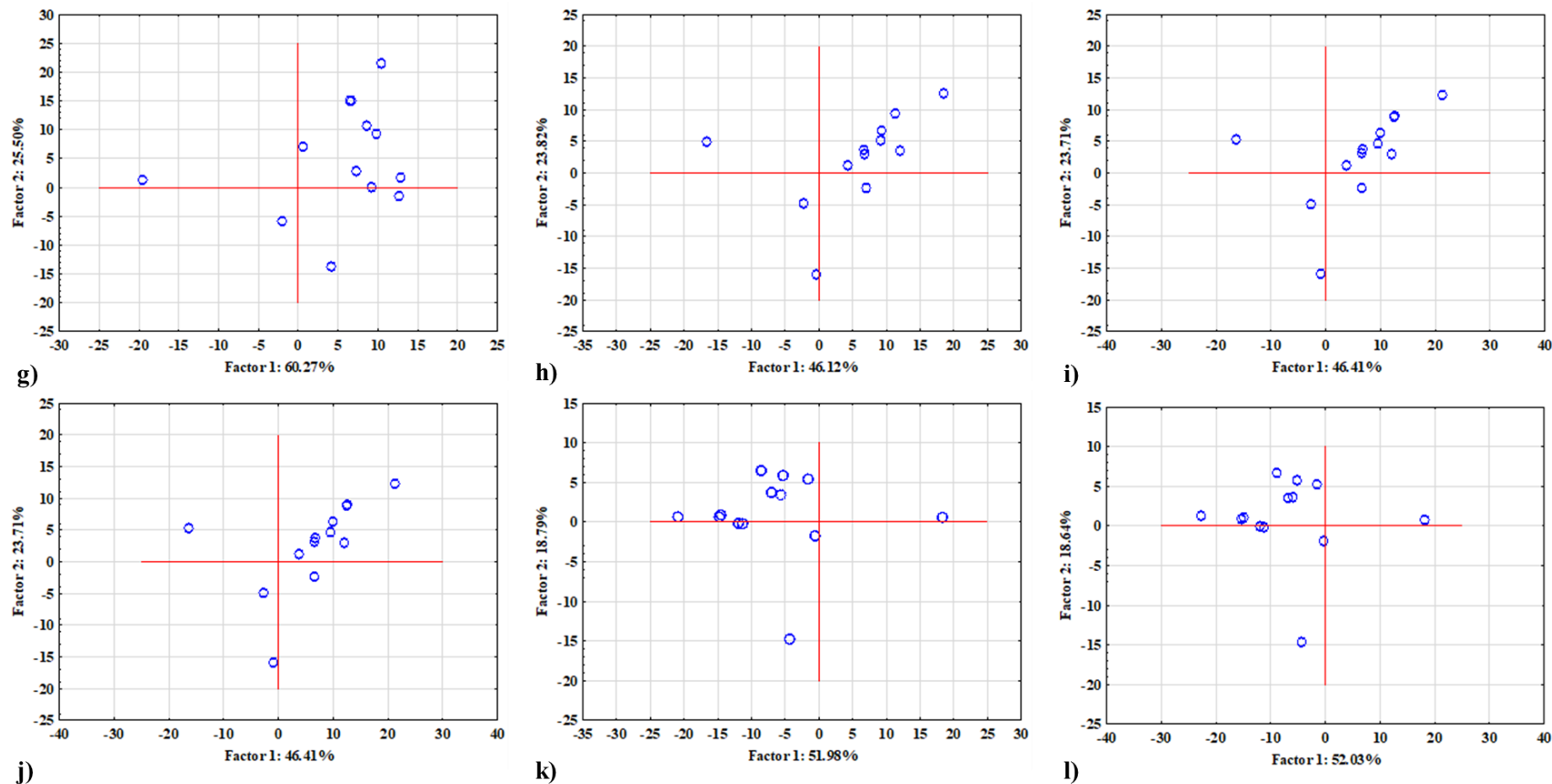
Figure 28. (*continuing*) Principal component analysis (PCA) of g) smoothing+SNV; h) smoothing+MSC; i) SG1D+SNV; j) SG1D+MSC; k) SG2D+SNV and l) SG2D+MSC average NIR spectra of compost samples gathered using NIR spectrometer (AvaSpec-NIR256-2.5-HSC-EVO, Avantes, USA) (smoothing+SNV= smoothing followed by standard normal variate; smoothing+MSC= smoothing followed by multiplicative scatter corrections; SG1D+SNV=first-order Savitzky-Golay derivative followed by standard normal variate; SG1D+MSC= smoothing followed by multiplicative scatter corrections; SG2D+SNV= second-order Savitzky-Golay derivative followed by standard normal variate; SG2D+MSC= second-order Savitzky-Golay derivative followed by multiplicative scatter corrections)
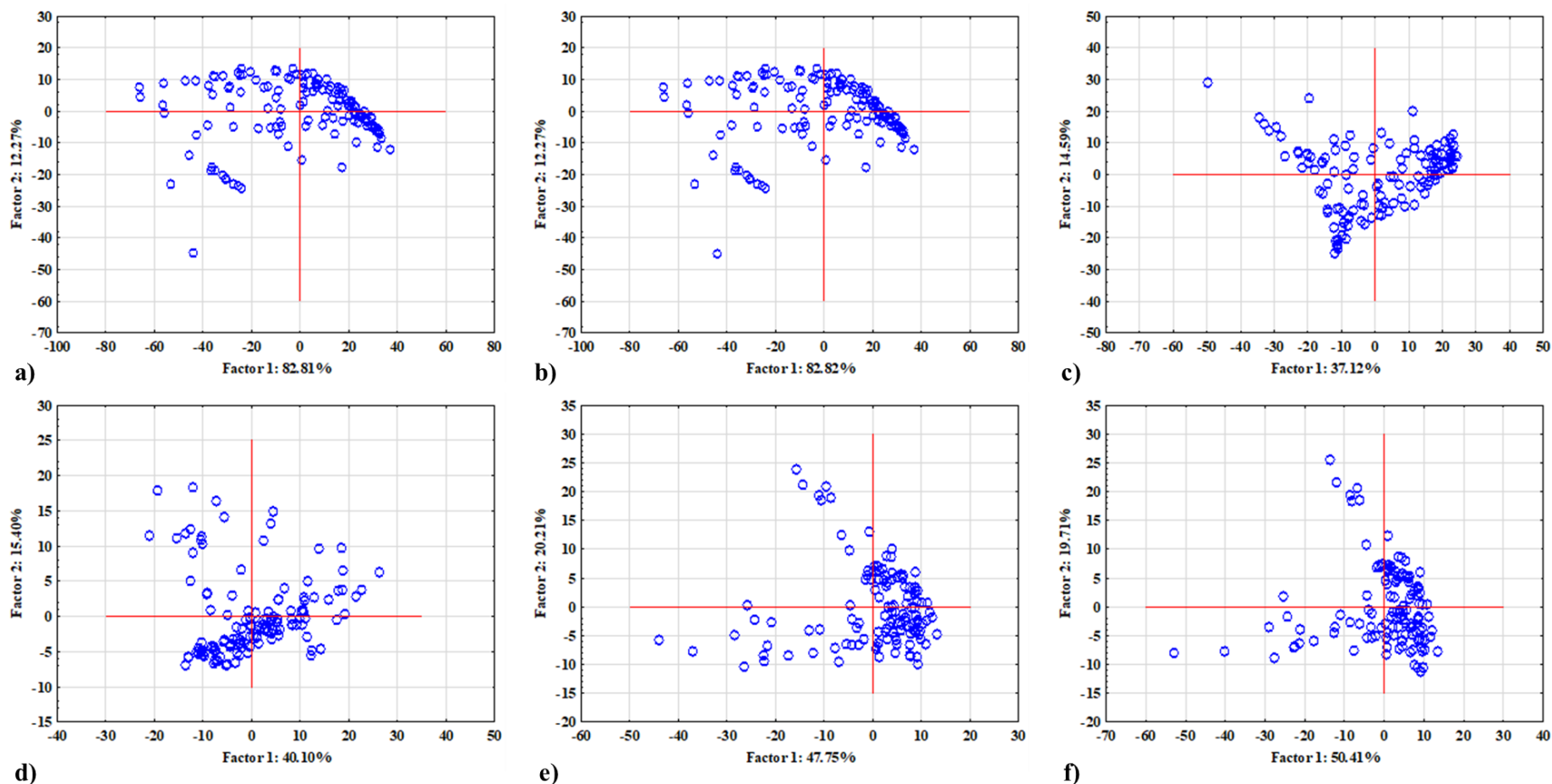
Figure 29. Principal component analysis (PCA) of a) raw and preprocessed b) smoothing; c) SG1D; d) SG2D; e) SNV and f) MSC average NIR spectra of compost extracts samples gathered using NIR spectrometer (AvaSpec-NIR256-2.5-HSC-EVO, Avantes, USA) (SG1D= first-order Savitzky-Golay derivative; SG2D= second-order Savitzky-Golay derivative; SNV= standard normal variate; MSC= multiplicative scatter corrections)
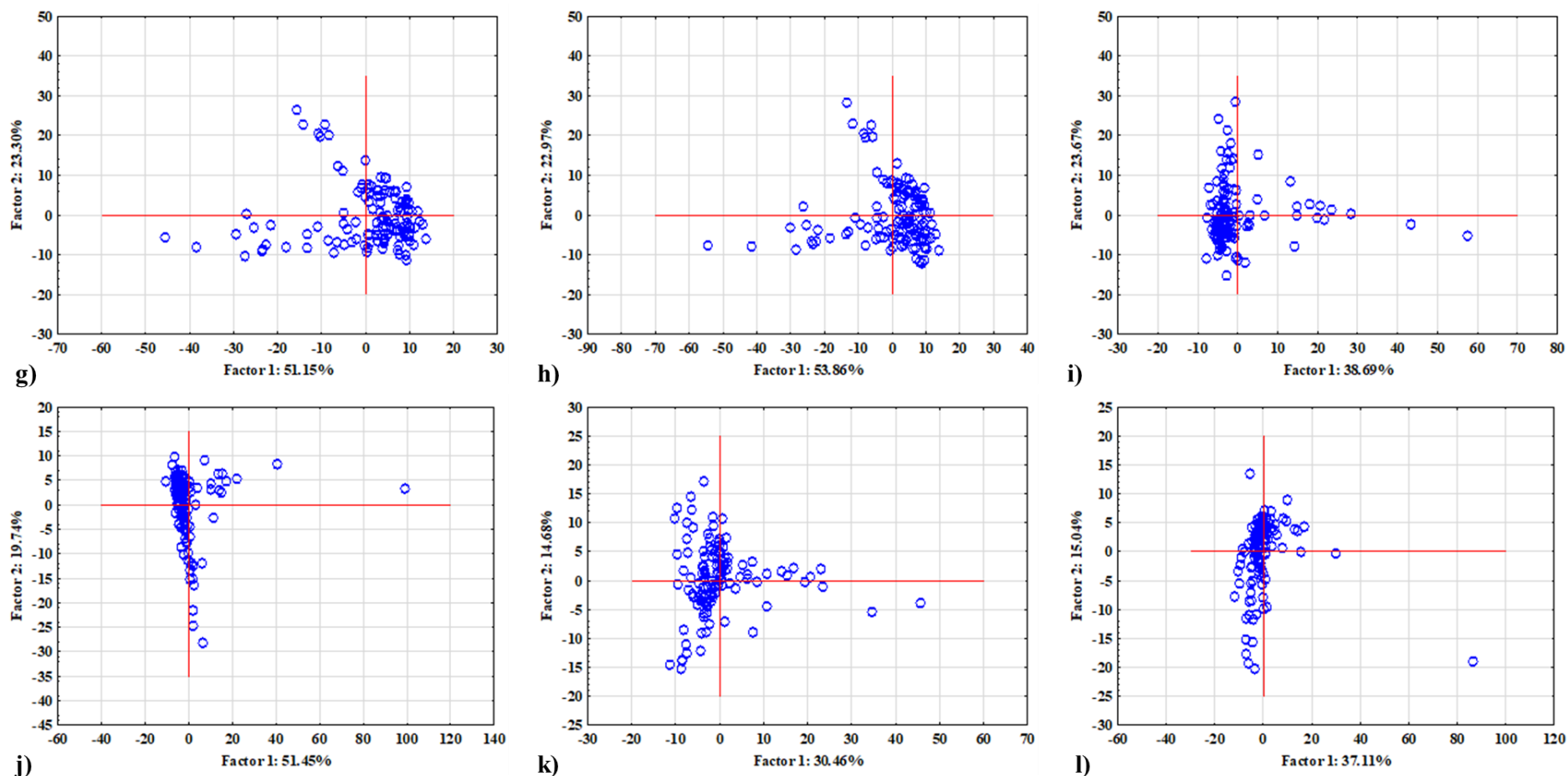
Figure 29. (*continuing*) Principal component analysis (PCA) of g) smoothing+SNV; h) smoothing+MSC; i) SG1D+SNV; j) SG1D+MSC; k) SG2D+SNV; l) SG2D+MSC average NIR spectra of compost extracts samples gathered using NIR spectrometer (AvaSpec-NIR256-2.5-HSC-EVO, Avantes, USA) (smoothing+SNV= smoothing followed by standard normal variate; smoothing+MSC= smoothing followed by multiplicative scatter corrections; SG1D+SNV=first-order Savitzky-Golay derivative followed by standard normal variate; SG1D+MSC= smoothing followed by multiplicative scatter corrections; SG2D+SNV= second-order Savitzky-Golay derivative followed by standard normal variate; SG2D+MSC= second-order Savitzky-Golay derivative followed by multiplicative scatter corrections)

4.1.8. Artificial neural network (ANN) models for the prediction of physicochemical properties of compost samples and compost extracts samples during the composting process

Due to complexity of the NIR spectra, the preprocessing of spectra has been applied in order to obtain important infromation about physicochemical properties of compost. Furthermore, the artificial neural network models were developed based on the recorded NIR spectra for the compost samples and compost extracts. The developed ANN models based on NIR spectra obtained using the NIR spectrometer (NIR-128-1.7-USB/6.25/50 μm, Control Development Inc., USA) for each property of the samples are shown in Tables 17-29. The developed ANN models based on NIR spectra obtained using the another NIR spectrometer (AvaSpec-NIR256-2.5-HSC-EVO, Avantes, USA) for each property of the samples are shown in Tables 30-42. In the tables, the preprocessing method with the greatest *RER* (the ratio of the error range) values are in bold.

Table 17. Artificial neural network (ANN) models for prediction of day of composting of the compost samples during the composting process based on the NIR spectra gathered using NIR spectrometer (NIR-128-1.7-USB/6.25/50 μm, Control Development Inc., USA) (R_{pred}^2=coefficient of determination for prediction; $R_{pred}^2{}_{adj}$=adjusted coefficient of determination for prediction; $RMSEP$=root mean square of prediction; SEP=standard error of prediction; RPD=ratio of prediction to deviation; RER=ratio of the error range). Pretreatment selected as optimal is marked bold

Output variable	NIR spectra pretreatment	Network name	Calibration					Prediction					
			Training perf. Training error	Test perf. Test error	Validation perf. Validation error	Hidden activation	Output activation	R_{pred}^2	$R_{pred}^2{}_{adj}$	$RMSEP$	SEP	RPD	RER
Day of composting	raw	MLP 5-6-1	0.5839 29.1725	0.5073 30.7158	0.4369 41.3116	Exponential	Identity	0.2570	0.1968	8.4320	1.3332	1.0399	3.5579
	smoothing	MLP 5-8-1	0.7939 16.6205	0.7856 21.1921	0.7033 26.4817	Exponential	Tanh	0.1926	0.1271	14.8561	2.3489	0.6191	1.8848
	SG1D	MLP 5-8-1	0.7885 16.6205	0.7277 21.1921	0.6944 26.4817	Tanh	Identity	0.2886	0.2309	8.0964	1.2802	1.1508	3.7053
	SG2D	MLP 5-9-1	0.8298 13.0341	0.8144 13.4357	0.8050 17.8252	Tanh	Logistic	0.3805	0.3303	8.1962	1.2959	1.1777	3.6602
	SNV	**MLP 5-7-1**	**0.8455 12.0252**	**0.8310 16.8627**	**0.7549 25.0996**	**Exponential**	**Tanh**	**0.3632**	**0.3116**	**7.1749**	**1.1345**	**1.2612**	**4.1812**
	MSC	MLP 5-5-1	0.8353 14.1384	0.8129 15.2955	0.8044 19.0774	Tanh	Logistic	0.4021	0.3537	7.2720	1.1498	1.2146	3.8504
	smoothing+SNV	MLP 5-10-1	0.8343 14.1021	0.8076 16.5322	0.7096 19.2098	Tanh	Identity	0.2834	0.2253	8.7789	1.3881	1.0743	3.4173
	smoothing+MSC	MLP 5-7-1	0.8468 12.2032	0.7223 23.1928	0.6980 26.5952	Exponential	Tanh	0.1708	0.1036	10.3614	1.6383	0.8474	2.8954
	SG1D+SNV	MLP 5-4-1	0.7370 19.1375	0.6667 24.1200	0.6483 28.8962	Exponential	Exponential	0.0839	0.0097	9.1916	1.4533	0.9796	3.2639
	SG1D+MSC	MLP 5-9-1	0.8464 17.1428	0.7913 19.3368	0.6789 24.4542	Exponential	Logistic	0.3401	0.2866	7.9816	1.2620	1.0046	3.7586
	SG2D+SNV	MLP 5-9-1	0.8616 11.2582	0.8608 16.7532	0.8592 17.4223	Tanh	Logistic	0.0730	0.0021	11.4968	1.8178	0.7667	2.4355
	SG2D+MSC	MLP 5-9-1	0.6221 12.6195	0.5947 22.6195	0.4258 30.6758	Logistic	Tanh	0.1450	0.0756	10.1399	1.6033	1.0116	2.9586

Table 18. Artificial neural network (ANN) models for prediction of moisture content of the compost samples during the composting process based on the NIR spectra gathered using NIR spectrometer (NIR-128-1.7-USB/6.25/50 μm, Control Development Inc., USA) (R_{pred}^2=coefficient of determination for prediction; $R_{pred}^2{}_{adj}$=adjusted coefficient of determination for prediction; $RMSEP$=root mean square of prediction; SEP=standard error of prediction; RPD=ratio of prediction to deviation; RER=ratio of the error range). Pretreatment selected as optimal is marked bold

Output variable	NIR spectra pretreatment	Network name	Calibration					Prediction					
			Training perf. Training error	Test perf. Test error	Validation perf. Validation error	Hidden activation	Output activation	R_{pred}^2	$R_{pred}^2{}_{adj}$	$RMSEP$	SEP	RPD	RER
Moisture content	raw	MLP 5-8-1	0.5554 10.1205	0.3965 12.8554	0.3468 15.0513	Exponential	Identity	0.1025	0.0297	4.5645	0.7217	0.6321	3.1844
	smoothing	**MLP 5-5-1**	**0.9987 0.0378**	**0.9985 0.0387**	**0.9984 0.0539**	**Tanh**	**Exponential**	**0.9944**	**0.9939**	**0.4156**	**0.0657**	**13.4585**	**44.9551**
	SG1D	MLP 5-3-1	0.7878 3.4105	0.7687 5.9458	0.7455 6.2540	Tanh	Logistic	0.1070	0.0346	4.7219	0.7466	1.0250	4.1544
	SG2D	MLP 5-10-1	0.7557 5.4142	0.7263 10.4748	0.5286 10.47482	Tanh	Tanh	0.1890	0.1233	5.6728	0.8969	1.0281	3.3758
	SNV	MLP 5-10-1	0.8391 5.6338	0.7916 7.8180	0.6835 8.1232	Tanh	Tanh	0.1469	0.0777	5.5791	0.8821	0.8968	3.2018
	MSC	MLP 5-6-1	0.8222 6.8479	0.6265 8.4008	0.6075 10.2232	Logistic	Identity	0.3231	0.2682	4.9427	0.7815	1.1826	4.0970
	smoothing+SNV	MLP 5-4-1	0.9962 0.1174	0.9961 0.1893	0.9882 0.2926	Exponential	Tanh	0.9341	0.9287	1.3664	0.2161	3.8809	14.1278
	smoothing+MSC	MLP 5-6-1	0.8148 4.7146	0.7941 6.7456	0.7159 10.7376	Tanh	Exponential	0.1590	0.0908	5.9338	0.9382	0.9896	3.2273
	SG1D+SNV	MLP 5-10-1	0.6492 8.7858	0.6693 10.7573	0.6388 28.1358	Exponential	Identity	0.0985	0.0254	4.3328	0.6851	0.6659	3.3547
	SG1D+MSC	MLP 5-4-1	0.6454 10.4415	0.6348 17.9331	0.6146 20.5429	Logistic	Logistic	0.2379	0.1761	5.0581	0.7997	1.0137	3.4753
	SG2D+SNV	MLP 5-6-1	0.6464 8.8084	0.6347 11.7853	0.6369 12.3354	Tanh	Exponential	0.2640	0.2044	4.4200	0.6989	1.0904	3.7116
	SG2D+MSC	MLP 5-4-1	0.6291 12.3123	0.5874 18.3346	0.6540 22.9185	Logistic	Exponential	0.2216	0.1585	4.2093	0.6655	1.1159	4.3594

Table 19. Artificial neural network (ANN) models for prediction of dry matter content of the compost samples during the composting process based on the NIR spectra gathered using NIR spectrometer (NIR-128-1.7-USB/6.25/50 μm, Control Development Inc., USA) (R_{pred}^2=coefficient of determination for prediction; $R_{pred}^2{}_{adj}$=adjusted coefficient of determination for prediction; $RMSEP$=root mean square of prediction; SEP=standard error of prediction; RPD=ratio of prediction to deviation; RER=ratio of the error range). Pretreatment selected as optimal is marked bold
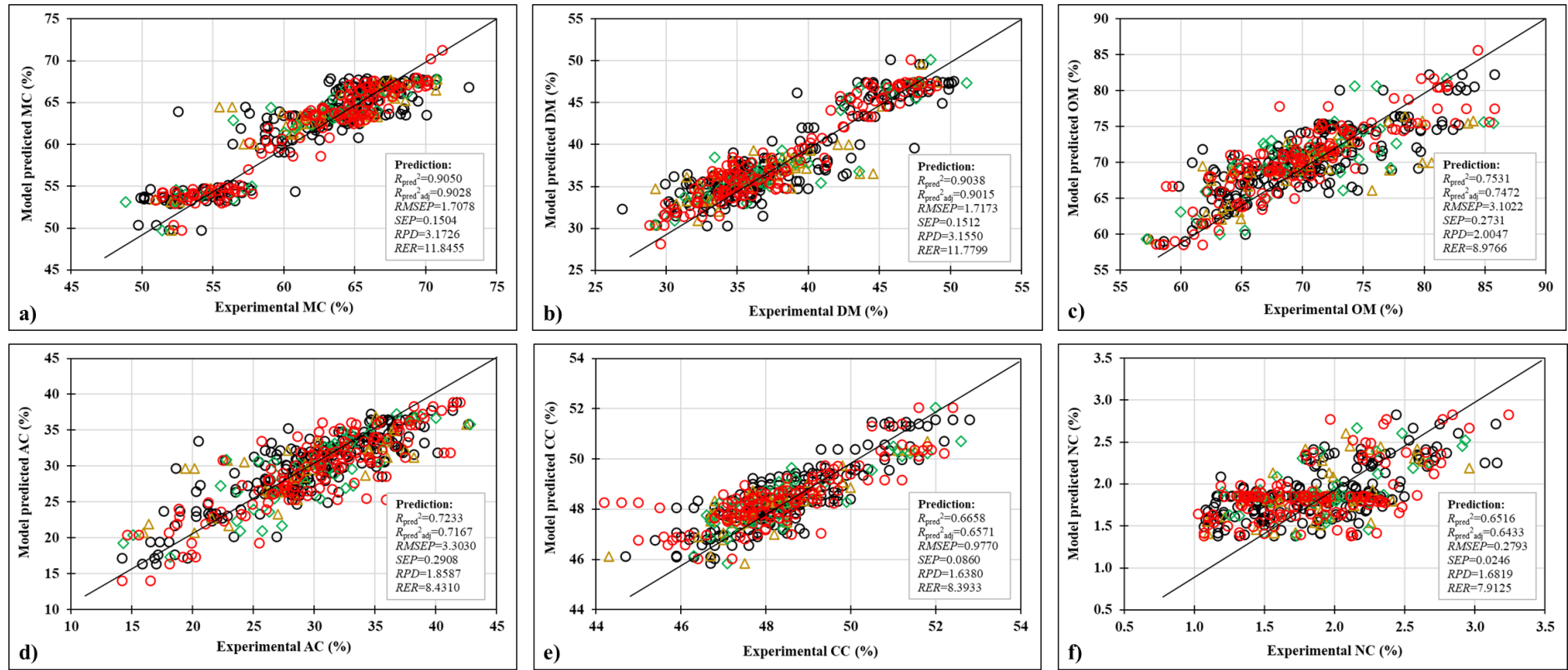
Output variable	NIR spectra pretreatment	Network name	Calibration					Prediction					
			Training perf. Training error	Test perf. Test error	Validation perf. Validation error	Hidden activation	Output activation	R_{pred}^2	$R_{pred}^2{}_{adj}$	$RMSEP$	SEP	RPD	RER
Dry matter content	raw	MLP 5-9-1	0.8396 3.1692	0.8115 7.1564	0.6106 9.9352	Exponential	Tanh	0.1703	0.1031	5.6055	0.8863	0.5147	2.5930
	smoothing	**MLP 5-4-1**	**0.9993 0.0294**	**0.9987 0.0355**	**0.9985 0.0361**	**Tanh**	**Identity**	**0.9977**	**0.9975**	**0.2981**	**0.0471**	**18.7653**	**62.6811**
	SG1D	MLP 5-7-1	0.8747 3.0552	0.8433 7.4561	0.8346 7.4794	Tanh	Identity	0.0797	0.0050	5.0719	0.8019	0.9542	3.8676
	SG2D	MLP 5-10-1	0.7557 8.4152	0.7262 10.4748	0.7242 10.4784	Tanh	Tanh	0.2439	0.1826	6.0184	0.9516	0.9690	3.1819
	SNV	MLP 5-9-1	0.8015 5.5261	0.7944 6.2238	0.6877 8.7895	Tanh	Logistic	0.1768	0.1100	5.2705	0.8333	0.9493	3.3892
	MSC	MLP 5-10-1	0.8025 7.1751	0.6269 9.1600	0.6043 10.5574	Tanh	Tanh	0.3823	0.3323	6.9697	1.1020	0.8387	2.9054
	smoothing+SNV	MLP 5-3-1	0.9962 0.1203	0.9935 0.3073	0.9876 0.3289	Tanh	Exponential	0.9193	0.9128	1.5141	0.2394	3.5024	12.7496
	smoothing+MSC	MLP 5-6-1	0.7324 4.7705	0.7337 9.2733	0.7118 12.4026	Exponential	Tanh	0.1481	0.0791	5.6978	0.9009	1.0306	3.3609
	SG1D+SNV	MLP 5-7-1	0.6946 7.8542	0.6533 10.6772	0.6338 22.5355	Exponential	Tanh	0.1695	0.1022	4.4191	0.6987	0.6529	3.2892
	SG1D+MSC	MLP 5-8-1	0.6558 8.8885	0.6480 16.8209	0.6366 16.9902	Logistic	Logistic	0.5179	0.4788	3.5357	0.5590	1.4501	4.9716
	SG2D+SNV	MLP 5-8-1	0.5725 10.1402	0.5668 11.6237	0.5597 13.2283	Logistic	Logistic	0.3851	0.3352	4.0671	0.6431	1.1850	4.0336
	SG2D+MSC	MLP 5-7-1	0.5985 11.2443	0.5405 15.8488	0.50322 20.9274	Logistic	Exponential	0.2687	0.2094	4.1359	0.6539	1.1356	4.4367

Table 20. Artificial neural network (ANN) models for prediction of organic matter content of the compost samples during the composting process based on the NIR spectra gathered using NIR spectrometer (NIR-128-1.7-USB/6.25/50 μm, Control Development Inc., USA) (R_{pred}^2=coefficient of determination for prediction; $R_{pred}^2{}_{adj}$=adjusted coefficient of determination for prediction; *RMSEP*=root mean square of prediction; *SEP*=standard error of prediction; *RPD*=ratio of prediction to deviation; *RER*=ratio of the error range). Pretreatment selected as optimal is marked bold

| Output variable	NIR spectra pretreatment	Network name	Calibration					Prediction					
			Training perf. Training error	Test perf. Test error	Validation perf. Validation error	Hidden activation	Output activation	R_{pred}^2	$R_{pred}^2{}_{adj}$	*RMSEP*	*SEP*	*RPD*	*RER*
Organic matter content	raw	MLP 5-4-1	0.7807 6.8654	0.7504 9.0871	0.6569 18.0756	Tanh	Identity	0.2003	0.1354	5.2444	0.8292	0.8030	3.6361
	smoothing	**MLP 5-5-1**	**0.9975 0.1078**	**0.9973 0.1127**	**0.9937 0.1777**	**Tanh**	**Tanh**	**0.9840**	**0.9827**	**0.8323**	**0.1316**	**6.8072**	**25.3339**
	SG1D	MLP 5-3-1	0.8611 5.0615	0.7658 8.8748	0.6910 10.1300	Exponential	Tanh	0.1340	0.0638	5.3500	0.8459	0.9571	3.9148
	SG2D	MLP 5-9-1	0.7802 4.6659	0.7202 9.1399	0.6805 10.9684	Logistic	Tanh	0.2443	0.1831	5.2732	0.8338	0.9898	4.5794
	SNV	MLP 5-8-1	0.8619 5.0063	0.8374 5.3625	0.8017 6.1832	Tanh	Logistic	0.1941	0.1288	5.3619	0.8478	1.0657	4.4413
	MSC	MLP 5-4-1	0.7807 6.8654	0.7504 9.0871	0.6569 18.0756	Tanh	Identity	0.2932	0.2359	11.4443	1.8095	0.5330	2.2559
	smoothing+SNV	MLP 5-4-1	0.9938 0.2655	0.9906 0.2845	0.9842 0.5154	Logistic	Logistic	0.9335	0.9281	1.4880	0.2353	3.7873	17.3503
	smoothing+MSC	MLP 5-11-1	0.8024 5.2829	0.7838 9.4680	0.6478 11.8055	Tanh	Exponential	0.2154	0.1518	5.5593	0.8790	0.9327	4.1566
	SG1D+SNV	MLP 5-6-1	0.7878 8.0126	0.6896 10.0793	0.6335 10.4021	Exponential	Identity	0.1114	0.0393	4.1936	0.6631	1.0042	4.5473
	SG1D+MSC	MLP 5-10-1	0.7305 7.9336	0.7034 10.6153	0.6221 13.5745	Tanh	Identity	0.2277	0.1650	4.2133	0.6662	1.0957	5.6781
	SG2D+SNV	MLP 5-7-1	0.8419 4.0228	0.6630 7.5049	0.6062 6.4536	Tanh	Logistic	0.3403	0.2868	5.3565	0.8469	1.1892	4.6073
	SG2D+MSC	MLP 5-10-1	0.6614 9.9115	0.6503 11.8159	0.6405 16.4807	Logistic	Identity	0.5036	0.4633	3.6485	0.5769	1.3392	6.8154

Table 21. Artificial neural network (ANN) models for prediction of ash content of the compost samples during the composting process based on the NIR spectra gathered using NIR spectrometer (NIR-128-1.7-USB/6.25/50 μm, Control Development Inc., USA) (R_{pred}^2=coefficient of determination for prediction; $R_{pred}^2{}_{adj}$=adjusted coefficient of determination for prediction; *RMSEP*=root mean square of prediction; *SEP*=standard error of prediction; *RPD*=ratio of prediction to deviation; *RER*=ratio of the error range). Pretreatment selected as optimal is marked bold

Output variable	NIR spectra pretreatment	Network name	Calibration					Prediction					
			Training perf. Training error	Test perf. Test error	Validation perf. Validation error	Hidden activation	Output activation	R_{pred}^2	$R_{pred}^2{}_{adj}$	*RMSEP*	*SEP*	*RPD*	*RER*
Ash content	raw spectra	MLP 5-10-1	0.7726 7.9259	0.6606 16.0589	0.6491 45.4394	Tanh	Tanh	0.1765	0.1098	5.1692	0.8173	0.8147	3.6890
	smoothing	**MLP 5-5-1**	**0.9953 0.1677**	**0.9947 0.1885**	**0.9922 0.2307**	**Tanh**	**Exponential**	**0.9870**	**0.9860**	**0.7509**	**0.1187**	**7.5449**	**28.0795**
	SG1D	MLP 5-3-1	0.8611 5.0615	0.7657 8.8749	0.6910 17.1300	Exponential	Tanh	0.2062	0.1419	5.1289	0.8109	0.9983	4.0836
	SG2D	MLP 5-9-1	0.8184 5.7771	0.8075 9.5782	0.7966 12.1156	Exponential	Tanh	0.1685	0.1011	6.3966	1.0114	0.8160	3.7752
	SNV	MLP 5-7-1	0.7671 7.4257	0.6907 8.6351	0.6755 10.2968	Exponential	Logistic	0.2282	0.1656	5.1504	0.8144	1.1094	4.6237
	MSC	MLP 5-4-1	0.7660 7.4257	0.7158 9.1354	0.5527 14.8834	Logistic	Exponential	0.3113	0.2554	5.3251	0.8420	1.1480	4.8483
	smoothing+SNV	MLP 5-4-1	0.9962 0.2103	0.9961 0.2285	0.9886 0.4207	Logistic	Tanh	0.3964	0.3474	4.7627	0.7531	1.1821	5.4208
	smoothing+MSC	MLP 5-4-1	0.8231 6.4884	0.7882 9.4326	0.6978 10.2335	Tanh	Logistic	0.1823	0.1160	5.7999	0.9170	0.8940	3.9842
	SG1D+SNV	MLP 5-8-1	0.8241 5.9648	0.7752 7.2075	0.6383 9.1979	Tanh	Logistic	0.0079	-0.0725	4.9874	0.7886	0.8443	3.8235
	SG1D+MSC	MLP 5-6-1	0.7255 7.4415	0.6733 13.6290	0.6483 16.2272	Exponential	Logistic	0.1647	0.0969	7.1078	1.1238	0.6495	3.3658
	SG2D+SNV	MLP 5-5-1	0.9319 4.2353	0.6673 4.5598	0.6517 7.6032	Exponential	Exponential	0.3193	0.2641	5.4346	0.8593	1.1541	4.5411
	SG2D+MSC	MLP 5-9-1	0.7148 8.4457	0.6279 12.9839	0.6272 16.1628	Exponential	Logistic	0.3934	0.3443	4.1159	0.6508	1.1871	6.0414

Table 22. Artificial neural network (ANN) models for prediction of carbon content of the compost samples during the composting process based on the NIR spectra gathered using NIR spectrometer (NIR-128-1.7-USB/6.25/50 μm, Control Development Inc., USA) (R_{pred}^2=coefficient of determination for prediction; $R_{pred}^2{}_{adj}$=adjusted coefficient of determination for prediction; $RMSEP$=root mean square of prediction; SEP=standard error of prediction; RPD=ratio of prediction to deviation; RER=ratio of the error range). Pretreatment selected as optimal is marked bold

Output variable	NIR spectra pretreatment	Network name	Calibration					Prediction					
			Training perf. Training error	Test perf. Test error	Validation perf. Validation error	Hidden activation	Output activation	R_{pred}^2	$R_{pred}^2{}_{adj}$	$RMSEP$	SEP	RPD	RER
Carbon content	raw spectra	MLP 5-9-1	0.6063 0.6764	0.5386 1.1052	0.5109 1.5937	Logistic	Tanh	0.1233	0.0522	1.9459	0.3077	0.6666	3.1862
	smoothing	**MLP 5-7-1**	**0.8455 0.5655**	**0.7850 0.8072**	**0.7129 0.8455**	**Logistic**	**Logistic**	**0.3470**	**0.2940**	**1.2353**	**0.1953**	**1.0916**	**5.1000**
	SG1D	MLP 5-9-1	0.7785 0.6363	0.6884 0.9542	0.6398 1.1121	Exponential	Identity	0.0856	0.0114	2.0568	0.3252	0.7523	3.3548
	SG2D	MLP 5-8-1	0.8319 0.6267	0.7469 0.7072	0.7367 0.8768	Logistic	Logistic	0.3032	0.2467	1.4222	0.2249	1.1294	4.9923
	SNV	MLP 5-6-1	0.8284 0.4996	0.8049 1.1271	0.7387 1.1511	Tanh	Tanh	0.4389	0.3934	1.4910	0.2358	1.2406	4.6948
	MSC	MLP 5-6-1	0.8284 0.4996	0.8049 1.1271	0.7387 1.1511	Tanh	Exponential	0.3216	0.2666	7.4291	1.1746	0.2343	1.0903
	smoothing+SNV	MLP 5-7-1	0.8443 0.4725	0.8245 0.6527	0.6953 0.9373	Tanh	Exponential	0.2625	0.2027	1.8450	0.2917	1.0019	4.2277
	smoothing+MSC	MLP 5-11-1	0.8812 0.2925	0.8435 0.5856	0.7615 0.7037	Tanh	Identity	0.2095	0.1454	1.8599	0.2941	0.9798	4.2476
	SG1D+SNV	MLP 5-9-1	0.8565 0.7429	0.7319 0.8321	0.6219 0.8454	Logistic	Identity	0.0884	0.0144	1.3292	0.2102	0.9759	4.6644
	SG1D+MSC	MLP 5-10-1	0.8756 0.4251	0.8033 0.6122	0.7118 0.7077	Tanh	Identity	0.2876	0.2298	1.5533	0.2456	1.1386	4.8284
	SG2D+SNV	MLP 5-5-1	0.8484 0.4510	0.8327 0.5913	0.7533 0.6592	Tanh	Tanh	0.2682	0.2089	1.6223	0.2565	1.0895	4.7463
	SG2D+MSC	MLP 5-11-1	0.8081 0.5704	0.7641 0.6353	0.7431 0.8397	Tanh	Tanh	0.1386	0.0688	1.9068	0.3015	0.9767	4.2479

Table 23. Artificial neural network (ANN) models for prediction of nitrogen content of the compost samples during the composting process based on the NIR spectra gathered using NIR spectrometer (NIR-128-1.7-USB/6.25/50 μm, Control Development Inc., USA) (R_{pred}^2=coefficient of determination for prediction; $R_{pred}^2{}_{adj}$=adjusted coefficient of determination for prediction; $RMSEP$=root mean square of prediction; SEP=standard error of prediction; RPD=ratio of prediction to deviation; RER=ratio of the error range). Pretreatment selected as optimal is marked bold

Output variable	NIR spectra pretreatment	Network name	Calibration					Prediction					
			Training perf. Training error	Test perf. Test error	Validation perf. Validation error	Hidden activation	Output activation	R_{pred}^2	$R_{pred}^2{}_{adj}$	$RMSEP$	SEP	RPD	RER
Nitrogen content	raw spectra	MLP 5-9-1	0.7698 0.0140	0.7621 0.2231	0.6965 0.0259	Logistic	Exponential	0.0930	0.0195	0.4429	0.0700	0.8976	3.0708
	smoothing	MLP 5-8-1	0.9326 0.0040	0.8911 0.011	0.8376 0.0012	Tanh	Exponential	0.7024	0.6783	0.1936	0.0306	1.3959	5.5788
	SG1D	MLP 5-4-1	0.6655 0.0269	0.6549 0.0319	0.6219 0.0398	Logistic	Exponential	0.2339	0.1718	0.2759	0.0436	1.1315	5.4004
	SG2D	MLP 5-3-1	0.7271 0.0242	0.6177 0.0368	0.60526 0.0662	Logistic	Identity	0.0801	0.0055	0.2693	0.0426	0.8973	3.8983
	SNV	MLP 5-9-1	0.9197 0.0066	0.6515 0.0088	0.6400 0.0406	Logistic	Tanh	0.2613	0.2014	0.2317	0.0366	1.1295	4.4461
	MSC	MLP 5-9-1	0.6587 0.0151	0.6214 0.0264	0.6103 0.0387	Exponential	Exponential	0.1474	0.0782	0.4745	0.0750	0.7143	2.8661
	smoothing+SNV	**MLP 5-4-1**	**0.9406 0.0042**	**0.9463 0.0043**	**0.9456 0.0054**	**Identity**	**Exponential**	**0.8730**	**0.8627**	**0.1229**	**0.0194**	**2.7410**	**10.4991**
	smoothing+MSC	MLP 5-11-1	0.8038 0.0130	0.7923 0.0205	0.6555 0.0245	Tanh	Tanh	0.1488	0.0798	0.2966	0.0469	0.8895	4.3491
	SG1D+SNV	MLP 5-4-1	0.6291 0.0143	0.5909 0.0169	0.5712 0.0241	Logistic	Logistic	0.2089	0.1448	0.4075	0.0644	0.9756	3.3375
	SG1D+MSC	MLP 5-11-1	0.7204 0.0154	0.6452 0.0166	0.6114 0.0345	Tanh	Exponential	0.1964	0.1312	0.2606	0.0412	1.1335	4.3354
	SG2D+SNV	MLP 5-9-1	0.7269 0.0156	0.6954 0.02748	0.5405 0.0618	Logistic	Exponential	0.1215	0.0503	0.2810	0.0444	0.9406	3.4873
	SG2D+MSC	MLP 5-4-1	0.8710 0.0045	0.6581 0.0111	0.5587 0.0279	Tanh	Logistic	0.1167	0.0451	0.3718	0.0588	1.0289	4.2230

Table 24. Artificial neural network (ANN) models for prediction of carbon to nitrogen (C/N) ratio of the compost samples during the composting process based on the NIR spectra gathered using NIR spectrometer (NIR-128-1.7-USB/6.25/50 μm, Control Development Inc., USA) (R_{pred}^2=coefficient of determination for prediction; $R_{pred}^2{}_{adj}$=adjusted coefficient of determination for prediction; $RMSEP$=root mean square of prediction; SEP=standard error of prediction; RPD=ratio of prediction to deviation; RER=ratio of the error range). Pretreatment selected as optimal is marked bold

Output variable	NIR spectra pretreatment	Network name	Calibration					Prediction					
			Training perf. Training error	Test perf. Test error	Validation perf. Validation error	Hidden activation	Output activation	R_{pred}^2	$R_{pred}^2{}_{adj}$	$RMSEP$	SEP	RPD	RER
C/N ratio	raw spectra	MLP 5-4-1	0.7896 2.2447	0.7240 4.3708	0.7094 6.1104	Logistic	Identity	0.1301	0.0595	5.6899	0.8996	0.9379	2.9412
	smoothing	MLP 5-3-1	0.8355 1.0221	0.8218 3.4094	0.7558 5.3590	Tanh	Identity	0.6162	0.5850	2.9096	0.4600	1.3807	5.3292
	SG1D	MLP 5-3-1	0.7039 5.9997	0.6884 6.0806	0.6494 6.6891	Tanh	Logistic	0.2346	0.1725	4.1277	0.6526	1.1365	5.5631
	SG2D	MLP 5-9-1	0.7988 3.5978	0.6935 13.2147	0.6405 15.8150	Tanh	Identity	0.1072	0.0348	6.9096	1.0925	0.5749	2.7718
	SNV	MLP 5-9-1	0.9017 2.3570	0.6662 6.1312	0.6404 8.4362	Tanh	Exponential	0.3418	0.2885	3.3222	0.5253	1.1553	4.5319
	MSC	MLP 5-10-1	0.8301 3.4459	0.6267 5.6548	0.6200 6.0675	Tanh	Logistic	0.1798	0.1133	5.8185	0.9200	0.7810	2.9292
	smoothing+SNV	**MLP 5-10-1**	**0.9603 0.4904**	**0.9594 0.7338**	**0.9252 1.0411**	**Logistic**	**Identity**	**0.8082**	**0.7927**	**2.3779**	**0.3760**	**2.2158**	**9.1270**
	smoothing+MSC	MLP 5-4-1	0.8072 3.4172	0.7552 4.2922	0.6415 5.8031	Logistic	Identity	0.1751	0.1082	4.5907	0.7259	0.9034	4.7276
	SG1D+SNV	MLP 5-5-1	0.7506 2.7989	0.5408 4.9562	0.5107 6.0275	Tanh	Identity	0.1539	0.0853	5.7170	0.9039	0.9335	2.9273
	SG1D+MSC	MLP 5-4-1	0.8404 4.2823	0.7111 4.3788	0.6341 6.8592	Tanh	Identity	0.1067	0.0343	4.5570	0.7205	0.9619	3.6254
	SG2D+SNV	MLP 5-3-1	0.7551 3.6321	0.6945 5.1385	0.6301 9.3871	Logistic	Identity	0.2461	0.1849	3.5432	0.5602	1.1140	3.8640
	SG2D+MSC	MLP 5-11-1	0.6553 4.9327	0.6528 5.7809	0.6553 10.4168	Exponential	Logistic	0.1871	0.1212	5.3415	0.8446	1.0315	4.2989

Table 25. Artificial neural network (ANN) models for prediction of total color change (ΔE) of the compost samples during the composting process based on the NIR spectra gathered using NIR spectrometer (NIR-128-1.7-USB/6.25/50 µm, Control Development Inc., USA) (R_{pred}^2=coefficient of determination for prediction; $R_{pred}^2{}_{adj}$=adjusted coefficient of determination for prediction; $RMSEP$=root mean square of prediction; SEP=standard error of prediction; RPD=ratio of prediction to deviation; RER=ratio of the error range). Pretreatment selected as optimal is marked bold

| Output variable | NIR spectra pretreatment | Network name | Calibration | | | | | Prediction | | | | | |
			Training perf. Training error	Test perf. Test error	Validation perf. Validation error	Hidden activation	Output activation	R_{pred}^2	$R_{pred}^2{}_{adj}$	$RMSEP$	SEP	RPD	RER
ΔE (compost)	raw spectra	MLP 5-6-1	0.7424 3.4734	0.6787 9.2355	0.6244 11.9412	Tanh	Exponential	0.0942	0.0207	3.4393	0.5438	0.3848	2.1338
	smoothing	MLP 5-6-1	0.8569 1.1366	0.7273 1.9281	0.6584 4.3033	Logistic	Tanh	0.4125	0.3649	2.9245	0.4624	1.2270	4.4150
	SG1D	MLP 5-5-1	0.7810 2.1722	0.7707 2.1356	0.7494 4.0141	Logistic	Logistic	0.2186	0.1552	3.7100	0.5866	1.1211	3.9601
	SG2D	MLP 5-7-1	0.7087 2.7437	0.5726 4.5634	0.5384 7.9037	Logistic	Tanh	0.3798	0.3296	3.8014	0.6011	1.1286	4.1178
	SNV	MLP 5-5-1	0.8727 1.5759	0.8552 2.2630	0.8550 1.8319	Exponential	Logistic	0.4992	0.4586	3.3709	0.5330	1.1764	4.6771
	MSC	MLP 5-9-1	0.8829 2.1708	0.8368 2.5036	0.7803 3.1918	Exponential	Tanh	0.4715	0.4287	3.4576	0.5467	1.0709	3.9268
	smoothing+SNV	MLP 5-5-1	0.7929 2.1084	0.7744 2.8104	0.7257 3.4392	Tanh	Logistic	0.5385	0.5011	5.1408	0.8128	0.7464	2.8205
	smoothing+MSC	MLP 5-3-1	0.8153 2.6231	0.6616 4.0326	0.6241 6.8165	Identity	Exponential	0.3921	0.3428	2.9918	0.4730	1.1969	4.2904
	SG1D+SNV	MLP 5-7-1	0.7664 3.1687	0.7132 4.9811	0.6203 7.7434	Logistic	Exponential	0.0886	0.0147	3.3658	0.5322	0.3932	2.1804
	SG1D+MSC	MLP 5-3-1	0.8163 2.5131	0.7948 3.0431	0.7354 3.1932	Tanh	Logistic	0.0807	0.0062	4.2238	0.6678	0.8709	3.6154
	SG2D+SNV	MLP 5-8-1	0.8135 2.6061	0.7320 2.7189	0.7316 3.2914	Logistic	Logistic	0.3170	0.2617	3.2809	0.5188	1.0907	3.9901
	SG2D+MSC	**MLP 5-9-1**	**0.7438 4.6378**	**0.5752 4.8578**	**0.5654 4.8228**	**Tanh**	**Logistic**	**0.1909**	**0.1252**	**3.1987**	**0.5058**	**1.1569**	**4.8341**

Table 26. Artificial neural network (ANN) models for prediction of pH of the compost samples during the composting process based on the NIR spectra gathered using NIR spectrometer (NIR-128-1.7-USB/6.25/50 µm, Control Development Inc., USA) (R_{pred}^2=coefficient of determination for prediction; $R_{pred}^2{}_{adj}$=adjusted coefficient of determination for prediction; $RMSEP$=root mean square of prediction; SEP=standard error of prediction; RPD=ratio of prediction to deviation; RER=ratio of the error range). Pretreatment selected as optimal is marked bold

Output variable	NIR spectra pretreatment	Network name	Calibration					Prediction					
			Training perf. Training error	Test perf. Test error	Validation perf. Validation error	Hidden activation	Output activation	R_{pred}^2	$R_{pred}^2{}_{adj}$	$RMSEP$	SEP	RPD	RER
pH	raw spectra	MLP 5-10-1	0.7971 0.2629	0.5478 0.5377	0.5200 0.5415	Exponential	Tanh	0.1393	0.0696	1.0777	0.1704	0.9910	3.7208
	smoothing	MLP 5-5-1	0.7127 0.3439	0.5484 0.4227	0.5199 0.5952	Logistic	Logistic	0.1559	0.0875	1.2684	0.2006	0.8420	3.1614
	SG1D	MLP 5-7-1	0.7246 0.3849	0.6663 0.4221	0.4295 0.4349	Logistic	Tanh	0.1193	0.0479	1.1461	0.1812	0.9319	3.4989
	SG2D	MLP 5-5-1	0.7675 0.3587	0.6958 0.3604	0.6853 0.3655	Exponential	Tanh	0.1562	0.0878	2.9358	0.4642	0.3638	1.3659
	SNV	**MLP 5-5-1**	**0.7348 0.3218**	**0.5594 0.4127**	**0.5518 0.5995**	**Exponential**	**Tanh**	**0.4194**	**0.3723**	**0.8386**	**0.1326**	**1.2735**	**4.7817**
	MSC	MLP 5-8-1	0.6781 0.3788	0.5857 0.4955	0.5087 0.5452	Logistic	Tanh	0.1259	0.0550	1.1758	0.1859	0.9083	3.4104
	smoothing+SNV	MLP 5-8-1	0.7722 0.2769	0.7506 0.3825	0.5575 0.4262	Exponential	Identity	0.4294	0.3831	3.7730	0.5966	0.2831	1.0628
	smoothing+MSC	MLP 5-9-1	0.7377 0.3189	0.5293 0.4356	0.5032 0.6423	Exponential	Tanh	0.0873	0.0133	1.5669	0.2477	0.6816	2.5592
	SG1D+SNV	MLP 5-6-1	0.6299 0.3634	0.5919 0.5328	0.4881 0.6386	Tanh	Exponential	0.1366	0.0666	1.1667	0.1845	0.9154	3.4370
	SG1D+MSC	MLP 5-10-1	0.6396 0.49476	0.5415 0.54482	0.4917 0.7533	Tanh	Identity	0.1708	0.1036	1.1073	0.1751	0.9645	3.6215
	SG2D+SNV	MLP 5-5-1	0.7880 0.3088	0.6315 0.4201	0.5035 0.5245	Exponential	Identity	0.1028	0.0301	2.4212	0.3828	0.4411	1.6562
	SG2D+MSC	MLP 5-4-1	0.8417 0.4322	0.6312 0.5032	0.5295 0.8417	Exponential	Identity	0.1881	0.1223	2.4305	0.3843	0.4394	1.6499

Table 27. Artificial neural network (ANN) models for prediction of total dissolved solids (TDS) of the compost samples during the composting process based on the NIR spectra gathered using NIR spectrometer (NIR-128-1.7-USB/6.25/50 μm, Control Development Inc., USA) (R_{pred}^2=coefficient of determination for prediction; $R_{pred}^2{}_{adj}$=adjusted coefficient of determination for prediction; $RMSEP$=root mean square of prediction; SEP=standard error of prediction; RPD=ratio of prediction to deviation; RER=ratio of the error range). Pretreatment selected as optimal is marked bold

Output variable	NIR spectra pretreatment	Network name	Calibration					Prediction					
			Training perf. Training error	Test perf. Test error	Validation perf. Validation error	Hidden activation	Output activation	R_{pred}^2	$R_{pred}^2{}_{adj}$	$RMSEP$	SEP	RPD	RER
TDS	raw spectra	MLP 5-8-1	0.8277 3293.66	0.7902 42884.49	0.7845 44982.81	Exponential	Tanh	0.1597	0.0916	363.8039	57.5224	0.9000	3.5385
	smoothing	MLP 5-5-1	0.8082 3374.04	0.7811 4382.53	0.7443 5086.81	Logistic	Exponential	0.2569	0.1966	326.7202	51.6590	1.0021	3.9402
	SG1D	MLP 5-9-1	0.6766 5360.69	0.6173 6840.51	0.6005 7613.86	Tanh	Exponential	0.4329	0.3869	262.4615	41.4988	1.2475	4.9048
	SG2D	MLP 5-3-1	0.6338 5395.63	0.6118 7913.51	0.5187 8199.49	Tanh	Exponential	0.2536	0.1931	307.8960	48.6826	1.0634	4.1811
	SNV	**MLP 5-4-1**	**0.8193 3943.03**	**0.7677 4912.67**	**0.7375 4989.54**	**Tanh**	**Tanh**	**0.7684**	**0.7497**	**157.8980**	**24.9659**	**2.0736**	**8.1529**
	MSC	MLP 5-3-1	0.8127 4004.38	0.7345 4995.52	0.7321 5980.21	Tanh	Logistic	0.5089	0.4691	256.0765	40.4892	1.2786	5.0271
	smoothing+SNV	MLP 5-11-1	0.8310 3982.42	0.7518 4844.85	0.7358 5174.37	Exponential	Logistic	0.3689	0.3177	280.2602	44.3130	1.1683	4.5934
	smoothing+MSC	MLP 5-6-1	0.8352 4007.53	0.7225 4138.17	0.7066 5498.95	Tanh	Logistic	0.5092	0.4694	238.6703	37.7371	1.3718	5.3938
	SG1D+SNV	MLP 5-10-1	0.6947 5136.58	0.6446 6248.66	0.6372 7307.48	Logistic	Exponential	0.1151	0.0434	331.7226	52.4499	0.9870	3.8808
	SG1D+MSC	MLP 5-8-1	0.6925 5392.38	0.6292 6605.55	0.6139 7417.76	Tanh	Exponential	0.3249	0.2701	290.1861	45.8824	1.1283	4.4362
	SG2D+SNV	MLP 5-8-1	0.6779 5453.38	0.6248 6843.55	0.6064 7987.76	Identity	Identity	0.3249	0.4139	243.8320	38.5532	1.3428	5.2796
	SG2D+MSC	MLP 5-8-1	0.6837 6186.93	0.6068 6656.89	0.6001 9567.62	Tanh	Identity	0.4294	0.3832	277.5859	43.8902	1.1795	4.6376

Table 28. Artificial neural network (ANN) models for prediction of conductivity (S) of the compost samples during the composting process based on the NIR spectra gathered using NIR spectrometer (NIR-128-1.7-USB/6.25/50 μm, Control Development Inc., USA) (R_{pred}^2=coefficient of determination for prediction; $R_{pred}^2{}_{adj}$=adjusted coefficient of determination for prediction; $RMSEP$=root mean square of prediction; SEP=standard error of prediction; RPD=ratio of prediction to deviation; RER=ratio of the error range). Pretreatment selected as optimal is marked bold

| Output variable | NIR spectra pretreatment | Network name | Calibration | | | | | Prediction | | | | | |
			Training perf. Training error	Test perf. Test error	Validation perf. Validation error	Hidden activation	Output activation	R_{pred}^2	$R_{pred}^2{}_{adj}$	$RMSEP$	SEP	RPD	RER
S	raw spectra	MLP 5-9-1	0.7686 1325.07	0.7612 2207.31	0.7362 2267.74	Logistic	Tanh	0.5250	0.4865	482.1836	76.2399	1.3386	5.0548
	smoothing	MLP 5-8-1	0.7921 1423.19	0.7496 2198.88	0.7205 2407.58	Exponential	Logistic	0.4825	0.4405	515.2234	81.4640	1.2528	4.7306
	SG1D	MLP 5-5-1	0.6333 19690.00	0.6258 2638.12	0.6158 3352.84	Exponential	Identity	0.5608	0.5251	440.0957	69.5852	1.4666	5.5382
	SG2D	MLP 5-11-1	0.6117 2060.00	0.6025 3126.43	0.5286 3713.62	Logistic	Exponential	0.5256	0.4872	463.8397	73.3395	1.3916	5.2547
	SNV	MLP 5-6-1	0.8072 1459.75	0.7422 2157.56	0.7356 2310.91	Exponential	Logistic	0.5485	0.5118	458.7013	72.5270	1.4072	5.3136
	MSC	**MLP 5-11-1**	**0.8515 1564.50**	**0.8471 1594.70**	**0.7129 233.02**	**Tanh**	**Identity**	**0.5528**	**0.5165**	**440.0167**	**69.5728**	**1.4669**	**5.5392**
	smoothing+SNV	MLP 5-6-1	0.8085 1349.44	0.7805 1997.37	0.7649 2072.15	Exponential	Logistic	0.4904	0.4490	617.5374	97.6412	1.0452	3.9469
	smoothing+MSC	MLP 5-11-1	0.8318 1518.20	0.7782 1853.39	0.7315 2371.72	Tanh	Identity	0.1317	0.0613	879.9875	139.1382	0.7335	2.7697
	SG1D+SNV	MLP 5-9-1	0.6938 1928.46	0.6787 2379.83	0.6406 3154.77	Logistic	Exponential	0.3806	0.3304	521.7969	82.5033	1.2370	4.6710
	SG1D+MSC	MLP 5-6-1	0.6521 1936.46	0.6366 2638.83	0.6228 3172.77	Logistic	Exponential	0.3837	0.3337	508.8868	80.4621	1.2684	4.7895
	SG2D+SNV	MLP 5-9-1	0.6321 2025.57	0.6311 2713.23	0.6151 3405.15	Logistic	Exponential	0.2770	0.2184	578.9056	91.5330	1.1150	4.2102
	SG2D+MSC	MLP 5-4-1	0.6851 2176.81	0.6212 2788.24	0.5727 3263.69	Logistic	Exponential	0.4801	0.4379	474.1152	74.9642	1.3614	5.1408

Table 29. Artificial neural network (ANN) models for prediction of total color change (ΔE) of the compost extracts during the composting process based on the NIR spectra gathered using NIR spectrometer (NIR-128-1.7-USB/6.25/50 μm, Control Development Inc., USA) (R_{pred}^2=coefficient of determination for prediction; $R_{pred}^2{}_{adj}$=adjusted coefficient of determination for prediction; $RMSEP$=root mean square of prediction; SEP=standard error of prediction; RPD=ratio of prediction to deviation; RER=ratio of the error range). Pretreatment selected as optimal is marked bold

| Output variable | NIR spectra pretreatment | Network name | Calibration | | | | | Prediction | | | | | |
			Training perf. Training error	Test perf. Test error	Validation perf. Validation error	Hidden activation	Output activation	R_{pred}^2	$R_{pred}^2{}_{adj}$	$RMSEP$	SEP	RPD	RER
ΔE (extracts)	raw spectra	MLP 5-10-1	0.8809 0.1153	0.7816 0.3835	0.7278 0.3318	Exponential	Tanh	0.1782	0.1116	1.2128	0.1918	0.8607	3.0021
	smoothing	MLP 5-10-1	0.9389 0.0455	0.9764 0.0611	0.7843 0.3508	Exponential	Logistic	0.2198	0.1565	1.2144	0.1920	0.8595	2.9982
	SG1D	MLP 5-11-1	0.9601 0.0991	0.8983 0.1194	0.8411 0.3510	Exponential	Exponential	0.2201	0.1569	1.2911	0.2041	0.8085	2.8200
	SG2D	MLP 5-8-1	0.9804 0.0603	0.9434 0.0455	0.8363 0.3287	Tanh	Logistic	0.1450	0.0757	1.6654	0.2633	0.6268	2.1863
	SNV	MLP 5-9-1	0.9697 0.1094	0.8497 0.1436	0.7624 0.3084	Tanh	Logistic	0.0899	0.0161	28.9539	4.5780	0.0361	0.1258
	MSC	MLP 5-9-1	0.9318 0.1496	0.8445 0.1804	0.7622 0.3441	Exponential	Exponential	0.3660	0.3146	0.9776	0.1546	1.0678	3.7246
	smoothing+SNV	**MLP 5-10-1**	**0.8454 0.1480**	**0.8186 0.3707**	**0.7484 0.4824**	**Tanh**	**Exponential**	**0.4696**	**0.4265**	**0.7025**	**0.1111**	**1.4075**	**5.1832**
	smoothing+MSC	MLP 5-6-1	0.9545 0.1453	0.8462 0.1456	0.7523 0.3101	Exponential	Logistic	0.1643	0.0965	1.0412	0.1646	1.0025	3.4969
	SG1D+SNV	MLP 5-4-1	0.9122 0.1778	0.8297 0.2176	0.7721 0.2367	Exponential	Exponential	0.1138	0.0420	1.0231	0.1618	1.0203	3.5588
	SG1D+MSC	MLP 5-4-1	0.8498 0.1437	0.8473 0.2417	0.8347 0.3653	Exponential	Tanh	0.2538	0.1933	1.0322	0.1632	1.0113	3.5275
	SG2D+SNV	MLP 5-9-1	0.9340 0.1545	0.8505 0.3064	0.8373 0.3818	Exponential	Exponential	0.3692	0.3180	1.0281	0.1626	1.0153	3.5415
	SG2D+MSC	MLP 5-10-1	0.7782 0.2536	0.7567 0.3897	0.7123 0.3194	Exponential	Logistic	0.3324	0.2782	0.9046	0.1430	1.1540	4.0252

Table 30. Artificial neural network (ANN) models for prediction of day of composting of the compost samples during the composting process based on the NIR spectra gathered using NIR spectrometer (AvaSpec-NIR256-2.5-HSC-EVO, Avantes, USA) (R_{pred}^2=coefficient of determination for prediction; $R_{pred}^2{}_{adj}$=adjusted coefficient of determination for prediction; $RMSEP$=root mean square of prediction; SEP=standard error of prediction; RPD=ratio of prediction to deviation; RER=ratio of the error range). Pretreatment selected as optimal is marked bold

Output variable	NIR spectra pretreatment	Network name	Calibration					Prediction					
			Training perf. Training error	Test perf. Test error	Validation perf. Validation error	Hidden activation	Output activation	R_{pred}^2	$R_{pred}^2{}_{adj}$	$RMSEP$	SEP	RPD	RER
Day of composting	raw	MLP 5-9-1	0.8708 9.2180	0.7603 13.7170	0.7559 24.1615	Tanh	Exponential	0.6230	0.5925	6.1155	0.9669	1.5684	4.3653
	smoothing	MLP 5-5-1	0.9518 3.9955	0.8321 19.9636	0.7598 22.0526	Tanh	Tanh	0.2850	0.2270	8.4941	1.3430	1.1139	3.3683
	SG1D	**MLP 5-7-1**	**0.8791 9.8650**	**0.7923 19.9727**	**0.7199 26.0503**	**Tanh**	**Logistic**	**0.7514**	**0.7313**	**3.9939**	**0.6315**	**1.9212**	**6.4896**
	SG2D	MLP 5-5-1	0.8094 0.7703	0.7703 13.7108	0.7136 31.9012	Tanh	Identity	0.4374	0.3918	7.1666	1.1331	1.3203	3.9762
	SNV	MLP 5-11-1	0.5993 24.8182	0.5855 23.6472	0.5936 26.7255	Logistic	Exponential	0.2837	0.2256	8.1719	1.2921	1.1415	3.8146
	MSC	MLP 5-11-1	0.5653 27.7587	0.5638 26.6818	0.54788 31.5666	Exponential	Exponential	0.4000	0.3513	6.8439	1.0821	1.2896	3.8222
	smoothing+SNV	MLP 5-11-1	0.5898 18.7570	0.5082 16.5465	0.4787 22.4013	Logistic	Logistic	0.1736	0.1066	8.4605	1.3377	1.0569	3.4209
	smoothing+MSC	MLP 5-6-1	0.6153 20.8299	0.5924 21.2048	0.5643 24.3679	Logistic	Exponential	0.1761	0.1093	8.8900	1.4056	1.0530	3.8585
	SG1D+SNV	MLP 5-10-1	0.8249 20.6933	0.6227 25.2481	0.5763 27.5441	Exponential	Tanh	0.3496	0.2969	8.4531	1.3365	1.0893	3.5490
	SG1D+MSC	MLP 5-5-1	0.6264 31.1937	0.5253 32.8967	0.5177 34.0949	Tanh	Exponential	0.0537	0.0230	8.2739	1.3082	1.1098	3.1758
	SG2D+SNV	MLP 5-7-1	0.5467 31.1253	0.4880 36.5562	0.4303 37.9323	Exponential	Exponential	0.2510	0.1903	7.8556	1.2421	1.1532	3.7123
	SG2D+MSC	MLP 5-7-1	0.5085 35.0756	0.4826 36.0271	0.4676 36.7027	Exponential	Identity	0.4567	0.4127	6.0449	0.9558	1.3490	5.1029

Table 31. Artificial neural network (ANN) models for prediction of moisture content of the compost samples during the composting process based on the NIR spectra gathered using NIR spectrometer (AvaSpec-NIR256-2.5-HSC-EVO, Avantes, USA) (R_{pred}^2=coefficient of determination for prediction; $R_{pred}^2{}_{adj}$=adjusted coefficient of determination for prediction; $RMSEP$=root mean square of prediction; SEP=standard error of prediction; RPD=ratio of prediction to deviation; RER=ratio of the error range). Pretreatment selected as optimal is marked bold

Output variable	NIR spectra pretreatment	Network name	Calibration					Prediction					
			Training perf. Training error	Test perf. Test error	Validation perf. Validation error	Hidden activation	Output activation	R_{pred}^2	$R_{pred}^2{}_{adj}$	$RMSEP$	SEP	RPD	RER
Moisture content	raw	MLP 5-8-1	0.8852 2.1320	0.8023 7.9806	0.6538 10.6045	Logistic	Logistic	0.3209	0.2658	4.8194	0.7620	1.1566	2.9182
	smoothing	MLP 5-7-1	0.9237 2.9241	0.7281 4.9638	0.7140 6.0292	Tanh	Logistic	0.0003	-0.0808	10.1943	1.6119	0.5623	1.2222
	SG1D	MLP 5-5-1	0.7676 5.5117	0.7236 8.5644	0.6105 9.3526	Logistic	Logistic	0.6448	0.6160	3.4176	0.5404	1.6796	5.0555
	SG2D	MLP 5-9-1	0.7410 5.1612	0.7031 5.9118	0.6596 7.4896	Tanh	Tanh	0.3696	0.3185	4.5619	0.7213	1.2566	4.0497
	SNV	MLP 5-9-1	0.7652 5.6178	0.6891 7.7789	0.5807 13.8809	Tanh	Logistic	0.5080	0.4682	3.5303	0.5582	1.4083	4.0803
	MSC	MLP 5-3-1	0.8528 3.8738	0.8398 4.6513	0.7983 4.7017	Tanh	Tanh	0.3200	0.2648	5.0248	0.7945	1.1735	3.0512
	smoothing+SNV	MLP 5-8-1	0.6467 4.7510	0.6338 8.2945	0.5268 10.3276	Logistic	Exponential	0.4222	0.3753	4.2915	0.6785	1.3129	3.6039
	smoothing+MSC	MLP 5-11-1	0.7381 5.3863	0.7035 7.7037	0.7198 8.0772	Exponential	Logistic	0.3091	0.2531	10.9955	1.7385	0.5143	1.3302
	SG1D+SNV	MLP 5-11-1	0.7257 6.8732	0.7024 6.9796	0.6898 7.5256	Exponential	Logistic	0.2608	0.2009	4.9864	0.7884	1.0883	3.8509
	SG1D+MSC	MLP 5-4-1	0.7936 6.8286	0.7203 7.0167	0.6173 11.6551	Logistic	Tanh	0.0501	0.0269	5.9699	4.7827	0.5888	2.4780
	SG2D+SNV	MLP 5-4-1	0.7264 6.6300	0.6558 8.2128	0.6605 11.3279	Logistic	Exponential	0.4146	0.3672	3.9556	0.6254	1.1910	3.3613
	SG2D+MSC	**MLP 5-6-1**	**0.7869 4.8395**	**0.6209 11.0523**	**0.6116 13.2731**	**Exponential**	**Tanh**	**0.4752**	**0.4327**	**3.9093**	**0.6181**	**1.3377**	**5.1029**

Table 32. Artificial neural network (ANN) models for prediction of dry matter content of the compost samples during the composting process based on the NIR spectra gathered using NIR spectrometer (AvaSpec-NIR256-2.5-HSC-EVO, Avantes, USA) (R_{pred}^2=coefficient of determination for prediction; $R_{pred}^2{}_{adj}$=adjusted coefficient of determination for prediction; *RMSEP*=root mean square of prediction; *SEP*=standard error of prediction; *RPD*=ratio of prediction to deviation; *RER*=ratio of the error range). Pretreatment selected as optimal is marked bold

Output variable	NIR spectra pretreatment	Network name	Calibration					Prediction					
			Training perf. Training error	Test perf. Test error	Validation perf. Validation error	Hidden activation	Output activation	R_{pred}^2	$R_{pred}^2{}_{adj}$	*RMSEP*	*SEP*	*RPD*	*RER*
Dry matter content	raw	MLP 5-7-1	0.8591 2.5862	0.7898 8.3500	0.6488 10.5606	Logistic	Exponential	0.4476	0.4028	4.2467	0.6715	1.3126	4.3133
	smoothing	MLP 5-10-1	0.9269 2.9191	0.7499 4.8763	0.6709 7.0524	Exponential	Exponential	0.6788	0.6527	6.3010	0.9963	0.9098	3.1909
	SG1D	MLP 5-3-1	0.7547 5.6135	0.7174 8.7338	0.6010 10.0737	Logistic	Identity	0.6391	0.6099	3.4870	0.5514	1.6462	4.3154
	SG2D	MLP 5-7-1	0.7063 5.7590	0.7053 6.5681	0.6668 7.8324	Exponential	Exponential	0.4645	0.4211	4.2652	0.6744	1.3441	3.7541
	SNV	MLP 5-7-1	0.7606 5.7156	0.7073 7.5432	0.5848 13.6541	Logistic	Exponential	0.5127	0.4732	3.4990	0.5532	1.4209	4.7655
	MSC	MLP 5-5-1	0.8498 3.6871	0.8429 4.7022	0.7982 5.0744	Logistic	Logistic	0.3052	0.2489	8.5169	1.3466	0.6923	2.6512
	smoothing+SNV	MLP 5-9-1	0.7122 4.7408	0.6949 6.8418	0.6305 7.9142	Exponential	Logistic	0.4222	0.3753	25.9965	4.1104	0.2167	1.4144
	smoothing+MSC	MLP 5-4-1	0.7305 5.6842	0.7241 7.1305	0.6392 10.2632	Exponential	Identity	0.3383	0.2847	7.3777	1.1665	0.7665	2.1930
	SG1D+SNV	MLP 5-10-1	0.7256 6.1505	0.6362 10.044	0.6020 10.5207	Tanh	Tanh	0.0490	0.0758	6.9296	1.0957	0.7831	2.8240
	SG1D+MSC	MLP 5-3-1	0.7578 7.0436	0.7097 7.8531	0.6396 10.9381	Logistic	Tanh	0.1488	0.0798	3.2979	0.5214	1.0658	3.9936
	SG2D+SNV	MLP 5-10-1	0.7083 6.7543	0.6931 8.4387	0.6365 9.5411	Logistic	Exponential	0.5507	0.5142	3.3393	0.5280	1.4108	4.9673
	SG2D+MSC	**MLP 5-10-1**	**0.7552 5.4691**	**0.7088 9.5505**	**0.6025 12.3802**	**Logistic**	**Exponential**	**0.4683**	**0.4252**	**3.8773**	**0.6131**	**1.3488**	**5.1029**

Table 33. Artificial neural network (ANN) models for prediction of organic matter content of the compost samples during the composting process based on the NIR spectra gathered using NIR spectrometer (AvaSpec-NIR256-2.5-HSC-EVO, Avantes, USA) (R_{pred}^2=coefficient of determination for prediction; $R_{pred}^2{}_{adj}$=adjusted coefficient of determination for prediction; $RMSEP$=root mean square of prediction; SEP=standard error of prediction; RPD=ratio of prediction to deviation; RER=ratio of the error range). Pretreatment selected as optimal is marked bold

Output variable	NIR spectra pretreatment	Network name	Calibration					Prediction					
			Training perf. Training error	Test perf. Test error	Validation perf. Validation error	Hidden activation	Output activation	R_{pred}^2	$R_{pred}^2{}_{adj}$	$RMSEP$	SEP	RPD	RER
Organic matter content	raw	MLP 5-8-1	0.7094 8.8137	0.6687 9.8357	0.6426 11.3482	Logistic	Logistic	0.1967	0.1315	5.6342	0.8909	1.1110	3.3775
	smoothing	MLP 5-8-1	0.5267 10.6582	0.5156 12.4395	0.5262 16.1719	Identity	Tanh	0.2631	0.2033	5.5515	0.8778	1.1050	2.8329
	SG1D	MLP 5-6-1	0.7241 6.1728	0.7219 10.9347	0.6341 16.2974	Exponential	Logistic	0.2589	0.1988	5.6257	0.8895	1.1533	3.9125
	SG2D	MLP 5-7-1	0.5356 9.4053	0.5425 11.5147	0.5215 19.8569	Exponential	Exponential	0.3980	0.3492	4.8119	0.7608	1.2749	4.0070
	SNV	MLP 5-10-1	0.5355 9.999	0.5222 11.7308	0.5156 23.7156	Exponential	Tanh	0.0652	0.0106	5.4177	0.8566	0.9884	3.0894
	MSC	MLP 5-5-1	0.5815 8.8137	0.5149 9.8357	0.5523 11.3482	Logistic	Logistic	0.0016	0.0793	7.1255	1.1266	0.9267	2.7155
	smoothing+SNV	MLP 5-7-1	0.5678 10.0433	0.5186 12.8924	0.5022 27.2434	Exponential	Logistic	0.0299	0.0488	4.9449	0.7819	0.9882	3.2483
	smoothing+MSC	MLP 5-5-1	0.5577 11.2427	0.5129 13.3040	0.5277 13.4023	Tanh	Logistic	0.0642	0.0117	12.3840	1.9581	0.4929	1.3056
	SG1D+SNV	MLP 5-10-1	0.7112 2.3727	0.6429 9.5798	0.5376 14.1735	Tanh	Identity	0.0551	0.0210	16.8734	2.6679	0.3986	3.3752
	SG1D+MSC	MLP 5-10-1	0.5379 9.5309	0.4376 12.8379	0.4144 25.8489	Tanh	Identity	0.0908	0.0705	2.1710	0.3433	0.9616	3.6298
	SG2D+SNV	MLP 5-10-1	0.5379 9.5309	0.4376 12.8379	0.4144 25.8489	Tanh	Identity	0.1088	0.0365	3.9223	0.6202	1.0583	2.8945
	SG2D+MSC	**MLP 5-4-1**	**0.5379 11.3571**	**0.4378 15.2671**	**0.4098 18.4410**	**Logistic**	**Tanh**	**0.1453**	**0.0760**	**5.2690**	**0.8331**	**1.0662**	**5.1029**

Table 34. Artificial neural network (ANN) models for prediction of ash content of the compost samples during the composting process based on the NIR spectra gathered using NIR spectrometer (AvaSpec-NIR256-2.5-HSC-EVO, Avantes, USA) (R_{pred}^2=coefficient of determination for prediction; $R_{pred}^2{}_{adj}$=adjusted coefficient of determination for prediction; $RMSEP$=root mean square of prediction; SEP=standard error of prediction; RPD=ratio of prediction to deviation; RER=ratio of the error range). Pretreatment selected as optimal is marked bold

Output variable	NIR spectra pretreatment	Network name	Calibration					Prediction					
			Training perf. Training error	Test perf. Test error	Validation perf. Validation error	Hidden activation	Output activation	R_{pred}^2	$R_{pred}^2{}_{adj}$	$RMSEP$	SEP	RPD	RER
Ash content	raw spectra	MLP 5-7-1	0.6632 7.5883	0.6319 8.6492	0.5505 11.9075	Logistic	Exponential	0.2117	0.1478	5.5863	0.8833	1.1205	3.6109
	smoothing	MLP 5-7-1	0.5617 11.0265	0.5416 11.5828	0.5414 15.5546	Identity	Tanh	0.2730	0.2141	5.2264	0.8264	1.1525	3.3400
	SG1D	MLP 5-10-1	0.7399 7.0438	0.6766 10.3819	0.5416 15.6905	Exponential	Logistic	0.0780	0.0032	6.2307	0.9852	1.0237	3.7371
	SG2D	MLP 5-8-1	0.5761 8.8124	0.5137 11.5264	0.5457 20.4258	Tanh	Exponential	0.2897	0.2321	5.0821	0.8035	1.1852	4.0783
	SNV	MLP 5-10-1	0.5534 10.0425	0.5067 16.9378	0.5039 27.1165	Logistic	Exponential	0.0423	0.0354	5.4072	0.8550	0.9671	3.1572
	MSC	MLP 5-5-1	0.5881 8.9561	0.5145 8.9944	0.5508 13.0699	Logistic	Identity	0.0031	0.0777	7.0109	1.1085	0.9418	2.4711
	smoothing+SNV	MLP 5-3-1	0.6149 9.9663	0.5805 10.0037	0.5911 16.9587	Logistic	Identity	0.0569	0.0196	4.8518	0.7671	1.0071	2.8377
	smoothing+MSC	MLP 5-5-1	0.5782 9.9663	0.5805 10.0037	0.5911 16.9587	Exponential	Logistic	0.0701	0.0053	7.4861	1.1837	0.8002	2.1728
	SG1D+SNV	MLP 5-6-1	0.5790 3.3243	0.5753 9.7665	0.5072 15.9806	Exponential	Logistic	0.0009	0.0801	8.1383	1.2868	0.8265	2.0882
	SG1D+MSC	MLP 5-4-1	0.5187 10.6129	0.4605 16.4466	0.4543 21.0789	Tanh	Identity	0.1205	0.0492	3.8461	2.3679	0.8792	1.6859
	SG2D+SNV	MLP 5-6-1	0.5865 15.1234	0.5369 15.4188	0.4369 27.1024	Exponential	Identity	0.0928	0.0193	5.0113	0.7924	1.0481	3.4215
	SG2D+MSC	**MLP 5-9-1**	**0.6672 12.8377**	**0.5783 15.3933**	**0.5703 16.7527**	**Tanh**	**Tanh**	**0.0567**	**0.0198**	**5.5291**	**0.8742**	**1.0161**	**5.1029**

Table 35. Artificial neural network (ANN) models for prediction of carbon content of the compost samples during the composting process based on the NIR spectra gathered using NIR spectrometer (AvaSpec-NIR256-2.5-HSC-EVO, Avantes, USA) (R_{pred}^2=coefficient of determination for prediction; $R_{pred}^2{}_{adj}$=adjusted coefficient of determination for prediction; $RMSEP$=root mean square of prediction; SEP=standard error of prediction; RPD=ratio of prediction to deviation; RER=ratio of the error range). Pretreatment selected as optimal is marked bold

| Output variable | NIR spectra pretreatment | Network name | Calibration | | | | | Prediction | | | | | |
			Training perf. Training error	Test perf. Test error	Validation perf. Validation error	Hidden activation	Output activation	R_{pred}^2	$R_{pred}^2{}_{adj}$	$RMSEP$	SEP	RPD	RER
Carbon content	raw spectra	MLP 5-5-1	0.5976 0.7878	0.5239 0.7897	0.5148 1.4499	Logistic	Exponential	0.0996	0.0266	2.3265	0.3678	0.7187	4.5181
	smoothing	MLP 5-9-1	0.7867 0.5476	0.5394 0.7934	0.5235 1.3379	Logistic	Tanh	0.1533	0.0846	2.0280	0.3207	0.9263	3.4348
	SG1D	MLP 5-9-1	0.7532 0.5776	0.6287 0.9224	0.5920 1.3778	Tanh	Logistic	0.1638	0.0121	1.8789	0.2971	0.9278	3.7954
	SG2D	MLP 5-6-1	0.7638 0.9781	0.5185 1.2359	0.5593 1.3978	Logistic	Exponential	0.1837	0.1176	1.7659	0.2792	1.0638	3.6419
	SNV	MLP 5-11-1	0.7356 0.2787	0.5987 1.2170	0.5801 1.5206	Identity	Identity	0.1815	0.0070	1.6810	0.2658	1.0280	2.8263
	MSC	MLP 5-3-1	0.6561 0.9327	0.6294 1.0678	0.5814 1.2818	Exponential	Tanh	0.2002	0.0809	1.9423	0.3071	0.8100	2.8102
	smoothing+SNV	MLP 5-9-1	0.6971 0.7606	0.6839 1.0291	0.5814 1.9307	Logistic	Logistic	0.1295	0.0589	1.7077	0.2700	1.0239	2.8450
	smoothing+MSC	MLP 5-5-1	0.6505 0.9511	0.6209 1.2392	0.6148 1.9482	Logistic	Logistic	0.1684	0.0072	7.6851	1.2151	0.2473	0.5446
	SG1D+SNV	MLP 5-8-1	0.6795 0.9268	0.6577 1.1162	0.5979 1.7956	Tanh	Logistic	0.1346	0.0437	2.1925	0.3467	0.7462	3.0558
	SG1D+MSC	MLP 5-8-1	0.5541 1.2667	0.5273 1.2862	0.5254 1.7446	Exponential	Logistic	0.1320	0.0465	1.4141	3.5373	0.9384	3.2306
	SG2D+SNV	MLP 5-8-1	0.7625 1.1622	0.5249 1.7380	0.5147 2.1809	Tanh	Exponential	0.2826	0.2244	1.5114	0.2390	1.1709	3.3735
	SG2D+MSC	**MLP 5-11-1**	**0.6497 0.9001**	**0.6367 1.1801**	**0.5305 1.8672**	**Exponential**	**Tanh**	**0.1767**	**0.1100**	**1.7089**	**0.2702**	**1.0858**	**5.1029**

Table 36. Artificial neural network (ANN) models for prediction of nitrogen content of the compost samples during the composting process based on the NIR spectra gathered using NIR spectrometer (AvaSpec-NIR256-2.5-HSC-EVO, Avantes, USA) (R_{pred}^2=coefficient of determination for prediction; $R_{pred}^2{}_{adj}$=adjusted coefficient of determination for prediction; $RMSEP$=root mean square of prediction; SEP=standard error of prediction; RPD=ratio of prediction to deviation; RER=ratio of the error range). Pretreatment selected as optimal is marked bold

Output variable	NIR spectra pretreatment	Network name	Calibration					Prediction					
			Training perf. Training error	Test perf. Test error	Validation perf. Validation error	Hidden activation	Output activation	R_{pred}^2	$R_{pred}^2{}_{adj}$	$RMSEP$	SEP	RPD	RER
Nitrogen content	raw spectra	MLP 5-7-1	0.7333 0.0459	0.6467 0.0294	0.5759 0.0478	Tanh	Exponential	0.3541	0.3017	0.2665	0.0421	1.2261	4.2961
	smoothing	MLP 5-7-1	0.7279 0.0195	0.5859 0.0226	0.5854 0.0321	Logistic	Tanh	0.3383	0.2846	0.3517	0.0556	0.8749	4.0068
	SG1D	**MLP 5-4-1**	**0.8497 0.0181**	**0.7179 0.0229**	**0.7092 0.0377**	**Tanh**	**Exponential**	**0.3452**	**0.2921**	**0.2130**	**0.0337**	**1.1975**	**5.1944**
	SG2D	MLP 5-7-1	0.7565 0.0233	0.6965 0.0337	0.5362 0.0339	Exponential	Logistic	0.1011	0.0282	0.3090	0.0489	0.9960	3.0756
	SNV	MLP 5-11-1	0.6623 0.0239	0.5843 0.0363	0.5975 0.0393	Exponential	Tanh	0.1210	0.0497	0.3063	0.0484	1.0571	2.3129
	MSC	MLP 5-11-1	0.6219 0.0306	0.5816 0.0382	0.5064 0.0528	Logistic	Logistic	0.0544	0.0223	0.2620	0.0414	1.0016	2.5937
	smoothing+SNV	MLP 5-5-1	0.5453 0.0447	0.5107 0.0449	0.5256 0.0537	Exponential	Exponential	0.1204	0.0491	0.2690	0.0425	0.9460	3.8854
	smoothing+MSC	MLP 5-5-1	0.5363 0.0296	0.5308 0.0388	0.5443 0.0406	Exponential	Exponential	0.1898	0.0160	0.4310	0.0682	0.7202	1.5470
	SG1D+SNV	MLP 5-9-1	0.5165 0.0317	0.5308 0.0467	0.5169 0.0545	Logistic	Tanh	0.1365	0.0416	0.4313	0.0682	0.6460	3.5698
	SG1D+MSC	MLP 5-9-1	0.7071 0.0041	0.5419 0.0412	0.5367 0.0516	Exponential	Identity	0.1522	0.0246	0.3046	0.1519	1.1578	2.4271
	SG2D+SNV	MLP 5-9-1	0.7314 0.0199	0.6374 0.0277	0.5367 0.0377	Exponential	Logistic	0.2374	0.1756	0.3124	0.0494	1.1229	2.5471
	SG2D+MSC	MLP 5-9-1	0.8019 0.0199	0.6084 0.0277	0.5782 0.0377	Logistic	Tanh	0.1784	0.1118	0.2529	0.0400	1.0946	5.1029

Table 37. Artificial neural network (ANN) models for prediction of carbon to nitrogen (C/N) ratio of the compost samples during the composting process based on the NIR spectra gathered using NIR spectrometer (AvaSpec-NIR256-2.5-HSC-EVO, Avantes, USA) (R_{pred}^2=coefficient of determination for prediction; $R_{pred}^2{}_{adj}$=adjusted coefficient of determination for prediction; $RMSEP$=root mean square of prediction; SEP=standard error of prediction; RPD=ratio of prediction to deviation; RER=ratio of the error range). Pretreatment selected as optimal is marked bold

Output variable	NIR spectra pretreatment	Network name	Calibration					Prediction					
			Training perf. Training error	Test perf. Test error	Validation perf. Validation error	Hidden activation	Output activation	R_{pred}^2	$R_{pred}^2{}_{adj}$	$RMSEP$	SEP	RPD	RER
C/N ratio	raw spectra	MLP 5-3-1	0.8470 4.4319	0.6994 5.1314	0.5261 7.5236	Tanh	Exponential	0.2067	0.1424	4.2000	0.6641	1.1204	3.8666
	smoothing	MLP 5-3-1	0.6903 5.2072	0.6114 8.8076	0.6244 7.4899	Logistic	Exponential	0.3693	0.3182	3.5632	0.5634	1.2152	4.6461
	SG1D	**MLP 5-11-1**	**0.8096 3.6539**	**0.7282 6.7419**	**0.7180 7.6625**	**Tanh**	**Exponential**	**0.1157**	**0.0641**	**8.6840**	**1.3731**	**0.3998**	**6.7000**
	SG2D	MLP 5-6-1	0.7206 3.5274	0.6458 5.9614	0.6021 12.9069	Logistic	Logistic	0.3638	0.3122	3.6200	0.5724	1.1961	6.2847
	SNV	MLP 5-4-1	0.6251 5.3792	0.6142 7.2593	0.5632 13.0790	Exponential	Logistic	0.1762	0.1094	4.0220	0.6359	1.0973	3.1673
	MSC	MLP 5-10-1	0.6763 8.1299	0.6573 8.2752	0.6107 8.5829	Exponential	Exponential	0.1534	0.0233	3.6239	0.5730	0.9567	3.9720
	smoothing+SNV	MLP 5-5-1	0.5761 7.7038	0.5405 8.8335	0.4833 14.3421	Logistic	Identity	0.1665	0.0990	3.7724	0.5965	1.0580	4.0702
	smoothing+MSC	MLP 5-9-1	0.6301 6.7115	0.5672 8.0646	0.5033 9.0108	Exponential	Tanh	0.1500	0.0810	18.5759	2.9371	0.2356	0.1351
	SG1D+SNV	MLP 5-9-1	0.5103 6.8812	0.4834 8.7677	0.4479 12.0440	Exponential	Exponential	0.2803	0.0057	5.3510	0.8461	0.7945	2.8967
	SG1D+MSC	MLP 5-3-1	0.6235 6.8812	0.4118 8.7677	0.4399 12.0440	Exponential	Exponential	0.0589	0.0174	4.6211	2.0586	1.1542	2.5513
	SG2D+SNV	MLP 5-7-1	0.7101 4.6788	0.6012 5.4176	0.5975 7.8612	Tanh	Tanh	0.2079	0.1437	4.9198	0.7779	1.0910	2.5475
	SG2D+MSC	MLP 5-7-1	0.5654 7.9397	0.5341 9.3655	0.4372 9.9355	Tanh	Tanh	0.2040	0.1394	3.1760	0.5022	1.3762	5.1029

Table 38. Artificial neural network (ANN) models for prediction of total color change (ΔE) of the compost samples during the composting process based on the NIR spectra gathered using NIR spectrometer (AvaSpec-NIR256-2.5-HSC-EVO, Avantes, USA) (R_{pred}^2=coefficient of determination for prediction; $R_{pred\,adj}^2$=adjusted coefficient of determination for prediction; *RMSEP*=root mean square of prediction; *SEP*=standard error of prediction; *RPD*=ratio of prediction to deviation; *RER*=ratio of the error range)

Output variable	NIR spectra pretreatment	Network name	Calibration					Prediction					
			Training perf. Training error	Test perf. Test error	Validation perf. Validation error	Hidden activation	Output activation	R_{pred}^2	$R_{pred\,adj}^2$	*RMSEP*	*SEP*	*RPD*	*RER*
ΔE (compost)	raw spectra	MLP 5-3-1	0.8585 2.0064	0.8513 2.2827	0.7609 7.7643	Exponential	Tanh	0.7559	0.7361	10.4435	1.6513	1.2222	4.1511
	smoothing	MLP 5-5-1	0.8878 1.7988	0.8452 1.9355	0.8156 2.3641	Exponential	Logistic	0.1433	0.0739	4.6093	0.7288	0.8775	3.2376
	SG1D	**MLP 5-7-1**	**0.8517 2.0796**	**0.8295 2.2513**	**0.7348 3.5186**	**Tanh**	**Tanh**	**0.6763**	**0.6500**	**2.0776**	**0.3285**	**1.5680**	**5.7912**
	SG2D	MLP 5-6-1	0.9514 0.6534	0.7715 2.9019	0.7069 4.0695	Exponential	Logistic	0.3460	0.2930	3.5224	0.5569	1.1010	3.6528
	SNV	MLP 5-4-1	0.6907 3.2362	0.6827 4.0307	0.6390 4.0529	Logistic	Identity	0.4259	0.3794	3.9409	0.6231	0.9534	2.6651
	MSC	MLP 5-8-1	0.8735 2.9304	0.6633 5.7105	0.6465 6.9668	Exponential	Exponential	0.5200	0.4810	2.9845	0.4719	1.3666	3.8798
	smoothing+SNV	MLP 5-8-1	0.7331 2.7385	0.7254 4.2297	0.6099 2.2385	Exponential	Exponential	0.3526	0.3001	3.4819	0.5505	1.0722	3.0269
	smoothing+MSC	MLP 5-11-1	0.7980 2.3892	0.7509 6.1508	0.7432 7.2686	Exponential	Tanh	0.5776	0.5434	3.5536	0.5619	1.0776	3.3357
	SG1D+SNV	MLP 5-7-1	0.8634 1.6898	0.8457 1.9293	0.8269 3.8333	Logistic	Tanh	0.4148	0.3673	3.0081	0.4756	1.2260	4.3402
	SG1D+MSC	MLP 5-7-1	0.7229 1.6898	0.6788 1.9293	0.6463 3.8333	Tanh	Identity	0.3965	0.3475	2.4631	0.3895	1.2457	4.7794
	SG2D+SNV	MLP 5-8-1	0.8242 2.2318	0.7691 2.7707	0.7094 7.7577	Exponential	Tanh	0.2869	0.2290	4.3598	0.6893	0.7623	2.6524
	SG2D+MSC	MLP 5-4-1	0.7664 1.6908	0.7235 4.0213	0.6849 4.5053	Tanh	Tanh	0.5860	0.5524	2.7539	0.4354	1.2989	5.1029

Table 39. Artificial neural network (ANN) models for prediction of pH of the compost samples during the composting process based on the NIR spectra gathered using NIR spectrometer (AvaSpec-NIR256-2.5-HSC-EVO, Avantes, USA) (R_{pred}^2=coefficient of determination for prediction; $R_{pred}^2{}_{adj}$=adjusted coefficient of determination for prediction; $RMSEP$=root mean square of prediction; SEP=standard error of prediction; RPD=ratio of prediction to deviation; RER=ratio of the error range). Pretreatment selected as optimal is marked bold

Output variable	NIR spectra pretreatment	Network name	Calibration					Prediction					
			Training perf. Training error	Test perf. Test error	Validation perf. Validation error	Hidden activation	Output activation	R_{pred}^2	$R_{pred}^2{}_{adj}$	RMSEP	SEP	RPD	RER
pH	raw spectra	MLP 5-7-1	0.8364 0.1497	0.8573 0.1606	0.8285 0.7553	Tanh	Logistic	0.7366	0.6682	1.0562	0.1670	0.9711	3.6464
	smoothing	MLP 5-5-1	0.8364 0.1497	0.8573 0.1606	0.8285 0.7553	Tanh	Logistic	0.1528	0.0857	1.2431	0.1965	0.8251	3.0982
	SG1D	MLP 5-9-1	0.6723 0.4589	0.5700 0.6703	0.5830 0.6928	Exponential	Logistic	0.1169	0.0469	1.1231	0.1776	0.9132	3.4289
	SG2D	MLP 5-5-1	0.6005 0.3626	0.5786 0.4751	0.5566 0.9673	Exponential	Logistic	0.1531	0.0860	2.8771	0.4549	0.3565	1.3386
	SNV	**MLP 5-8-1**	**0.5815 0.6527**	**0.5659 0.8131**	**0.5424 0.9149**	**Identity**	**Exponential**	**0.4110**	**0.3648**	**0.8218**	**0.1299**	**1.2480**	**4.6861**
	MSC	MLP 5-5-1	0.6628 0.3289	0.6164 0.3782	0.6112 0.6261	Tanh	Exponential	0.1233	0.0539	1.1523	0.1822	0.8901	3.3422
	smoothing+SNV	MLP 5-3-1	0.7088 0.4527	0.5856 0.5155	0.5378 0.5856	Logistic	Tanh	0.4208	0.3755	3.6976	0.5846	0.2774	1.0415
	smoothing+MSC	MLP 5-8-1	0.6150 0.4530	0.5546 0.5374	0.5346 0.6169	Tanh	Exponential	0.0856	0.0130	1.5355	0.2428	0.6680	2.5081
	SG1D+SNV	MLP 5-9-1	0.9105 0.1009	0.8182 0.4015	0.6424 0.4155	Tanh	Identity	0.1339	0.0653	1.1434	0.1808	0.8971	3.3682
	SG1D+MSC	MLP 5-7-1	0.5925 0.4867	0.5809 0.5477	0.5489 0.6499	Logistic	Tanh	0.1674	0.1015	1.0851	0.1716	0.9452	3.5490
	SG2D+SNV	MLP 5-11-1	0.7353 0.3051	0.6792 0.4402	0.6510 0.4524	Logistic	Tanh	0.1008	0.0295	2.3728	0.3752	0.4323	1.6231
	SG2D+MSC	MLP 5-9-1	0.9563 0.4706	0.8059 0.8006	0.6706 0.9563	Exponential	Tanh	0.1843	0.1198	2.3818	0.3766	0.4306	1.6169

Table 40. Artificial neural network (ANN) models for prediction of total dissolved solids (TDS) of the compost samples during the composting process based on the NIR spectra gathered using NIR spectrometer (AvaSpec-NIR256-2.5-HSC-EVO, Avantes, USA) (R_{pred}^2=coefficient of determination for prediction; $R_{pred}^2{}_{adj}$=adjusted coefficient of determination for prediction; $RMSEP$=root mean square of prediction; SEP=standard error of prediction; RPD=ratio of prediction to deviation; RER=ratio of the error range). Pretreatment selected as optimal is marked bold

Output variable	NIR spectra pretreatment	Network name	Calibration					Prediction					
			Training perf. Training error	Test perf. Test error	Validation perf. Validation error	Hidden activation	Output activation	R_{pred}^2	$R_{pred}^2{}_{adj}$	$RMSEP$	SEP	RPD	RER
TDS	raw spectra	MLP 5-9-1	0.8679 2280.05	0.8062 2378.98	0.7366 7909.23	Tanh	Logistic	0.6076	0.6191	472.9451	74.7792	1.1700	4.6001
	smoothing	MLP 5-5-1	0.6742 4996.69	0.5597 6170.44	0.5447 7386.53	Tanh	Logistic	0.3339	0.2556	424.7362	67.1567	1.3028	5.1222
	SG1D	MLP 5-10-1	0.6107 5398.83	0.5394 8905.41	0.5699 9700.38	Logistic	Tanh	0.5628	0.5030	341.1999	53.9484	1.6217	6.3763
	SG2D	MLP 5-10-1	0.6595 6180.83	0.6221 6453.83	0.5624 8910.25	Tanh	Identity	0.3297	0.2511	400.2648	63.2874	1.3824	5.4354
	SNV	**MLP 5-3-1**	**0.8509 3429.10**	**0.8228 34845.81**	**0.8036 3564.99**	**Tanh**	**Logistic**	**0.7990**	**0.7746**	**205.2674**	**32.4556**	**2.6957**	**10.5988**
	MSC	MLP 5-10-1	0.5961 4700.75	0.5712 7741.21	0.5261 9356.56	Tanh	Identity	0.6616	0.6099	332.8994	52.6360	1.6622	6.5353
	smoothing+SNV	MLP 5-6-1	0.9744 1441.66	0.9389 4695.09	0.7509 9000.27	Tanh	Exponential	0.4796	0.4131	364.3382	57.6069	1.5187	5.9714
	smoothing+MSC	MLP 5-6-1	0.7366 4926.36	0.6888 5077.72	0.6576 5405.81	Logistic	Logistic	0.6620	0.6103	310.2714	49.0582	1.7834	7.0119
	SG1D+SNV	MLP 5-5-1	0.7178 3372.16	0.5829 5553.26	0.5584 6022.28	Tanh	Logistic	0.1497	0.0564	431.2394	68.1849	1.2831	5.0450
	SG1D+MSC	MLP 5-3-1	0.7280 6794.31	0.6003 6905.73	0.6187 6985.35	Tanh	Logistic	0.4223	0.3512	377.2419	59.6472	1.4668	5.7671
	SG2D+SNV	MLP 5-10-1	0.8697 3200.84	0.8687 3625.73	0.7651 3758.29	Exponential	Identity	0.5952	0.5381	316.9816	50.1192	1.7456	6.8635
	SG2D+MSC	MLP 5-5-1	0.8915 1562.49	0.7354 3504.27	0.7213 3779.62	Tanh	Exponential	0.5583	0.4981	360.8616	57.0572	1.5334	6.0289

Table 41. Artificial neural network (ANN) models for prediction of conductivity (S) of the compost samples during the composting process based on the NIR spectra gathered using NIR spectrometer (AvaSpec-NIR256-2.5-HSC-EVO, Avantes, USA) (R_{pred}^2=coefficient of determination for prediction; $R_{pred}^2{}_{adj}$=adjusted coefficient of determination for prediction; $RMSEP$=root mean square of prediction; SEP=standard error of prediction; RPD=ratio of prediction to deviation; RER=ratio of the error range). Pretreatment selected as optimal is marked bold

Output variable	NIR spectra pretreatment	Network name	Calibration					Prediction					
			Training perf. Training error	Test perf. Test error	Validation perf. Validation error	Hidden activation	Output activation	R_{pred}^2	$R_{pred}^2{}_{adj}$	$RMSEP$	SEP	RPD	RER
S	raw spectra	MLP 5-9-1	0.8507 1099.72	0.8021 3620.79	0.8263 8471.81	Tanh	Logistic	0.5512	0.5108	506.2927	80.0519	1.4056	5.3075
	smoothing	MLP 5-9-1	0.6910 1905.44	0.6419 2336.58	0.6356 2760.47	Exponential	Identitiy	0.5066	0.4625	540.9845	85.5372	1.3154	4.9672
	SG1D	MLP 5-9-1	0.6302 2244.20	0.5512 2648.75	0.5441 2993.24	Tanh	Identitiy	0.5888	0.5514	462.1005	73.0645	1.5400	5.8151
	SG2D	MLP 5-3-1	0.7817 1519.44	0.6419 2093.58	0.5827 3415.20	Exponential	Tanh	0.5519	0.5115	487.0317	77.0065	1.4611	5.5174
	SNV	MLP 5-7-1	0.7243 1884.62	0.7209 2058.36	0.6179 3058.97	Exponential	Tanh	0.5759	0.5374	481.6364	76.1534	1.4775	5.5792
	MSC	**MLP 5-5-1**	**0.8372 1929.25**	**0.6781 2967.52**	**0.6679 9984.17**	**Tanh**	**Exponential**	**0.5804**	**0.5424**	**462.0175**	**73.0514**	**1.5402**	**5.8161**
	smoothing+SNV	MLP 5-9-1	0.9332 1929.25	0.8915 2967.52	0.7874 9984.17	Logistic	Exponential	0.5149	0.4715	648.4143	102.5233	1.0975	4.1442
	smoothing+MSC	MLP 5-10-1	0.7312 1920.25	0.6942 1988.05	0.6455 22235.55	Tanh	Tanh	0.1382	0.0643	923.9869	146.0952	0.7702	2.9082
	SG1D+SNV	MLP 5-5-1	0.7780 1153.75	0.5527 2047.64	0.5524 2485.56	Logistic	Tanh	0.3996	0.3469	547.8867	86.6285	1.2988	4.9046
	SG1D+MSC	MLP 5-3-1	0.8386 2242.91	0.6052 2488.32	0.5884 6843.32	Logistic	Logistic	0.4029	0.3504	534.3312	84.4852	1.3318	5.0290
	SG2D+SNV	MLP 5-8-1	0.8554 1170.64	0.8542 1304.39	0.7845 1548.71	Exponential	Tanh	0.2909	0.2293	607.8509	96.1097	1.1707	4.4208
	SG2D+MSC	MLP 5-11-1	0.6421 1884.23	0.5403 1947.70	0.5385 3781.56	Tanh	Exponential	0.5041	0.4598	497.8210	78.7124	1.4295	5.3978

Table 42. Artificial neural network (ANN) models for prediction of total color change (ΔE) of the compost extract samples during the composting process based on the NIR spectra gathered using NIR spectrometer (AvaSpec-NIR256-2.5-HSC-EVO, Avantes, USA) (R_{pred}^2=coefficient of determination for prediction; $R_{pred}^2{}_{adj}$=adjusted coefficient of determination for prediction; $RMSEP$=root mean square of prediction; SEP=standard error of prediction; RPD=ratio of prediction to deviation; RER=ratio of the error range). Pretreatment selected as optimal is marked bold

Output variable	NIR spectra pretreatment	Network name	Calibration					Prediction					
			Training perf. Training error	Test perf. Test error	Validation perf. Validation error	Hidden activation	Output activation	R_{pred}^2	$R_{pred}^2{}_{adj}$	$RMSEP$	SEP	RPD	RER
ΔE (extracts)	raw spectra	MLP 5-6-1	0.7451 0.1497	0.6439 0.1606	0.5022 0.7553	Logistic	Logistic	0.1924	0.1205	1.3099	0.2071	0.9295	3.2423
	smoothing	MLP 5-6-1	0.8291 0.2584	0.6220 0.3624	0.5178 0.4296	Logistic	Logistic	0.2373	0.1690	1.3116	0.2074	0.9283	3.2380
	SG1D	MLP 5-4-1	0.6705 0.2485	0.6398 0.3419	0.5720 0.3641	Tanh	Identity	0.2377	0.1695	1.3944	0.2205	0.8731	3.0456
	SG2D	MLP 5-7-1	0.7301 0.1852	0.6939 0.3611	0.5472 0.5034	Logistic	Identity	0.1566	0.0818	1.7986	0.2844	0.6769	2.3612
	SNV	MLP 5-11-1	0.8351 0.1656	0.7777 0.2657	0.5016 0.8600	Logistic	logistic	0.0971	0.0174	31.2702	4.9443	0.0389	0.1358
	MSC	MLP 5-6-1	0.6191 0.2691	0.5996 0.3498	0.5599 0.5885	Logistic	Identity	0.3953	0.3398	1.0558	0.1669	1.1532	4.0225
	smoothing+SNV	**MLP 5-7-1**	**0.6629 0.3185**	**0.6578 0.3643**	**0.5217 0.4217**	**Exponential**	**Logistic**	**0.5071**	**0.4607**	**0.7587**	**0.1200**	**1.5200**	**5.5979**
	smoothing+MSC	MLP 5-8-1	0.9247 0.1154	0.8463 0.3490	0.5931 0.4265	Exponential	Exponential	0.1774	0.1042	1.1245	0.1778	1.0827	3.7766
	SG1D+SNV	MLP 5-7-1	0.7101 0.1864	0.5459 0.3986	0.5417 0.4633	Logistic	Exponential	0.1229	0.0453	1.1050	0.1747	1.1019	3.8435
	SG1D+MSC	MLP 5-4-1	0.8204 0.2428	0.7102 0.2932	0.5335 0.7235	Tanh	Logistic	0.2741	0.2088	1.1148	0.1763	1.0922	3.8097
	SG2D+SNV	MLP 5-5-1	0.7827 0.1811	0.7399 0.2183	0.6988 0.3191	Tanh	Logistic	0.3987	0.3435	1.1104	0.1756	1.0965	3.8248
	SG2D+MSC	MLP 5-5-1	0.7021 0.2897	0.6955 0.2897	0.5285 0.4304	Exponential	Exponential	0.3590	0.3005	0.9769	0.1545	1.2463	4.3473

4.1.9. Artificial neural network (ANN) models for the prediction of number of microorganisms during the composting process

The preprocessing methods were applied for the prediction of number of bacteria and fungi, and for the total number of microorganisms during the composting processes. The developed ANN models based on NIR spectra obtained using the NIR spectrometer (NIR-128-1.7-USB/6.25/50 μm, Control Development Inc., USA) for the prediction of number of microorganisms are shown in Tables 43-45. The developed ANN models based on NIR spectra obtained using the another NIR spectrometer (AvaSpec-NIR256-2.5-HSC-EVO, Avantes, USA) for the prediction of number of microorganisms are shown in Tables 46-48. In the tables, the preprocessing method with the greatest *RER* (the ratio of the error range) values are in bold.

Table 43. Artificial neural network (ANN) models for prediction of number of bacteria during the composting process based on the NIR spectra gathered using NIR spectrometer (NIR-128-1.7-USB/6.25/50 μm, Control Development Inc., USA) (R_{pred}^2=coefficient of determination for prediction; $R_{pred}^2{}_{adj}$=adjusted coefficient of determination for prediction; $RMSEP$=root mean square of prediction; SEP=standard error of prediction; RPD=ratio of prediction to deviation; RER=ratio of the error range). Pretreatment selected as optimal is marked bold

Output variable	NIR spectra pretreatment	Network name	Calibration					Prediction					
			Training perf. Training error	Test perf. Test error	Validation perf. Validation error	Hidden activation	Output activation	R_{pred}^2	$R_{pred}^2{}_{adj}$	$RMSEP$	SEP	RPD	RER
logCFU$_{bacteria}$	raw	MLP 5-7-1	0.9198 0.0106	0.7429 0.3337	0.7509 0.3578	Tanh	Tanh	0.7411	0.6866	0.8380	0.1787	1.9520	7.2188
	smoothing	**MLP 5-6-1**	**0.8849 0.2101**	**0.7944 0.3011**	**0.7850 0.3211**	**Tanh**	**Tanh**	**0.8411**	**0.8077**	**0.5974**	**0.1274**	**2.4955**	**10.0839**
	SG1D	MLP 5-6-1	0.9084 0.0122	0.6961 0.3877	0.6733 0.3444	Tanh	Identity	0.4808	0.3715	1.2666	0.2700	1.3123	4.7563
	SG2D	MLP 5-9-1	0.9525 0.0514	0.9200 0.2414	0.7788 0.4004	Tanh	Identity	0.6214	0.5417	1.0515	0.2242	1.6136	5.7578
	SNV	MLP 5-6-1	0.9862 0.0028	0.9083 0.0111	0.8981 0.1222	Tanh	Exponential	0.8198	0.7818	0.6173	0.1316	2.3340	9.8000
	MSC	MLP 5-11-1	0.9518 0.0255	0.7829 0.3696	0.7151 0.3999	Tanh	Logistic	0.6404	0.5647	1.0511	0.2241	1.6310	5.7553
	smoothing+SNV	MLP 5-3-1	0.9848 0.0021	0.9143 0.0054	0.8689 0.0125	Tanh	Exponential	0.7409	0.6864	0.8187	0.1745	1.6639	6.9579
	smoothing+MSC	MLP 5-8-1	0.9460 0.0055	0.8996 0.1247	0.8238 0.1474	Tanh	Tanh	0.5160	0.4142	1.0140	0.2162	1.2186	4.7747
	SG1D+SNV	MLP 5-7-1	0.9246 0.0788	0.8121 0.2555	0.6455 0.4012	Tanh	Logistic	0.6002	0.5160	0.8137	0.1735	1.4647	7.3612
	SG1D+MSC	MLP 5-4-1	0.9747 0.0322	0.9249 0.0888	0.7707 0.3555	Logistic	Logistic	0.8203	0.7825	0.5952	0.1269	2.3099	9.5244
	SG2D+SNV	MLP 5-6-1	0.9285 0.0171	0.8172 0.1244	0.7355 0.2577	Tanh	Tanh	0.8075	0.7670	0.7057	0.1505	2.2737	8.1261
	SG2D+MSC	MLP 5-9-1	0.8955 0.1499	0.8258 0.1874	0.6303 0.3772	Tanh	Logistic	0.5820	0.4940	0.7591	0.1618	1.4608	7.2212

Table 44. Artificial neural network (ANN) models for prediction of number of fungi during the composting process based on the NIR spectra gathered using NIR spectrometer (NIR-128-1.7-USB/6.25/50 μm, Control Development Inc., USA) (R_{pred}^2=coefficient of determination for prediction; $R_{pred}^2{}_{adj}$=adjusted coefficient of determination for prediction; $RMSEP$=root mean square of prediction; SEP=standard error of prediction; RPD=ratio of prediction to deviation; RER=ratio of the error range). Pretreatment selected as optimal is marked bold

Output variable	NIR spectra pretreatment	Network name	Calibration					Prediction					
			Training perf. Training error	Test perf. Test error	Validation perf. Validation error	Hidden activation	Output activation	R_{pred}^2	$R_{pred}^2{}_{adj}$	$RMSEP$	SEP	RPD	RER
logCFU$_{fungi}$	raw	MLP 5-7-1	0.9390 0.0206	0.7832 0.3787	0.7622 0.3578	Tanh	Tanh	0.3717	0.2395	0.7429	0.1584	1.0225	5.0860
	smoothing	MLP 5-6-1	0.8466 0.1998	0.8139 0.2147	0.6696 0.3471	Tanh	Tanh	0.7867	0.7418	0.4857	0.1035	2.1252	10.8946
	SG1D	MLP 5-6-1	0.7753 0.3491	0.7172 0.3654	0.7414 0.3578	Tanh	Identity	0.6374	0.5610	0.7156	0.1526	1.4737	7.5096
	SG2D	MLP 5-9-1	0.9937 0.0014	0.8377 0.2544	0.7220 0.3662	Tanh	Identity	0.6841	0.6176	0.7547	0.1609	1.5800	7.0111
	SNV	MLP 5-6-1	0.8749 0.0299	0.6947 0.1314	0.6431 0.4101	Tanh	Exponential	0.5197	0.4186	0.5693	0.1214	1.3628	6.4085
	MSC	MLP 5-11-1	0.9580 0.0455	0.7529 0.3777	0.7021 0.3822	Tanh	Logistic	0.6935	0.6290	0.6742	0.1437	1.7545	7.9711
	smoothing+SNV	MLP 5-3-1	0.8389 0.1996	0.8001 0.1984	0.7277 0.2013	Tanh	Exponential	0.7735	0.7258	0.5299	0.1130	1.9213	9.6040
	smoothing+MSC	MLP 5-8-1	0.9012 0.0166	0.8456 0.1642	0.8344 0.1474	Tanh	Tanh	0.5680	0.4771	0.7315	0.1560	1.2977	5.0626
	SG1D+SNV	MLP 5-7-1	0.9130 0.0774	0.8493 0.2014	0.6203 0.3885	Tanh	Logistic	0.5402	0.4434	0.2732	0.0583	1.4275	6.0197
	SG1D+MSC	MLP 5-4-1	0.9289 0.0622	0.8249 0.1444	0.7783 0.2577	Logistic	Logistic	0.6908	0.6258	0.4421	0.0943	1.7068	8.3769
	SG2D+SNV	MLP 5-6-1	0.9399 0.0077	0.7844 0.2111	0.7490 0.3887	Tanh	Tanh	0.8122	0.7726	0.4805	0.1024	2.1307	8.1091
	SG2D+MSC	**MLP 5-9-1**	**0.7496 0.2499**	**0.7392 0.2874**	**0.7736 0.4772**	**Tanh**	**Logistic**	**0.8842**	**0.8598**	**0.3487**	**0.0743**	**2.8852**	**15.0753**

Table 45. Artificial neural network (ANN) models for prediction of total number of microorganisms during the composting process based on the NIR spectra gathered using NIR spectrometer (NIR-128-1.7-USB/6.25/50 μm, Control Development Inc., USA) (R_{pred}^2=coefficient of determination for prediction; $R_{pred}^2{}_{adj}$=adjusted coefficient of determination for prediction; $RMSEP$=root mean square of prediction; SEP=standard error of prediction; RPD=ratio of prediction to deviation; RER=ratio of the error range). Pretreatment selected as optimal is marked bold

Output variable	NIR spectra pretreatment	Network name	Calibration					Prediction					
			Training perf. Training error	Test perf. Test error	Validation perf. Validation error	Hidden activation	Output activation	R_{pred}^2	$R_{pred}^2{}_{adj}$	$RMSEP$	SEP	RPD	RER
$logCFU_{total\ number\ of\ microorganism}$	raw	MLP 5-7-1	0.9485 0.0612	0.7382 0.3874	0.7063 0.3311	Tanh	Tanh	0.4757	0.3654	1.6044	0.3421	1.3165	5.3274
	smoothing	MLP 5-6-1	0.9108 0.0124	0.8164 0.2147	0.7714 0.3366	Tanh	Tanh	0.8520	0.8208	1.0523	0.2243	2.1408	9.9687
	SG1D	MLP 5-6-1	0.8910 0.2144	0.7287 0.3012	0.7107 0.3387	Tanh	Identity	0.6933	0.6288	1.3692	0.2919	1.7576	7.8623
	SG2D	MLP 5-9-1	0.9869 0.0013	0.9482 0.0152	0.7087 0.3997	Tanh	Identity	0.7048	0.6426	1.4576	0.3108	1.7919	7.3551
	SNV	MLP 5-6-1	0.9909 0.0021	0.9217 0.0074	0.8351 0.0124	Tanh	Exponential	0.8053	0.7643	0.8899	0.1897	2.2572	9.6048
	MSC	MLP 5-11-1	0.8703 0.1122	0.8484 0.1474	0.7614 0.2971	Tanh	Logistic	0.7487	0.6958	1.3507	0.2880	1.9771	7.9697
	smoothing+SNV	MLP 5-3-1	0.9586 0.0674	0.9345 0.0741	0.8714 0.2998	Tanh	Exponential	0.8334	0.7983	1.1263	0.2401	1.8629	8.7475
	smoothing+MSC	MLP 5-8-1	0.9426 0.0078	0.8622 0.1354	0.8392 0.1574	Tanh	Tanh	0.6736	0.6049	1.1894	0.2536	1.7423	6.5830
	SG1D+SNV	MLP 5-7-1	0.9493 0.0155	0.8198 0.2247	0.6909 0.3474	Tanh	Logistic	0.5452	0.4494	1.0000	0.2132	1.3973	7.0718
	SG1D+MSC	MLP 5-4-1	0.9779 0.0031	0.8769 0.1888	0.8546 0.2555	Logistic	Logistic	0.7362	0.6806	1.0225	0.2180	1.8785	7.8175
	SG2D+SNV	MLP 5-6-1	0.9466 0.0066	0.8330 0.1755	0.7438 0.3011	Tanh	Tanh	0.8122	0.7727	1.0199	0.2175	2.2724	8.4233
	SG2D+MSC	**MLP 5-9-1**	**0.8464 0.2263**	**0.8383 0.2556**	**0.6669 0.4322**	**Tanh**	**Logistic**	**0.8234**	**0.7862**	**0.8745**	**0.1864**	**2.3412**	**12.0403**

Table 46. Artificial neural network (ANN) models for prediction of number of bacteria during the composting process based on the NIR spectra gathered using NIR spectrometer (AvaSpec-NIR256-2.5-HSC-EVO, Avantes, USA) (R_{pred}^2=coefficient of determination for prediction; $R_{pred}^2{}_{adj}$=adjusted coefficient of determination for prediction; $RMSEP$=root mean square of prediction; SEP=standard error of prediction; RPD=ratio of prediction to deviation; RER=ratio of the error range). Pretreatment selected as optimal is marked bold

Output variable	NIR spectra pretreatment	Network name	Calibration					Prediction					
			Training perf. Training error	Test perf. Test error	Validation perf. Validation error	Hidden activation	Output activation	R_{pred}^2	$R_{pred}^2{}_{adj}$	$RMSEP$	SEP	RPD	RER
logCFU$_{bacteria}$	raw	MLP 5-8-1	0.8387 0.1774	0.7932 0.2147	0.7760 0.3247	Tanh	Tanh	0.7411	0.6866	0.8380	0.1787	1.9520	7.2188
	smoothing	**MLP 5-3-1**	**0.6594 0.3366**	**0.6550 0.3457**	**0.6399 0.3668**	**Exponential**	**Logistic**	**0.8411**	**0.8077**	**0.5974**	**0.1274**	**2.4955**	**10.0839**
	SG1D	MLP 5-5-1	0.9191 0.0012	0.8892 0.0247	0.7852 0.0236	Logistic	Identity	0.4808	0.3715	1.2666	0.2700	1.3123	4.7563
	SG2D	MLP 5-5-1	0.9491 0.0322	0.7241 0.2887	0.7165 0.2997	Exponential	Exponential	0.6214	0.5417	1.0515	0.2242	1.6136	5.7578
	SNV	MLP 5-6-1	0.9963 0.0012	0.9072 0.0198	0.7410 0.2887	Tanh	Identity	0.8198	0.7818	0.6173	0.1316	2.3340	9.8000
	MSC	MLP 5-5-1	0.7514 0.2115	0.7344 0.2887	0.7488 0.2997	Exponential	Logistic	0.6404	0.5647	1.0511	0.2241	1.6310	5.7553
	smoothing+SNV	MLP 5-6-1	0.6038 0.3998	0.6022 0.4117	0.6002 0.4122	Identity	Exponential	0.7409	0.6864	0.8187	0.1745	1.6639	6.9579
	smoothing+MSC	MLP 5-3-1	0.6747 0.3441	0.6708 0.3255	0.6381 0.3367	Logistic	Exponential	0.5160	0.4142	1.0140	0.2162	1.2186	4.7747
	SG1D+SNV	MLP 5-8-1	0.9178 0.0144	0.7507 0.2553	0.7073 0.2736	Exponential	Logistic	0.6002	0.5160	0.8137	0.1735	1.4647	7.3612
	SG1D+MSC	MLP 5-4-1	0.7970 0.1874	0.6322 0.2054	0.6209 0.2334	Logistic	Exponential	0.8203	0.7825	0.5952	0.1269	2.3099	9.5244
	SG2D+SNV	MLP 5-5-1	0.6942 0.2445	0.6453 0.2556	0.6176 0.3019	Identity	Identity	0.8075	0.7670	0.7057	0.1505	2.2737	8.1261
	SG2D+MSC	MLP 5-9-1	0.6703 0.3711	0.6323 0.3874	0.6033 0.3921	Tanh	Tanh	0.5820	0.4940	0.7591	0.1618	1.4608	7.2212

Table 47. Artificial neural network (ANN) models for prediction of number of fungi during the composting process based on the NIR spectra gathered using NIR spectrometer (AvaSpec-NIR256-2.5-HSC-EVO, Avantes, USA) (R_{pred}^2=coefficient of determination for prediction; $R_{pred}^2{}_{adj}$=adjusted coefficient of determination for prediction; $RMSEP$=root mean square of prediction; SEP=standard error of prediction; RPD=ratio of prediction to deviation; RER=ratio of the error range). Pretreatment selected as optimal is marked bold

Output variable	NIR spectra pretreatment	Network name	Calibration					Prediction					
			Training perf. Training error	Test perf. Test error	Validation perf. Validation error	Hidden activation	Output activation	R_{pred}^2	$R_{pred}^2{}_{adj}$	$RMSEP$	SEP	RPD	RER
logCFU$_{fungi}$	raw	MLP 5-8-1	0.6691 0.4112	0.6424 0.4257	0.6313 0.4449	Tanh	Tanh	0.5839	0.4963	0.5497	0.1172	1.3483	7.0882
	smoothing	MLP 5-3-1	0.6899 0.2366	0.6512 0.3852	0.6035 0.3999	Exponential	Logistic	0.7867	0.7418	0.4857	0.1035	2.1252	10.8946
	SG1D	MLP 5-5-1	0.9823 0.0044	0.7849 0.0457	0.7673 0.1001	Logistic	Identity	0.6704	0.6010	0.5824	0.1242	1.2385	6.5475
	SG2D	MLP 5-5-1	0.9677 0.0047	0.9605 0.0125	0.7777 0.2244	Exponential	Exponential	0.3488	0.2117	0.3863	0.0824	1.0669	3.9934
	SNV	MLP 5-6-1	0.9910 0.0021	0.9817 0.0199	0.7850 0.2555	Tanh	Identity	0.5119	0.4092	0.4596	0.0980	1.2361	5.5973
	MSC	MLP 5-5-1	0.7514 0.2977	0.6344 0.3225	0.6488 0.3251	Exponential	Logistic	0.6708	0.6014	0.4163	0.0888	1.6852	8.7647
	smoothing+SNV	MLP 5-6-1	0.6686 0.3885	0.6408 0.3969	0.6390 0.4024	Identity	Exponential	0.7735	0.7258	0.5299	0.1130	1.9213	9.6040
	smoothing+MSC	MLP 5-31	0.6410 0.4233	0.6353 0.4247	0.6018 0.4366	Logistic	Exponential	0.8673	0.8393	0.3868	0.0825	2.1360	9.8578
	SG1D+SNV	MLP 5-8-1	0.6253 0.2448	0.6233 0.2534	0.6345 0.2736	Exponential	Logistic	0.2756	0.1231	0.6678	0.1424	1.1190	5.4635
	SG1D+MSC	MLP 5-4-1	0.8632 0.1987	0.6541 0.3742	0.6221 0.3845	Logistic	Exponential	0.3957	0.2685	0.7812	0.1665	1.2667	4.9878
	SG2D+SNV	**MLP 5-5-1**	**0.6464 0.3144**	**0.6272 0.3215**	**0.6277 0.3538**	**Identity**	**Identity**	**0.8434**	**0.8104**	**0.4043**	**0.0862**	**2.4908**	**13.2922**
	SG2D+MSC	MLP 5-9-1	0.6719 0.3166	0.6645 0.3287	0.6277 0.3732	Tanh	Tanh	0.7725	0.7247	0.4075	0.0869	1.8620	9.2712

Table 48. Artificial neural network (ANN) models for prediction of total number of microorganisms during the composting process based on the NIR spectra gathered using NIR spectrometer (AvaSpec-NIR256-2.5-HSC-EVO, Avantes, USA) (R_{pred}^2=coefficient of determination for prediction; $R_{pred}^2{}_{adj}$=adjusted coefficient of determination for prediction; $RMSEP$=root mean square of prediction; SEP=standard error of prediction; RPD=ratio of prediction to deviation; RER=ratio of the error range). Pretreatment selected as optimal is marked bold

Output variable	NIR spectra pretreatment	Network name	Calibration					Prediction					
			Training perf. Training error	Test perf. Test error	Validation perf. Validation error	Hidden activation	Output activation	R_{pred}^2	$R_{pred}^2{}_{adj}$	$RMSEP$	SEP	RPD	RER
logCFU total number of microorganism	raw	MLP 5-8-1	0.7691 0.3112	0.7424 0.3257	0.7313 0.3449	Tanh	Tanh	0.4757	0.3654	1.6044	0.3421	1.3165	5.3274
	smoothing	MLP 5-3-1	0.7086 0.3122	0.6955 0.3552	0.6892 0.3621	Exponential	Logistic	0.8520	0.8208	1.0523	0.2243	2.1408	9.9687
	SG1D	MLP 5-5-1	0.9641 0.0102	0.8763 0.0355	0.7885 0.2211	Logistic	Identity	0.6933	0.6288	1.3692	0.2919	1.7576	7.8623
	SG2D	MLP 5-5-1	0.9444 0.0225	0.7683 0.1442	0.7217 0.1988	Exponential	Exponential	0.7048	0.6426	1.4576	0.3108	1.7919	7.3551
	SNV	MLP 5-6-1	0.9988 0.0022	0.8836 0.0211	0.7419 0.3007	Tanh	Identity	0.8053	0.7643	0.8899	0.1897	2.2572	9.6048
	MSC	MLP 5-5-1	0.8892 0.2244	0.6641 0.3778	0.6558 0.3874	Exponential	Logistic	0.7487	0.6958	1.3507	0.2880	1.9771	7.9697
	smoothing+SNV	MLP 5-6-1	0.6343 0.3966	0.6333 0.4225	0.6316 0.4356	Identity	Exponential	0.8334	0.7983	1.1263	0.2401	1.8629	8.7475
	smoothing+MSC	MLP 5-3-1	0.6439 0.4011	0.6457 0.4124	0.6275 0.4247	Logistic	Exponential	0.6736	0.6049	1.1894	0.2536	1.7423	6.5830
	SG1D+SNV	MLP 5-8-1	0.6539 0.3582	0.6315 0.3577	0.6012 0.3657	Exponential	Logistic	0.5452	0.4494	1.0000	0.2132	1.3973	7.0718
	SG1D+MSC	MLP 5-4-1	0.7162 0.3055	0.6071 0.3974	0.6044 0.3941	Logistic	Exponential	0.7362	0.6806	1.0225	0.2180	1.8785	7.8175
	SG2D+SNV	MLP 5-5-1	0.6518 0.3398	0.6019 0.3477	0.6008 0.3556	Identity	Identity	0.8122	0.7727	1.0199	0.2175	2.2724	8.4233
	SG2D+MSC	**MLP 5-9-1**	**0.6323 0.3222**	**0.6397 0.3155**	**0.6098 0.3606**	**Tanh**	**Tanh**	**0.8234**	**0.7862**	**0.8745**	**0.1864**	**2.3412**	**12.0403**

4.2. Extraction of bioactive molecules from grape skin

The extraction of bioactive molecules from grape skin under different conditions of extraction time, temperature, solid-liquid ratio and mixing rate was performed. The extraction conditions are presented in Table 10. In this chapter the physicochemical properties of grape skin extracts will be presented, and also the results of the principal component analysis (PCA). Furthermore, the results of optimization of the extraction conditions will be presented. The optimization was investigated using the chemical properties (total polyphenol content, and antioxidant activity determined using DPPH and FRAP method) as the output variables.

4.2.1. Physicochemical properties of aqueous grape skin extracts

The physicochemical properties of aqueous grape skin extracts were analyzed, and include the determination of pH, TDS, conductivity, extraction yield, Chroma and Hue values as the main color properties, total polyphenol content and antioxidant activity determined by FRAP and DPPH method. The results are shown in Tables 49 and 50.

Table 49. Physical characteristics of grape skin extracts (*S*=conductivity, TDS=total dissolved solids; *Y*=extraction yield)

Exp.	pH	*S* (µS/cm)	*TDS* (mg/L)	*Y* (%)
1.	3.89 ± 0.01	313.33 ± 2.08	152.80 ± 2.52	0.2332 ± 0.03
2.	3.93 ± 0.01	254.33 ± 1.53	128.87 ± 1.71	0.2219 ± 0.04
3.	3.84 ± 0.01	379.33 ± 5.13	186.67 ± 0.90	0.4160 ± 0.07
4.	3.95 ± 0.01	335.33 ± 1.53	169.57 ± 1.10	0.3338 ± 0.02
5.	3.88 ± 0.02	219.00 ± 2.65	106.77 ± 1.62	0.1359 ± 0.03
6.	3.81 ± 0.01	329.00 ± 1.00	163.27 ± 0.91	0.4101 ± 0.04
7.	3.79 ± 0.01	230.33 ± 7.64	112.83 ± 2.63	0.2245 ± 0.01
8.	3.76 ± 0.01	379.67 ± 3.21	191.40 ± 0.26	0.5113 ± 0.01
9.	3.94 ± 0.01	239.67 ± 0.58	122.67 ± 3.76	0.2825 ± 0.04
10.	3.87 ± 0.00	219.00 ± 1.73	108.67 ± 0.23	0.1923 ± 0.00
11.	4.00 ± 0.01	197.93 ± 0.21	99.30 ± 0.44	0.2357 ± 0.04
12.	3.90 ± 0.02	227.67 ± 0.58	113.67 ± 0.06	0.2193 ± 0.05
13.	3.86 ± 0.01	311.33 ± 0.58	154.97 ± 0.51	0.4154 ± 0.01
14.	4.07 ± 0.01	193.07 ± 9.48	93.73 ± 5.61	0.1610 ± 0.01
15.	3.95 ± 0.00	218.33 ± 0.58	109.33 ± 0.21	0.2465 ± 0.08
16.	3.76 ± 0.00	242.67 ± 1.15	121.33 ± 0.58	0.2338 ± 0.00
17.	3.78 ± 0.01	378.00 ± 1.00	187.97 ± 2.66	0.4515 ± 0.01
18.	3.85 ± 0.01	296.00 ± 3.61	141.93 ± 3.88	0.3330 ± 0.04
19.	3.94 ± 0.03	162.00 ± 1.00	81.27 ± 0.93	0.1889 ± 0.00
20.	4.03 ± 0.01	172.70 ± 0.10	86.47 ± 0.06	0.1740 ± 0.01
21.	3.84 ± 0.02	280.33 ± 0.58	139.00 ± 1.00	0.2875 ± 0.08
22.	3.82 ± 0.00	291.33 ± 0.58	145.93 ± 0.21	0.2944 ± 0.01
23.	3.93 ± 0.01	152.27 ± 8.95	81.97 ± 0.70	0.2350 ± 0.17
24.	3.79 ± 0.01	229.67 ± 0.58	114.67 ± 0.58	0.3160 ± 0.04
25.	3.83 ± 0.01	208.00 ± 1.00	106.57 ± 1.80	0.2008 ± 0.04
26.	3.69 ± 0.01	311.00 ± 5.57	158.47 ± 0.58	0.4133 ± 0.04
27.	3.82 ± 0.01	225.00 ± 1.73	114.13 ± 0.81	0.1241 ± 0.05
28.	3.77 ± 0.01	245.67 ± 0.58	123.57 ± 0.06	0.2882 ± 0.02
29.	3.72 ± 0.00	242.33 ± 0.58	121.27 ± 0.64	0.2848 ± 0.02
30.	3.73 ± 0.01	241.67 ± 0.58	121.33 ± 0.58	0.2755 ± 0.04

Table 50. Physicochemical characteristics of grape skin extracts (Chroma and Hue=color variables; TPC=total polyphenol content; DPPH=antioxidant activity determined using DPPH method; FRAP=antioxidant activity determined using FRAP method)

Exp.	Chroma	Hue	TPC (mg_{GAE}/g_{DM})	DPPH ($mmol_{Trolox}/g_{DM}$)	FRAP ($mmol_{FeSO4\cdot7H2O}/g_{DM}$)
1.	0.71 ± 0.01	83.38 ± 1.00	1.47 ± 0.00	0.0009 ± 0.0001	0.0082 ± 0.0002
2.	0.68 ± 0.01	87.77 ± 0.61	2.54 ± 0.32	0.0007 ± 0.0001	0.0098 ± 0.0021
3.	0.60 ± 0.01	77.32 ± 0.70	3.85 ± 0.06	0.0046 ± 0.0010	0.0295 ± 0.0002
4.	0.90 ± 0.31	87.63 ± 3.76	2.94 ± 0.16	0.0022 ± 0.0005	0.0287 ± 0.0006
5.	1.03 ± 0.01	98.50 ± 0.05	1.20 ± 0.06	0.0005 ± 0.0000	0.0059 ± 0.0002
6.	1.16 ± 0.01	96.46 ± 0.19	3.43 ± 0.06	0.0012 ± 0.0003	0.0192 ± 0.0005
7.	1.11 ± 0.01	95.10 ± 0.38	1.31 ± 0.01	0.0005 ± 0.0001	0.0050 ± 0.0001
8.	1.16 ± 0.02	134.81 ± 0.54	4.02 ± 0.06	0.0012 ± 0.0001	0.0431 ± 0.0013
9.	1.13 ± 0.01	91.27 ± 0.55	3.28 ± 0.16	0.0008 ± 0.0001	0.0088 ± 0.0006
10.	1.07 ± 0.01	96.61 ± 0.03	3.28 ± 0.04	0.0007 ± 0.0001	0.0155 ± 0.0012
11.	0.97 ± 0.01	100.03 ± 0.52	2.19 ± 0.06	0.0008 ± 0.0001	0.0133 ± 0.0026
12.	1.13 ± 0.01	94.63 ± 0.66	2.10 ± 0.02	0.0007 ± 0.0000	0.0200 ± 0.0005
13.	1.13 ± 0.01	93.61 ± 0.37	2.30 ± 0.34	0.0007 ± 0.0001	0.0264 ± 0.0001
14.	1.01 ± 0.01	99.54 ± 0.22	1.09 ± 0.04	0.0004 ± 0.0001	0.0028 ± 0.0002
15.	1.16 ± 0.01	92.93 ± 0.59	1.29 ± 0.03	0.0015 ± 0.0008	0.0129 ± 0.0004
16.	1.01 ± 0.01	97.33 ± 0.51	3.08 ± 0.03	0.0009 ± 0.0001	0.0253 ± 0.0014
17.	1.27 ± 0.01	91.75 ± 0.21	8.24 ± 0.21	0.0301 ± 0.0009	0.0483 ± 0.0001
18.	1.12 ± 0.01	133.64 ± 0.23	2.93 ± 0.24	0.0008 ± 0.0001	0.0105 ± 0.0001
19.	1.04 ± 0.02	140.69 ± 0.37	1.98 ± 0.05	0.0003 ± 0.0000	0.0030 ± 0.0003
20.	1.06 ± 0.01	140.06 ± 0.52	1.96 ± 0.14	0.0003 ± 0.0000	0.0037 ± 0.0002
21.	1.12 ± 0.00	133.07 ± 0.68	4.74 ± 0.06	0.0021 ± 0.0004	0.0297 ± 0.0016
22.	1.12 ± 0.01	136.77 ± 0.02	4.30 ± 0.03	0.0010 ± 0.0001	0.025 ± 0.0011
23.	1.06 ± 0.01	143.73 ± 0.32	4.04 ± 0.32	0.0007 ± 0.0000	0.0055 ± 0.0007
24.	1.19 ± 0.02	130.53 ± 0.07	5.05 ± 0.04	0.0046 ± 0.0024	0.0236 ± 0.0004
25.	1.04 ± 0.01	142.59 ± 0.50	4.00 ± 0.38	0.0010 ± 0.0000	0.0088 ± 0.0000
26.	1.24 ± 0.01	120.61 ± 0.63	5.96 ± 0.32	0.0273 ± 0.0015	0.0314 ± 0.0007
27.	1.10 ± 0.01	137.85 ± 0.31	2.47 ± 0.22	0.0012 ± 0.0005	0.0144 ± 0.0010
28.	1.05 ± 0.02	131.98 ± 0.49	2.20 ± 0.04	0.0008 ± 0.0003	0.0183 ± 0.0002
29.	1.13 ± 0.01	132.79 ± 0.36	2.67 ± 0.18	0.0008 ± 0.0000	0.0160 ± 0.0001
30.	1.09 ± 0.01	134.65 ± 0.62	2.57 ± 0.04	0.0008 ± 0.0000	0.0173 ± 0.0001

4.2.2. Principal component analysis (PCA) and optimization of extraction conditions of bioactive molecules from grape skin

The relationship between extraction conditions and physicochemical properties of aqueous grape skin extracts was investigated using the PCA, and the results are shown in Figure 30.
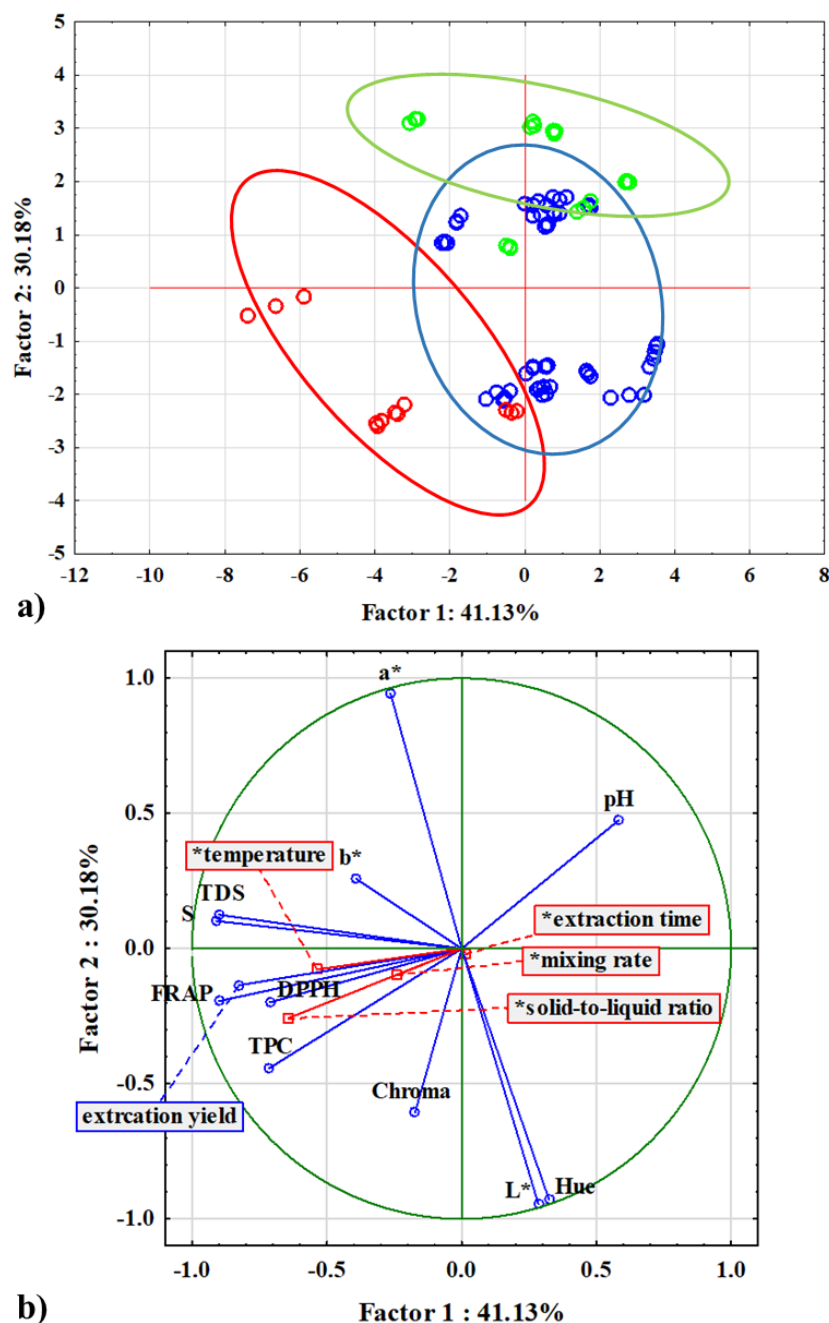
Figure 30. Principal component analysis (PCA): a) score plot (○ 80°C; ○ 60°C and ○ 40°C) and b) loading plot showing the relationship between extraction conditions and physicochemical properties of grape skin aqueous extracts

The effect of each parameter (extraction time, temperature, solid-liquid ratio and mixing speed) was analyzed at three levels, and 30 extraction experiments were performed according to the conditions shown in Table 10. Second-order polynomial equations with interactions term were used to fit the experimental data for the chemical properties (total polyphenol content and antioxidant activity determined using DPPH and FRAP method) of grape skin extracts and the regression coefficients and analysis of variance for purposed models are shown in Table 51.

Table 51. Regression coefficients and analysis of variance for response surface models used for TPC, DPPH and FRAP description (a significant coefficients are marked in bold, $p < 0.05$)

Dependent variable		Coefficient	St. error	Sum of squares (SS)	Degrees of freedom (df)	Mean squares (MS)	F value	p
Total polyhenol content (TPC)	β_0	**3.3463**	0.1310					<0.0001
	β_1	-0.2000	0.2485	0.36	1	0.360	0.65	0.4235
	β_{11}	0.3177	0.1644	2.08	1	2.076	3.73	0.0571
	β_2	**1.8555**	0.2485	30.99	1	30.986	55.74	<0.0001
	β_{22}	**-0.9169**	0.1644	17.29	1	17.293	31.11	<0.0001
	β_3	**3.1627**	0.2485	90.02	1	90.025	161.93	<0.0001
	β_{33}	-0.0547	0.1644	0.06	1	0.062	0.11	0.7402
	β_4	**0.0835**	0.2485	0.06	1	0.063	0.11	0.7377
	β_{44}	**-0.3344**	0.1644	2.30	1	2.301	4.14	0.0454
	β_{12}	**-0.9954**	0.4305	2.97	1	2.973	5.35	0.0235
	β_{13}	-0.2118	0.4305	0.13	1	0.135	0.24	0.6242
	β_{14}	0.6424	0.4305	1.24	1	1.238	2.23	0.1398
	β_{23}	**2.4815**	0.4305	18.47	1	18.473	33.23	<0.0001
	β_{24}	0.4730	0.4305	0.67	1	0.671	1.21	0.2754
	β_{34}	0.2436	0.4305	0.18	1	0.178	0.32	0.5732
	Lack-of-fit			38.7287	10	3.8787	14.8692	0.09074
	Pure error			2.9662	65	0.04563		
	Total SS			209.8053	89			
	R^2	0.8013						
	R^2_{adj}	0.7617						
Antioxidant activity determined using DPPH method	β_0	**0.0053**	0.0007					<0.0001
	β_1	-0.0006	0.0013	0.0000	1	0.0000	0.211	0.6472
	β_{11}	**0.0021**	0.0009	0.0001	1	0.0001	5.966	0.0169
	β_2	**0.0109**	0.0013	0.0011	1	0.0011	71.916	<0.0001
	β_{22}	**-0.0054**	0.0009	0.0006	1	0.0006	40.253	<0.0001
	β_3	**0.0063**	0.0013	0.0004	1	0.0004	24.016	<0.0001
	β_{33}	-0.0010	0.0009	0.0000	1	0.0000	1.499	0.2247
	β_4	**0.0038**	0.0013	0.0001	1	0.0001	8.686	0.0043
	β_{44}	-0.0010	0.0009	0.0000	1	0.0000	1.406	0.2395
	β_{12}	-0.0011	0.0022	0.0000	1	0.0000	0.249	0.6190
	β_{13}	-0.0006	0.0022	0.0000	1	0.0000	0.062	0.8035
	β_{14}	-0.0001	0.0022	0.0000	1	0.0000	0.001	0.9813
	β_{23}	**0.0140**	0.0022	0.0006	1	0.0006	39.321	<0.0001
	β_{24}	**0.0112**	0.0022	0.0004	1	0.0004	25.166	<0.0001
	β_{34}	0.0010	0.0022	0.0000	1	0.0000	0.000	0.9953
	Lack-of-fit			0.0011	10	0.0001	15.9500	0.6011
	Pure error			0.0000	65	0.0000		
	Total SS			0.0044	89			
	R^2	0.7477						
	R^2_{adj}	0.7006						

Table 51. (*continuing*) Regression coefficients and analysis of variance for response surface models used for TPC, DPPH and FRAP description (a significant coefficients are marked in bold, $p < 0.05$)

Dependent variable		Coefficient	St. error	Sum of squares (SS)	Degrees of freedom (df)	MS	F value	p
Antioxidant activity determined using FRAP method	β_0	**0.0202**	0.0005					<0.0001
	β_1	-0.0002	0.0009	0.000	1	0.0000	0.06	0.8041
	β_{11}	-0.0010	0.0006	0.0000	1	0.0000	2.78	0.0994
	β_2	**0.0190**	0.0009	0.0032	1	0.0032	413.62	<0.0001
	β_{22}	**-0.0037**	0.0006	0.0003	1	0.0003	35.60	<0.0001
	β_3	**0.0266**	0.0009	0.0063	1	0.0063	807.79	<0.0001
	β_{33}	**-0.0024**	0.0006	0.0001	1	0.0001	14.75	0.0003
	β_4	**0.0086**	0.0009	0.0007	1	0.0007	85.20	<0.0001
	β_{44}	**-0.0015**	0.0006	0.0000	1	0.0000	6.29	0.0143
	β_{12}	-0.0012	0.0016	0.0000	1	0.0000	0.56	0.4580
	β_{13}	-0.0025	0.0016	0.0000	1	0.0000	2.31	0.1330
	β_{14}	**-0.0042**	0.0016	0.0001	1	0.0001	6.90	0.0105
	β_{23}	**0.0065**	0.0016	0.0001	1	0.0001	15.98	0.0001
	β_{24}	0.0022	0.0016	0.0000	1	0.0000	1.91	0.1707
	β_{34}	**0.0124**	0.0016	0.0005	1	0.0005	59.11	<0.0001
	Lack-of-fit			0.0003	10	0.0000	9.3	0.1877
	Pure error			0.0002	65	0.0000		
	Total SS			0.0119	89			
	R^2	0.9505						
	R^2_{adj}	0.9413						

In Figure 31 are shown the effects of extraction time and solid-liquid ratio on total polyphenol content, antioxidant activity determined by DPPH and FRAP method.
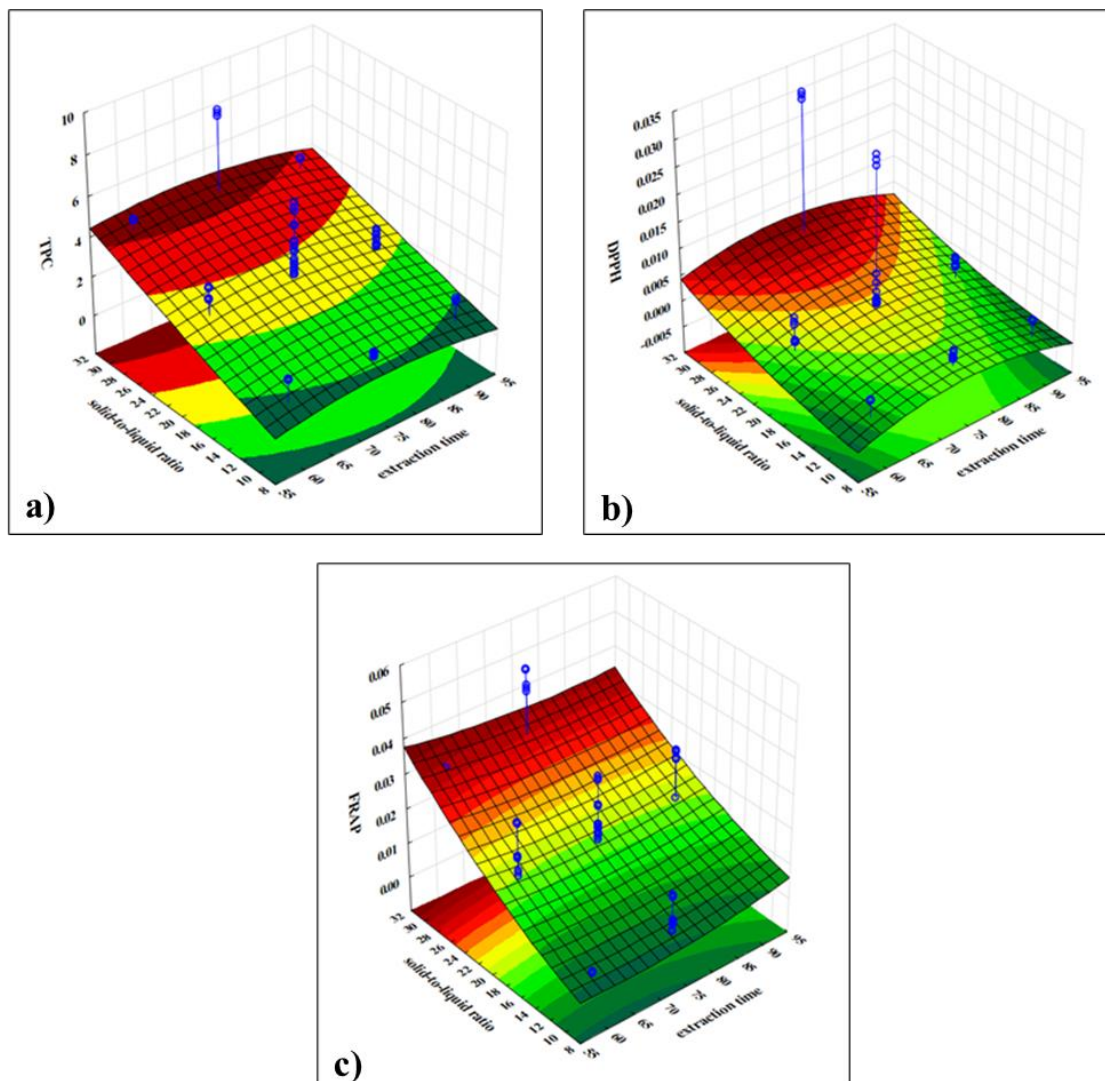
Figure 31. Response surface plots describing the dependence of a) TPC (mg$_{GAE}$/g$_{DM}$); b) DPPH (mmol$_{Trolox}$/g$_{DM}$) and c) FRAP (mmol$_{FeSO4·7H2O}$/g$_{DM}$) of grape skin aqueous extracts on extraction time and solid-liquid ratio

Figure 32 presents the predicted values for TPC, DPPH and FRAP obtained under the optimal extraction conditions of extraction time, temperature, solid-liquid ratio and mixing speed.
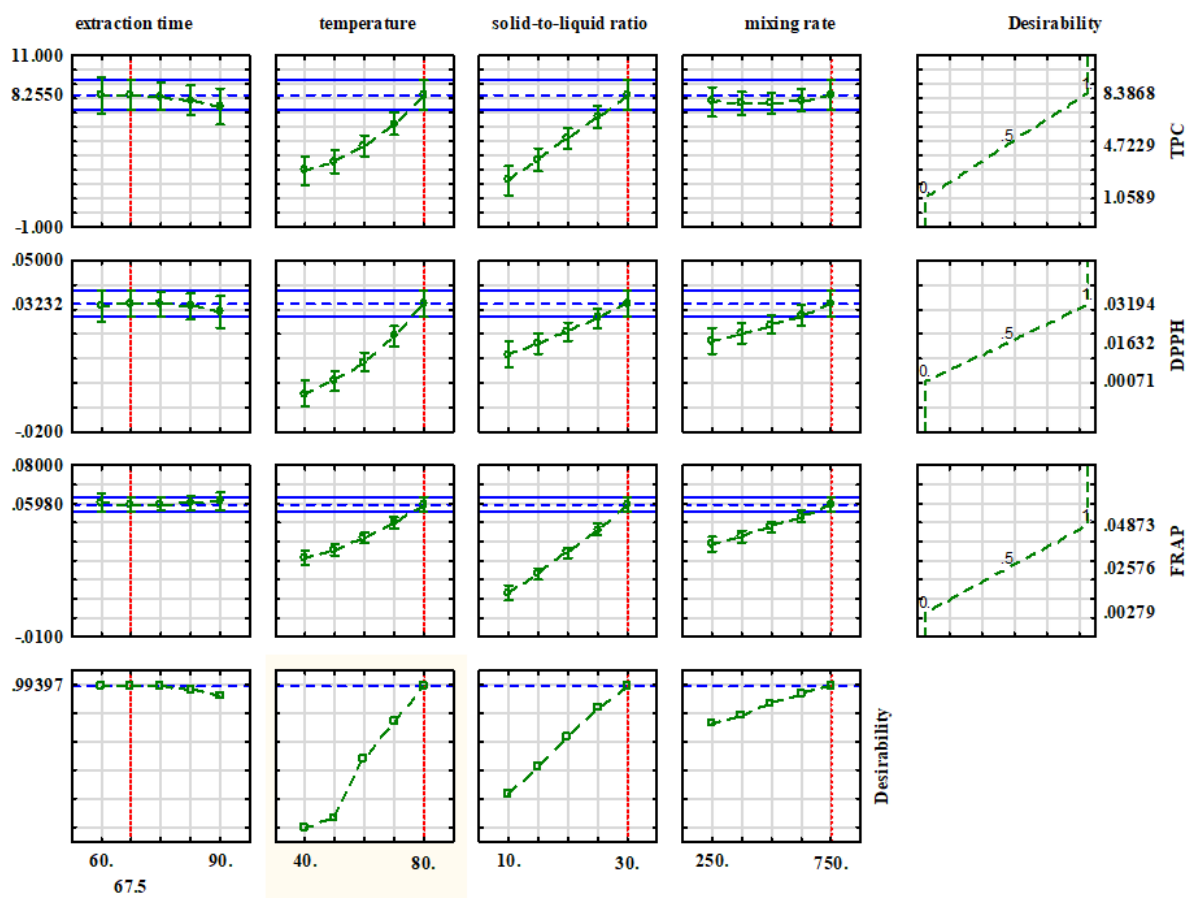
Figure 32. Profiles for predicted TPC (mg$_{GAE}$/g$_{DM}$), DPPH (mmol$_{Trolox}$/g$_{DM}$) and FRAP (mmol$_{FeSO4 \cdot 7H2O}$/g$_{DM}$) in grape skin aqueous extracts and estimated optimal extraction conditions

4.3. The effect of different pretreatments of grape skin on the efficiency of the composting process

The second set of composting experiments was carried out in order to investigate the effect of different pretreatments of grape skin on the efficiency of the composting process. To revise, the experiments were as follows: grape skin without pretreatment; ground grape skin without pretreatment; grape skin pretreated to extract bioactive molecules at 40 °C during the 90 minutes; ground grape skin pretreated to extract bioactive molecules at 40 °C during the 90 minutes; and the mixture of grape skin consisted of: grape skin without pretreatment (w/w = 43.93 %), ground grape skin without pretreatment (w/w = 8.11 %), grape skin pretreated to extract bioactive molecules at 40 °C during the 90 minutes (w/w = 14.25 %) and ground grape skin pretreated to extract bioactive molecules at 40 °C during the 90 minutes (w/w = 33.66 %).

In this chapter, the results of physicochemical analysis of compost samples and compost extracts will be presented, and microbiological analysis as well. Additionaly, the kinetics of organic matter degradation and microbial growth, descriptive statistical analysis, NIR spectra and the artificial neural network models for the prediction of compost properties will be presented.

4.3.1. Physicochemical and microbiological properties of compost samples and compost extracts during composting processes

The performed composting processes with different pretreated grape skin were monitored during the 30 days through important physicochemical properties. The temperature changes in reactors are shown in Figure 33.
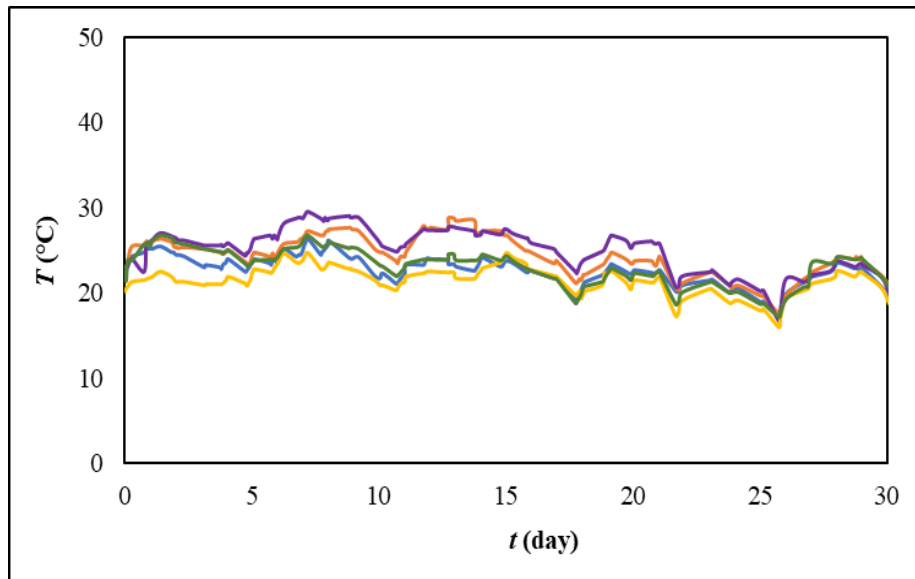
Figure 33. Temperature changes during the 30 days of grape skin composting process (•
experiment 1; • experiment 2; • experiment 3; • experiment 4; • experiment 5)

Figure 34 presents the appearance of grape skin before composting and after 30 days of
the process in reactors. Besides temperature, the processes were monitored through important
variables such as moisture and dry matter content, organic matter and ash content, carbon and
nitrogen content, C/N ratio, total color change of compost samples (ΔE compost), pH, total
dissolved solids (TDS), conductivity (S) and total color change of compost extract samples (ΔE
extract), and the results are shown in Figure 35.

a) Exp. 1   Exp. 2   Exp. 3   Exp. 4   Exp. 5

b)

Figure 34. a) Fresh or pretreated grape skin before composting and b) Grape skin compost after 30 days of composting process
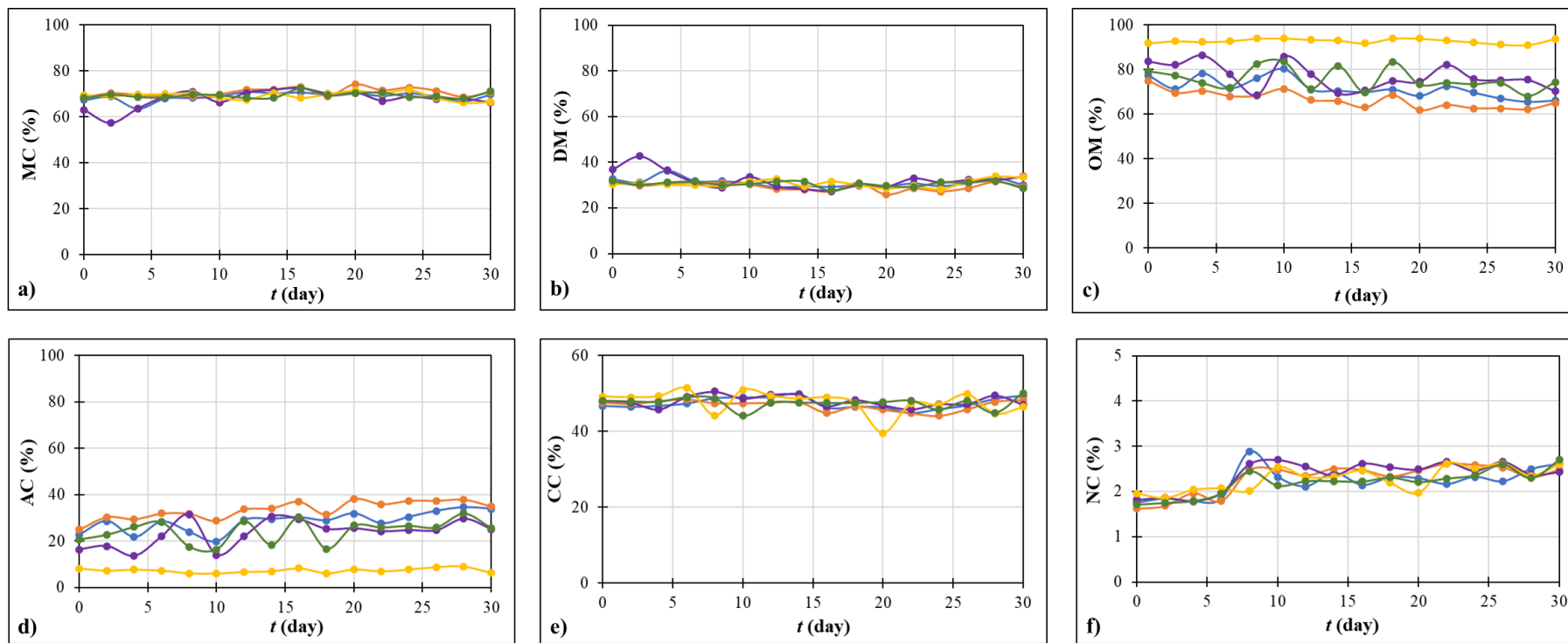
Figure 35. Changes in: a) MC; b) DM; c) OM; d) AC; e) CC and f) NC during the 30 days of grape skin composting process (• experiment 1; • experiment 2; • experiment 3; • experiment 4; • experiment 5) (MC=moisture content; DM=dry matter content; OM= organic matter content; AC= ash content; CC=carbon content; NC= nitrogen content)
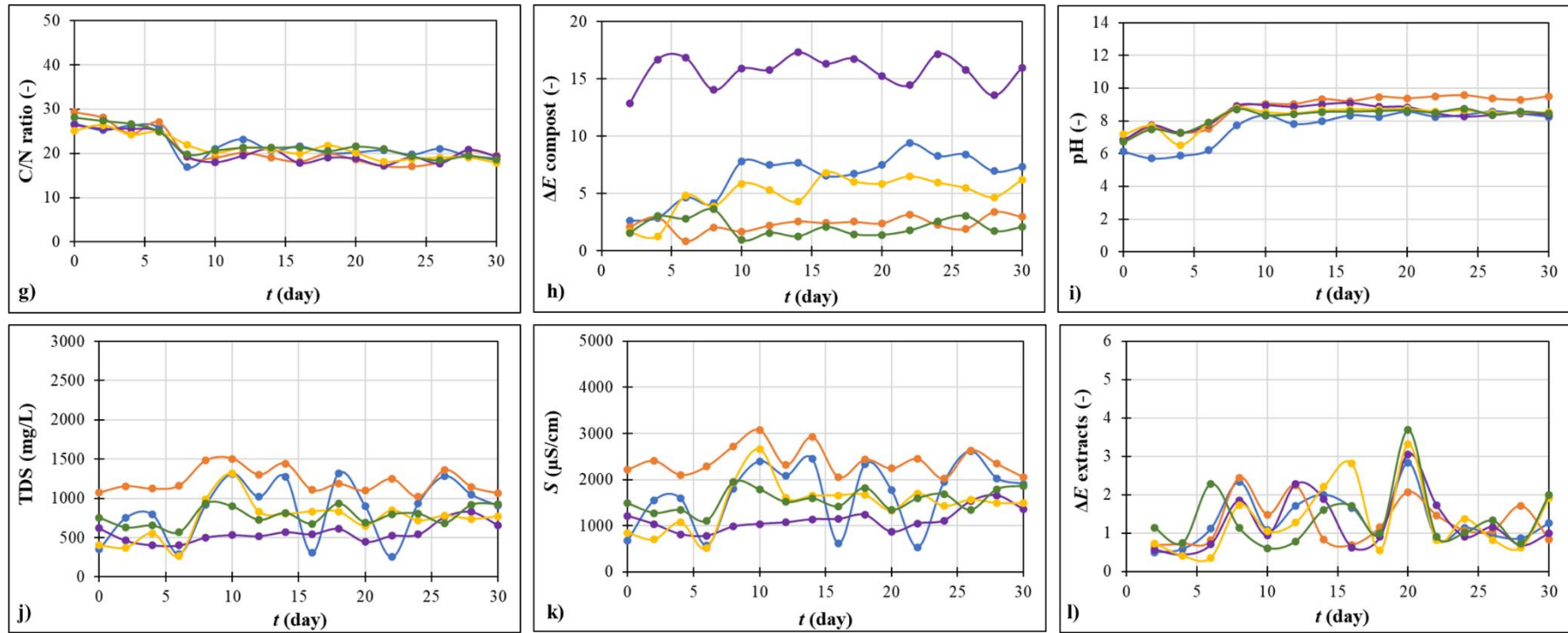
Figure 35. (*continuing*) Changes in: g) C/N ratio; h) ΔE compost; i) pH; j) TDS; k) S and l) ΔE extracts during the 30 days of grape skin composting process (• experiment 1; • experiment 2; • experiment 3; • experiment 4; • experiment 5) (ΔE compost=total color change of compost samples; TDS=total dissolved solids; S=conductivity; ΔE extracts=total color change of compost extracts)

The results of microbiological analysis during the composting processes in reactors with different pretreatment of grape skin are shown in Figure 36. The microbial growth was monitored every 96 hours.
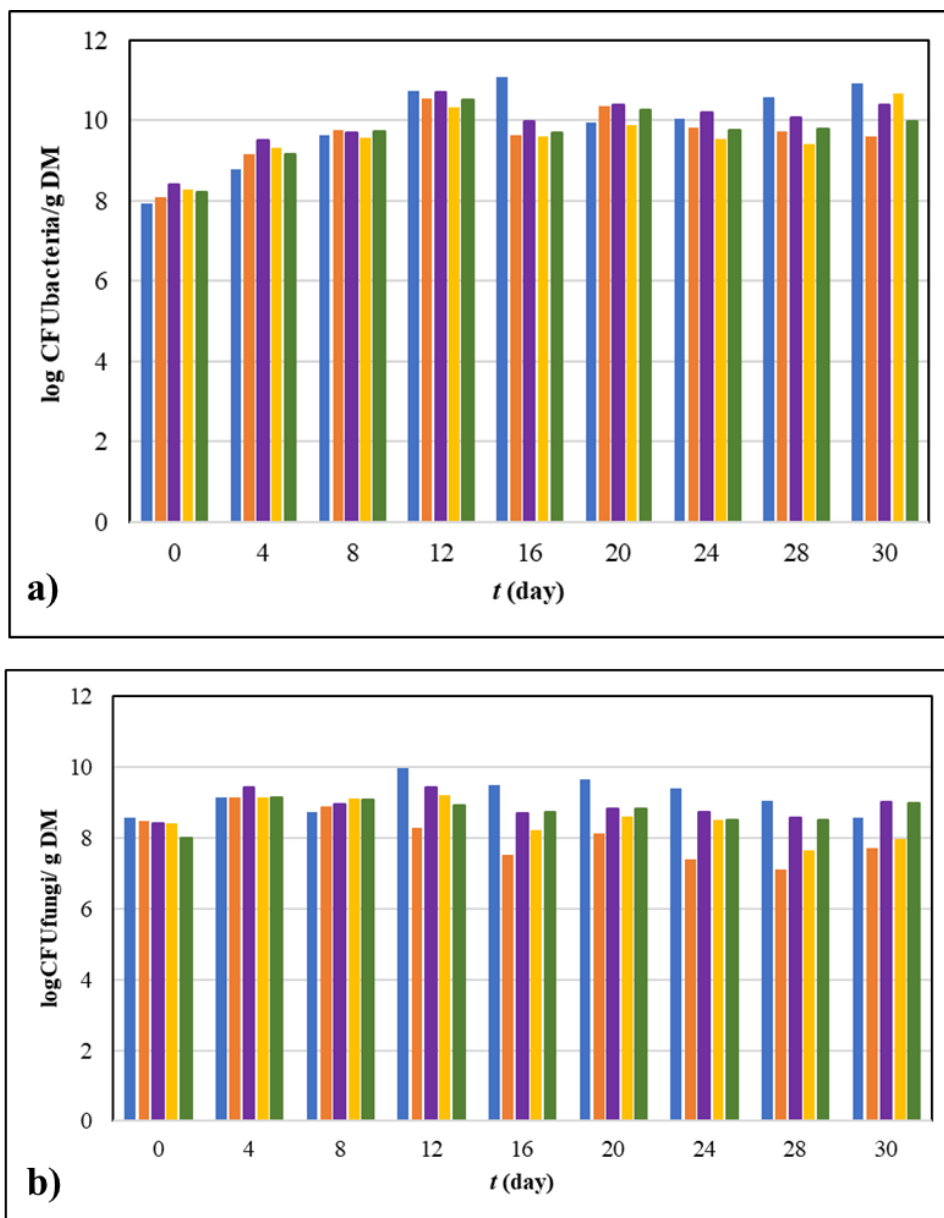
Figure 36. Microbial growth during the 30 days of grape skin composting process: a) Bacterial growth and b) Growth of fungi (• experiment 1; • experiment 2; • experiment 3; • experiment 4; • experiment 5)

The changes in germination index in reactors during the 30 days of composting processes are shown in Figure 37. To a final composts, bulk density and porosity were determined and the results are shown in Table 52.
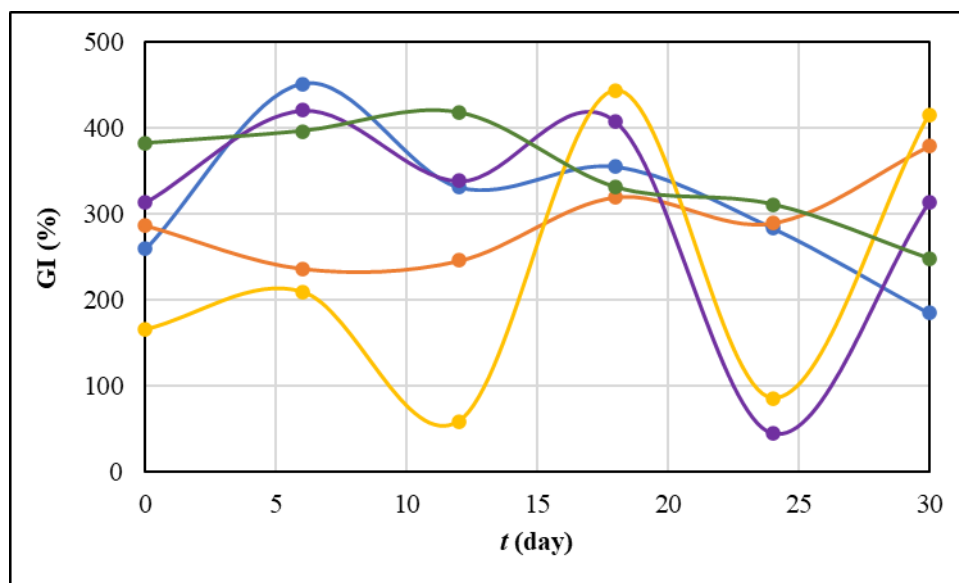
Figure 37. Changes in germination index (GI) during the 30 days of grape skin composting process (• experiment 1; • experiment 2; • experiment 3; • experiment 4; • experiment 5)

Table 52. The results of bulk density and porosity obtained for final composts

Experiment	Bulk density (ρ) ± S.D. (kg/ m^3)	Porosity (ε) ± S.D. (%)
1.	448.08 ± 10.941	68.709 ± 0.764
2.	403.212 ± 39.067	71.479 ± 2.764
3.	314.421 ± 8.078	77.482 ± 0.267
4.	292.666 ± 2.396	80.536 ± 0.079
5.	378.690 ± 0.607	73.014 ± 0.021

4.3.2. Kinetics of degradation of organic matter and microbial growth

As for the previous set of composting processes, organic matter degradation was described by first-order kinetic model, because the experimental data for the organic matter change during the time following the exponential decay. Furthermore, the bacterial growth was also described by first-order kinetic model, and the fungal growth was described using logistic model. The kinetic parameters and the corresponding statistical analysis are shown in Table 53.

Table 53. Kinetic parameters and corresponding statistical analysis for description of organic matter degradation and bacterial and fungal growth (k=degradation rate; OM_0=degraded organic matter content; μ=specific growth rate of bacteria or fungi; X=the number of bacterial/fungal cells; R^2 = coefficient of determination; R_{adj}^2= adjusted coefficient of determination; RMSE=root mean square error; χ^2= Chi-square; EF=modelling efficiency)

<table>
<tr><th></th><th>Exp.</th><th>k (1/day)</th><th>OM₀ (%)</th><th>R²</th><th>R²adj</th><th>RMSE</th><th>χ²</th><th>EF</th></tr>
<tr><td rowspan="5">Organic matter degradation</td><td>1.</td><td>0.0048 ± 0.0011 (p<0.0001)</td><td>76.9469 ± 1.43267 (p<0.0001)</td><td>0.5814</td><td>0.4767</td><td>2.7184</td><td>9.0955</td><td>0.5814</td></tr>
<tr><td>2.</td><td>0.0051 ± 0.0009 (p<0.0001)</td><td>71.7322 ± 1.0934 (p<0.0001)</td><td>0.6911</td><td>0.6138</td><td>2.0715</td><td>5.2813</td><td>0.6910</td></tr>
<tr><td>3.</td><td>0.0039 ± 0.0018 (p<0.0001)</td><td>81.5019 ± 2.5598 (p<0.0001)</td><td>0.2370</td><td>0.0436</td><td>4.8879</td><td>29.4058</td><td>0.2371</td></tr>
<tr><td>4.</td><td>0.0001 ± 0.002 (p<0.0001)</td><td>92.9764 ± 0.4884 (p<0.0001)</td><td>0.2343</td><td>0.0125</td><td>6.9561</td><td>1.1253</td><td>0.0125</td></tr>
<tr><td>5.</td><td>0.0001 ± 0.002 (p<0.0001)</td><td>92.9764 ± 0.4884 (p<0.0001)</td><td>0.1835</td><td>0.0206</td><td>5.4042</td><td>1.4262</td><td>0.8271</td></tr>
<tr><th></th><th>Exp.</th><th>μ (1/day)</th><th>X (logCFU/gDM)</th><th>R²</th><th>R²adj</th><th>RMSE</th><th>χ²</th><th>EF</th></tr>
<tr><td rowspan="5">Bacterial growth</td><td>1.</td><td>0.0075 ± 0.0031 (p<0.0001)</td><td>8.8363 ± 0.4925 (p<0.0001)</td><td>0.5026</td><td>0.2042</td><td>0.4883</td><td>0.2934</td><td>0.5023</td></tr>
<tr><td>2.</td><td>0.0045 ± 0.0026 (p<0.0001)</td><td>9.0357 ± 0.4160 (p<0.0001)</td><td>0.3392</td><td>0.1741</td><td>0.4051</td><td>0.21998</td><td>0.3399</td></tr>
<tr><td>3.</td><td>0.0047 ± 0.0021 (p<0.0001)</td><td>9.2205 ± 0.3490 (p<0.0001)</td><td>0.4544</td><td>0.3180</td><td>0.3434</td><td>0.1425</td><td>0.4543</td></tr>
<tr><td>4.</td><td>0.0028 ± 0.0022 (p<0.0001)</td><td>9.1224 ± 0.3568 (p<0.0001)</td><td>0.2075</td><td>0.0094</td><td>0.3440</td><td>0.1456</td><td>0.2075</td></tr>
<tr><td>5.</td><td>0.0043 ± 0.0024 (p<0.0001)</td><td>9.0645 ± 0.3812 (p<0.0001)</td><td>0.3575</td><td>0.1969</td><td>0.3708</td><td>0.1692</td><td>0.3574</td></tr>
<tr><th></th><th>Exp.</th><th>μ (1/day)</th><th>X (logCFU/gDM)</th><th>R²</th><th>R²adj</th><th>RMSE</th><th>χ²</th><th>EF</th></tr>
<tr><td rowspan="5">Fungal growth</td><td>1.</td><td>0.0021 ± 0.0019 (p<0.0001)</td><td>8.9766 ± 0.2941 (p<0.0001)</td><td>0.3765</td><td>0.3132</td><td>0.2824</td><td>0.0981</td><td>0.1792</td></tr>
<tr><td>2.</td><td>0.0076 ± 0.0019 (p<0.0001)</td><td>9.0208 ± 0.2795 (p<0.0001)</td><td>0.7193</td><td>0.6491</td><td>0.2544</td><td>0.0796</td><td>0.7192</td></tr>
<tr><td>3.</td><td>0.0011 ± 0.0019 (p<0.0001)</td><td>9.0189 ± 0.2514 (p<0.0001)</td><td>0.2652</td><td>0.1684</td><td>0.2371</td><td>0.0691</td><td>0.0652</td></tr>
<tr><td>4.</td><td>0.0036 ± 0.0019 (p<0.0001)</td><td>9.0645 ± 0.3146 (p<0.0001)</td><td>0.3371</td><td>0.1714</td><td>0.2925</td><td>0.1053</td><td>0.3371</td></tr>
<tr><td>5.</td><td>0.0001 ± 0.0001 (p<0.0001)</td><td>8.7296 ± 0.2606 (p<0.0001)</td><td>0.3272</td><td>0.2489</td><td>0.2474</td><td>0.0751</td><td>0.0019</td></tr>
</table>

141

Results

4.3.3. Basic statistical analysis

The results of the statistical analysis of physicochemical properties of compost samples and compost extracts at the beginning of the composting process and at the end of the process for all reactors are shown in Table 54.

Table 54. Mean values of physicochemical properties of compost at the beginning and the end of the composting process. [A-E] The same capital letters in the row indicate that there is no significant difference ($p > 0.05$) between samples in different experiments according to two-way ANOVA and Tukey's post hoc test. [a-b] The same lowercase letters in the column indicate that there is no significant difference ($p > 0.05$) between the samples at the beginning and end of the composting process according to two-way analysis of variance and Tukey's post hoc test. (MC=moisture content; DM=dry matter content; OM= organic matter content; AC= ash content; CC=carbon content; NC= nitrogen content; TDS=total dissolved solids; S=conductivity)

Variable	Day	Exp.1	Exp.2	Exp.3	Exp.4	Exp.5
MC (%)	0.	$67.364 \pm 0.809^{A.a}$	$68.340 \pm 0.052^{A.a}$	$63.186 \pm 1.963^{A.a}$	$69.606 \pm 1.205^{A.a}$	$68.308 \pm 0.793^{A.a}$
	30.	$69.868 \pm 2.218^{A.a}$	$70.774 \pm 1.914^{A.a}$	$66.245 \pm 9.171^{A.a}$	$66.558 \pm 0.282^{A.a}$	$71.303 \pm 1.344^{A.a}$
DM (%)	0.	$32.636 \pm 0.809^{A.a}$	$31.660 \pm 0.052^{A.a}$	$36.814 \pm 1.963^{A.a}$	$30.394 \pm 1.205^{A.a}$	$31.692 \pm 0.793^{A.a}$
	30.	$30.132 \pm 2.218^{A.a}$	$29.226 \pm 1.914^{A.a}$	$33.755 \pm 9.171^{A.a}$	$33.442 \pm 0.282^{A.a}$	$28.697 \pm 1.344^{A.a}$
OM (%)	0.	$77.271 \pm 5.645^{B.a}$	$74.996 \pm 0.043^{B.a}$	$83.649 \pm 2.809^{B.a}$	$91.790 \pm 0.340^{A.a}$	$79.294 \pm 2.124^{B.a}$
	30.	$66.086 \pm 1.201^{B.b}$	$65.042 \pm 1.415^{B.a}$	$70.394 \pm 0.795^{B.b}$	$93.765 \pm 0.162^{A.a}$	$74.444 \pm 8.805^{B.a}$
AC (%)	0.	$22.729 \pm 5.645^{B.b}$	$25.004 \pm 0.043^{B.a}$	$16.351 \pm 2.809^{B.a}$	$8.210 \pm 0.340^{A.a}$	$20.707 \pm 2.124^{B.a}$
	30.	$33.914 \pm 1.201^{B.a}$	$34.958 \pm 1.415^{B.a}$	$25.128 \pm 10.429^{B.a}$	$6.235 \pm 0.162^{A.a}$	$25.557 \pm 8.805^{B.a}$
CC (%)	0.	$44.817 \pm 3.274^{B.a}$	$43.498 \pm 0.025^{B.a}$	$48.516 \pm 1.629^{B.a}$	$53.238 \pm 0.197^{A.b}$	$45.990 \pm 1.232^{B.a}$
	30.	$38.330 \pm 0.696^{A.b}$	$37.724 \pm 0.821^{D.b}$	$43.426 \pm 6.049^{B.b}$	$54.384 \pm 0.094^{A.a}$	$43.177 \pm 5.107^{C.b}$
NC (%)	0.	$1.750 \pm 0.004^{A,b}$	$1.610 \pm 0.004^{A,b}$	$1.820 \pm 0.004^{A,b}$	$1.960 \pm 0.004^{A,b}$	$1.710 \pm 0.004^{A,b}$
	30.	$2.610 \pm 0.004^{A,a}$	$2.480 \pm 0.004^{A,a}$	$2.430 \pm 0.004^{A,a}$	$2.600 \pm 0.004^{A,a}$	$2.700 \pm 0.004A,a$
C/N ratio	0.	$26.690 \pm 0.004^{A,b}$	$29.380 \pm 0.004^{A,b}$	$26.4286 \pm 0.004^{A,b}$	$25.1020 \pm 0.004^{A,b}$	$28.1287 \pm 0.004^{A,b}$
	30.	$18.930 \pm 0.004^{A,a}$	$19.440 \pm 0.004^{A,a}$	$19.3827 \pm 0.004^{A,a}$	$17.8462 \pm 0.004^{A,a}$	$18.5565 \pm 0.004^{A,a}$
pH	0.	$6.123 \pm 0.006^{E.b}$	$6.837 \pm 0.006^{C.b}$	$6.847 \pm 0.006^{B.b}$	$7.167 \pm 0.012^{A.b}$	$6.723 \pm 0.006^{D.b}$
	30.	$8.237 \pm 0.023^{D.a}$	$9.506 \pm 0.023^{D.a}$	$8.357 \pm 0.025^{C.a}$	$8.507 \pm 0.015^{A.a}$	$8.437 \pm 0.038^{B.a}$
TDS (mg/L)	0.	$353.000 \pm 1.000^{E.b}$	$1076.670 \pm 12.503^{A.a}$	$620.333 \pm 2.517^{C.a}$	$401.333 \pm 9.019^{D.b}$	$752.667 \pm 1.528^{B.b}$
	30.	$905.667 \pm 34.020^{A.a}$	$1066.000 \pm 34.020^{A.b}$	$659.333 \pm 12.583^{C.a}$	$773.333 \pm 0.577^{B.a}$	$929.667 \pm 1.155^{A.a}$
S (μS/cm)	0.	$682.000 \pm 12.000^{E.b}$	$2220.000 \pm 20.000^{A.a}$	$1213.670 \pm 11.676^{C.b}$	$846.667 \pm 10.408^{D.b}$	$1486.670 \pm 8.505^{B.b}$
	30.	$1905.000 \pm 9.539^{A.a}$	$2056.667 \pm 9.539^{A.b}$	$1363.330 \pm 8.622^{C.a}$	$1489.000 \pm 2.000^{B.a}$	$1868.330 \pm 4.933^{A.a}$

4.3.4. Principal Component Analysis (PCA)

The effect of sampling day on physicochemical properties of compost and compost extracts during the composting process was analysed using the principal component analysis and the results are shown in Figure 38.
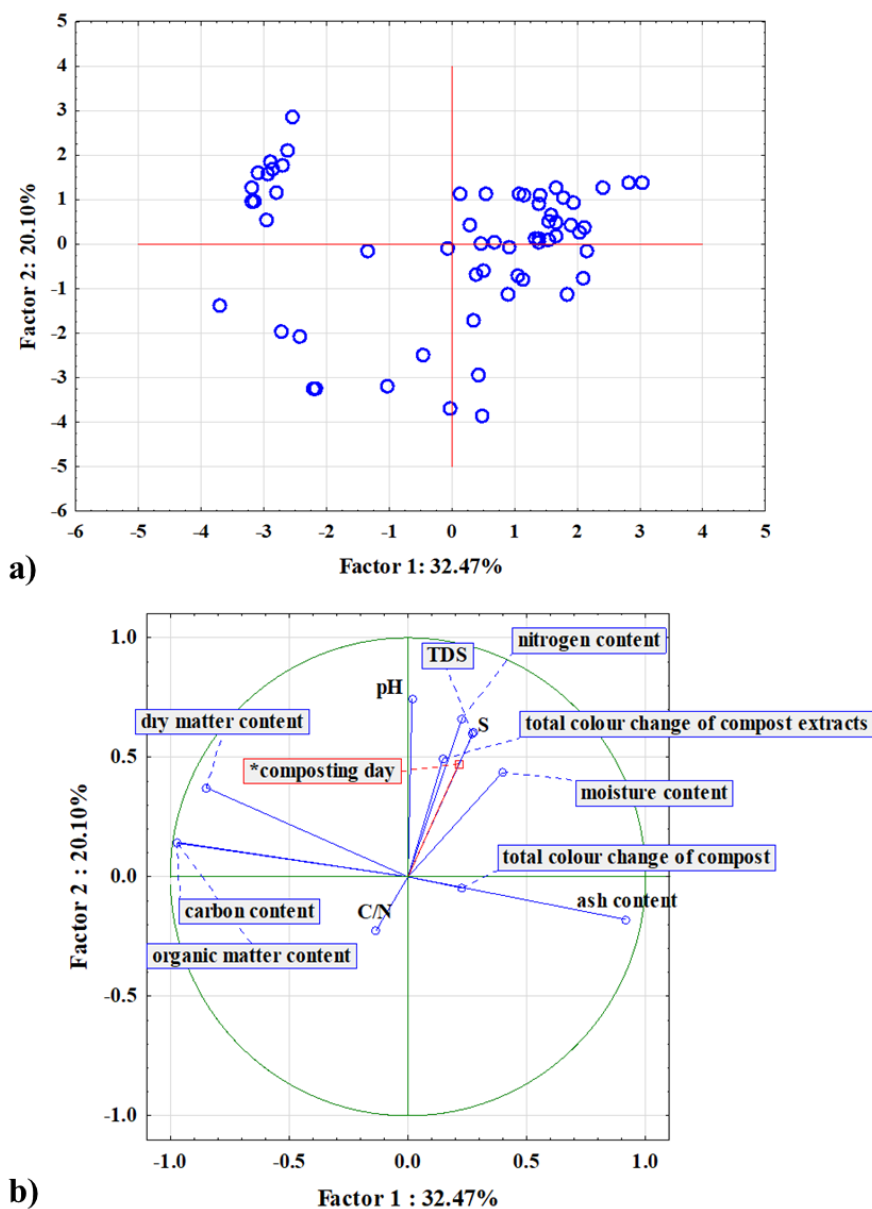
Figure 38. Principal component analysis (PCA): a) score plot and b) loading plot showing the relationship between sampling day and physicochemical properties of compost during the composting process

4.3.5. NIR spectra of compost samples and compost extract samples

During the composting processes, the NIR spectra were recorded for all compost samples and compost extract samples with different NIR instruments. The recorded spectra are shown in Figures 39-41.
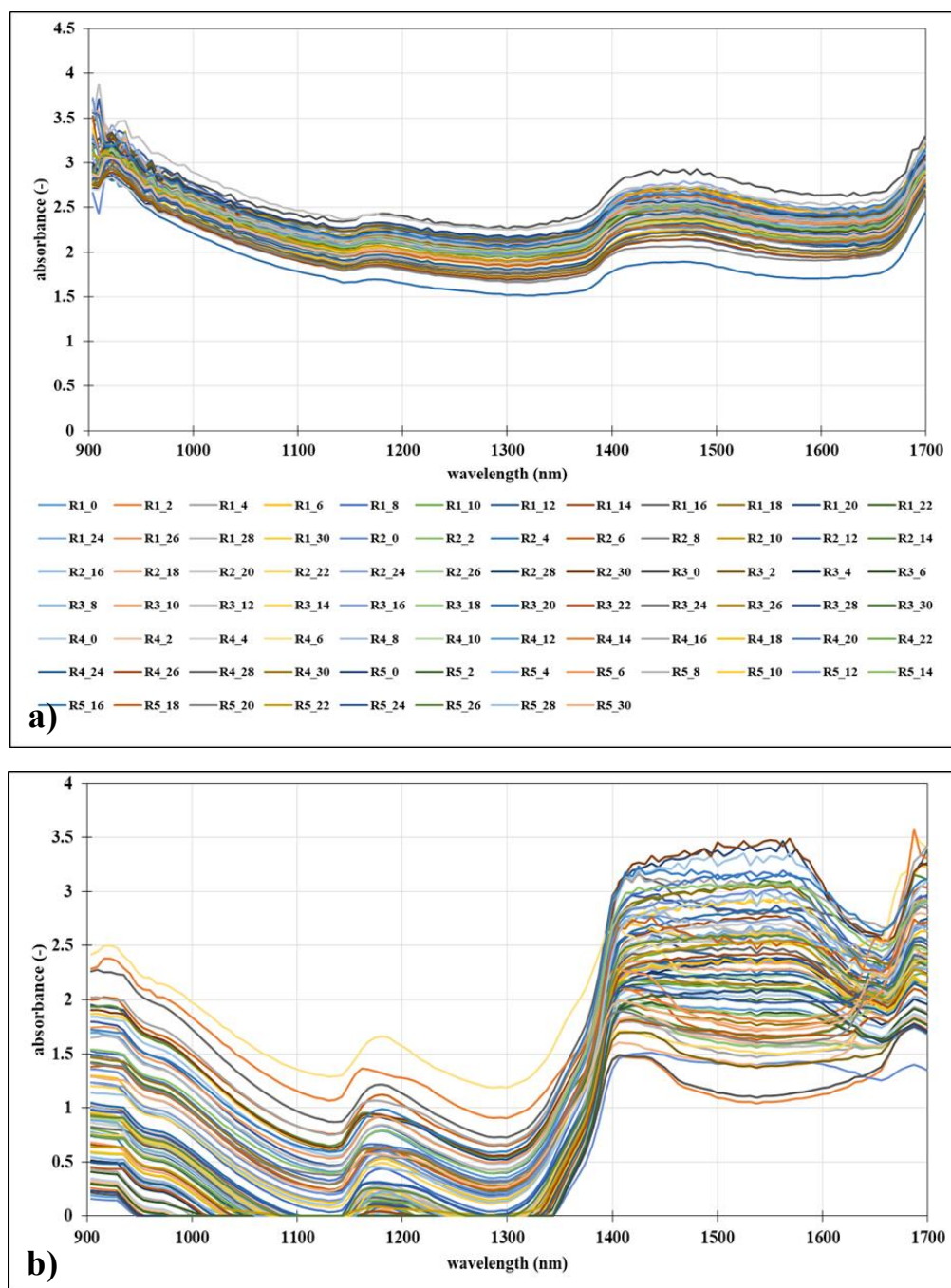
Figure 39. Average NIR spectra of a) compost samples and b) compost extracts gathered using NIR spectrometer (NIR-128-1.7-USB/6.25/50 μm, Control Development Inc., USA) (the legend from figure a) is applicable for figure b))
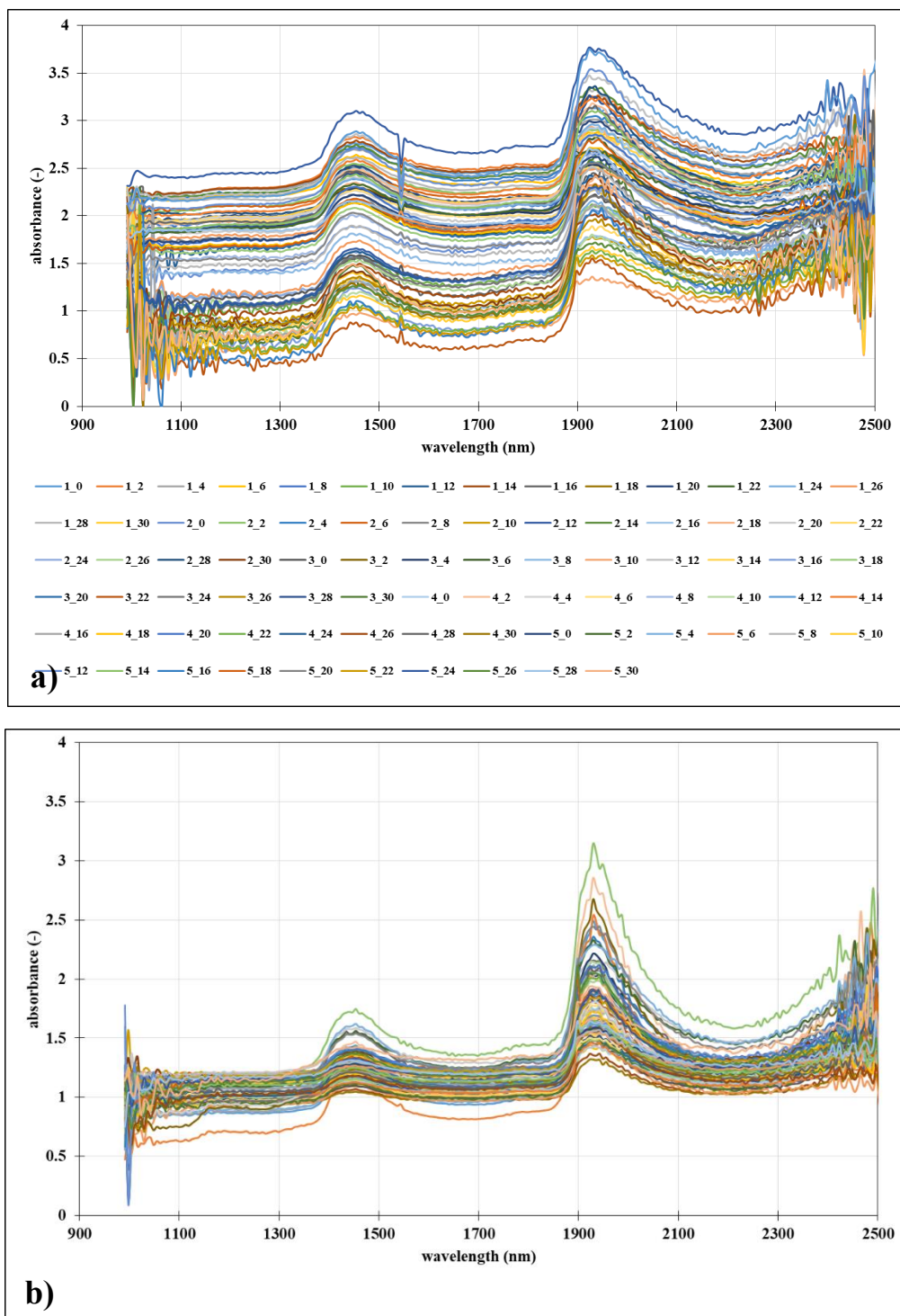
Figure 40. Average NIR spectra of a) compost samples and b) compost extracts gathered using NIR spectrometer (AvaSpec-NIR256-2.5-HSC-EVO, Avantes, USA) (the legend from figure a) is applicable for figure b))

146
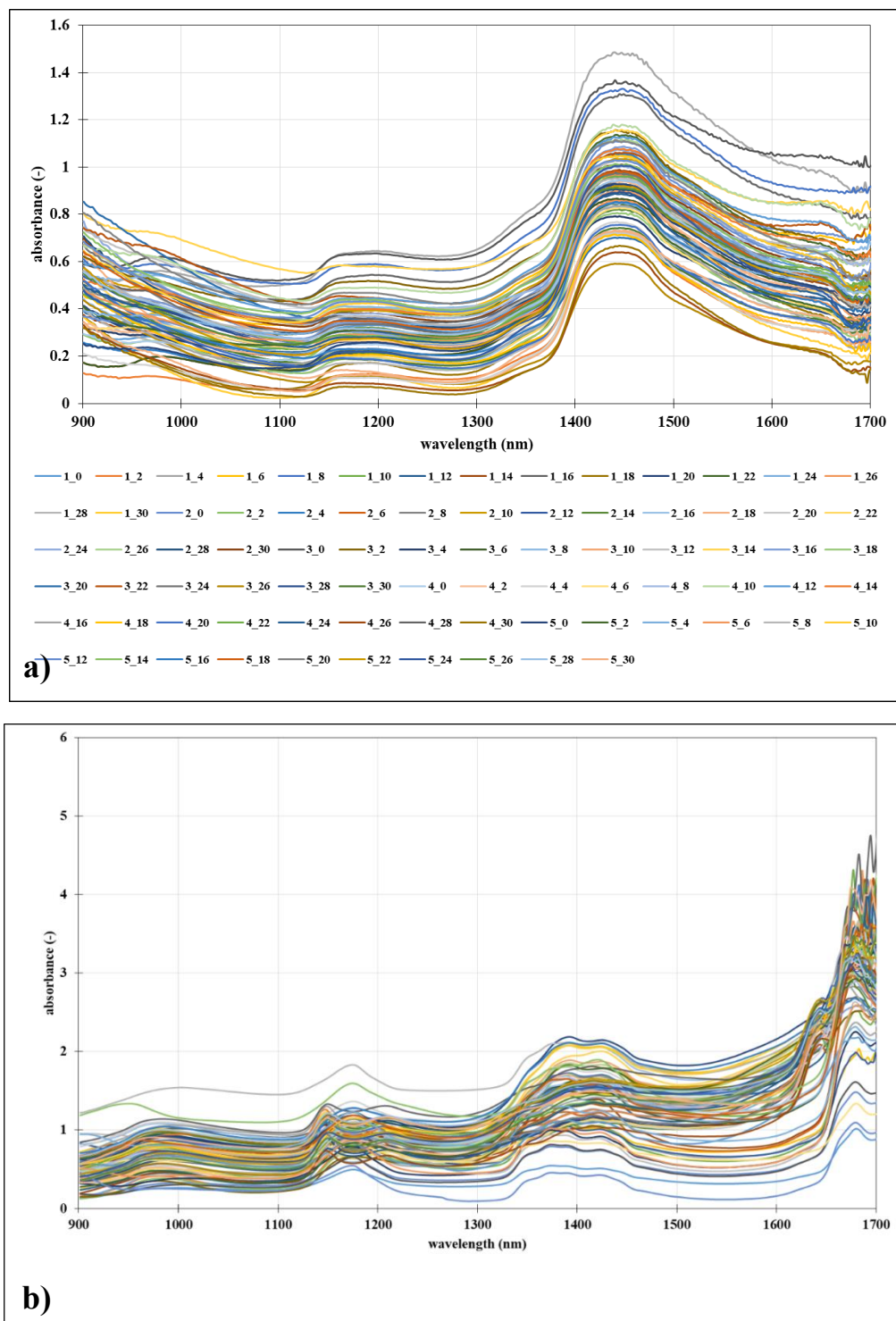
Figure 41. Average NIR spectra of a) compost samples gathered with portable NIR spectrometer (NIR-S-G1, InnoSpectra, Taiwan) and b) compost extracts gathered with portable NIR spectrometer (NIR-M-R2, InnoSpectra, Taiwan) (the legend from figure a) is applicable for figure b))

147

4.3.6. Principal component analysis (PCA) of NIR spectra of compost samples and compost extracts

The principal component analysis (PCA) was performed for the average NIR spectra of compost samples and compost extracts recorded with different NIR instruments and the results are shown in figures below (Figures 42-44).
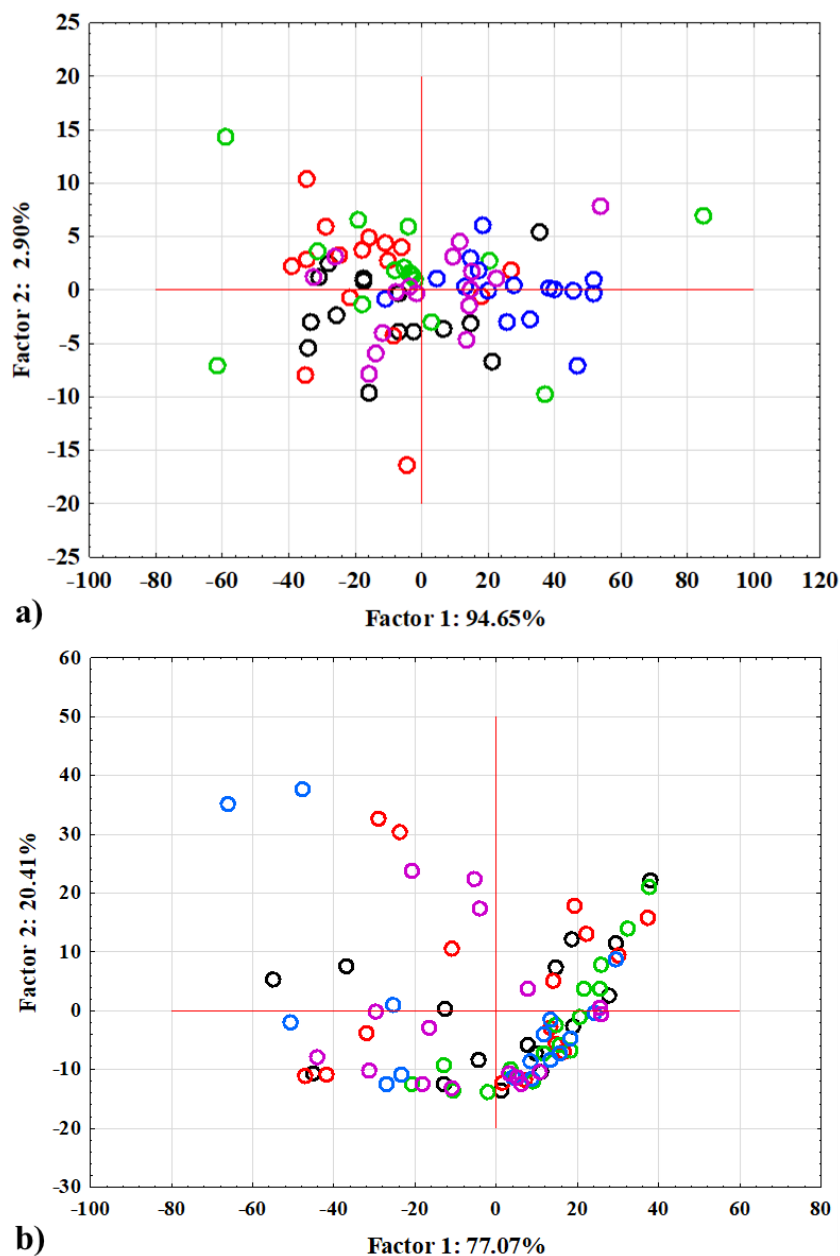
Figure 42. Principal component analysis (PCA) of mean values of NIR spectra of a) compost samples and b) compost extracts during the composting process recorded with a NIR spectrometer (NIR-128-1.7-USB/6.25/50 μm, Control Development Inc., USA) (○ - experiment 1, ○ - experiment 2, ○ - experiment 3, ○ - experiment 4, ○ - experiment 5)
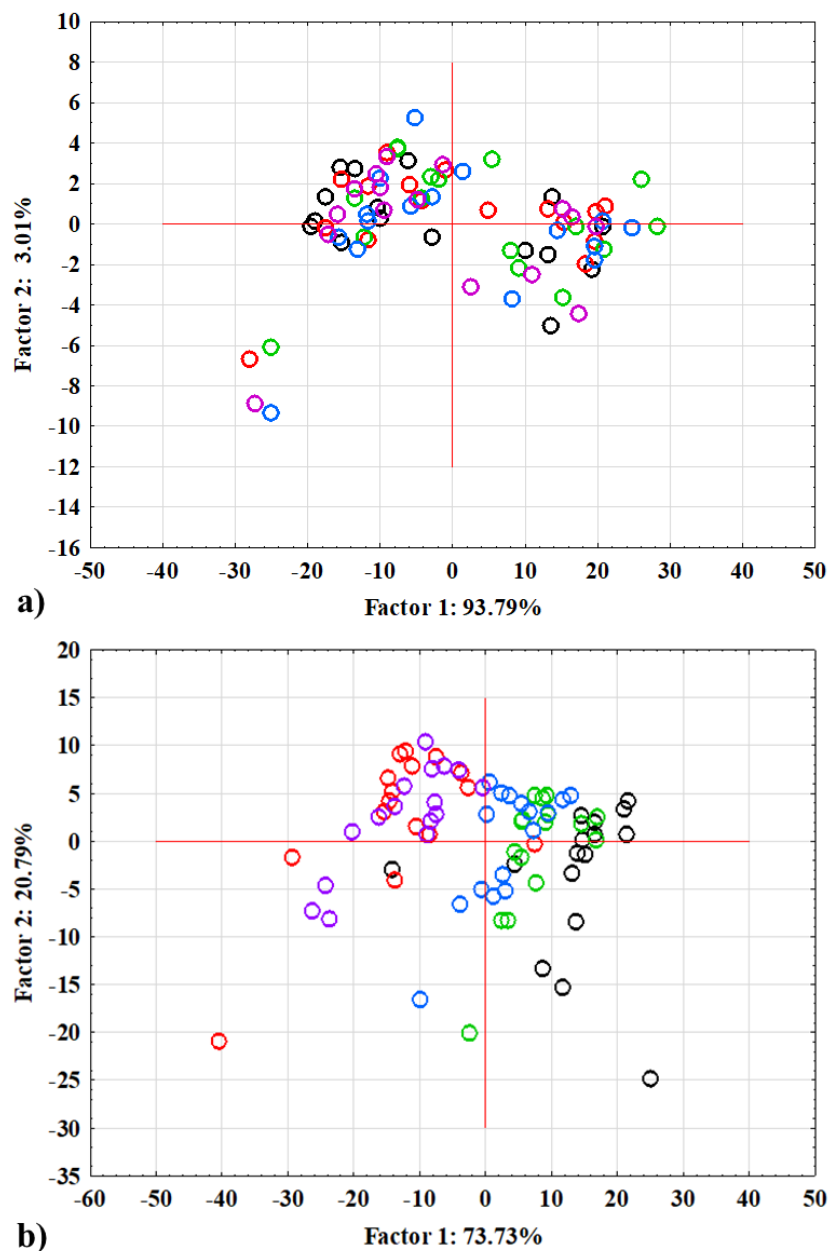
Figure 43. Principal component analysis (PCA) of mean values of NIR spectra of a) compost samples and b) compost extracts during the composting process recorded with a NIR spectrometer (AvaSpec- NIR256-2.5-HSC-EVO, Avantes, USA) (○ - experiment 1, ○ - experiment 2, ○ - experiment 3, ○ - experiment 4, ○ - experiment 5)
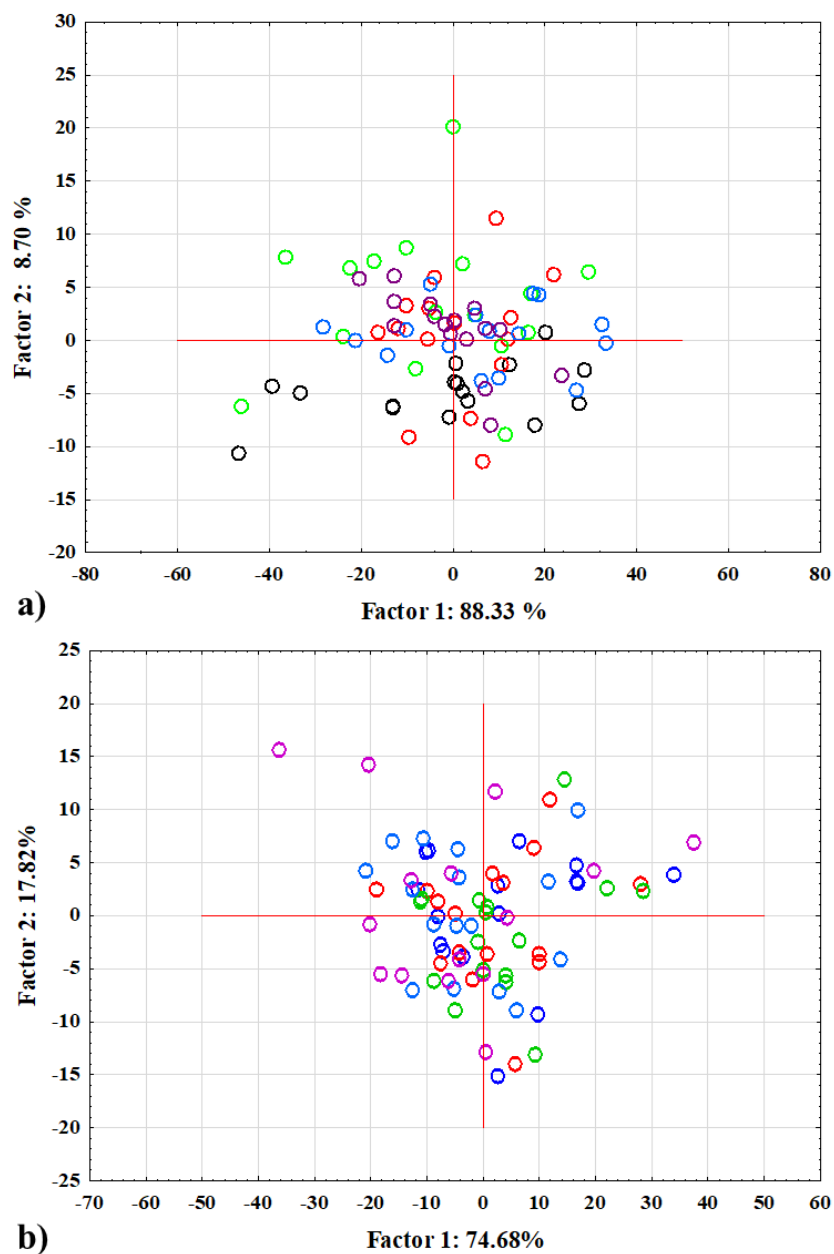
Figure 44. Principal component analysis (PCA) of mean values of NIR spectra of a) compost samples gathered with portable NIR spectrometer (NIR-S-G1, InnoSpectra, Taiwan) and b) compost extracts gathered with portable NIR spectrometer (NIR-M-R2, InnoSpectra, Taiwan) (○ - experiment 1, ○ - experiment 2, ○ - experiment 3, ○ - experiment 4, ○ - experiment 5)

4.3.7. Artificial neural network (ANN) models for the prediction of physicochemical properties of compost samples and compost extracts samples during the composting process

As mentioned before, due to complexity of the NIR spectra, the preprocessing of spectra has been applied in order to obtain important infromation about physicochemical properties of compost. Furthermore, the artificial neural network (ANN) models were developed based on the recorded NIR spectra for the compost samples and compost extracts. The developed ANN models based on NIR spectra obtained using the NIR spectrometer (NIR-128-1.7-USB/6.25/50 µm, Control Development Inc., USA) for each property of the samples are shown in Tables 55-67. The developed ANN models based on NIR spectra obtained using the another NIR spectrometer (AvaSpec-NIR256-2.5-HSC-EVO, Avantes, USA) for each property of the samples are shown in Tables 68-80. Furthermore, in this set of composting experiments the portable NIR spectrometer was used. The developed ANN models based on NIR spectra obtained using the portable NIR spectrometers NIR-S-G1 (InnoSpectra, Taiwan) and NIR-M-R2 (InnoSpectra, Taiwan) for each property of the compost samples and compost extracts are shown in Tables 81-93.

Table 55. Artificial neural network (ANN) models for prediction of day of composting of compost samples during the composting process based on the NIR spectra gathered using NIR spectrometer (NIR-128-1.7-USB/6.25/50 μm, Control Development inc., USA) (R_{pred}^2=coefficient of determination for prediction; $R_{pred}^2{}_{adj}$=adjusted coefficient of determination for prediction; *RMSEP*=root mean square of prediction; *SEP*=standard error of prediction; *RPD*=ratio of prediction to deviation; *RER*=ratio of the error range). Pretreatment selected as optimal is marked bold

Output variable	NIR spectra pretreatment	Network name	Calibration					Prediction					
			Training perf. Training error	Test perf. Test error	Validation perf. Validation error	Hidden activation	Output activation	R_{pred}^2	$R_{pred}^2{}_{adj}$	*RMSEP*	*SEP*	*RPD*	*RER*
Day of composting	raw	MLP 5-5-1	0.6880 4.9815	0.4470 10.6643	0.3867 12.2619	Exponential	Logistic	0.5418	0.4453	6.0822	1.2967	1.3436	4.6036
	smoothing	MLP 5-4-1	0.9482 1.9305	0.8888 6.1594	0.8452 8.8907	Tanh	Tanh	0.5283	0.4290	7.5016	1.5994	1.3014	3.9991
	SG1D	MLP 5-11-1	0.9881 0.9010	0.9443 4.5704	0.9401 5.3793	Tanh	Tanh	0.7002	0.6370	5.6360	1.2016	1.8011	5.3229
	SG2D	MLP 5-8-1	0.9392 3.5679	0.9375 5.3863	0.8834 6.8795	Tanh	Exponential	0.7453	0.6917	6.7432	1.4377	1.4829	4.4489
	SNV	**MLP 5-8-1**	**0.9793 2.3423**	**0.9322 5.6986**	**0.8395 8.6103**	**Logistic**	**Exponential**	**0.8172**	**0.7788**	**4.9774**	**1.0612**	**1.9190**	**6.0272**
	MSC	MLP 5-6-1	0.7753 4.3423	0.7778 6.6986	0.7711 10.6103	Logistic	Exponential	0.4982	0.3925	5.3458	1.1397	1.3864	4.4895
	smoothing+SNV	MLP 5-6-1	0.9714 4.1333	0.9648 4.1855	0.9423 4.6354	Tanh	Tanh	0.2213	0.0574	11.5404	2.4604	0.9055	2.5996
	smoothing+MSC	MLP 5-5-1	0.9453 1.2705	0.9357 5.6351	0.8835 7.6948	Exponential	Tanh	0.1758	0.0022	10.7694	2.2960	0.9350	2.7857
	SG1D+SNV	MLP 5-7-1	0.7326 7.5858	0.7288 10.4818	0.7068 12.4170	Tanh	Tanh	0.2075	0.0407	11.2212	2.3924	0.8681	2.6735
	SG1D+MSC	MLP 5-4-1	0.9730 1.9622	0.9605 2.4375	0.8188 13.2513	Logistic	Logistic	0.6536	0.5806	6.2236	1.3269	1.5070	4.8203
	SG2D+SNV	MLP 5-5-1	0.9310 1.9622	0.8963 2.4375	0.8779 13.2513	Exponential	Identity	0.2298	0.0676	15.2684	3.2552	0.6155	1.9648
	SG2D+MSC	MLP 5-4-1	0.9564 0.9564	0.8807 13.0187	0.8078 12.4674	Tanh	Exponential	0.3320	0.1913	9.1491	1.9506	1.0940	3.2790

Table 56. Artificial neural network (ANN) models for prediction of moisture content of compost samples during the composting process based on the NIR spectra gathered using NIR spectrometer (NIR-128-1.7-USB/6.25/50 μm, Control Development inc., USA) (R_{pred}^2=coefficient of determination for prediction; $R_{pred}^2{}_{adj}$=adjusted coefficient of determination for prediction; $RMSEP$=root mean square of prediction; SEP=standard error of prediction; RPD=ratio of prediction to deviation; RER=ratio of the error range). Pretreatment selected as optimal is marked bold

Output variable	NIR spectra pretreatment	Network name	Calibration					Prediction					
			Training perf. Training error	Test perf. Test error	Validation perf. Validation error	Hidden activation	Output activation	R_{pred}^2	$R_{pred}^2{}_{adj}$	$RMSEP$	SEP	RPD	RER
Moisture content	raw	MLP 5-5-1	0.4867 15.9815	0.4842 16.6643	0.4605 22.2619	Exponential	Logistic	0.2605	0.1048	1.4403	0.3071	0.9626	4.1119
	smoothing	MLP 5-9-1	0.8008 0.6975	0.7691 0.8653	0.7421 10.8649	Tanh	Logistic	0.2966	0.1485	2.3388	0.4986	0.9974	4.1557
	SG1D	MLP 5-9-1	0.9575 0.5727	0.7365 1.1361	0.7046 10.1685	Exponential	Exponential	0.4772	0.3671	2.4341	0.5190	1.3312	6.2301
	SG2D	MLP 5-10-1	0.5811 2.0029	0.5444 2.0969	0.5213 12.3422	Exponential	Logistic	0.3916	0.2636	2.2121	0.4716	1.1169	4.9776
	SNV	MLP 5-9-1	0.9343 0.8048	0.9238 1.9119	0.7422 12.3422	Tanh	Exponential	0.2740	0.1212	1.9077	0.4067	1.0714	5.4999
	MSC	MLP 5-4-1	0.8986 0.6459	0.8683 0.6993	0.7203 1.7553	Logistic	Tah	0.3726	0.2405	2.2531	0.4804	1.0313	4.1295
	smoothing+SNV	MLP 5-4-1	0.6344 0.7875	0.6202 2.5123	0.6178 4.3582	Logistic	Logistic	0.2769	0.1246	1.9028	0.4057	1.0049	3.5409
	smoothing+MSC	MLP 5-4-1	0.8848 0.5754	0.8416 12.5482	0.6359 14.9051	Tanh	Logistic	0.4207	0.2987	2.2880	0.4878	1.0532	4.2060
	SG1D+SNV	MLP 5-7-1	0.7326 5.8584	0.6688 10.4868	0.6228 14.1700	Tanh	Tanh	0.2207	0.0566	1.8938	0.4038	1.0151	4.6337
	SG1D+MSC	MLP 5-5-1	0.7822 0.6071	0.7315 3.8585	0.6255 14.3333	Logistic	Tanh	0.2337	0.0724	1.8992	0.4049	1.1259	5.5245
	SG2D+SNV	MLP 5-6-1	0.8594 0.5363	0.8128 3.0637	0.6307 16.2538	Tanh	Identity	0.2116	0.0457	2.1730	0.4633	0.9589	4.8283
	SG2D+MSC	**MLP 5-11-1**	**0.5505 1.7287**	**0.5484 1.8351**	**0.5406 1.9043**	**Identity**	**Exponential**	**0.5496**	**0.4548**	**2.1901**	**0.4669**	**1.4450**	**6.5937**

Table 57. Artificial neural network (ANN) models for prediction of dry matter content of compost samples during the composting process based on the NIR spectra gathered using NIR spectrometer (NIR-128-1.7-USB/6.25/50 μm, Control Development inc., USA) (R_{pred}^2=coefficient of determination for prediction; $R_{pred}^2{}_{adj}$=adjusted coefficient of determination for prediction; *RMSEP*=root mean square of prediction; *SEP*=standard error of prediction; *RPD*=ratio of prediction to deviation; *RER*=ratio of the error range). Pretreatment selected as optimal is marked bold

Output variable	NIR spectra pretreatment	Network name	Calibration					Prediction					
			Training perf. Training error	Test perf. Test error	Validation perf. Validation error	Hidden activation	Output activation	R_{pred}^2	$R_{pred}^2{}_{adj}$	*RMSEP*	*SEP*	*RPD*	*RER*
Dry matter content	raw	MLP 5-5-1	0.9596 5.9815	0.7237 6.6643	0.6237 6.2619	Exponential	Logistic	0.2778	0.1257	18.5393	3.9526	1.0296	2.3985
	smoothing	MLP 5-5-1	0.9874 9.7684	0.9689 11.4916	0.9690 13.6093	Exponential	Exponential	0.3087	0.1632	18.9897	4.0486	0.9561	2.3900
	SG1D	MLP 5-4-1	0.8375 16.5789	0.7666 18.6236	0.7593 19.9545	Logistic	Tanh	0.1758	0.0023	44.3421	9.4538	0.3588	0.9748
	SG2D	MLP 5-10-1	0.8884 15.9666	0.8068 16.2229	0.7518 19.4808	Tanh	Exponential	0.3345	0.1944	21.3243	4.5464	0.8952	2.1536
	SNV	MLP 5-11-1	0.9966 0.8166	0.8131 12.4388	0.7817 13.4666	Tanh	Logistic	0.3975	0.2707	16.7432	3.5697	1.1507	2.6649
	MSC	MLP 5-11-1	0.9749 1.4666	0.9011 5.6656	0.7073 19.7444	Exponential	Exponential	0.2632	0.1081	8.6712	1.8487	1.0042	3.4985
	smoothing+SNV	MLP 5-11-1	0.7965 14.3755	0.7573 15.3868	0.7060 20.4738	Logistic	Logistic	0.3111	0.1661	8.8677	1.8906	1.1853	3.5839
	smoothing+MSC	MLP 5-11-1	0.8221 12.6576	0.7778 13.0459	0.6519 23.3879	Logistic	Identity	0.5677	0.4767	6.8560	1.4617	1.5128	4.6492
	SG1D+SNV	MLP 5-7-1	0.7326 10.4816	0.6685 14.1700	0.6289 24.8168	Tanh	Tanh	0.4421	0.3247	13.8902	2.9614	0.7095	2.2880
	SG1D+MSC	MLP 5-7-1	0.9179 1.8899	0.8699 17.2666	0.7022 33.3729	Tanh	Exponential	0.3775	0.2464	9.2703	1.9764	1.1194	3.3984
	SG2D+SNV	**MLP 5-7-1**	**0.6616 23.6706**	**0.6251 27.7735**	**0.6125 35.0022**	**Identity**	**Exponential**	**0.5255**	**0.4256**	**6.0335**	**1.2863**	**1.4497**	**5.1817**
	SG2D+MSC	MLP 5-8-1	0.6787 24.1258	0.6025 28.1117	0.6005 40.1287	Identity	Exponential	0.2778	0.1257	18.5393	3.9526	1.0296	2.3985

Table 58. Artificial neural network (ANN) models for prediction of organic matter content of compost samples during the composting process based on the NIR spectra gathered using NIR spectrometer (NIR-128-1.7-USB/6.25/50 μm, Control Development inc., USA) (R_{pred}^2=coefficient of determination for prediction; $R_{pred}^2{}_{adj}$=adjusted coefficient of determination for prediction; $RMSEP$=root mean square of prediction; SEP=standard error of prediction; RPD=ratio of prediction to deviation; RER=ratio of the error range). Pretreatment selected as optimal is marked bold

Output variable	NIR spectra pretreatment	Network name	Calibration					Prediction					
			Training perf. Training error	Test perf. Test error	Validation perf. Validation error	Hidden activation	Output activation	R_{pred}^2	$R_{pred}^2{}_{adj}$	$RMSEP$	SEP	RPD	RER
Organic matter content	raw	MLP 5-5-1	0.9552 11.9815	0.7275 26.6643	0.7249 26.2619	Exponential	Logistic	0.4902	0.3829	8.5126	1.8149	1.0817	3.2981
	smoothing	MLP 5-5-1	0.7259 22.8094	0.7184 26.0954	0.7651 31.9065	Tanh	Exponential	0.3014	0.1543	8.1752	1.7430	1.1228	3.8876
	SG1D	MLP 5-10-1	0.9986 12.1583	0.7791 32.1538	0.7182 33.9546	Tanh	Exponential	0.2356	0.0747	9.3361	1.9905	1.0374	3.1015
	SG2D	MLP 5-9-1	0.9738 11.6541	0.9103 14.4402	0.7221 34.4495	Identity	Logistic	0.4787	0.3690	8.2577	1.7605	1.2866	3.8969
	SNV	MLP 5-9-1	0.9264 5.4544	0.8683 21.6969	0.6375 45.5463	Tanh	Exponential	0.3357	0.1958	10.3493	2.2065	1.1564	3.1002
	MSC	MLP 5-9-1	0.9910 0.8889	0.7593 31.1526	0.7370 39.3008	Tanh	Identity	0.2632	0.1081	8.6712	1.8487	1.0042	3.4985
	smoothing+SNV	MLP 5-6-1	0.6994 16.9185	0.6837 30.6468	0.6505 37.9984	Exponential	Logistic	0.3111	0.1661	8.8677	1.8906	1.1853	3.5839
	smoothing+MSC	MLP 5-10-1	0.6639 42.247	0.6518 46.2150	0.6442 51.0743	Logistic	Logistic	0.5677	0.4767	6.8560	1.4617	1.5128	4.6492
	SG1D+SNV	MLP 5-8-1	0.6868 24.3051	0.6205 32.9494	0.6357 40.9408	Exponential	Exponential	0.4421	0.3247	13.8902	2.9614	0.7095	2.2880
	SG1D+MSC	MLP 5-7-1	0.9734 21.5857	0.6364 27.8978	0.6347 35.1044	Exponential	Tanh	0.3775	0.2464	9.2703	1.9764	1.1194	3.3984
	SG2D+SNV	**MLP 5-7-1**	**0.9905 6.9524**	**0.7739 21.2221**	**0.7228 24.9967**	**Logistic**	**Exponential**	**0.5255**	**0.4256**	**6.0335**	**1.2863**	**1.4497**	**5.1817**
	SG2D+MSC	MLP 5-7-1	0.7351 23.7887	0.6573 27.0438	0.5539 44.4045	Logistic	Logistic	0.1849	0.0134	9.1488	1.9505	1.0208	3.4737

Table 59. Artificial neural network (ANN) models for prediction of ash content of compost samples during the composting process based on the NIR spectra gathered using NIR spectrometer (NIR-128-1.7-USB/6.25/50 µm, Control Development inc., USA) (R_{pred}^2=coefficient of determination for prediction; $R_{pred}^2{}_{adj}$=adjusted coefficient of determination for prediction; $RMSEP$=root mean square of prediction; SEP=standard error of prediction; RPD=ratio of prediction to deviation; RER=ratio of the error range). Pretreatment selected as optimal is marked bold

Output variable	NIR spectra pretreatment	Network name	Calibration					Prediction					
			Training perf. Training error	Test perf. Test error	Validation perf. Validation error	Hidden activation	Output activation	R_{pred}^2	$R_{pred}^2{}_{adj}$	$RMSEP$	SEP	RPD	RER
Ash content	raw spectra	MLP 5-5-1	0.8181 25.9815	0.7999 26.6643	0.7991 36.2619	Exponential	Logistic	0.5678	0.4768	7.2724	1.5505	1.2470	3.8605
	smoothing	MLP 5-9-1	0.8675 23.2449	0.7757 24.3663	0.7535 42.8754	Tanh	Tanh	0.3169	0.1731	7.6366	1.6281	1.2017	4.1618
	SG1D	MLP 5-6-1	0.71669 22.2224	0.6943 24.4915	0.6801 23.6644	Logistic	Logistic	0.1745	0.0007	9.6588	2.0593	1.0036	2.9978
	SG2D	MLP 5-4-1	0.7876 14.7013	0.7492 20.6848	0.7372 24.0687	Logistic	Tanh	0.3894	0.2608	8.8291	1.8824	1.2113	3.6447
	SNV	MLP 5-9-1	0.9431 8.6188	0.7883 20.1882	0.7458 23.7699	Exponential	Logistic	0.3226	0.1800	10.3286	2.2021	1.1495	3.1064
	MSC	MLP 5-4-1	0.9179 0.5564	0.7119 8.1867	0.6564 32.2927	Tanh	Identity	0.3380	0.1987	8.3225	1.7744	1.0359	3.6451
	smoothing+SNV	MLP 5-4-1	0.9644 9.1109	0.6479 27.8775	0.6327 29.4764	Exponential	Exponential	0.1897	0.0191	11.0469	2.3552	1.0227	3.4287
	smoothing+MSC	MLP 5-8-1	0.5507 23.3937	0.5049 42.0034	0.5048 42.0217	Exponential	Tanh	0.4444	0.3275	8.2489	1.7587	1.3278	4.5917
	SG1D+SNV	MLP 5-7-1	0.5591 20.2923	0.5269 37.3775	0.5255 41.3683	Identity	Identity	0.3153	0.1711	10.5689	2.2533	0.9293	2.9521
	SG1D+MSC	MLP 5-7-1	0.9734 21.5857	0.6367 27.8798	0.6343 35.1045	Exponential	Tanh	0.3736	0.2417	8.5684	1.8268	1.2024	3.6768
	SG2D+SNV	**MLP 5-5-1**	**0.9129 21.5857**	**0.8608 27.8798**	**0.7591 35.1045**	**Logistic**	**Tanh**	**0.5023**	**0.3975**	**7.5851**	**1.6172**	**1.2935**	**5.0337**
	SG2D+MSC	MLP 5-5-1	0.8822 24.0061	0.6241 28.6931	0.6153 32.5692	Tanh	Logistic	0.4111	0.2871	7.3610	1.5694	1.2875	4.3174

Table 60. Artificial neural network (ANN) models for prediction of carbon content of compost samples during the composting process based on the NIR spectra gathered using NIR spectrometer (NIR-128-1.7-USB/6.25/50 μm, Control Development inc., USA) (R_{pred}^2=coefficient of determination for prediction; $R_{pred}^2{}_{adj}$=adjusted coefficient of determination for prediction; *RMSEP*=root mean square of prediction; *SEP*=standard error of prediction; *RPD*=ratio of prediction to deviation; *RER*=ratio of the error range). Pretreatment selected as optimal is marked bold

Output variable	NIR spectra pretreatment	Network name	Calibration					Prediction					
			Training perf. Training error	Test perf. Test error	Validation perf. Validation error	Hidden activation	Output activation	R_{pred}^2	$R_{pred}^2{}_{adj}$	*RMSEP*	*SEP*	*RPD*	*RER*
Carbon content	raw spectra	MLP 5-5-1	0.9426 5.9815	0.8081 6.6643	0.7999 6.2619	Exponential	Logistic	0.5270	0.4275	4.6642	0.9944	1.1277	3.4912
	smoothing	MLP 5-10-1	0.8731 4.1226	0.6490 10.1885	0.6370 10.8787	Tanh	Exponential	0.2671	0.1128	4.9728	1.0602	1.0704	3.7069
	SG1D	MLP 5-7-1	0.8062 7.6876	0.7493 10.6267	0.7292 15.8156	Logistic	Exponential	0.0084	-0.2004	6.5514	1.3968	0.8582	2.5635
	SG2D	MLP 5-9-1	0.7885 5.0459	0.7168 14.7678	0.7247 15.6335	Exponential	Exponential	0.1785	0.0056	12.8877	2.7477	0.4813	1.4482
	SNV	MLP 5-4-1	0.8238 4.2457	0.7247 11.3780	0.7003 14.5123	Logistic	Logistic	0.2342	0.0730	6.4493	1.3750	1.0677	2.8855
	MSC	MLP 5-4-1	0.9197 1.1867	0.7119 13.2927	0.6647 15.3221	Tanh	Identity	0.1857	0.0143	5.8725	1.2520	0.8515	2.9962
	smoothing+SNV	MLP 5-4-1	0.8737 0.0102	0.8485 0.0128	0.8441 0.0193	Exponential	Logistic	0.3558	0.2202	4.8543	1.0349	1.2402	3.7806
	smoothing+MSC	MLP 5-4-1	0.5952 10.4655	0.5613 11.2187	0.5096 13.9106	Identity	Tanh	0.3674	0.2342	5.0019	1.0664	1.2029	3.6960
	SG1D+SNV	MLP 5-4-1	0.5992 10.3598	0.5648 11.2551	0.5249 13.0905	Identity	Tanh	0.4358	0.3171	11.4330	2.4375	0.4982	1.5828
	SG1D+MSC	MLP 5-4-1	0.9818 0.4809	0.9253 2.2372	0.8708 15.6307	Logistic	Exponential	0.2785	0.1266	6.6494	1.4176	0.8987	2.7480
	SG2D+SNV	MLP 5-7-1	0.9089 4.4291	0.8532 4.6675	0.6928 13.4011	Tanh	Identity	0.2801	0.1286	6.5456	1.3955	0.7793	2.7702
	SG2D+MSC	**MLP 5-3-1**	**0.8653 7.3790**	**0.6356 10.0576**	**0.6241 15.4391**	**Exponential**	**Identity**	**0.2938**	**0.1451**	**4.9252**	**1.0500**	**1.1161**	**3.7426**

Table 61. Artificial neural network (ANN) models for prediction of nitrogen content of compost samples during the composting process based on the NIR spectra gathered using NIR spectrometer (NIR-128-1.7-USB/6.25/50 μm, Control Development inc., USA) (R_{pred}^2=coefficient of determination for prediction; $R_{pred}^2{}_{adj}$=adjusted coefficient of determination for prediction; $RMSEP$=root mean square of prediction; SEP=standard error of prediction; RPD=ratio of prediction to deviation; RER=ratio of the error range). Pretreatment selected as optimal is marked bold

Output variable	NIR spectra pretreatment	Network name	Calibration					Prediction					
			Training perf. Training error	Test perf. Test error	Validation perf. Validation error	Hidden activation	Output activation	R_{pred}^2	$R_{pred}^2{}_{adj}$	$RMSEP$	SEP	RPD	RER
Nitrogen content	raw spectra	MLP 5-5-1	0.6925 0.0199	0.6498 0.0211	0.6164 0.0211	Exponential	Logistic	0.2653	0.1107	0.2865	0.0611	0.9797	4.1886
	smoothing	**MLP 5-10-1**	**0.9134 0.0088**	**0.7416 0.0190**	**0.7302 0.0195**	**Logistic**	**Identity**	**0.3072**	**0.1614**	**0.2351**	**0.0501**	**1.1267**	**4.8074**
	SG1D	MLP 5-10-1	0.8837 0.0096	0.7977 0.0195	0.7534 0.0198	Tanh	Logistic	0.4372	0.3187	0.2266	0.0483	1.3214	4.0158
	SG2D	MLP 5-7-1	0.9183 0.0111	0.8363 0.0141	0.8214 0.0159	Logistic	Identity	0.5738	0.4840	0.2161	0.0461	1.4158	4.2111
	SNV	MLP 5-6-1	0.9439 0.0111	0.8948 0.0186	0.7707 0.0147	Logistic	Exponential	0.5573	0.4641	0.2282	0.0486	1.2482	4.4701
	MSC	MLP 5-6-1	0.8918 0.0066	0.8641 0.0091	0.8399 0.0136	Tanh	Logistic	0.3196	0.1764	0.2833	0.0604	1.1708	4.2351
	smoothing+SNV	MLP 5-5-1	0.8021 0.3454	0.5832 1.1378	0.5434 1.4926	Exponential	Exponential	0.2812	0.1299	0.2940	0.0627	0.9924	4.0812
	smoothing+MSC	MLP 5-11-1	0.7900 0.0116	0.7897 0.0162	0.7683 0.0186	Exponential	Logistic	0.2439	0.0848	0.3073	0.0655	1.0231	3.0589
	SG1D+SNV	MLP 5-4-1	0.8365 0.0109	0.7869 0.0148	0.7658 0.0189	Exponential	Logistic	0.1769	0.0036	0.5160	0.1100	0.5951	1.7634
	SG1D+MSC	MLP 5-4-1	0.9285 0.0086	0.9031 0.0021	0.8650 0.0183	Tanh	Tanh	0.3501	0.2133	0.2567	0.0547	1.1689	4.2077
	SG2D+SNV	MLP 5-6-1	0.9898 0.0028	0.9707 0.0063	0.9102 0.0073	Exponential	Tanh	0.4238	0.3025	11.3795	2.4261	1.1101	3.0325
	SG2D+MSC	MLP 5-6-1	0.9756 0.0385	0.7128 0.0401	0.6155 0.04312	Identity	Tanh	0.5476	0.4523	3.1537	0.6724	1.2111	4.5747

Table 62. Artificial neural network (ANN) models for prediction of carbon to nitrogen ratio of compost samples during the composting process based on the NIR spectra gathered using NIR spectrometer (NIR-128-1.7-USB/6.25/50 μm, Control Development inc., USA) (R_{pred}^2=coefficient of determination for prediction; $R_{pred}^2{}_{adj}$=adjusted coefficient of determination for prediction; $RMSEP$=root mean square of prediction; SEP=standard error of prediction; RPD=ratio of prediction to deviation; RER=ratio of the error range). Pretreatment selected as optimal is marked bold

Output variable	NIR spectra pretreatment	Network name	Calibration					Prediction					
			Training perf. Training error	Test perf. Test error	Validation perf. Validation error	Hidden activation	Output activation	R_{pred}^2	$R_{pred}^2{}_{adj}$	$RMSEP$	SEP	RPD	RER
C/N ratio	raw spectra	MLP 5-5-1	0.7079 3.9815	0.6685 6.6643	0.6022 16.2619	Exponential	Logistic	0.3820	0.2519	12.5656	2.6790	0.9766	2.6213
	smoothing	MLP 5-3-1	0.7125 2.8799	0.7011 4.3693	0.6929 12.1493	Tanh	Tanh	0.2231	0.0595	13.8001	2.9422	0.8906	2.3578
	SG1D	MLP 5-9-1	0.9931 3.7729	0.9903 4.2944	0.7454 10.6211	Exponential	Tanh	0.0033	-0.2065	20.2030	4.3073	0.4415	1.5362
	SG2D	MLP 5-11-1	0.8672 3.7729	0.7803 4.2944	0.7282 10.6211	Identity	Logistic	0.8300	0.7942	5.7267	1.2209	2.1603	5.8639
	SNV	MLP 5-3-1	0.9778 4.3039	0.7877 6.7555	0.6127 13.0395	Logistic	Tanh	0.5997	0.5155	8.5191	1.8163	1.1368	3.9720
	MSC	MLP 5-10-1	0.8338 3.9302	0.7704 6.8894	0.7507 19.1963	Exponential	Exponential	0.6686	0.5988	4.7555	1.0139	1.6170	4.9828
	smoothing+SNV	MLP 5-8-1	0.8521 5.8379	0.6779 6.7604	0.6684 23.6887	Exponential	Exponential	0.3099	0.1646	2.3812	0.5077	1.0171	4.5774
	smoothing+MSC	MLP 5-5-1	0.6447 2.8943	0.6424 4.7760	0.6215 6.1178	Tanh	Logistic	0.6475	0.5733	2.7528	0.5869	1.6841	5.3968
	SG1D+SNV	MLP 5-7-1	0.6400 3.6132	0.6395 4.2383	0.6301 6.0411	Identity	Identity	0.6487	0.5748	7.5633	1.6125	1.5509	4.4003
	SG1D+MSC	**MLP 5-8-1**	**0.6865 4.4660**	**0.6758 8.0220**	**0.6422 9.0307**	**Tanh**	**Identity**	**0.9865**	**0.9837**	**2.2970**	**0.4897**	**4.9313**	**14.4576**
	SG2D+SNV	MLP 5-9-1	0.8073 1.0513	0.7473 5.4258	0.7166 8.6591	Tanh	Exponential	0.4238	0.3025	11.3795	2.4261	1.1101	3.0325
	SG2D+MSC	MLP 5-4-1	0.7973 4.5153	0.7478 6.1320	0.7328 6.6498	Logistic	Tanh	0.5476	0.4523	3.1537	0.6724	1.2111	4.5747

Table 63. Artificial neural network (ANN) models for prediction of total color change (ΔE) of compost samples during the composting process based on the NIR spectra gathered using NIR spectrometer (NIR-128-1.7-USB/6.25/50 μm, Control Development inc., USA) (R_{pred}^2=coefficient of determination for prediction; $R_{pred}^2{}_{adj}$=adjusted coefficient of determination for prediction; $RMSEP$=root mean square of prediction; SEP=standard error of prediction; RPD=ratio of prediction to deviation; RER=ratio of the error range). Pretreatment selected as optimal is marked bold

Output variable	NIR spectra pretreatment	Network name	Calibration					Prediction					
			Training perf. Training error	Test perf. Test error	Validation perf. Validation error	Hidden activation	Output activation	R_{pred}^2	$R_{pred}^2{}_{adj}$	$RMSEP$	SEP	RPD	RER
ΔE (compost)	raw spectra	MLP 5-5-1	0.6901 5.9815	0.6225 10.6643	0.6118 12.2619	Exponential	Logistic	0.2953	0.1470	4.4844	0.9561	1.0882	3.6163
	smoothing	MLP 5-10-1	0.6554 7.9889	0.6548 11.2936	0.6496 13.9478	Logistic	Tanh	0.2028	0.0350	4.2190	0.8995	0.9825	3.7887
	SG1D	MLP 5-4-1	0.6317 7.9889	0.6248 11.2936	0.5845 13.9478	Exponential	Exponential	0.0209	-0.1852	6.8129	1.4525	0.8776	2.4612
	SG2D	MLP 5-10-1	0.9435 2.2868	0.6882 7.2063	0.6555 9.1088	Exponential	Tanh	0.4925	0.3856	3.6650	0.7814	1.3635	4.6871
	SNV	MLP 5-10-1	0.7639 4.7961	0.7666 6.3157	0.6379 12.7597	Logistic	Identity	0.2629	0.1078	4.1818	0.8916	1.0631	3.8225
	MSC	MLP 5-10-1	0.9507 1.0811	0.9403 8.7366	0.6266 9.7684	Logistic	Tanh	0.0875	-0.1046	10.3084	2.1978	0.4924	1.6664
	smoothing+SNV	MLP 5-7-1	0.6384 2.2899	0.5123 7.7061	0.5100 12.8081	Tanh	Exponential	0.4621	0.3488	4.1372	0.8821	1.2098	4.1521
	smoothing+MSC	MLP 5-7-1	0.9567 2.4895	0.8880 3.0065	0.7474 12.6391	Tanh	Identity	0.2982	0.1504	4.3709	0.9319	1.1250	3.9302
	SG1D+SNV	MLP 5-8-1	0.8925 10.9165	0.8227 11.4143	0.7217 15.5953	Identity	Exponential	0.4332	0.3139	3.2704	0.6972	1.3187	4.6504
	SG1D+MSC	MLP 5-5-1	0.5633 7.9440	0.5335 10.7665	0.5053 17.6218	Identity	Exponential	0.2391	0.0790	4.3903	0.9360	1.0900	3.9430
	SG2D+SNV	MLP 5-3-1	0.7553 4.2802	0.6963 6.2664	0.6786 7.6362	Exponential	Identity	0.2079	0.0411	3.9480	0.8417	1.1124	4.1360
	SG2D+MSC	**MLP 5-9-1**	**0.6104 10.7815**	**0.5809 13.0136**	**0.5411 16.2869**	**Tanh**	**Exponential**	**0.5910**	**0.5049**	**3.4396**	**0.7333**	**1.5283**	**4.8943**

Table 64. Artificial neural network (ANN) models for prediction of pH of compost samples during the composting process based on the NIR spectra gathered using NIR spectrometer (NIR-128-1.7-USB/6.25/50 μm, Control Development inc., USA) (R_{pred}^2=coefficient of determination for prediction; $R_{pred}^2{}_{adj}$=adjusted coefficient of determination for prediction; $RMSEP$=root mean square of prediction; SEP=standard error of prediction; RPD=ratio of prediction to deviation; RER=ratio of the error range). Pretreatment selected as optimal is marked bold

Output variable	NIR spectra pretreatment	Network name	Calibration					Prediction					
			Training perf. Training error	Test perf. Test error	Validation perf. Validation error	Hidden activation	Output activation	R_{pred}^2	$R_{pred}^2{}_{adj}$	$RMSEP$	SEP	RPD	RER
pH	raw spectra	MLP 5-3-1	0.9422 0.0736	0.8576 0.1110	0.7616 0.1566	Logistic	Identity	0.4856	0.3773	0.5787	0.1234	1.3733	5.4431
	smoothing	MLP 5-7-1	0.9439 0.0292	0.9417 0.0394	0.8929 0.1961	Tanh	Logistic	0.4268	0.3061	0.6993	0.1491	1.2064	4.5949
	SG1D	MLP 5-11-1	0.9928 0.0111	0.9752 0.0505	0.9278 0.7757	Logistic	Logistic	0.3747	0.2431	0.7729	0.1648	0.6183	2.8894
	SG2D	MLP 5-8-1	0.9088 0.0254	0.8385 0.0669	0.7282 0.1576	Logistic	Tanh	0.2787	0.1268	0.6540	0.1394	0.9778	3.4864
	SNV	MLP 5-3-1	0.9984 0.0171	0.7361 0.0895	0.6611 0.2142	Tanh	Logistic	0.2427	0.0833	0.6349	0.1354	1.0791	4.5204
	MSC	MLP 5-8-1	0.9931 0.0181	0.9019 0.1036	0.7849 0.1139	Tanh	Tanh	0.2731	0.1200	1.5041	0.3207	0.5466	1.8195
	smoothing+SNV	MLP 5-10-1	0.9638 0.0149	0.9158 0.0159	0.8663 0.4065	Tanh	Tanh	0.2781	0.1261	1.4768	0.3149	0.6648	2.2842
	smoothing+MSC	MLP 5-10-1	0.9602 0.0307	0.9272 0.0563	0.8827 0.0726	Tanh	Logistic	0.4131	0.2895	0.7791	0.1661	0.9764	4.1243
	SG1D+SNV	MLP 5-8-1	0.9707 0.0093	0.9350 0.0486	0.8599 0.0923	Tanh	Logistic	0.4363	0.3176	0.6388	0.1362	1.0523	4.4925
	SG1D+MSC	**MLP 5-11-1**	**0.8953 0.0477**	**0.8853 0.0548**	**0.6940 0.0681**	**Logistic**	**Logistic**	**0.7756**	**0.7284**	**0.3706**	**0.0790**	**1.8646**	**7.6733**
	SG2D+SNV	MLP 5-3-1	0.8319 0.0477	0.8155 0.0548	0.7471 0.0681	Logistic	Tanh	0.6384	0.5622	0.5305	0.1131	1.6262	6.0567
	SG2D+MSC	MLP 5-3-1	0.9173 0.095	0.6629 0.1019	0.6201 0.1274	Identity	Tanh	0.5060	0.4020	0.7173	0.1529	1.3855	4.7030

Table 65. Artificial neural network (ANN) models for prediction of total dissolved solids (TDS) of compost samples during the composting process based on the NIR spectra gathered using NIR spectrometer (NIR-128-1.7-USB/6.25/50 μm, Control Development inc., USA) (R_{pred}^2=coefficient of determination for prediction; $R_{pred}^2{}_{adj}$=adjusted coefficient of determination for prediction; $RMSEP$=root mean square of prediction; SEP=standard error of prediction; RPD=ratio of prediction to deviation; RER=ratio of the error range). Pretreatment selected as optimal is marked bold

Output variable	NIR spectra pretreatment	Network name	Calibration					Prediction					
			Training perf. Training error	Test perf. Test error	Validation perf. Validation error	Hidden activation	Output activation	R_{pred}^2	$R_{pred}^2{}_{adj}$	$RMSEP$	SEP	RPD	RER
TDS	raw spectra	MLP 5-7-1	0.9049 100.121	0.7651 357.77	0.7178 800.15	Logistic	Identity	0.2605	0.1048	1.4403	0.3071	0.9626	4.1119
	smoothing	MLP 5-9-1	0.8275 206.51	0.7116 347.84	0.7023 800.84	Exponential	Exponential	0.2966	0.1485	2.3388	0.4986	0.9974	4.1557
	SG1D	MLP 5-9-1	0.9545 116.94	0.9231 188.38	0.6633 2277.57	Logistic	Logistic	0.4772	0.3671	2.4341	0.5190	1.3312	6.2301
	SG2D	MLP 5-11-1	0.9579 134.21	0.8711 160.50	0.6882 1386.84	Tanh	Exponential	0.3916	0.2636	2.2121	0.4716	1.1169	4.9776
	SNV	MLP 5-4-1	0.7444 1565.86	0.6661 1832.51	0.6657 1922.51	Tanh	Tanh	0.2740	0.1212	1.9077	0.4067	1.0714	5.4999
	MSC	MLP 5-7-1	0.7889 1339.38	0.6215 2800.06	0.5778 3600.01	Exponential	Tanh	0.3726	0.2405	2.2531	0.4804	1.0313	4.1295
	smoothing+SNV	MLP 5-11-1	0.9098 1885.16	0.7517 2861.30	0.7261 2373.69	Logistic	Logistic	0.2769	0.1246	1.9028	0.4057	1.0049	3.5409
	smoothing+MSC	MLP 5-6-1	0.5621 1845.56	0.5415 3412.29	0.5401 3774.77	Logistic	Identity	0.4207	0.2987	2.2880	0.4878	1.0532	4.2060
	SG1D+SNV	MLP 5-10-1	0.7159 1739.82	0.6595 2640.33	0.6512 4053.44	Exponential	Tanh	0.2207	0.0566	1.8938	0.4038	1.0151	4.6337
	SG1D+MSC	MLP 5-6-1	0.9432 725.91	0.9251 741.41	0.7215 2015.97	Exponential	Identity	0.2337	0.0724	1.8992	0.4049	1.1259	5.5245
	SG2D+SNV	MLP 5-7-1	0.7846 843.33	0.7661 2006.20	0.7752 2997.78	Logistic	Identity	0.2116	0.0457	2.1730	0.4633	0.9589	4.8283
	SG2D+MSC	**MLP 5-10-1**	**0.9252 838.32**	**0.8346 2062.25**	**0.6955 2949.01**	**Logistic**	**Logistic**	**0.5496**	**0.4548**	**2.1901**	**0.4669**	**1.4450**	**6.5937**

Table 66. Artificial neural network (ANN) models for prediction of conductivity (*S*) of compost samples during the composting process based on the NIR spectra gathered using NIR spectrometer (NIR-128-1.7-USB/6.25/50 μm, Control Development inc., USA) (R_{pred}^2=coefficient of determination for prediction; $R_{pred}^2{}_{adj}$=adjusted coefficient of determination for prediction; *RMSEP*=root mean square of prediction; *SEP*=standard error of prediction; *RPD*=ratio of prediction to deviation; *RER*=ratio of the error range). Pretreatment selected as optimal is marked bold

Output variable	NIR spectra pretreatment	Network name	Calibration					Prediction					
			Training perf. Training error	Test perf. Test error	Validation perf. Validation error	Hidden activation	Output activation	R_{pred}^2	$R_{pred}^2{}_{adj}$	*RMSEP*	*SEP*	*RPD*	*RER*
S	raw spectra	MLP 5-9-1	0.9033 886.12	0.7925 887.48	0.6903 4810.42	Logistic	Identity	0.3485	0.2113	454.5514	96.9107	1.0557	4.0912
	smoothing	MLP 5-3-1	0.9296 621.74	0.7465 917.75	0.7214 986.39	Exponential	Exponential	0.2923	0.1433	516.1319	110.0397	1.1501	4.1585
	SG1D	MLP 5-5-1	0.9391 621.36	0.9328 879.28	0.7496 946.39	Logistic	Exponential	0.2479	0.0896	568.4630	121.1967	1.0437	3.7757
	SG2D	MLP 5-3-1	0.7109 961.62	0.6224 966.29	0.6161 965.43	Tanh	Identity	0.3521	0.2157	442.7759	94.4001	1.0899	4.8474
	SNV	MLP 5-6-1	0.7805 937.55	0.5578 1028.82	0.5314 1691.42	Exponential	Tanh	0.4997	0.3944	414.2253	88.3131	1.3493	5.0359
	MSC	MLP 5-3-1	0.7935 1169.55	0.6429 1211.66	0.6418 1216.61	Logistic	Exponential	0.3689	0.2361	520.1934	110.9056	1.2561	4.1260
	smoothing+SNV	MLP 5-4-1	0.7781 1077.75	0.6601 1197.78	0.6129 1777.89	Logistic	Logistic	0.3049	0.1586	477.6226	101.8295	1.1853	4.4938
	smoothing+MSC	MLP 5-6-1	0.7765 1323.33	0.7507 1834.37	0.6525 1842.89	Logistic	Identity	0.2194	0.0551	562.4688	119.9188	1.0392	3.7744
	SG1D+SNV	MLP 5-5-1	0.7238 1031.37	0.6589 1500.71	0.6549 1803.24	Tanh	Tanh	0.3871	0.2580	466.8582	99.5345	1.1794	3.9834
	SG1D+MSC	MLP 5-8-1	0.9676 797.22	0.7335 1636.11	0.6693 1706.27	Exponential	Tanh	0.5655	0.4741	330.6280	70.4901	1.4358	5.5279
	SG2D+SNV	MLP 5-4-1	0.8924 762.45	0.7777 1114.95	0.7555 1632.26	Tanh	Logistic	0.4708	0.3594	405.1278	86.3735	1.1838	4.6232
	SG2D+MSC	**MLP 5-11-1**	**0.9844 647.11**	**0.9046 976.89**	**0.8999 1047.41**	**Tanh**	**Logistic**	**0.7350**	**0.6792**	**302.9299**	**64.5849**	**1.6959**	**6.8861**

Table 67. Artificial neural network (ANN) models for prediction of total color change (ΔE) of compost extracts during the composting process based on the NIR spectra gathered using NIR spectrometer (NIR-128-1.7-USB/6.25/50 μm, Control Development inc., USA) (R_{pred}^2=coefficient of determination for prediction; $R_{pred}^2{}_{adj}$=adjusted coefficient of determination for prediction; $RMSEP$=root mean square of prediction; SEP=standard error of prediction; RPD=ratio of prediction to deviation; RER=ratio of the error range). Pretreatment selected as optimal is marked bold

| Output variable | NIR spectra pretreatment | Network name | Calibration | | | | | Prediction | | | | | |
			Training perf. Training error	Test perf. Test error	Validation perf. Validation error	Hidden activation	Output activation	R_{pred}^2	$R_{pred}^2{}_{adj}$	$RMSEP$	SEP	RPD	RER
ΔE (extracts)	raw spectra	MLP 5-10-1	0.9136 0.0032	0.9009 0.0398	0.8180 0.0966	Tanh	Exponential	0.5578	0.4647	0.5389	0.1149	1.4948	6.8590
	smoothing	MLP 5-10-1	0.8816 0.0382	0.8323 0.0745	0.8295 0.1605	Logistic	Tanh	0.2922	0.1432	0.8268	0.1763	0.8882	3.4246
	SG1D	MLP 5-5-1	0.7221 0.1573	0.6953 0.2598	0.6548 0.2995	Identity	Tanh	0.2722	0.1190	0.8386	0.1788	1.1242	4.4079
	SG2D	MLP 5-5-1	0.9846 0.0133	0.9104 0.0384	0.8652 0.1334	Logistic	Logistic	0.2923	0.1433	0.7956	0.1696	1.0791	4.6457
	SNV	MLP 5-10-1	0.7382 0.1121	0.7321 0.3594	0.6356 0.4488	Exponential	Exponential	0.2744	0.1217	0.8945	0.1907	0.7503	3.1425
	MSC	MLP 5-5-1	0.7221 0.1573	0.6953 0.2598	0.6548 0.2995	Identity	Tanh	0.3718	0.2395	0.5785	0.1233	1.1319	4.6572
	smoothing+SNV	**MLP 5-4-1**	**0.7163 0.0895**	**0.7116 0.1502**	**0.6302 0.3994**	**Tanh**	**Exponential**	**0.5399**	**0.4431**	**0.6565**	**0.1400**	**1.3940**	**5.6305**
	smoothing+MSC	MLP 5-7-1	0.8772 0.0790	0.7779 0.2817	0.7376 0.3111	Tanh	Logistic	0.2819	0.1307	0.5261	0.1122	0.9085	3.3171
	SG1D+SNV	MLP 5-8-1	0.8618 0.0785	0.8163 0.0866	0.7154 0.4829	Logistic	Identity	0.3416	0.2029	0.6793	0.1448	1.0612	4.8912
	SG1D+MSC	MLP 5-3-1	0.9803 0.0699	0.7019 0.1473	0.6935 0.2965	Exponential	Tanh	0.5172	0.4155	0.6015	0.1282	1.3378	4.7076
	SG2D+SNV	MLP 5-11-1	0.9142 0.0448	0.8506 0.0539	0.7538 0.1711	Exponential	Exponential	0.3140	0.1696	0.5639	0.1202	1.1700	4.1357
	SG2D+MSC	MLP 5-7-1	0.9819 0.0144	0.9605 0.0271	0.9026 0.1185	Tanh	Logistic	0.3044	0.1580	0.6248	0.1332	0.8321	3.0885

Table 68. Artificial neural network (ANN) models for prediction of day of composting of the compost samples during the composting process based on the NIR spectra gathered using NIR spectrometer (AvaSpec-NIR256-2.5-HSC-EVO, Avantes, USA) (R_{pred}^2=coefficient of determination for prediction; $R_{pred}^2{}_{adj}$=adjusted coefficient of determination for prediction; *RMSEP*=root mean square of prediction; *SEP*=standard error of prediction; *RPD*=ratio of prediction to deviation; *RER*=ratio of the error range). Pretreatment selected as optimal is marked bold

Output variable	NIR spectra pretreatment	Network name	Calibration					Prediction					
			Training perf. Training error	Test perf. Test error	Validation perf. Validation error	Hidden activation	Output activation	R_{pred}^2	$R_{pred}^2{}_{adj}$	*RMSEP*	*SEP*	*RPD*	*RER*
Day of composting	raw	MLP 5-6-1	0.8319 4.2596	0.8235 12.1156	0.8066 14.1024	Tanh	Logistic	0.6407	0.5650	7.1752	1.5297	1.5422	4.1811
	smoothing	MLP 5-4-1	0.8087 8.3964	0.7532 17.9277	0.7357 20.8557	Tanh	Logistic	0.5523	0.4581	6.8658	1.4638	1.2209	4.3695
	SG1D	MLP 5-3-1	0.9646 5.9462	0.8368 12.4119	0.6543 26.6692	Identity	Tanh	0.3722	0.2400	7.7641	1.6553	1.0779	3.3487
	SG2D	MLP 5-8-1	0.8851 8.4844	0.7943 10.7610	0.7559 26.7813	Exponential	Exponential	0.6902	0.6250	5.1119	1.0899	1.6845	5.4774
	SNV	**MLP 5-5-1**	**0.9807 3.3566**	**0.8985 7.5995**	**0.8624 25.6706**	**Exponential**	**Tanh**	**0.7878**	**0.7431**	**4.1187**	**0.8781**	**2.1060**	**6.7982**
	MSC	MLP 5-6-1	0.9093 12.4992	0.8025 17.1209	0.7907 19.1609	Tanh	Exponential	0.3952	0.2678	6.7265	1.4341	1.2720	4.1626
	smoothing+SNV	MLP 5-9-1	0.9089 8.5084	0.7407 13.9499	0.7268 21.6321	Exponential	Logistic	0.2810	0.1296	7.1520	1.5248	1.1447	3.9150
	smoothing+MSC	MLP 5-5-1	0.8884 7.9151	0.7894 10.1948	0.7085 43.0589	Tanh	Logistic	0.5855	0.4982	5.6797	1.2109	1.5453	5.2820
	SG1D+SNV	MLP 5-4-1	0.9260 5.5684	0.8866 6.2794	0.7184 29.33352	Tanh	Identity	0.2184	0.0538	9.5976	2.0462	1.0828	3.1258
	SG1D+MSC	MLP 5-11-1	0.9652 2.9321	0.9034 17.3169	0.7866 17.5149	Exponential	Logistic	0.1747	0.0010	10.4068	2.2187	0.8282	2.8827
	SG2D+SNV	MLP 5-8-1	0.9128 13.6460	0.8748 14.3989	0.8135 19.1849	Exponential	Identity	0.3111	0.1661	8.2391	1.7566	1.1069	3.6412
	SG2D+MSC	MLP 5-10-1	0.9481 6.7494	0.8651 10.6277	0.7068 28.2824	Exponential	Exponential	0.3700	0.2374	11.3993	2.4303	0.7840	2.6317

Table 69. Artificial neural network (ANN) models for prediction of moisture content of the compost samples during the composting process based on the NIR spectra gathered using NIR spectrometer (AvaSpec-NIR256-2.5-HSC-EVO, Avantes, USA) (R_{pred}^2=coefficient of determination for prediction; $R_{pred}^2{}_{adj}$=adjusted coefficient of determination for prediction; $RMSEP$=root mean square of prediction; SEP=standard error of prediction; RPD=ratio of prediction to deviation; RER=ratio of the error range). Pretreatment selected as optimal is marked bold

Output variable	NIR spectra pretreatment	Network name	Calibration					Prediction					
			Training perf. Training error	Test perf. Test error	Validation perf. Validation error	Hidden activation	Output activation	R_{pred}^2	$R_{pred}^2{}_{adj}$	$RMSEP$	SEP	RPD	RER
Moisture content	raw	MLP 5-8-1	0.6628 0.3407	0.6407 0.9766	0.6178 2.3291	Tanh	Tanh	0.6766	0.6085	1.8095	0.3858	1.7336	8.5529
	smoothing	MLP 5-7-1	0.9729 0.0883	0.7397 0.2709	0.7223 0.8905	Tanh	Identity	0.3797	0.2491	2.6544	0.5659	0.8993	3.6254
	SG1D	MLP 5-7-1	0.8116 1.3067	0.6443 1.3202	0.5827 8.1559	Exponential	Logistic	0.2162	0.0512	1.5235	0.3248	0.9604	3.3959
	SG2D	MLP 5-4-1	0.5965 0.4348	0.5314 2.3788	0.5303 2.9613	Logistic	Exponential	0.2218	0.0579	1.9227	0.4099	1.1280	4.7893
	SNV	MLP 5-10-1	0.9439 0.4481	0.8976 1.0939	0.8442 1.3516	Tanh	Tanh	0.6029	0.5193	1.0111	0.2156	1.3891	4.9226
	MSC	MLP 5-10-1	0.6359 2.4121	0.6224 2.5710	0.6124 5.0436	Logistic	Identity	0.2929	0.1441	1.3525	0.2883	0.9729	4.0537
	smoothing+SNV	MLP 5-9-1	0.9605 0.5482	0.9167 0.5966	0.7592 4.5389	Tanh	Identity	0.2181	0.0535	1.4228	0.3033	1.0192	4.5994
	smoothing+MSC	**MLP 5-10-1**	**0.9193 2.3384**	**0.7755 4.0151**	**0.7531 4.1124**	**Tanh**	**Logistic**	**0.4826**	**0.3736**	**2.4116**	**0.5141**	**1.4040**	**6.9930**
	SG1D+SNV	MLP 5-7-1	0.6882 1.4943	0.6369 1.6634	0.5047 7.9108	Exponential	Identity	0.3472	0.2098	1.6686	0.3557	1.2494	5.4560
	SG1D+MSC	MLP 5-10-1	0.9168 0.3816	0.8637 1.2829	0.7928 4.4284	Logistic	Exponential	0.1880	0.0171	2.5156	0.5363	0.8847	3.4140
	SG2D+SNV	MLP 5-9-1	0.7835 0.7835	0.7166 1.3746	0.6818 2.4276	Tanh	Exponential	0.4698	0.3582	1.9268	0.4108	1.2187	5.7146
	SG2D+MSC	MLP 5-7-1	0.9908 0.5930	0.7701 1.7557	0.7555 3.1759	Tanh	Logistic	0.2200	0.0557	1.6276	0.3470	1.0334	4.9334

Table 70. Artificial neural network (ANN) models for prediction of dry matter content of the compost samples during the composting process based on the NIR spectra gathered using NIR spectrometer (AvaSpec-NIR256-2.5-HSC-EVO, Avantes, USA) (R_{pred}^2=coefficient of determination for prediction; $R_{pred}^2{}_{adj}$=adjusted coefficient of determination for prediction; *RMSEP*=root mean square of prediction; *SEP*=standard error of prediction; *RPD*=ratio of prediction to deviation; *RER*=ratio of the error range). Pretreatment selected as optimal is marked bold

Output variable	NIR spectra pretreatment	Network name	Calibration					Prediction					
			Training perf. Training error	Test perf. Test error	Validation perf. Validation error	Hidden activation	Output activation	R_{pred}^2	$R_{pred}^2{}_{adj}$	*RMSEP*	*SEP*	*RPD*	*RER*
Dry matter content	raw	MLP 5-7-1	0.8287 50.5951	0.6978 114.686	0.6203 130.018	Exponential	Logistic	0.4079	0.2832	15.6002	3.3260	1.1956	2.8549
	smoothing	**MLP 5-6-1**	**0.8041 93.0719**	**0.6864 94.3281**	**0.6533 165.0523**	**Tanh**	**Logistic**	**0.7188**	**0.6596**	**10.0603**	**2.1449**	**1.8332**	**4.5017**
	SG1D	MLP 5-4-1	0.5807 65.4073	0.5531 122.3091	0.5133 143.3091	Exponential	Tanh	0.5386	0.4414	12.1123	2.5823	1.4752	3.6611
	SG2D	MLP 5-3-1	0.5703 115.7967	0.5191 174.081	0.5004 196.005	Logistic	Exponential	0.5585	0.4655	12.8511	2.7399	1.5315	3.4656
	SNV	MLP 5-7-1	0.7262 104.785	0.7290 145.233	0.7031 155.232	Exponential	Identity	0.6677	0.5978	11.3995	2.4304	1.7502	3.8095
	MSC	MLP 5-4-1	0.9352 17.0853	0.6643 89.0257	0.6436 97.7175	Tanh	Exponential	0.5115	0.4087	13.6981	2.9205	1.4242	3.1710
	smoothing+SNV	MLP 5-7-1	0.6889 130.092	0.6375 139.083	0.6029 157.208	Identity	Identity	0.3420	0.2035	14.8247	3.1606	1.2565	3.0107
	smoothing+MSC	MLP 5-7-1	0.6540 116.8538	0.6839 131.0130	0.6393 131.0131	Logistic	Identity	0.1913	0.0211	18.6038	3.9663	1.0549	2.5090
	SG1D+SNV	MLP 5-7-1	0.7609 96.1859	0.6116 108.1010	0.6121 175.7196	Logistic	Logistic	0.1867	0.0155	16.9493	3.6136	1.1114	2.6106
	SG1D+MSC	MLP 5-7-1	0.8771 96.1859	0.6116 108.1010	0.6121 175.7196	Exponential	Tanh	0.3041	0.1576	18.5342	3.9515	1.0000	2.2930
	SG2D+SNV	MLP 5-10-1	0.7695 53.2770	0.7340 169.7627	0.7104 184.2132	Tanh	Tanh	0.5255	0.4256	13.8766	2.9585	1.4103	3.3637
	SG2D+MSC	MLP 5-4-1	0.6622 112.439	0.6244 120.1838	0.6425 204.0418	Exponential	Tanh	0.2165	0.0516	17.8724	3.8104	1.1365	2.5696

Table 71. Artificial neural network (ANN) models for prediction of organic matter content of the compost samples during the composting process based on the NIR spectra gathered using NIR spectrometer (AvaSpec-NIR256-2.5-HSC-EVO, Avantes, USA) (R_{pred}^2=coefficient of determination for prediction; $R_{pred}^2{}_{adj}$=adjusted coefficient of determination for prediction; *RMSEP*=root mean square of prediction; *SEP*=standard error of prediction; *RPD*=ratio of prediction to deviation; *RER*=ratio of the error range). Pretreatment selected as optimal is marked bold

Output variable	NIR spectra pretreatment	Network name	Calibration					Prediction					
			Training perf. Training error	Test perf. Test error	Validation perf. Validation error	Hidden activation	Output activation	R_{pred}^2	$R_{pred}^2{}_{adj}$	*RMSEP*	*SEP*	*RPD*	*RER*
Organic matter content	raw	MLP 5-8-1	0.6494 31.1234	0.6304 39.0577	0.6187 43.4670	Logistic	Identity	0.4116	0.2878	8.5073	1.8138	1.2686	3.7357
	smoothing	MLP 5-9-1	0.5864 23.7687	0.5472 43.4770	0.5435 44.8052	Tanh	Identity	0.5114	0.4085	6.8751	1.4658	1.4581	4.5298
	SG1D	MLP 5-10-1	0.9043 23.7719	0.5202 43.4376	0.5146 47.8168	Identity	Exponential	0.5125	0.4098	6.9862	1.4895	1.4296	4.4772
	SG2D	**MLP 5-7-1**	**0.6895 34.8358**	**0.6321 38.9542**	**0.6211 50.9587**	**Identity**	**Logistic**	**0.8064**	**0.7656**	**5.4703**	**1.1663**	**2.0486**	**5.7182**
	SNV	MLP 5-3-1	0.7423 19.0005	0.6656 21.3227	0.6555 34.3656	Tanh	Exponential	0.3446	0.2066	10.4255	2.2227	0.9793	3.0006
	MSC	MLP 5-7-1	0.9339 19.0005	0.8769 21.3227	0.8526 34.3656	Tanh	Identity	0.5053	0.4012	7.6387	1.6286	1.2803	3.3838
	smoothing+SNV	MLP 5-5-1	0.7842 25.3907	0.6613 26.9061	0.6610 41.4115	Tanh	Exponential	0.2280	0.0655	8.9578	1.9098	1.0515	3.4514
	smoothing+MSC	MLP 5-7-1	0.7742 25.3307	0.6713 26.9861	0.6710 43.4115	Tanh	Exponential	0.2100	0.0436	10.3425	2.2050	1.0212	3.1024
	SG1D+SNV	MLP 5-11-1	0.9327 3.2368	0.8272 19.4045	0.7103 20.8212	Tanh	Exponential	0.2267	0.0639	12.8923	2.7486	0.9259	2.4724
	SG1D+MSC	MLP 5-9-1	0.9257 4.0644	0.7162 15.1449	0.7137 18.7397	Logistic	Exponential	0.2182	0.0536	8.4120	1.7935	1.0883	3.7298
	SG2D+SNV	MLP 5-9-1	0.6850 21.0159	0.6714 38.4061	0.6457 41.75002	Logistic	Identity	0.2568	0.1004	10.1284	2.1594	1.0922	3.1679
	SG2D+MSC	MLP 5-8-1	0.6915 37.3135	0.6576 48.7848	0.6505 60.2009	Logistic	Identity	0.3610	0.2264	8.7912	1.8743	1.1628	3.6498

Table 72. Artificial neural network (ANN) models for prediction of ash content of the compost samples during the composting process based on the NIR spectra gathered using NIR spectrometer (AvaSpec-NIR256-2.5-HSC-EVO, Avantes, USA) (R_{pred}^2=coefficient of determination for prediction; $R_{pred}^2{}_{adj}$=adjusted coefficient of determination for prediction; *RMSEP*=root mean square of prediction; *SEP*=standard error of prediction; *RPD*=ratio of prediction to deviation; *RER*=ratio of the error range). Pretreatment selected as optimal is marked bold

Output variable	NIR spectra pretreatment	Network name	Calibration					Prediction					
			Training perf. Training error	Test perf. Test error	Validation perf. Validation error	Hidden activation	Output activation	R_{pred}^2	$R_{pred}^2{}_{adj}$	*RMSEP*	*SEP*	*RPD*	*RER*
Ash content	raw spectra	MLP 5-6-1	0.6491 36.2439	0.6029 44.1025	0.6001 50.7081	Identity	Exponential	0.3160	0.1719	9.3947	2.0030	1.1446	4.0317
	smoothing	MLP 5-8-1	0.6963 32.0268	0.6572 34.1225	0.6499 48.9172	Tanh	Exponential	0.6374	0.5611	7.0617	1.5056	1.5201	5.2930
	SG1D	MLP 5-4-1	0.7726 27.6719	0.6327 41.6622	0.6239 46.6281	Identity	Tanh	0.7468	0.6935	5.7402	1.2238	1.8333	6.4481
	SG2D	**MLP 5-4-1**	**0.6439 33.3382**	**0.6405 50.4654**	**0.6368 61.8984**	**Logistic**	**Exponential**	**0.8064**	**0.7656**	**5.4703**	**1.1663**	**2.0486**	**5.7182**
	SNV	MLP 5-5-1	0.6243 29.1815	0.6203 36.5296	0.6188 51.3880	Tanh	Logistic	0.3446	0.2066	10.4255	2.2227	0.9793	3.0006
	MSC	MLP 5-10-1	0.7459 17.2312	0.7416 33.5715	0.7401 62.9917	Tanh	Exponential	0.5053	0.4012	7.6387	1.6286	1.2803	3.3838
	smoothing+SNV	MLP 5-10-1	0.9046 8.6426	0.7733 69.9631	0.7445 81.6342	Tanh	Logistic	0.2280	0.0655	8.9578	1.9098	1.0515	3.4514
	smoothing+MSC	MLP 5-6-1	0.6917 35.0378	0.6478 49.1603	0.6386 49.97736	Exponential	Tanh	0.2100	0.0436	10.3425	2.2050	1.0212	3.1024
	SG1D+SNV	MLP 5-8-1	0.8577 29.3701	0.4331 42.8953	0.2182 45.5128	Tanh	Identity	0.2267	0.0639	12.8923	2.7486	0.9259	2.4724
	SG1D+MSC	MLP 5-7-1	0.8738 12.2474	0.7278 41.5926	0.7107 31.4377	Logistic	Identity	0.2182	0.0536	8.4120	1.7935	1.0883	3.7298
	SG2D+SNV	MLP 5-5-1	0.7737 32.6460	0.7411 38.7784	0.7277 61.6465	Exponential	Exponential	0.2568	0.1004	10.1284	2.1594	1.0922	3.1679
	SG2D+MSC	MLP 5-7-1	0.7864 31.4506	0.7330 58.2995	0.7034 58.8129	Identity	Logistic	0.3610	0.2264	8.7912	1.8743	1.1628	3.6498

Table 73. Artificial neural network (ANN) models for prediction of carbon content of the compost samples during the composting process based on the NIR spectra gathered using NIR spectrometer (AvaSpec-NIR256-2.5-HSC-EVO, Avantes, USA) (R_{pred}^2=coefficient of determination for prediction; $R_{pred}^2{}_{adj}$=adjusted coefficient of determination for prediction; $RMSEP$=root mean square of prediction; SEP=standard error of prediction; RPD=ratio of prediction to deviation; RER=ratio of the error range). Pretreatment selected as optimal is marked bold

Output variable	NIR spectra pretreatment	Network name	Calibration					Prediction					
			Training perf. Training error	Test perf. Test error	Validation perf. Validation error	Hidden activation	Output activation	R_{pred}^2	$R_{pred}^2{}_{adj}$	$RMSEP$	SEP	RPD	RER
Carbon content	raw spectra	MLP 5-6-1	0.6466 12.1134	0.6311 14.3357	0.6305 23.3100	Tanh	Identity	0.6061	0.5232	3.8246	0.8154	1.6231	4.7985
	smoothing	**MLP 5-7-1**	**0.5622 9.1416**	**0.5608 14.3268**	**0.5413 14.9574**	**Exponential**	**Tanh**	**0.7409**	**0.6863**	**2.8980**	**0.6178**	**2.0066**	**6.2329**
	SG1D	MLP 5-5-1	0.9458 2.2504	0.7491 12.6215	0.7212 17.9653	Exponential	Tanh	0.7334	0.6773	3.0896	0.6587	1.8727	5.7170
	SG2D	MLP 5-3-1	0.6405 10.9864	0.6403 19.6392	0.6266 19.9853	Logistic	Tanh	0.3584	0.2234	5.0838	1.0839	1.2681	3.5687
	SNV	MLP 5-4-1	0.6844 9.4819	0.6455 9.9866	0.6328 17.5049	Logistic	Logistic	0.3717	0.2394	5.2009	1.1088	1.1540	3.4886
	MSC	MLP 5-4-1	0.6714 14.8824	0.6216 15.6856	0.6044 21.9035	Tanh	Identity	0.4491	0.3331	4.3704	0.9318	1.2696	3.4302
	smoothing+SNV	MLP 5-9-1	0.7644 6.6128	0.7259 8.8317	0.6899 13.4297	Exponential	Identity	0.2982	0.1504	4.5400	0.9679	1.2122	3.9497
	smoothing+MSC	MLP 5-6-1	0.6479 9.5644	0.6364 9.6905	0.6191 23.6431	Exponential	Identity	0.3412	0.2026	5.1363	1.0951	1.2060	3.6232
	SG1D+SNV	MLP 5-4-1	0.6607 8.3545	0.6577 12.4886	0.6205 17.9153	Tanh	Logistic	0.2719	0.1186	5.8219	1.2412	1.1797	3.1755
	SG1D+MSC	MLP 5-3-1	0.6745 9.2604	0.6635 15.9024	0.6429 20.0897	Tanh	Logistic	0.4391	0.3211	4.1952	0.8944	1.2656	4.3378
	SG2D+SNV	MLP 5-3-1	0.6962 8.8690	0.6732 11.9472	0.6021 13.3680	Tanh	Exponential	0.3617	0.2273	5.2703	1.1236	1.2173	3.5311
	SG2D+MSC	MLP 5-3-1	0.8239 5.7875	0.6467 10.9011	0.6515 20.3882	Exponential	Logistic	0.5852	0.4979	3.7427	0.7980	1.5841	4.9723

Table 74. Artificial neural network (ANN) models for prediction of nitrogen content of the compost samples during the composting process based on the NIR spectra gathered using NIR spectrometer (AvaSpec-NIR256-2.5-HSC-EVO, Avantes, USA) (R_{pred}^2=coefficient of determination for prediction; $R_{pred}^2{}_{adj}$=adjusted coefficient of determination for prediction; *RMSEP*=root mean square of prediction; *SEP*=standard error of prediction; *RPD*=ratio of prediction to deviation; *RER*=ratio of the error range). Pretreatment selected as optimal is marked bold

Output variable	NIR spectra pretreatment	Network name	Calibration					Prediction					
			Training perf. Training error	Test perf. Test error	Validation perf. Validation error	Hidden activation	Output activation	R_{pred}^2	$R_{pred}^2{}_{adj}$	*RMSEP*	*SEP*	*RPD*	*RER*
Nitrogen content	raw spectra	MLP 5-9-1	0.7724 0.0202	0.6654 0.0372	0.6132 0.0327	Logistic	Logistic	0.4608	0.3472	0.2894	0.0617	1.1503	3.4557
	smoothing	MLP 5-4-1	0.6336 0.0146	0.6257 0.0372	0.6254 0.0521	Identity	Identity	0.3818	0.2516	0.2753	0.0587	1.0978	3.6319
	SG1D	MLP 5-4-1	0.9903 0.0045	0.9451 0.0154	0.8801 0.0332	Exponential	Exponential	0.2749	0.1222	0.3005	0.0641	1.0161	3.4614
	SG2D	MLP 5-6-1	0.9035 0.0078	0.7043 0.0268	0.7008 0.0535	Exponential	Exponential	0.5504	0.4558	0.2134	0.0455	1.2994	4.4048
	SNV	MLP 5-7-1	0.9018 0.0077	0.8921 0.0139	0.7744 0.7744	Exponential	Exponential	0.4218	0.3001	0.2566	0.0547	1.2701	4.0537
	MSC	MLP 5-10-1	0.9166 0.008	0.9153 0.0177	0.7887 0.0258	Tanh	Exponential	0.2428	0.0833	0.2892	0.0617	0.8886	2.8697
	smoothing+SNV	MLP 5-7-1	0.8873 0.0092	0.8724 0.0135	0.8435 0.0193	Tanh	Exponential	0.3543	0.2184	0.2098	0.0447	1.1754	4.0991
	smoothing+MSC	MLP 5-11-1	0.9872 0.0190	0.8543 0.0361	0.7552 0.0853	Tanh	Identity	0.3008	0.1536	0.2317	0.0494	1.2145	3.9275
	SG1D+SNV	MLP 5-6-1	0.9688 0.0081	0.9165 0.0155	0.7045 0.0649	Tanh	Identity	0.2337	0.0723	0.3326	0.0709	0.9090	2.9762
	SG1D+MSC	MLP 5-8-1	0.7948 0.0155	0.7495 0.0187	0.7236 0.0468	Tanh	Identity	0.3547	0.2189	0.2781	0.0593	1.1970	4.3157
	SG2D+SNV	MLP 5-8-1	0.8859 0.0115	0.8045 0.0174	0.7760 0.0240	Exponential	Logistic	0.2496	0.0917	0.2824	0.0602	1.0117	3.5053
	SG2D+MSC	**MLP 5-4-1**	**0.8703 0.0112**	**0.8446 0.0148**	**0.7519 0.0483**	**Tanh**	**Logistic**	**0.6148**	**0.5337**	**0.1889**	**0.0403**	**1.4339**	**4.8167**

Table 75. Artificial neural network (ANN) models for prediction of carbon to nitrogen (C/N) ratio of the compost samples during the composting process based on the NIR spectra gathered using NIR spectrometer (AvaSpec-NIR256-2.5-HSC-EVO, Avantes, USA) (R_{pred}^2=coefficient of determination for prediction; $R_{pred}^2{}_{adj}$=adjusted coefficient of determination for prediction; *RMSEP*=root mean square of prediction; *SEP*=standard error of prediction; *RPD*=ratio of prediction to deviation; *RER*=ratio of the error range). Pretreatment selected as optimal is marked bold

Output variable	NIR spectra pretreatment	Network name	Calibration					Prediction					
			Training perf. Training error	Test perf. Test error	Validation perf. Validation error	Hidden activation	Output activation	R_{pred}^2	$R_{pred}^2{}_{adj}$	*RMSEP*	*SEP*	*RPD*	*RER*
C/N ratio	raw spectra	MLP 5-8-1	0.5131 1.2228	0.5095 1.4291	0.5001 1.6262	Exponential	Tanh	0.7540	0.7022	1.1668	0.2488	1.8442	8.9987
	smoothing	MLP 5-9-1	0.5335 0.7308	0.5171 1.1078	0.5132 5.8746	Identity	Exponential	0.5416	0.4451	0.9860	0.2102	1.4877	5.9837
	SG1D	MLP 5-6-1	0.9337 1.0545	0.6456 1.1021	0.6471 1.4316	Tanh	Identitiy	0.4729	0.3620	1.4991	0.3196	1.0420	4.8696
	SG2D	MLP 5-6-1	0.5812 0.8755	0.5548 1.2261	0.5149 1.8253	Exponential	Identitiy	0.4923	0.3854	1.8251	0.3891	1.3656	6.2490
	SNV	MLP 5-9-1	0.6405 1.1973	0.6344 1.6765	0.6103 2.4489	Identity	Tanh	0.3804	0.2499	1.1355	0.2421	1.0363	4.8409
	MSC	MLP 5-9-1	0.69007 1.1245	0.6379 1.8657	0.6149 2.6305	Identity	Logistic	0.4379	0.3196	1.1315	0.2412	1.3633	5.6560
	smoothing+SNV	MLP 5-10-1	0.7237 0.9877	0.7037 1.7781	0.7026 2.6713	Tanh	Exponential	0.2368	0.0761	2.4741	0.5275	0.9999	4.7694
	smoothing+MSC	MLP 5-10-1	0.6434 1.3187	0.6152 2.4459	0.6066 2.6528	Tanh	Tanh	0.2191	0.0546	1.3415	0.2860	0.7996	3.8017
	SG1D+SNV	MLP 5-5-1	0.6851 0.7401	0.6311 1.4968	0.6144 1.4095	Logistic	Identity	0.2442	0.0851	1.6803	0.3582	1.0241	4.1065
	SG1D+MSC	MLP 5-4-1	0.6162 0.3384	0.5821 1.0377	0.5752 1.2523	Tanh	Logistic	0.1781	0.0051	1.9202	0.4094	1.0897	3.8018
	SG2D+SNV	MLP 5-10-1	0.7945 1.8025	0.6701 1.9182	0.6494 2.1799	Tanh	Logistic	0.2281	0.0657	1.6095	0.3431	1.0383	3.8521
	SG2D+MSC	**MLP 5-6-1**	**0.6614 1.0453**	**0.6842 1.4823**	**0.6256 2.9492**	**Identity**	**Identity**	**0.6456**	**0.5710**	**1.4003**	**0.2985**	**1.6441**	**7.5678**

Table 76. Artificial neural network (ANN) models for prediction of total color change (ΔE) of the compost samples during the composting process based on the NIR spectra gathered using NIR spectrometer (AvaSpec-NIR256-2.5-HSC-EVO, Avantes, USA) (R_{pred}^2=coefficient of determination for prediction; $R_{pred}^2{}_{adj}$=adjusted coefficient of determination for prediction; $RMSEP$=root mean square of prediction; SEP=standard error of prediction; RPD=ratio of prediction to deviation; RER=ratio of the error range). Pretreatment selected as optimal is marked bold

Output variable	NIR spectra pretreatment	Network name	Calibration					Prediction					
			Training perf. Training error	Test perf. Test error	Validation perf. Validation error	Hidden activation	Output activation	R_{pred}^2	$R_{pred}^2{}_{adj}$	$RMSEP$	SEP	RPD	RER
ΔE (compost)	raw spectra	MLP 54-1	0.8036 4.2429	0.7530 15.2136	0.7381 27.3952	Tanh	Logistic	0.6480	0.5739	2.7147	0.5788	1.6983	5.8213
	smoothing	**MLP 5-9-1**	**0.5681 9.2111**	**0.5261 11.0515**	**0.5187 30.2902**	**Identity**	**Logistic**	**0.8254**	**0.7887**	**2.0465**	**0.4363**	**2.4405**	**8.3939**
	SG1D	MLP 5-10-1	0.5752 8.6805	0.5278 9.2135	0.5122 23.1662	Logistic	Exponential	0.7412	0.6867	3.0045	0.6406	1.7752	5.6032
	SG2D	MLP 5-5-1	0.6962 9.1238	0.6499 9.7913	0.6088 11.4554	Logistic	Exponential	0.4924	0.3855	3.7374	0.7968	1.4236	4.2909
	SNV	MLP 5-3-1	0.8036 4.2429	0.7530 15.2136	0.7381 27.3952	Tanh	Logistic	0.4420	0.3246	3.9025	0.8320	1.2142	4.0512
	MSC	MLP 5-7-1	0.6901 0.2013	0.6324 12.6496	0.6214 14.0485	Identity	Tanh	0.5549	0.4612	3.5615	0.7593	1.3238	4.5907
	smoothing+SNV	MLP 5-10-1	0.6331 7.8368	0.6183 7.8929	0.6175 18.9017	Tanh	Logistic	0.4293	0.3091	3.7617	0.8020	1.3117	4.4753
	smoothing+MSC	MLP 5-11-1	0.6343 7.8368	0.6307 7.8929	0.6189 18.9017	Identity	Identity	0.2754	0.1229	4.6117	0.9832	1.1473	3.6360
	SG1D+SNV	MLP 5-3-1	0.5447 8.6629	0.5377 23.0492	0.5272 27.0605	Exponential	Identity	0.3255	0.1835	3.4605	0.7378	1.2196	4.7186
	SG1D+MSC	MLP 5-8-1	0.8882 6.8833	0.5931 8.6815	0.5654 20.4013	Logistic	Tanh	0.2613	0.1058	5.2115	1.1111	0.9361	3.2303
	SG2D+SNV	MLP 5-10-1	0.9244 5.4068	0.7341 9.1624	0.7353 11.3278	Exponential	Exponential	0.2123	0.0464	4.4759	0.9543	0.9908	3.5487
	SG2D+MSC	MLP 5-10-1	0.7814 4.6325	0.6784 5.0334	0.6213 10.9466	Tanh	Exponential	0.3651	0.2314	4.9485	1.0550	0.6823	3.0826

Table 77. Artificial neural network (ANN) models for prediction of pH of the compost samples during the composting process based on the NIR spectra gathered using NIR spectrometer (AvaSpec-NIR256-2.5-HSC-EVO, Avantes, USA) (R_{pred}^2=coefficient of determination for prediction; $R_{pred}^2{}_{adj}$=adjusted coefficient of determination for prediction; $RMSEP$=root mean square of prediction; SEP=standard error of prediction; RPD=ratio of prediction to deviation; RER=ratio of the error range). Pretreatment selected as optimal is marked bold

Output variable	NIR spectra pretreatment	Network name	Calibration					Prediction					
			Training perf. Training error	Test perf. Test error	Validation perf. Validation error	Hidden activation	Output activation	R_{pred}^2	$R_{pred}^2{}_{adj}$	RMSEP	SEP	RPD	RER
pH	raw spectra	MLP 5-3-1	0.9655 0.0139	0.7733 0.1140	0.7685 0.1485	Logistic	Identity	0.2658	0.1113	0.5954	0.1269	1.1192	4.5961
	smoothing	MLP 5-7-1	0.8655 0.0632	0.7915 0.0945	0.7641 1.2004	Tanh	Exponential	0.1827	0.0106	0.8526	0.1818	1.0417	3.3779
	SG1D	MLP 5-8-1	0.8553 0.0779	0.7439 0.0968	0.7220 0.3025	Exponential	Identity	0.4198	0.2977	0.6542	0.1395	1.1376	3.9181
	SG2D	MLP 5-7-1	0.8095 0.0937	0.7781 0.0947	0.7966 0.1753	Logistic	Tanh	0.4637	0.3508	0.6564	0.1399	1.2722	4.6720
	SNV	MLP 5-8-1	0.7907 0.0297	0.7376 0.1298	0.7403 0.2665	Logistic	Logistic	0.2844	0.1338	0.7111	0.1516	1.0962	4.5561
	MSC	MLP 5-3-1	0.7072 0.0993	0.6499 0.1307	0.6711 0.2092	Tanh	Exponential	0.2094	0.0430	0.7774	0.1657	0.9469	3.5933
	smoothing+SNV	MLP 5-7-1	0.6019 0.0365	0.6076 0.2305	0.5877 0.3551	Tanh	Tanh	0.2907	0.1414	0.9056	0.1931	1.0019	3.7248
	smoothing+MSC	MLP 5-5-1	0.6106 0.0368	0.5763 0.2694	0.5142 0.3235	Logistic	Exponential	0.2506	0.0928	0.6299	0.1343	1.0307	3.9369
	SG1D+SNV	MLP 5-5-1	0.7868 0.0206	0.7519 0.1013	0.7262 0.1224	Tanh	Tanh	0.2801	0.1285	0.9580	0.2043	0.9746	3.5211
	SG1D+MSC	MLP 5-10-1	0.7859 0.0972	0.7885 0.2361	0.7529 0.3456	Exponential	Tanh	0.1985	0.0298	0.7062	0.1506	1.1268	4.1865
	SG2D+SNV	**MLP 5-3-1**	**0.8126 0.1718**	**0.7803 0.1232**	**0.6471 0.2928**	**Tanh**	**Identity**	**0.3509**	**0.2143**	**0.4332**	**0.0924**	**1.2085**	**4.9785**
	SG2D+MSC	MLP 5-3-1	0.9972 0.0898	0.8627 0.1059	0.7320 0.2544	Logistic	Tanh	0.2959	0.1477	0.5478	0.1168	0.8050	2.7872

Table 78. Artificial neural network (ANN) models for prediction of total dissolved solids (TDS) of the compost samples during the composting process based on the NIR spectra gathered using NIR spectrometer (AvaSpec-NIR256-2.5-HSC-EVO, Avantes, USA) (R_{pred}^2=coefficient of determination for prediction; $R_{pred}^2{}_{adj}$=adjusted coefficient of determination for prediction; $RMSEP$=root mean square of prediction; SEP=standard error of prediction; RPD=ratio of prediction to deviation; RER=ratio of the error range). Pretreatment selected as optimal is marked bold

Output variable	NIR spectra pretreatment	Network name	Calibration					Prediction					
			Training perf. Training error	Test perf. Test error	Validation perf. Validation error	Hidden activation	Output activation	R_{pred}^2	$R_{pred}^2{}_{adj}$	$RMSEP$	SEP	RPD	RER
TDS	raw spectra	MLP 5-5-1	0.8298 261.714	0.6338 477.824	0.6045 963.623	Tanh	Identity	0.6448	0.5700	191.4392	40.8150	1.6577	5.3385
	smoothing	MLP 5-7-1	0.6142 243.215	0.6134 336.209	0.6113 673.828	Exponential	Exponential	0.3538	0.2177	244.2498	52.0742	1.1795	4.3303
	SG1D	MLP 5-10-1	0.8546 404.048	0.6411 650.004	0.6025 747.679	Tanh	Exponential	0.3126	0.1678	288.8486	61.5827	1.0684	3.5382
	SG2D	MLP 5-10-1	0.8254 233.901	0.6214 614.601	0.6452 725.004	Logistic	Logistic	0.2788	0.1269	276.7507	59.0034	1.0720	3.6760
	SNV	**MLP 5-5-1**	**0.6481 251.335**	**0.6281 430.585**	**0.6188 469.186**	**Exponential**	**Tanh**	**0.4077**	**0.2830**	**206.7229**	**44.0735**	**1.2559**	**4.9616**
	MSC	MLP 5-9-1	0.7224 232.291	0.6609 241.093	0.6810 556.568	Tanh	Logistic	0.2438	0.0846	280.9799	59.9051	0.9019	3.7808
	smoothing+SNV	MLP 5-9-1	0.9832 102.808	0.8662 339.116	0.8173 432.220	Exponential	Tanh	0.1867	0.0155	364.0683	77.6196	0.6328	2.7797
	smoothing+MSC	MLP 5-10-1	0.7305 388.73	0.7264 531.708	0.7094 742.00	Identity	Logistic	0.3722	0.2401	246.7725	52.6121	1.2777	4.1563
	SG1D+SNV	MLP 5-4-1	0.6362 744.01	0.5976 734.24	0.5177 797.59	Exponential	Exponential	0.3495	0.2125	304.6143	64.9440	1.0913	3.4875
	SG1D+MSC	MLP 5-7-1	0.7976 390.49	0.7059 519.23	0.7036 625.42	Exponential	Exponential	0.2313	0.0695	249.4537	53.1837	1.0391	4.0782
	SG2D+SNV	MLP 5-5-1	0.9282 357.57	0.8372 515.15	0.7292 939.15	Exponential	Exponential	0.3989	0.2723	262.0604	55.8715	1.0778	4.0360
	SG2D+MSC	MLP 5-10-1	0.7115 525.10	0.6958 734.49	0.6887 1173.56	Tanh	Identity	0.2205	0.0564	308.0653	65.6797	1.1123	3.4484

Table 79. Artificial neural network (ANN) models for prediction of conductivity (S) of the compost samples during the composting process based on the NIR spectra gathered using NIR spectrometer (AvaSpec-NIR256-2.5-HSC-EVO, Avantes, USA) (R_{pred}^2=coefficient of determination for prediction; $R_{pred}^2{}_{adj}$=adjusted coefficient of determination for prediction; $RMSEP$=root mean square of prediction; SEP=standard error of prediction; RPD=ratio of prediction to deviation; RER=ratio of the error range). Pretreatment selected as optimal is marked bold

Output variable	NIR spectra pretreatment	Network name	Calibration					Prediction					
			Training perf. Training error	Test perf. Test error	Validation perf. Validation error	Hidden activation	Output activation	R_{pred}^2	$R_{pred}^2{}_{adj}$	*RMSEP*	*SEP*	*RPD*	*RER*
S	raw spectra	MLP 5-9-1	0.7915 601.35	0.7437 516.47	0.7350 1300.28	Exponential	Tanh	0.5032	0.3986	425.6701	90.7532	1.4243	4.9005
	smoothing	MLP 5-9-1	0.6897 689.76	0.6012 906.53	0.6107 1941.66	Exponential	Tanh	0.3695	0.2368	496.8508	105.9290	1.1322	3.7899
	SG1D	MLP 5-9-1	0.6625 1295.33	0.6605 1377.05	0.6518 1664.88	Identity	Exponential	0.6248	0.5458	427.0523	91.0479	1.3875	4.8846
	SG2D	**MLP 5-3-1**	**0.7232 1612.24**	**0.7355 1835.15**	**0.7163 1891.47**	**Tanh**	**Tanh**	**0.7270**	**0.6695**	**290.9070**	**62.0216**	**1.9319**	**6.4373**
	SNV	MLP 5-10-1	0.7772 1356.12	0.7588 1596.29	0.7440 1693.95	Exponential	Exponential	0.4504	0.3346	445.5420	94.9899	1.1575	4.6677
	MSC	MLP 5-5-1	0.7300 1038.68	0.7057 1300.98	0.7024 1585.53	Tanh	Identity	0.3223	0.1797	646.8077	137.8999	0.7413	2.7721
	smoothing+SNV	MLP 5-7-1	0.7550 1160.32	0.7231 1295.51	0.6999 1344.32	Exponential	Exponential	0.2081	0.0413	777.0794	165.6739	0.5895	2.7063
	smoothing+MSC	MLP 5-11-1	0.8341 1341.85	0.7867 1424.21	0.7572 1642.81	Exponential	Tanh	0.1749	0.0012	645.5912	137.6405	0.9828	3.2213
	SG1D+SNV	MLP 5-8-1	0.6047 1227.92	0.6018 1487.64	0.6002 1854.66	Tanh	Identity	0.2297	0.0676	588.2929	125.4245	1.0578	3.2858
	SG1D+MSC	MLP 5-7-1	0.7071 1214.06	0.6593 1227.90	0.6285 1478.16	Tanh	Exponential	0.3454	0.2076	430.9579	91.8805	1.2037	4.7398
	SG2D+SNV	MLP 5-5-1	0.8645 1082.22	0.8103 1162.68	0.7508 1800.40	Tanh	Tanh	0.1851	0.0135	506.5608	107.9991	1.0486	3.7699
	SG2D+MSC	MLP 5-3-1	0.8542 1047.45	0.7638 1724.00	0.7839 1894.40	Tanh	Tanh	0.2592	0.1033	0.5458	0.1164	1.0226	4.2730

Table 80. Artificial neural network (ANN) models for prediction of total color change (ΔE) of the compost extract samples during the composting process based on the NIR spectra gathered using NIR spectrometer (AvaSpec-NIR256-2.5-HSC-EVO, Avantes, USA) (R_{pred}^2=coefficient of determination for prediction; $R_{pred}^2{}_{adj}$=adjusted coefficient of determination for prediction; $RMSEP$=root mean square of prediction; SEP=standard error of prediction; RPD=ratio of prediction to deviation; RER=ratio of the error range). Pretreatment selected as optimal is marked bold

Output variable	NIR spectra pretreatment	Network name	Calibration					Prediction					
			Training perf. Training error	Test perf. Test error	Validation perf. Validation error	Hidden activation	Output activation	R_{pred}^2	$R_{pred}^2{}_{adj}$	$RMSEP$	SEP	RPD	RER
ΔE (extracts)	raw spectra	MLP 5-5-1	0.9476 0.1177	0.7123 0.2088	0.7095 0.2832	Tanh	Logistic	0.3580	0.2228	0.5679	0.1211	1.1452	4.9501
	smoothing	MLP 5-3-1	0.6439 0.1101	0.6339 0.1291	0.7616 0.2628	Exponential	Logistic	0.4345	0.3154	0.7319	0.1560	1.2833	4.1771
	SG1D	**MLP 5-6-1**	**0.9414 0.1262**	**0.7818 0.2442**	**0.7399 0.3463**	**Tanh**	**Exponential**	**0.5506**	**0.4560**	**0.5330**	**0.1136**	**1.3302**	**6.2344**
	SG2D	MLP 5-4-1	0.9293 0.0361	0.8569 0.0664	0.6697 0.6697	Logistic	Exponential	0.2006	0.0322	0.7730	0.1648	1.0894	4.7818
	SNV	MLP 5-4-1	0.9671 0.1762	0.7808 0.1993	0.7499 0.2553	Identity	Tanh	0.2613	0.1058	0.6876	0.1466	1.1867	4.1179
	MSC	MLP 5-4-1	0.5656 0.1271	0.5404 0.2375	0.5216 0.2469	Identity	Exponential	0.3650	0.2313	0.7203	0.1536	1.2518	5.1318
	smoothing+SNV	MLP 5-4-1	0.6484 0.1414	0.6439 0.4429	0.6057 0.5522	Exponential	Logistic	0.2021	0.0342	0.8619	0.1838	0.9089	3.8551
	smoothing+MSC	MLP 5-6-1	0.6467 0.1422	0.5877 0.1776	0.5612 0.4927	Tanh	Tanh	0.2594	0.1035	0.6836	0.1457	1.0729	4.1424
	SG1D+SNV	MLP 5-11-1	0.9707 0.2107	0.7693 0.2286	0.7024 0.2504	Identity	Exponential	0.2414	0.0817	0.6694	0.1427	0.8275	2.9888
	SG1D+MSC	MLP 5-11-1	0.7752 0.1418	0.7605 0.2439	0.7054 0.3654	Identity	Tanh	0.2480	0.0897	0.7448	0.1588	0.6524	2.3208
	SG2D+SNV	MLP 5-8-1	0.9098 0.0664	0.8720 0.0718	0.7707 0.2915	Exponential	Tanh	0.1829	0.0108	0.7771	0.1657	0.9596	3.6438
	SG2D+MSC	MLP 5-10-1	0.7388 0.0989	0.7044 0.3213	0.7029 0.3954	Tanh	Tanh	0.2592	0.1033	0.5458	0.1164	1.0226	4.2730

Table 81. Artificial neural network (ANN) models for prediction of day of composting of the compost samples during the composting process based on the NIR spectra gathered using portable NIR spectrometer (NIR-S-G1, InnoSpectra, Taiwan) (R_{pred}^2=coefficient of determination for prediction; $R_{pred}^2{}_{adj}$=adjusted coefficient of determination for prediction; $RMSEP$=root mean square of prediction; SEP=standard error of prediction; RPD=ratio of prediction to deviation; RER=ratio of the error range). Pretreatment selected as optimal is marked bold

Output variable	NIR spectra pretreatment	Network name	Calibration					Prediction					
			Training perf. / Training error	Test perf. / Test error	Validation perf. / Validation error	Hidden activation	Output activation	R_{pred}^2	$R_{pred}^2{}_{adj}$	$RMSEP$	SEP	RPD	RER
Day of composting	raw	MLP 5-3-1	0.8115 / 1.0589	0.7548 / 2.3713	0.7149 / 4.4954	Exponential	Tanh	0.7506	0.6981	4.1058	0.8754	1.9147	6.8196
	smoothing	MLP 5-3-1	0.8748 / 2.6317	0.7446 / 3.8431	0.7145 / 6.2397	Tanh	Tanh	0.4960	0.3899	6.6889	1.4261	1.2418	3.5880
	SG1D	MLP 5-3-1	0.8188 / 1.6578	0.8668 / 1.8747	0.8759 / 1.8755	Tanh	Logistic	0.3606	0.2260	7.7667	1.6559	1.2434	3.8627
	SG2D	MLP 5-8-1	0.7456 / 3.1002	0.7435 / 7.3674	0.7189 / 7.9008	Logistic	Logistic	0.2718	0.1186	8.1371	1.7348	1.1825	3.4410
	SNV	MLP 5-7-1	0.8873 / 1.9255	0.6887 / 8.1447	0.6403 / 8.2214	Logistic	Logistic	0.2856	0.1353	8.2339	1.7555	1.0779	3.4006
	MSC	MLP 5-8-1	0.7508 / 2.7730	0.7228 / 7.8741	0.6786 / 9.8058	Logistic	Logistic	0.3430	0.2046	7.3673	1.5707	1.1823	4.0721
	smoothing+SNV	MLP 5-7-1	0.8911 / 2.3461	0.7554 / 4.5563	0.7231 / 7.3942	Logistic	Logistic	0.3659	0.2324	7.9958	1.7047	1.1577	3.7520
	smoothing+MSC	**MLP 5-7-1**	**0.7164 / 1.9702**	**0.6974 / 4.5244**	**0.6527 / 8.5155**	**Logistic**	**Logistic**	**0.6796**	**0.6121**	**5.3438**	**1.1393**	**1.6585**	**5.6140**
	SG1D+SNV	MLP 5-11-1	0.8429 / 1.6922	0.7069 / 4.3745	0.7395 / 7.9365	Tanh	Exponential	0.4030	0.2774	7.7855	1.6599	1.2836	3.8533
	SG1D+MSC	MLP 5-11-1	0.9023 / 1.7707	0.7902 / 3.8514	0.7186 / 7.9531	Tanh	Exponential	0.5784	0.4897	6.2952	1.3421	1.5375	4.7655
	SG2D+SNV	MLP 5-11-1	0.9086 / 1.8877	0.6259 / 5.9983	0.6093 / 9.3434	Identity	Exponential	0.5151	0.4130	6.8585	1.4622	1.4170	4.3742
	SG2D+MSC	MLP 5-3-1	0.7835 / 1.2588	0.7314 / 6.5544	0.6638 / 11.5644	Tanh	Tanh	0.3686	0.2357	7.2411	1.5438	1.2670	4.1430

Table 82. Artificial neural network (ANN) models for prediction of moisture content of the compost samples during the composting process based on the NIR spectra gathered using portable NIR spectrometer (NIR-S-G1, InnoSpectra, Taiwan) (R_{pred}^2=coefficient of determination for prediction; $R_{pred}^2{}_{adj}$=adjusted coefficient of determination for prediction; $RMSEP$=root mean square of prediction; SEP=standard error of prediction; RPD=ratio of prediction to deviation; RER=ratio of the error range). Pretreatment selected as optimal is marked bold

Output variable	NIR spectra pretreatment	Network name	Calibration					Prediction					
			Training perf. Training error	Test perf. Test error	Validation perf. Validation error	Hidden activation	Output activation	R_{pred}^2	$R_{pred}^2{}_{adj}$	$RMSEP$	SEP	RPD	RER
Moisture content	raw	MLP 5-3-1	0.8665 0.0989	0.7762 2.3213	0.7335 7.3954	Exponential	Tanh	0.6338	0.5567	0.8748	0.1865	1.5659	6.7699
	smooth	MLP 5-3-1	0.7187 0.8537	0.6895 2.9987	0.6632 11.8527	Tanh	Tanh	0.2403	0.0804	1.7555	0.3743	1.0446	5.2406
	SG1D	MLP 5-3-1	0.7182 0.6317	0.7020 1.8431	0.6858 10.2397	Tanh	Logistic	0.3716	0.2393	2.0101	0.4286	1.0025	4.6286
	SG2D	MLP 5-8-1	0.7240 0.7477	0.7218 1.6674	0.7139 10.0012	Logistic	Logistic	0.2649	0.1101	1.6340	0.3484	0.9671	4.0756
	SNV	MLP 5-7-1	0.7543 0.9255	0.7291 1.1447	0.7386 9.2214	Logistic	Logistic	0.3285	0.1871	1.8119	0.3863	1.1862	4.8526
	MSC	MLP 5-8-1	0.7726 1.0011	0.7453 1.2587	0.7312 10.8857	Logistic	Logistic	0.2961	0.1479	1.4136	0.3014	1.1665	4.3411
	smoothing+SNV	**MLP 5-7-1**	**0.7421 1.3461**	**0.7145 1.5563**	**0.7187 11.3942**	**Logistic**	**Logistic**	**0.5847**	**0.4973**	**2.0514**	**0.4374**	**1.5362**	**7.5908**
	smoothing+MSC	MLP 5-7-1	0.7305 1.6492	0.7194 2.7084	0.7020 9.8758	Logistic	Logistic	0.3784	0.2475	2.1415	0.4566	1.1509	5.1418
	SG1D+SNV	MLP 5-11-1	0.7354 1.7998	0.7233 2.6904	0.7095 8.9365	Tanh	Exponential	0.2232	0.0596	2.5586	0.5455	0.7895	3.1079
	SG1D+MSC	MLP 5-11-1	0.6393 1.7126	0.6117 2.8288	0.6093 10.0085	Tanh	Exponential	0.2227	0.0591	1.1985	0.2555	0.9988	4.0080
	SG2D+SNV	MLP 5-11-1	0.7765 2.8877	0.7256 2.9983	0.7336 10.3434	Identity	Exponential	0.2959	0.1477	1.9344	0.4124	1.2032	4.9748
	SG2D+MSC	MLP 5-3-1	0.7791 2.9588	0.7606 2.8733	0.7347 11.9987	Tanh	Tanh	0.2247	0.0615	1.5788	0.3366	1.1450	5.0367

Table 83. Artificial neural network (ANN) models for prediction of dry matter content of the compost samples during the composting process based on the NIR spectra gathered using portable NIR spectrometer (NIR-S-G1, InnoSpectra, Taiwan) (R_{pred}^2=coefficient of determination for prediction; $R_{pred}^2{}_{adj}$=adjusted coefficient of determination for prediction; $RMSEP$=root mean square of prediction; SEP=standard error of prediction; RPD=ratio of prediction to deviation; RER=ratio of the error range). Pretreatment selected as optimal is marked bold

Output variable	NIR spectra pretreatment	Network name	Calibration					Prediction					
			Training perf. Training error	Test perf. Test error	Validation perf. Validation error	Hidden activation	Output activation	R_{pred}^2	$R_{pred}^2{}_{adj}$	RMSEP	SEP	RPD	RER
Dry matter content	raw	MLP 5-3-1	0.9562 9.5989	0.7476 10.3213	0.7210 21.3954	Exponential	Tanh	0.7444	0.6906	9.8743	2.1052	1.8987	4.5033
	smoothing	MLP 5-3-1	0.7635 11.8746	0.7351 13.8752	0.7029 31.5234	Exponential	Tanh	0.4054	0.2802	15.7192	3.3513	1.2512	2.8393
	SG1D	MLP 5-9-1	0.9974 8.6317	0.9405 8.8431	0.8461 11.2397	Tanh	Logistic	0.2096	0.0432	19.6227	4.1836	0.9358	2.2235
	SG2D	MLP 5-8-1	0.6625 11.5523	0.6431 21.4425	0.6337 31.2154	Logistic	Logistic	0.3805	0.2500	14.0458	2.9946	1.2930	3.1571
	SNV	MLP 5-7-1	0.8591 9.7742	0.6971 22.6221	0.6645 29.2287	Logistic	Logistic	0.5457	0.4500	12.3684	2.6370	1.5097	3.6365
	MSC	MLP 5-8-1	0.7726 9.6634	0.7453 14.6742	0.7312 30.9733	Logistic	Logistic	0.3532	0.2170	16.8994	3.6030	1.1354	2.6169
	smoothing+SNV	MLP 5-7-1	0.8845 3.1642	0.8180 10.6354	0.7123 29.6545	Logistic	Logistic	0.3590	0.2240	18.9136	4.0324	0.8905	2.2407
	smoothing+MSC	MLP 5-9-1	0.8422 3.9471	0.7665 11.4022	0.7406 27.9102	Logistic	Tanh	0.4584	0.3444	13.0178	2.7754	1.3301	3.4220
	SG1D+SNV	MLP 5-11-1	0.9687 1.7998	0.8717 9.6904	0.7936 18.9365	Tanh	Exponential	0.2720	0.1187	17.2956	3.6874	0.9579	2.6553
	SG1D+MSC	**MLP 5-5-1**	**0.8691 1.8610**	**0.8513 10.1217**	**0.7701 18.610**	**Tanh**	**Identity**	**0.6669**	**0.5967**	**10.7766**	**2.2976**	**1.7172**	**3.8772**
	SG2D+SNV	MLP 5-11-1	0.9958 1.2444	0.7708 18.3367	0.7517 22.7484	Identity	Exponential	0.2830	0.1320	16.0731	3.4268	1.1853	2.7709
	SG2D+MSC	MLP 5-3-1	0.8203 2.0017	0.6218 12.5423	0.6166 24.6682	Tanh	Tanh	0.3456	0.2078	15.0276	3.2039	1.2389	3.0278

Table 84. Artificial neural network (ANN) models for prediction of organic matter content of the compost samples during the composting process based on the NIR spectra gathered using portable NIR spectrometer (NIR-S-G1, InnoSpectra, Taiwan) (R_{pred}^2=coefficient of determination for prediction; $R_{pred}^2{}_{adj}$=adjusted coefficient of determination for prediction; $RMSEP$=root mean square of prediction; SEP=standard error of prediction; RPD=ratio of prediction to deviation; RER=ratio of the error range). Pretreatment selected as optimal is marked bold

Output variable	NIR spectra pretreatment	Network name	Calibration					Prediction					
			Training perf. Training error	Test perf. Test error	Validation perf. Validation error	Hidden activation	Output activation	R_{pred}^2	$R_{pred}^2{}_{adj}$	$RMSEP$	SEP	RPD	RER
Organic matter content	raw	MLP 5-3-1	0.6360 10.1111	0.6131 14.3613	0.6056 23.7854	Exponential	Tanh	0.4958	0.3896	6.9953	1.4914	1.3268	4.0135
	smoothing	MLP 5-3-1	0.6425 11.5236	0.6415 18.3587	0.6002 24.8745	Exponential	Tanh	0.2095	0.0430	9.4867	2.0226	1.1161	3.3500
	SG1D	MLP 5-9-1	0.7122 10.1223	0.7114 12.2365	0.6718 23.3254	Tanh	Logistic	0.4215	0.2997	8.2493	1.7588	1.2933	3.7480
	SG2D	MLP 5-8-1	0.8883 8.5224	0.7428 11.9978	0.7156 16.1657	Logistic	Logistic	0.3501	0.2133	7.9376	1.6923	1.1918	4.0038
	SNV	**MLP 5-7-1**	**0.8645 7.1447**	**0.8268 10.1447**	**0.6913 25.3663**	**Logistic**	**Logistic**	**0.7224**	**0.6640**	**5.3037**	**1.1308**	**1.6700**	**5.3577**
	MSC	MLP 5-8-1	0.6939 10.2441	0.6489 14.2557	0.6187 24.1744	Logistic	Logistic	0.6328	0.5555	6.2752	1.3379	1.6198	4.9851
	smoothing+SNV	MLP 5-7-1	0.8516 11.4572	0.7746 13.2340	0.7786 24.6784	Logistic	Logistic	0.4489	0.3329	7.4947	1.5979	1.3197	4.1860
	smoothing+MSC	MLP 5-9-1	0.7558 9.7493	0.7533 14.9022	0.7329 20.7910	Logistic	Tanh	0.5217	0.4210	7.4466	1.5876	1.4639	4.3213
	SG1D+SNV	MLP 5-11-1	0.7973 11.7998	0.6904 20.6904	0.6325 28.9365	Tanh	Exponential	0.3665	0.2332	9.0591	1.9314	1.2720	3.5418
	SG1D+MSC	MLP 5-5-1	0.9531 9.0222	0.8391 18.6920	0.7516 20.0928	Tanh	Identity	0.4270	0.3064	8.1962	1.7474	1.3123	3.8167
	SG2D+SNV	MLP 5-11-1	0.7859 10.1444	0.7714 19.9958	0.7212 25.1297	Identity	Exponential	0.3189	0.1755	10.0446	2.1415	1.0977	3.1641
	SG2D+MSC	MLP 5-3-1	0.8800 7.7915	0.8552 17.1777	0.7465 27.8555	Tanh	Tanh	0.3988	0.2722	8.6619	1.8467	1.3049	3.7150

Table 85. Artificial neural network (ANN) models for prediction of ash content of the compost samples during the composting process based on the NIR spectra gathered using portable NIR spectrometer (NIR-S-G1, InnoSpectra, Taiwan) (R_{pred}^2=coefficient of determination for prediction; $R_{pred}^2{}_{adj}$=adjusted coefficient of determination for prediction; $RMSEP$=root mean square of prediction; SEP=standard error of prediction; RPD=ratio of prediction to deviation; RER=ratio of the error range). Pretreatment selected as optimal is marked bold

Output variable	NIR spectra pretreatment	Network name	Calibration					Prediction					
			Training perf. Training error	Test perf. Test error	Validation perf. Validation error	Hidden activation	Output activation	R_{pred}^2	$R_{pred}^2{}_{adj}$	$RMSEP$	SEP	RPD	RER
Ash content	raw spectra	MLP 5-3-1	0.7695 5.1254	0.7624 14.2572	0.7347 25.1478	Exponential	Tanh	0.4200	0.2979	7.3888	1.5753	1.2273	3.7997
	smoothing	MLP 5-3-1	0.6697 7.3648	0.6309 15.7458	0.6064 22.8742	Exponential	Tanh	0.4993	0.3939	7.5547	1.6107	1.4015	4.2067
	SG1D	MLP 5-9-1	0.6838 5.6317	0.6489 12.8431	0.6478 21.2397	Tanh	Logistic	0.2528	0.0955	9.2233	1.9664	1.1455	3.3522
	SG2D	MLP 5-8-1	0.7487 3.2287	0.7306 3.3357	0.7090 23.0206	Logistic	Logistic	0.5664	0.4751	7.1341	1.5210	1.2829	4.3733
	SNV	MLP 5-7-1	0.8229 4.1104	0.7764 8.2877	0.6985 24.2214	Logistic	Logistic	0.2204	0.0563	8.5923	1.8319	1.0175	3.3071
	MSC	MLP 5-8-1	0.6541 6.9912	0.6321 15.2587	0.6195 25.8857	Logistic	Logistic	0.5401	0.4432	6.8826	1.4674	1.4723	4.5452
	smoothing+SNV	**MLP 5-7-1**	**0.8416 4.2147**	**0.7815 8.7755**	**0.7516 20.8910**	**Logistic**	**Logistic**	**0.4266**	**0.3059**	**7.9233**	**1.6893**	**1.3078**	**4.6714**
	smoothing+MSC	MLP 5-9-1	0.6516 8.8336	0.6478 9.1293	0.6120 31.2939	Logistic	Tanh	0.3268	0.1850	8.8448	1.8857	1.2325	3.6382
	SG1D+SNV	MLP 5-11-1	0.7739 9.7998	0.7350 12.6904	0.6676 28.9365	Tanh	Exponential	0.2778	0.1258	10.6636	2.2735	1.1197	3.5805
	SG1D+MSC	MLP 5-5-1	0.8582 9.5316	0.8036 12.6716	0.7232 29.9019	Tanh	Identity	0.4480	0.3318	8.2069	1.7497	1.3105	3.8118
	SG2D+SNV	MLP 5-11-1	0.8031 8.5699	0.7598 14.4414	0.7299 29.9712	Identity	Exponential	0.2297	0.0675	10.6208	2.2644	1.0554	3.5663
	SG2D+MSC	MLP 5-3-1	0.8678 8.5522	0.7691 10.1718	0.7457 27.7667	Tanh	Tanh	0.3044	0.1580	9.7124	2.0707	1.1506	3.3132

Table 86. Artificial neural network (ANN) models for prediction of carbon content of the compost samples during the composting process based on the NIR spectra gathered using portable NIR spectrometer (NIR-S-G1, InnoSpectra, Taiwan) (R_{pred}^2=coefficient of determination for prediction; $R_{pred}^2{}_{adj}$=adjusted coefficient of determination for prediction; $RMSEP$=root mean square of prediction; SEP=standard error of prediction; RPD=ratio of prediction to deviation; RER=ratio of the error range). Pretreatment selected as optimal is marked bold

Output variable	NIR spectra pretreatment	Network name	Calibration					Prediction					
			Training perf. Training error	Test perf. Test error	Validation perf. Validation error	Hidden activation	Output activation	R_{pred}^2	$R_{pred}^2{}_{adj}$	$RMSEP$	SEP	RPD	RER
Carbon content	raw spectra	MLP 5-3-1	0.7809 0.9987	0.7278 2.7416	0.7030 10.1287	Exponential	Tanh	0.3007	0.1535	4.8940	1.0434	1.0747	3.3273
	smoothing	MLP 5-3-1	0.6997 0.8978	0.6409 3.1978	0.6028 12.6874	Tanh	Tanh	0.2250	0.0618	5.7453	1.2249	1.0689	3.2083
	SG1D	MLP 5-9-1	0.7594 1.0112	0.7012 2.7426	0.7077 8.9875	Tanh	Logistic	0.4319	0.3123	4.9008	1.0449	1.2504	3.6591
	SG2D	MLP 5-8-1	0.8463 0.8747	0.7981 1.2274	0.7011 9.0014	Logistic	Logistic	0.4299	0.3099	4.8870	1.0419	1.0862	3.7029
	SNV	MLP 5-7-1	0.8667 0.9075	0.8265 1.1132	0.6985 13.2258	Logistic	Logistic	0.3855	0.2561	4.0089	0.8547	1.2648	4.1111
	MSC	**MLP 5-8-1**	**0.6931 1.0011**	**0.6549 3.2271**	**0.6190 13.3331**	**Logistic**	**Logistic**	**0.6823**	**0.6154**	**3.3527**	**0.7148**	**1.7530**	**5.4118**
	smoothing+SNV	MLP 5-7-1	0.8419 1.3368	0.7819 4.1562	0.7495 10.1614	Logistic	Logistic	0.4574	0.3432	4.3224	0.9215	1.3433	4.2098
	smoothing+MSC	MLP 5-9-1	0.7534 1.2011	0.7367 5.5158	0.7313 15.3334	Logistic	Tanh	0.5191	0.4178	4.3363	0.9245	1.4581	4.3041
	SG1D+SNV	MLP 5-11-1	0.8946 1.0998	0.7350 5.6904	0.6917 10.9365	Tanh	Exponential	0.3569	0.2215	5.3224	1.1347	1.2563	3.4965
	SG1D+MSC	MLP 5-5-1	0.9686 1.6177	0.8591 8.0368	0.7232 11.0983	Tanh	Identity	0.3929	0.2650	4.8427	1.0325	1.2881	3.7467
	SG2D+SNV	MLP 5-11-1	0.7873 1.8355	0.7653 5.8732	0.6499 11.5541	Identity	Exponential	0.2492	0.0911	5.7748	1.2312	1.1085	3.1920
	SG2D+MSC	MLP 5-3-1	0.8775 1.3577	0.8517 5.0996	0.7457 13.2100	Tanh	Tanh	0.3288	0.1875	5.2473	1.1187	1.2352	3.5568

Table 87. Artificial neural network (ANN) models for prediction of nitrogen content of the compost samples during the composting process based on the NIR spectra gathered using portable NIR spectrometer (NIR-S-G1, InnoSpectra, Taiwan) (R_{pred}^2=coefficient of determination for prediction; $R_{pred}^2{}_{adj}$=adjusted coefficient of determination for prediction; $RMSEP$=root mean square of prediction; SEP=standard error of prediction; RPD=ratio of prediction to deviation; RER=ratio of the error range). Pretreatment selected as optimal is marked bold

Output variable	NIR spectra pretreatment	Network name	Calibration					Prediction					
			Training perf. Training error	Test perf. Test error	Validation perf. Validation error	Hidden activation	Output activation	R_{pred}^2	$R_{pred}^2{}_{adj}$	$RMSEP$	SEP	RPD	RER
Nitrogen content	raw spectra	MLP 5-3-1	0.7564 0.0147	0.7441 0.0155	0.7364 0.1278	Exponential	Tanh	0.3319	0.1912	0.2417	0.0515	1.1612	4.9644
	smoothing	MLP 5-3-1	0.6717 0.0112	0.6582 0.0122	0.6399 0.1368	Tanh	Tanh	0.4339	0.3148	0.2063	0.0440	1.3093	4.4606
	SG1D	MLP 5-9-1	0.8063 0.0101	0.7728 0.0177	0.7580 0.1257	Tanh	Logistic	0.3610	0.2265	0.2332	0.0497	1.2261	4.3742
	SG2D	MLP 5-8-1	0.7548 0.0097	0.7499 0.0101	0.7159 0.0997	Logistic	Logistic	0.3509	0.2142	0.2505	0.0534	1.1108	3.9128
	SNV	MLP 5-7-1	0.8265 0.0117	0.8004 0.0144	0.7576 0.1122	Logistic	Logistic	0.4046	0.2793	0.2615	0.0558	1.2075	3.9007
	MSC	MLP 5-8-1	0.9117 0.0099	0.7922 0.0155	0.7735 0.1244	Logistic	Logistic	0.4420	0.3246	0.1983	0.0423	1.3617	4.7901
	smoothing+SNV	MLP 5-7-1	0.8168 0.0133	0.7809 0.0160	0.7133 0.1225	Logistic	Logistic	0.2303	0.0683	0.3066	0.0654	1.0632	3.3920
	smoothing+MSC	**MLP 5-9-1**	**0.9129 0.0120**	**0.7875 0.0158**	**0.7566 0.1857**	**Logistic**	**Tanh**	**0.5113**	**0.4084**	**0.1992**	**0.0425**	**1.4312**	**5.4709**
	SG1D+SNV	MLP 5-11-1	0.9258 0.0170	0.7749 0.0196	0.7646 0.0787	Tanh	Exponential	0.3213	0.1784	0.3332	0.0710	0.7980	2.7311
	SG1D+MSC	MLP 5-5-1	0.8069 0.0188	0.7162 0.0199	0.7047 0.0978	Tanh	Identity	0.3131	0.1685	0.2708	0.0577	1.2082	4.4310
	SG2D+SNV	MLP 5-11-1	0.8944 0.0155	0.8549 0.0441	0.7554 0.1222	Identity	Exponential	0.2311	0.0692	0.2624	0.0560	1.1251	3.4674
	SG2D+MSC	MLP 5-3-1	0.9766 0.0111	0.6899 0.0177	0.6033 0.1878	Tanh	Tanh	0.2126	0.0468	0.2402	0.0512	1.1267	3.5811

Table 88. Artificial neural network (ANN) models for prediction of carbon to nitrogen ratio /C/N) of the compost samples during the composting process based on the NIR spectra gathered using portable NIR spectrometer (NIR-S-G1, InnoSpectra, Taiwan) (R_{pred}^2=coefficient of determination for prediction; $R_{pred}^2{}_{adj}$=adjusted coefficient of determination for prediction; $RMSEP$=root mean square of prediction; SEP=standard error of prediction; RPD=ratio of prediction to deviation; RER=ratio of the error range). Pretreatment selected as optimal is marked bold

Output variable	NIR spectra pretreatment	Network name	Calibration					Prediction					
			Training perf. Training error	Test perf. Test error	Validation perf. Validation error	Hidden activation	Output activation	R_{pred}^2	$R_{pred}^2{}_{adj}$	$RMSEP$	SEP	RPD	RER
C/N ratio	**raw spectra**	MLP 5-3-1	0.7442 2.1287	0.7227 4.4768	0.7144 8.3578	Exponential	Tanh	0.4133	0.2898	9.9009	2.1109	1.2394	3.3268
	smoothing	MLP 5-3-1	0.6828 3.0144	0.6057 4.3587	0.6014 8.9878	Tanh	Tanh	0.2632	0.1081	1.6484	0.3514	1.1129	4.3679
	SG1D	MLP 5-9-1	0.6467 4.3578	0.6289 7.2665	0.6195 9.3377	Tanh	Logistic	0.3200	0.1768	1.2720	0.2712	1.2205	5.4247
	SG2D	MLP 5-8-1	0.6296 3.7722	0.6287 8.0014	0.6013 9.5532	Logistic	Logistic	0.3337	0.1934	1.1815	0.2519	1.2508	4.5706
	SNV	MLP 5-8-1	0.6967 2.9912	0.6656 7.2587	0.6043 8.8857	Logistic	Logistic	0.5626	0.4705	2.2782	0.4857	0.9662	5.0040
	MSC	**MLP 5-8-1**	**0.6304 2.5002**	**0.6494 5.7747**	**0.6281 9.5677**	**Logistic**	**Logistic**	**0.6055**	**0.5225**	**1.6143**	**0.3442**	**1.3970**	**7.0620**
	smoothing+SNV	MLP 5-7-1	0.6868 2.3461	0.6507 4.5563	0.6131 7.3942	Logistic	Logistic	0.5338	0.4357	1.6944	0.3612	1.4576	6.9643
	smoothing+MSC	MLP 5-9-1	0.6401 3.1201	0.6315 5.6347	0.6284 9.3670	Logistic	Tanh	0.4988	0.3933	1.7885	0.3813	1.4261	6.5977
	SG1D+SNV	MLP 5-11-1	0.7071 2.7998	0.7322 4.6904	0.7126 9.9365	Tanh	Exponential	0.4414	0.3238	2.2839	0.4869	1.0461	4.9915
	SG1D+MSC	MLP 5-5-1	0.6886 2.3203	0.6823 8.3280	0.6494 9.0262	Tanh	Identity	0.4292	0.3091	1.8278	0.3897	1.2933	6.4558
	SG2D+SNV	MLP 5-11-1	0.6696 2.9918	0.6352 5.3811	0.6014 9.9966	Identity	Exponential	0.3633	0.2293	1.4930	0.3183	1.0850	4.0858
	SG2D+MSC	MLP 5-3-1	0.6600 3.1713	0.6377 7.4574	0.6195 15.6677	Tanh	Tanh	0.3560	0.2205	1.3569	0.2893	1.1770	4.7910

Table 89. Artificial neural network (ANN) models for prediction of total color change (ΔE) of the compost samples during the composting process based on the NIR spectra gathered using portable NIR spectrometer (NIR-S-G1, InnoSpectra, Taiwan) (R_{pred}^2=coefficient of determination for prediction; $R_{pred}^2{}_{adj}$=adjusted coefficient of determination for prediction; $RMSEP$=root mean square of prediction; SEP=standard error of prediction; RPD=ratio of prediction to deviation; RER=ratio of the error range). Pretreatment selected as optimal is marked bold

Output variable	NIR spectra pretreatment	Network name	Calibration					Prediction					
			Training perf. Training error	Test perf. Test error	Validation perf. Validation error	Hidden activation	Output activation	R_{pred}^2	$R_{pred}^2{}_{adj}$	$RMSEP$	SEP	RPD	RER
ΔE (compost)	raw spectra	MLP 5-3-1	0.9523 2.0117	0.7523 9.2387	0.7128 12.1573	Exponential	Tanh	0.3749	0.2433	3.9169	0.8351	1.2459	4.1403
	smoothing	MLP 5-3-1	0.6559 3.9874	0.6407 10.3678	0.63001 15.1247	Tanh	Tanh	0.3166	0.1728	4.0551	0.8645	1.0903	3.9145
	SG1D	MLP 5-9-1	0.8632 2.1234	0.7369 8.8821	0.7226 8.9902	Tanh	Logistic	0.5357	0.4379	3.8523	0.8213	1.4765	4.4593
	SG2D	MLP 5-8-1	0.7446 2.7712	0.7131 9.3674	0.7123 11.9008	Logistic	Logistic	0.3005	0.1533	1.3372	0.2851	0.7790	2.7033
	SNV	MLP 5-8-1	0.7528 3.0012	0.7530 8.9877	0.7191 12.1174	Logistic	Logistic	0.4854	0.3771	4.3305	0.9233	1.3343	3.6729
	MSC	MLP 5-4-1	0.6932 3.1174	0.6248 9.5441	0.6088 15.5541	Logistic	Logistic	0.5575	0.4643	4.3757	0.9329	1.2749	3.8321
	smoothing+SNV	MLP 5-7-1	0.7803 2.9878	0.7834 7.8423	0.7491 12.3535	Logistic	Logistic	0.6633	0.5924	3.8817	0.8276	1.4526	4.4595
	smoothing+MSC	MLP 5-9-1	0.6540 3.2233	0.6519 8.2936	0.6493 14.3129	Logistic	Tanh	0.2423	0.0828	2.9701	0.6332	1.0290	3.4612
	SG1D+SNV	MLP 5-11-1	0.6824 3.5026	0.6690 8.9464	0.6009 12.6214	Tanh	Exponential	0.5320	0.4335	3.5041	0.7471	1.4774	4.9401
	SG1D+MSC	MLP 5-5-1	0.7549 2.6177	0.7453 8.0368	0.7439 11.0983	Tanh	Identity	0.2620	0.1066	4.0593	0.8654	1.1583	4.1472
	SG2D+SNV	**MLP 5-11-1**	**0.9209 1.0011**	**0.7199 9.6787**	**0.7007 12.1227**	**Identity**	**Exponential**	**0.6749**	**0.6065**	**3.2693**	**0.6970**	**1.6087**	**5.1056**
	SG2D+MSC	MLP 5-3-1	0.8788 2.5588	0.7474 9.9733	0.6024 14.1516	Tanh	Tanh	0.2937	0.1450	4.6523	0.9919	1.1955	3.7209

Table 90. Artificial neural network (ANN) models for prediction of pH of the compost extract samples during the composting process based on the NIR spectra gathered using portable NIR spectrometer (NIR-M-R2, InnoSpectra, Taiwan) (R_{pred}^2=coefficient of determination for prediction; $R_{pred}^2{}_{adj}$=adjusted coefficient of determination for prediction; $RMSEP$=root mean square of prediction; SEP=standard error of prediction; RPD=ratio of prediction to deviation; RER=ratio of the error range). Pretreatment selected as optimal is marked bold

Output variable	NIR spectra pretreatment	Network name	Calibration					Prediction					
			Training perf. Training error	Test perf. Test error	Validation perf. Validation error	Hidden activation	Output activation	R_{pred}^2	$R_{pred}^2{}_{adj}$	$RMSEP$	SEP	RPD	RER
pH	raw spectra	MLP 5-9-1	0.8488 0.0752	0.7553 0.1261	0.7232 0.2542	Exponential	Exponential	0.5459	0.4503	0.5391	0.1149	1.5130	5.7130
	smoothing	MLP 5-6-1	0.6852 0.1101	0.6384 0.2485	0.6628 0.3326	Logistic	Identity	0.2019	0.0339	0.3727	0.0795	1.0026	3.8997
	SG1D	MLP 5-6-1	0.8050 0.0520	0.7959 0.1139	0.6161 0.1871	Logistic	Tanh	0.2439	0.0847	0.7123	0.1519	1.1640	3.9635
	SG2D	MLP 5-5-1	0.7048 0.1586	0.6804 0.1749	0.6909 0.1873	Tanh	Identity	0.2690	0.1151	0.8743	0.1864	0.8692	3.6755
	SNV	MLP 5-5-1	0.6688 0.1277	0.6328 0.3001	0.6402 0.2977	Logistic	Identity	0.1778	0.0047	0.6666	0.1421	1.1350	4.8603
	MSC	MLP 5-5-1	0.8860 0.0877	0.8088 0.0971	0.8044 0.1144	Exponential	Logistic	0.2529	0.0956	0.6392	0.1363	0.9563	3.9477
	smoothing+SNV	MLP 5-10-1	0.8483 0.0890	0.7655 0.0999	0.7303 0.1012	Logistic	Logistic	0.3047	0.1583	0.6108	0.1302	1.1743	4.4802
	smoothing+MSC	MLP 5-8-1	0.8738 0.1541	0.7402 0.1678	0.7267 0.2001	Exponential	Logistic	0.3974	0.2705	0.4120	0.0878	1.2618	4.8953
	SG1D+SNV	MLP 5-4-1	0.6337 0.2551	0.6296 0.2987	0.6011 0.2675	Exponential	Identity	0.2216	0.0578	0.6035	0.1287	1.1480	4.4908
	SG1D+MSC	MLP 5-3-1	0.6535 0.3012	0.6404 0.3147	0.6328 0.3471	Tanh	Identity	0.1907	0.0203	0.8000	0.1706	1.1356	3.8498
	SG2D+SNV	**MLP 5-10-1**	**0.8391 0.2525**	**0.7390 0.2645**	**0.7326 0.3102**	**Tanh**	**Tanh**	**0.4232**	**0.3017**	**0.4996**	**0.1065**	**1.3339**	**5.4238**
	SG2D+MSC	MLP 5-3-1	0.7620 0.3112	0.6310 0.3221	0.6277 0.3887	Tanh	Identity	0.2606	0.1049	0.9610	0.2049	0.9978	3.3715

Table 91. Artificial neural network (ANN) models for prediction of total dissolved solids (TDS) of the compost extract samples during the composting process based on the NIR spectra gathered using portable NIR spectrometer (NIR-M-R2, InnoSpectra, Taiwan) (R_{pred}^2=coefficient of determination for prediction; $R_{pred}^2{}_{adj}$=adjusted coefficient of determination for prediction; $RMSEP$=root mean square of prediction; SEP=standard error of prediction; RPD=ratio of prediction to deviation; RER=ratio of the error range). Pretreatment selected as optimal is marked bold

Output variable	NIR spectra pretreatment	Network name	Calibration					Prediction					
			Training perf. Training error	Test perf. Test error	Validation perf. Validation error	Hidden activation	Output activation	R_{pred}^2	$R_{pred}^2{}_{adj}$	$RMSEP$	SEP	RPD	RER
TDS	raw spectra	MLP 5-71	0.7541 1312.224	0.7313 1302.637	0.6962 1335.471	Exponential	Logistic	0.6538	0.5809	216.4670	46.1509	1.3299	4.8445
	smoothing	**MLP 5-6-1**	**0.6852 1606.68**	**0.6384 1874.34**	**0.6628 1868.97**	**Tanh**	**Logistic**	**0.6993**	**0.6360**	**175.3826**	**37.3917**	**1.8362**	**5.9793**
	SG1D	MLP 5-7-1	0.9066 1558.80	0.7276 1568.42	0.7179 1867.17	Exponential	Identity	0.1957	0.0264	350.8866	74.8093	0.8854	2.9886
	SG2D	MLP 5-4-1	0.7468 1220.86	0.7436 1870,84	0.7028 1876.47	Exponential	Tanh	0.1873	0.0162	251.4775	53.6152	1.0688	4.1515
	SNV	MLP 5-5-1	0.6934 1627.07	0.6625 1832.01	0.6398 1900.29	Logistic	Identity	0.1866	0.0154	189.1040	40.3171	1.1326	4.8368
	MSC	MLP 5-5-1	0.9198 997.21	0.7423 1754.77	0.7215 1860.50	Exponential	Logistic	0.2426	0.0832	273.4225	58.2939	1.1566	3.8853
	smoothing+SNV	MLP 5-10-1	0.8286 1020.23	0.7536 1325.74	0.7352 1900.77	Logistic	Logistic	0.2881	0.1383	215.4688	45.9381	1.1743	4.7431
	smoothing+MSC	MLP 5-8-1	0.6329 1425.77	0.6418 1678.96	0.6218 1965.63	Exponential	Logistic	0.1905	0.0201	101.6569	21.6733	0.9974	3.6299
	SG1D+SNV	MLP 5-4-1	0.7537 1358.22	0.7216 1597.36	0.7025 1879.96	Exponential	Identity	0.2538	0.0967	273.0433	58.2130	1.1686	3.7564
	SG1D+MSC	MLP 5-3-1	0.6328 1577.41	0.6120 1885.22	0.6004 1963.66	Tanh	Identity	0.2886	0.1389	256.0654	54.5933	1.2084	3.9729
	SG2D+SNV	MLP 5-10-1	0.8984 1235.55	0.7298 1687.32	0.7177 1702.36	Tanh	Tanh	0.1971	0.0280	258.1370	55.0350	1.1066	3.9204
	SG2D+MSC	MLP 5-3-1	0.8915 1344.21	0.7379 1664.51	0.7156 1788.50	Tanh	Identity	0.2537	0.0966	256.1528	54.6120	1.1359	3.9716

Table 92. Artificial neural network (ANN) models for prediction of conductivity (*S*) of the compost extract samples during the composting process based on the NIR spectra gathered using portable NIR spectrometer (NIR-M-R2, InnoSpectra, Taiwan) (R_{pred}^2=coefficient of determination for prediction; $R_{pred}^2{}_{adj}$=adjusted coefficient of determination for prediction; *RMSEP*=root mean square of prediction; *SEP*=standard error of prediction; *RPD*=ratio of prediction to deviation; *RER*=ratio of the error range). Pretreatment selected as optimal is marked bold

Output variable	NIR spectra pretreatment	Network name	Calibration					Prediction					
			Training perf. Training error	Test perf. Test error	Validation perf. Validation error	Hidden activation	Output activation	R_{pred}^2	$R_{pred}^2{}_{adj}$	*RMSEP*	*SEP*	*RPD*	*RER*
S	raw spectra	MLP 5-6-1	0.7333 1381.17	0.7451 1486.97	0.7192 1897.25	Exponential	Logistic	0.6018	0.5180	419.7386	89.4886	1.3324	5.1135
	smoothing	**MLP 5-5-1**	**0.7527 1058.69**	**0.7252 1574.77**	**0.7032 2254.75**	**Identity**	**Logistic**	**0.7074**	**0.6458**	**328.9654**	**70.1357**	**1.8436**	**6.5245**
	SG1D	MLP 5-11-1	0.9024 1461.56	0.6476 1756.14	0.6256 1884.16	Logistic	Identity	0.3040	0.1575	524.7410	111.8752	1.1069	3.5884
	SG2D	MLP 5-5-1	0.6193 1027.88	0.6279 1214.44	0.6036 1989.93	Exponential	Tanh	0.1934	0.0236	558.6773	119.1104	0.9051	3.3705
	SNV	MLP 5-5-1	0.7294 1027.07	0.6762 1432.01	0.6453 1989.29	Logistic	Identity	0.1898	0.0193	341.6746	72.8453	1.1265	4.7248
	MSC	MLP 5-5-1	0.9485 998.73	0.7427 1324.23	0.7238 1878.87	Exponential	Logistic	0.2620	0.1067	517.3556	110.3006	1.1661	3.7363
	smoothing+SNV	MLP 5-10-1	0.8549 1124.88	0.7557 1578.22	0.7583 1854.52	Logistic	Logistic	0.2946	0.1461	390.6578	83.2885	1.1775	4.6656
	smoothing+MSC	MLP 5-8-1	0.6946 1754.55	0.6450 1978.15	0.6323 2314.12	Exponential	Logistic	0.2465	0.0879	220.7936	47.0734	0.9204	3.8045
	SG1D+SNV	MLP 5-4-1	0.7591 1660.06	0.6860 1993.24	0.6013 2323.11	Exponential	Identity	0.2493	0.0913	540.0331	115.1354	1.1630	3.8510
	SG1D+MSC	MLP 5-3-1	0.6262 1656.50	0.6035 1988.78	0.6156 2345.55	Tanh	Identity	0.2368	0.0761	519.6832	110.7968	1.1693	3.9306
	SG2D+SNV	MLP 5-10-1	0.9488 935.55	0.7396 1558.74	0.7226 2024.54	Tanh	Tanh	0.2090	0.0425	533.8834	113.8243	1.0698	3.9391
	SG2D+MSC	MLP 5-3-1	0.8776 1122.47	0.6408 1345.56	0.6184 2024.50	Tanh	Identity	0.2239	0.0605	497.4528	106.0573	1.1300	3.7645

Table 93. Artificial neural network (ANN) models for prediction of total color change (ΔE) of the compost extract samples during the composting process based on the NIR spectra gathered using portable NIR spectrometer (NIR-M-R2, InnoSpectra, Taiwan) (R_{pred}^2=coefficient of determination for prediction; $R_{pred\,adj}^2$=adjusted coefficient of determination for prediction; $RMSEP$=root mean square of prediction; SEP=standard error of prediction; RPD=ratio of prediction to deviation; RER=ratio of the error range). Pretreatment selected as optimal is marked bold

Output variable	NIR spectra pretreatment	Network name	Calibration					Prediction					
			Training perf. Training error	Test perf. Test error	Validation perf. Validation error	Hidden activation	Output activation	R_{pred}^2	$R_{pred\,adj}^2$	$RMSEP$	SEP	RPD	RER
ΔE (extracts)	raw spectra	MLP 5-5-1	0.8988 0.0697	0.8843 0.1031	0.7264 0.1706	Exponential	Logistic	0.5503	0.4556	0.5665	0.1208	1.1703	5.8655
	smoothing	MLP 5-11-1	0.9480 0.0354	0.8004 0.1312	0.7426 0.6799	Logistic	Exponential	0.5633	0.4714	0.5309	0.1132	1.1608	4.6498
	SG1D	MLP 5-6-1	0.9308 0.0529	0.7954 0.0888	0.6576 0.2406	Logistic	Identity	0.1835	0.0116	0.8983	0.1915	0.9600	3.1523
	SG2D	**MLP 5-6-1**	**0.8358 0.0585**	**0.7904 0.0754**	**0.6782 0.3560**	**Tanh**	**Exponential**	**0.4308**	**0.3109**	**0.5665**	**0.1208**	**1.3309**	**5.8657**
	SNV	MLP 5-5-1	0.6630 0.1277	0.6476 0.1787	0.6318 0.7444	Logistic	Identity	0.2872	0.1371	0.7010	0.1495	0.8575	4.0393
	MSC	MLP 5-5-1	0.9267 0.0771	0.6980 0.1887	0.6462 0.6745	Exponential	Logistic	0.2830	0.1320	0.8376	0.1786	1.1511	4.4127
	smoothing+SNV	MLP 5-10-1	0.8314 0.1032	0.7633 0.1888	0.7365 0.1912	Logistic	Logistic	0.2521	0.0946	0.7873	0.1679	1.1743	4.6948
	smoothing+MSC	MLP 5-8-1	0.8247 0.1541	0.6999 0.1678	0.6544 0.2001	Exponential	Logistic	0.3660	0.2326	0.7302	0.1557	1.2597	5.0621
	SG1D+SNV	MLP 5-4-1	0.6473 0.2001	0.6404 0.2324	0.6044 0.2578	Exponential	Identity	0.2448	0.0858	0.7127	0.1519	1.1521	4.6623
	SG1D+MSC	MLP 5-3-1	0.6400 0.2578	0.6278 0.2877	0.6174 0.2884	Tanh	Identity	0.2799	0.1283	0.6116	0.1304	1.1844	4.9985
	SG2D+SNV	MLP 5-10-1	0.8391 0.2741	0.7390 0.3001	0.7326 0.3257	Tanh	Tanh	0.2901	0.1406	0.6826	0.1455	1.1733	4.1484
	SG2D+MSC	MLP 5-3-1	0.8901 0.3112	0.8029 0.3221	0.7315 0.3887	Tanh	Identity	0.2780	0.1260	0.8472	0.1806	1.1404	4.3631

4.3.8. Artificial neural network (ANN) models for the prediction of number of microorganisms during the composting process

As mentioned before, due to complexity of the NIR spectra, the preprocessing of spectra has been applied in order to obtain important infromation about the microbiological properties of compost. Furthermore, the artificial neural network (ANN) models were developed based on the recorded NIR spectra for the compost samples. The developed ANN models based on NIR spectra obtained using the NIR spectrometer (NIR-128-1.7-USB/6.25/50 μm, Control Development Inc., USA) for microbiological properties of the samples are shown in Tables 94-96, and the developed ANN models based on NIR spectra obtained using the another NIR spectrometer (AvaSpec-NIR256-2.5-HSC-EVO, Avantes, USA) are shown in Tables 97 and 98. Furthermore, in this set of composting experiment, the portable NIR spectrometer was used. The developed ANN models based on NIR spectra obtained using the portable NIR spectrometers NIR-S-G1 (InnoSpectra, Taiwan) and NIR-M-R2 (InnoSpectra, Taiwan) for microbiological properties of the compost samples are shown in Table 99.

Table 94. Artificial neural network (ANN) models for prediction of number of bacteria during the composting process based on the NIR spectra gathered using NIR spectrometer (NIR-128-1.7-USB/6.25/50 μm, Control Development Inc., USA) (R_{pred}^2=coefficient of determination for prediction; $R_{pred}^2{}_{adj}$=adjusted coefficient of determination for prediction; $RMSEP$=root mean square of prediction; SEP=standard error of prediction; RPD=ratio of prediction to deviation; RER=ratio of the error range). Pretreatment selected as optimal is marked bold

Output variable	NIR spectra pretreatment	Network name	Calibration					Prediction					
			Training perf. Training error	Test perf. Test error	Validation perf. Validation error	Hidden activation	Output activation	R_{pred}^2	$R_{pred}^2{}_{adj}$	$RMSEP$	SEP	RPD	RER
logCFU$_{bacteria}$	raw	MLP 5-8-1	0.8877 0.1224	0.6947 0.3277	0.6951 0.3455	Logistic	Logistic	0.3494	0.2251	0.6983	0.1489	0.9611	4.7808
	smoothing	MLP 5-6-1	0.6268 0.3447	0.6386 0.3578	0.6006 0.3997	Logistic	Tanh	0.6395	0.6973	0.4565	0.0973	1.9977	9.2409
	SG1D	MLP 5-7-1	0.6571 0.3577	0.6430 0.3655	0.6248 0.4012	Logistic	Logistic	0.5991	0.5274	0.6727	0.1434	1.3853	7.0590
	SG2D	MLP 5-6-1	0.6757 0.2852	0.6354 0.2961	0.6353 0.2933	Logistic	Logistic	0.6431	0.5805	0.7094	0.1512	1.4852	6.5904
	SNV	MLP 5-6-1	0.8333 0.1198	0.7891 0.1992	0.6924 0.3004	Tanh	Logistic	0.4886	0.3935	0.5352	0.1141	1.2811	6.0240
	MSC	MLP 5-8-1	0.8525 0.2024	0.7540 0.2307	0.7315 0.3112	Exponential	Exponential	0.6519	0.5913	0.6337	0.1351	1.6492	7.4928
	smoothing+SNV	MLP 5-7-1	0.6221 0.3114	0.6131 0.3221	0.6138 0.3255	Logistic	Identity	0.7271	0.6823	0.4981	0.1062	1.8061	9.0278
	smoothing+MSC	MLP 5-6-1	0.8138 0.2101	0.6366 0.3125	0.6149 0.3336	Identity	Identity	0.5339	0.4485	0.6876	0.1466	1.2199	4.7589
	SG1D+SNV	MLP 5-8-1	0.9181 0.0099	0.8047 0.1223	0.7995 0.2155	Exponential	Identity	0.5078	0.4168	0.2568	0.0548	1.3419	5.6585
	SG1D+MSC	MLP 5-6-1	0.6628 0.3971	0.6260 0.4011	0.6262 0.4167	Tanh	Identity	0.6494	0.5882	0.4156	0.0886	1.6043	7.8743
	SG2D+SNV	MLP 5-6-1	0.7765 0.2101	0.6995 0.4114	0.6787 0.4235	Logistic	Exponential	0.6634	0.7263	0.4516	0.0963	2.0029	7.6225
	SG2D+MSC	**MLP 5-9-1**	**0.8416 0.4063**	**0.8137 0.4341**	**0.8144 0.4544**	**Exponential**	**Exponential**	**0.6311**	**0.8082**	**0.3277**	**0.0699**	**2.7121**	**10.1708**

Table 95. Artificial neural network (ANN) models for prediction of number of fungi during the composting process based on the NIR spectra gathered using NIR spectrometer (NIR-128-1.7-USB/6.25/50 μm, Control Development Inc., USA) (R_{pred}^2=coefficient of determination for prediction; $R_{pred}^2{}_{adj}$=adjusted coefficient of determination for prediction; *RMSEP*=root mean square of prediction; *SEP*=standard error of prediction; *RPD*=ratio of prediction to deviation; *RER*=ratio of the error range). Pretreatment selected as optimal is marked bold

Output variable	NIR spectra pretreatment	Network name	Calibration					Prediction					
			Training perf. Training error	Test perf. Test error	Validation perf. Validation error	Hidden activation	Output activation	R_{pred}^2	$R_{pred}^2{}_{adj}$	*RMSEP*	*SEP*	*RPD*	*RER*
logCFU_{fungi}	raw	MLP 5-8-1	0.7522 0.2336	0.6490 0.3897	0.6068 0.3574	Logistic	Logistic	0.6967	0.6454	0.7878	0.1680	1.8349	6.7857
	smoothing	**MLP 5-6-1**	**0.9605 0.0213**	**0.8501 0.2441**	**0.8421 0.3547**	**Logistic**	**Tanh**	**0.7907**	**0.7592**	**0.5616**	**0.1197**	**2.3458**	**9.4789**
	SG1D	MLP 5-7-1	0.8731 0.2101	0.8339 0.2242	0.8039 0.2677	Logistic	Logistic	0.4520	0.3492	1.1906	0.2538	1.2336	4.4709
	SG2D	MLP 5-6-1	0.7254 0.2997	0.7349 0.3221	0.7040 0.3514	Logistic	Logistic	0.5841	0.5092	0.9884	0.2107	1.5167	5.4123
	SNV	MLP 5-6-1	0.6227 0.3650	0.6305 0.3447	0.6019 0.3742	Tanh	Logistic	0.7706	0.7349	0.5803	0.1237	2.1939	9.2120
	MSC	MLP 5-8-1	0.7578 0.2024	0.7511 0.2307	0.6933 0.3112	Exponential	Exponential	0.6020	0.5308	0.9881	0.2107	1.5331	5.4099
	smoothing+SNV	MLP 5-7-1	0.8264 0.2114	0.7525 0.3221	0.7374 0.3255	Logistic	Identity	0.6965	0.6452	0.7695	0.1641	1.5640	6.5404
	smoothing+MSC	MLP 5-6-1	0.6839 0.3354	0.6351 0.3547	0.6131 0.3839	Identity	Identity	0.4851	0.3893	0.9531	0.2032	1.1455	4.4882
	SG1D+SNV	MLP 5-8-1	0.9542 0.0122	0.8417 0.1998	0.7089 0.2987	Exponential	Identity	0.5642	0.4851	0.7649	0.1631	1.3768	6.9195
	SG1D+MSC	MLP 5-6-1	0.9781 0.0087	0.7512 0.3011	0.7139 0.3255	Tanh	Identity	0.7711	0.7356	0.5595	0.1193	2.1713	8.9529
	SG2D+SNV	MLP 5-6-1	0.8232 0.1974	0.7651 0.1998	0.7316 0.2147	Logistic	Exponential	0.7591	0.7210	0.6634	0.1414	2.1373	7.6385
	SG2D+MSC	MLP 5-9-1	0.6848 0.3941	0.6334 0.3997	0.6255 0.4122	Exponential	Exponential	0.5471	0.4644	0.7136	0.1521	1.3732	6.7879

Table 96. Artificial neural network (ANN) models for prediction of total number of microorganisms during the composting process based on the NIR spectra gathered using NIR spectrometer (NIR-128-1.7-USB/6.25/50 μm, Control Development Inc., USA) (R_{pred}^2=coefficient of determination for prediction; $R_{pred}^2{}_{adj}$=adjusted coefficient of determination for prediction; $RMSEP$=root mean square of prediction; SEP=standard error of prediction; RPD=ratio of prediction to deviation; RER=ratio of the error range). Pretreatment selected as optimal is marked bold

Output variable	NIR spectra pretreatment	Network name	Calibration					Prediction					
			Training perf. Training error	Test perf. Test error	Validation perf. Validation error	Hidden activation	Output activation	R_{pred}^2	$R_{pred}^2{}_{adj}$	$RMSEP$	SEP	RPD	RER
logCFU$_{total\ number\ of\ microorganism}$	raw	MLP 5-8-1	0.6625 0.2336	0.6401 0.3897	0.6058 0.3574	Logistic	Logistic	0.4472	0.3434	1.5081	0.3215	1.2375	5.0077
	smoothing	MLP 5-6-1	0.6604 0.3225	0.6585 0.3578	0.6494 0.3687	Logistic	Tanh	0.8009	0.7716	0.9891	0.2109	2.0124	9.3706
	SG1D	MLP 5-7-1	0.6969 0.3221	0.6263 0.3466	0.6288 0.3422	Logistic	Logistic	0.6517	0.5910	1.2870	0.2744	1.6522	7.3905
	SG2D	MLP 5-6-1	0.6701 0.3541	0.6323 0.3321	0.6464 0.3455	Logistic	Logistic	0.6625	0.6040	1.3701	0.2921	1.6844	6.9138
	SNV	MLP 5-6-1	0.8315 0.1198	0.8126 0.1992	0.6689 0.3004	Tanh	Logistic	0.7570	0.7184	0.8365	0.1783	2.1218	9.0285
	MSC	MLP 5-8-1	0.6288 0.3621	0.6332 0.3544	0.6247 0.3741	Exponential	Exponential	0.7037	0.6540	1.2697	0.2707	1.8585	7.4915
	smoothing+SNV	MLP 5-7-1	0.7725 0.2144	0.6973 0.3271	0.6052 0.3755	Logistic	Identity	0.7834	0.7504	1.0587	0.2257	1.7511	8.2226
	smoothing+MSC	MLP 5-6-1	0.7063 0.3001	0.6855 0.3125	0.6412 0.3336	Identity	Identity	0.6332	0.5686	1.1180	0.2384	1.6378	6.1880
	SG1D+SNV	MLP 5-8-1	0.8292 0.1878	0.8030 0.2774	0.7635 0.3115	Exponential	Identity	0.5125	0.4224	0.9400	0.2004	1.3135	6.6475
	SG1D+MSC	MLP 5-6-1	0.6230 0.3574	0.6178 0.3456	0.6097 0.3824	Tanh	Identity	0.6920	0.6398	0.9612	0.2049	1.7658	7.3485
	SG2D+SNV	MLP 5-6-1	0.8437 0.1988	0.7759 0.2111	0.7578 0.2258	Logistic	Exponential	0.7635	0.7263	0.9587	0.2044	2.1361	7.9179
	SG2D+MSC	**MLP 5-9-1**	**0.8413 0.4122**	**0.8188 0.4342**	**0.8031 0.4725**	**Exponential**	**Exponential**	**0.7740**	**0.7390**	**0.8220**	**0.1752**	**2.2007**	**11.3179**

Table 97. Artificial neural network (ANN) models for prediction of number of bacteria during the composting process based on the NIR spectra gathered using NIR spectrometer (AvaSpec-NIR256-2.5-HSC-EVO, Avantes, USA) (R_{pred}^2=coefficient of determination for prediction; $R_{pred}^2{}_{adj}$=adjusted coefficient of determination for prediction; $RMSEP$=root mean square of prediction; SEP=standard error of prediction; RPD=ratio of prediction to deviation; RER=ratio of the error range). Pretreatment selected as optimal is marked bold

Output variable	NIR spectra pretreatment	Network name	Calibration					Prediction					
			Training perf. / Training error	Test perf. / Test error	Validation perf. / Validation error	Hidden activation	Output activation	R_{pred}^2	$R_{pred}^2{}_{adj}$	RMSEP	SEP	RPD	RER
logCFU_bacteria	raw	MLP 5-9-1	0.6413 0.4122	0.6188 0.4342	0.6031 0.4725	Exponential	Exponential	0.6477	0.6001	0.7324	0.1562	1.7061	6.3092
	smoothing	**MLP 5-6-1**	**0.8268 0.4498**	**0.8386 0.4534**	**0.8009 0.4874**	**Logistic**	**Tanh**	**0.7352**	**0.7059**	**0.5221**	**0.1113**	**2.1811**	**8.8134**
	SG1D	MLP 5-5-1	0.7343 0.2087	0.7444 0.2334	0.7008 0.3514	Tanh	Tanh	0.4202	0.3247	1.1070	0.2360	1.1469	4.1570
	SG2D	MLP 5-5-1	0.7343 0.2087	0.7444 0.2334	0.7008 0.3514	Tanh	Tanh	0.5431	0.4734	0.9190	0.1959	1.4102	5.0323
	SNV	MLP 5-10-1	0.6969 0.3698	0.6139 0.3852	0.6335 0.3514	Exponential	Logistic	0.7165	0.6833	0.5395	0.1150	2.0399	8.5652
	MSC	MLP 5-3-1	0.6955 0.3198	0.6302 0.3556	0.6112 0.3758	Exponential	Identity	0.5597	0.4936	0.9187	0.1959	1.4255	5.0301
	smoothing+SNV	MLP 5-7-1	0.7740 0.3099	0.7318 0.3132	0.7199 0.3355	Exponential	Logistic	0.6476	0.5999	0.7155	0.1525	1.4542	6.0812
	smoothing+MSC	MLP 5-6-1	0.6393 0.3224	0.6208 0.3444	0.6044 0.6742	Tanh	Logistic	0.4510	0.3620	0.8862	0.1889	1.0651	4.1731
	SG1D+SNV	MLP 5-3-1	0.7475 0.3198	0.7203 0.3556	0.7119 0.3758	Exponential	Identity	0.5246	0.4510	0.7112	0.1516	1.2801	6.4337
	SG1D+MSC	MLP 5-6-1	0.6066 0.3814	0.6338 0.3234	0.6033 0.6742	Tanh	Exponential	0.7170	0.6839	0.5202	0.1109	2.0189	8.3243
	SG2D+SNV	MLP 5-8-1	0.6411 0.3544	0.6385 0.3577	0.6188 0.3874	Exponential	Logistic	0.7058	0.6703	0.6168	0.1315	1.9872	7.1022
	SG2D+MSC	MLP 5-6-1	0.8853 0.3188	0.8518 0.3435	0.8087 0.4001	Exponential	Exponential	0.5087	0.4318	0.6635	0.1415	1.2768	6.3113

Table 97. (*continuing*) Artificial neural network (ANN) models for prediction of number of fungi during the composting process based on the NIR spectra gathered using NIR spectrometer (AvaSpec-NIR256-2.5-HSC-EVO, Avantes, USA) (R_{pred}^2=coefficient of determination for prediction; $R_{pred}^2{}_{adj}$=adjusted coefficient of determination for prediction; $RMSEP$=root mean square of prediction; SEP=standard error of prediction; RPD=ratio of prediction to deviation; RER=ratio of the error range). Pretreatment selected as optimal is marked bold

Output variable	NIR spectra pretreatment	Network name	Calibration					Prediction					
			Training perf. Training error	Test perf. Test error	Validation perf. Validation error	Hidden activation	Output activation	R_{pred}^2	$R_{pred}^2{}_{adj}$	$RMSEP$	SEP	RPD	RER
logCFU$_{fungi}$	raw	MLP 5-9-1	0.6513 0.4277	0.6289 0.4644	0.6110 0.4821	Exponential	Exponential	0.3249	0.2093	0.6493	0.1384	0.8936	4.4451
	smoothing	**MLP 5-6-1**	**0.9605 0.0125**	**0.7501 0.3241**	**0.7412 0.3455**	**Logistic**	**Tanh**	**0.6876**	**0.6484**	**0.4245**	**0.0905**	**1.8574**	**9.5219**
	SG1D	MLP 5-5-1	0.7598 0.2227	0.7329 0.2255	0.7333 0.3101	Tanh	Tanh	0.5571	0.4903	0.6255	0.1333	1.2880	6.5634
	SG2D	MLP 5-5-1	0.7343 0.2087	0.7444 0.2334	0.7008 0.3514	Tanh	Tanh	0.5979	0.5398	0.6596	0.1406	1.3809	6.1277
	SNV	MLP 5-10-1	0.6969 0.3698	0.6139 0.3852	0.6335 0.3514	Exponential	Logistic	0.4543	0.3659	0.4976	0.1061	1.1911	5.6010
	MSC	MLP 5-3-1	0.6435 0.3222	0.6307 0.3145	0.6207 0.3474	Exponential	Identity	0.6061	0.5497	0.5892	0.1256	1.5334	6.9667
	smoothing+SNV	MLP 5-7-1	0.7436 0.3156	0.7009 0.3567	0.7002 0.3885	Exponential	Logistic	0.6761	0.6344	0.4631	0.0987	1.6793	8.3939
	smoothing+MSC	MLP 5-6-1	0.7000 0.2667	0.6824 0.3115	0.6001 0.3774	Tanh	Logistic	0.4965	0.4170	0.6393	0.1363	1.1342	4.4247
	SG1D+SNV	MLP 5-6-1	0.6942 0.3166	0.6301 0.3355	0.6198 0.3874	Tanh	Exponential	0.4721	0.3875	0.2388	0.0509	1.2477	5.2612
	SG1D+MSC	MLP 5-6-1	0.6126 0.3825	0.6024 0.3355	0.6001 0.6877	Tanh	Exponential	0.6038	0.5469	0.3864	0.0824	1.4917	7.3214
	SG2D+SNV	MLP 5-8-1	0.6235 0.3644	0.6116 0.3724	0.6037 0.3844	Exponential	Logistic	0.7098	0.6753	0.4199	0.0895	1.8622	7.0873
	SG2D+MSC	MLP 5-8-1	0.8936 0.2998	0.8428 0.3487	0.8192 0.3811	Exponential	Logistic	0.7728	0.7514	0.3047	0.0650	2.5217	9.1758

Table 98. Artificial neural network (ANN) models for prediction of total number of microorganisms during the composting process based on the NIR spectra gathered using NIR spectrometer (AvaSpec-NIR256-2.5-HSC-EVO, Avantes, USA) (R_{pred}^2=coefficient of determination for prediction; $R_{pred}^2{}_{adj}$=adjusted coefficient of determination for prediction; $RMSEP$=root mean square of prediction; SEP=standard error of prediction; RPD=ratio of prediction to deviation; RER=ratio of the error range). Pretreatment selected as optimal is marked bold

Output variable	NIR spectra pretreatment	Network name	Calibration					Prediction					
			Training perf. Training error	Test perf. Test error	Validation perf. Validation error	Hidden activation	Output activation	R_{pred}^2	$R_{pred}^2{}_{adj}$	$RMSEP$	SEP	RPD	RER
logCFU total number of microorganism	raw	MLP 5-9-1	0.7522 0.3244	0.7241 0.3399	0.7110 0.3488	Exponential	Exponential	0.4158	0.3193	1.4022	0.2990	1.1506	4.6561
	smoothing	MLP 5-6-1	0.6604 0.3125	0.6577 0.3241	0.6494 0.3455	Logistic	Tanh	0.7446	0.7174	0.9197	0.1961	1.8711	8.7127
	SG1D	MLP 5-5-1	0.7501 0.2187	0.7409 0.2225	0.6455 0.3391	Tanh	Tanh	0.6060	0.5495	1.1967	0.2551	1.5362	6.8716
	SG2D	MLP 5-5-1	0.7343 0.2087	0.7444 0.2334	0.7008 0.3514	Tanh	Tanh	0.6160	0.5616	1.2739	0.2716	1.5661	6.4283
	SNV	MLP 5-10-1	0.6449 0.3598	0.6258 0.3712	0.6031 0.3514	Exponential	Logistic	0.7038	0.6680	0.7778	0.1658	1.9728	8.3946
	MSC	MLP 5-3-1	0.6635 0.3333	0.6107 0.3458	0.6006 0.3996	Exponential	Identity	0.6543	0.6081	1.1805	0.2517	1.7280	6.9655
	smoothing+SNV	MLP 5-7-1	0.9015 0.0122	0.8577 0.0997	0.8058 0.1988	Exponential	Logistic	0.7284	0.6977	0.9844	0.2099	1.6281	7.6453
	smoothing+MSC	MLP 5-6-1	0.9335 0.0102	0.9188 0.0111	0.7726 0.2774	Tanh	Logistic	0.5888	0.5287	1.0395	0.2216	1.5228	5.7535
	SG1D+SNV	MLP 5-3-1	0.7444 0.3598	0.7203 0.3656	0.7009 0.3844	Exponential	Identity	0.4765	0.3928	0.8740	0.1863	1.2213	6.1807
	SG1D+MSC	MLP 5-6-1	0.6432 0.3566	0.6281 0.3755	0.6069 0.3974	Tanh	Exponential	0.6434	0.5949	0.8937	0.1905	1.6418	6.8325
	SG2D+SNV	MLP 5-8-1	0.9529 0.0522	0.7816 0.3457	0.6866 0.3577	Exponential	Logistic	0.7099	0.6753	0.8914	0.1901	1.9861	7.3619
	SG2D+MSC	**MLP 5-8-1**	**0.7373 0.3778**	**0.7543 0.3645**	**0.7314 0.3874**	**Exponential**	**Logistic**	**0.7196**	**0.6871**	**0.7643**	**0.1629**	**2.0462**	**10.5232**

Table 99. Artificial neural network (ANN) models for prediction of number of bacteria during the composting process based on the NIR spectra gathered using portable NIR spectrometer (NIR-S-G1, InnoSpectra, Taiwan) (R_{pred}^2=coefficient of determination for prediction; $R_{pred}^2{}_{adj}$=adjusted coefficient of determination for prediction; $RMSEP$=root mean square of prediction; SEP=standard error of prediction; RPD=ratio of prediction to deviation; RER=ratio of the error range). Pretreatment selected as optimal is marked bold

| Output variable | NIR spectra pretreatment | Network name | Calibration | | | | | Prediction | | | | | |
			Training perf. Training error	Test perf. Test error	Validation perf. Validation error	Hidden activation	Output activation	R_{pred}^2	$R_{pred}^2{}_{adj}$	$RMSEP$	SEP	RPD	RER
logCFU$_{bacteria}$	raw	MLP 5-4-1	0.6761 0.3316	0.6157 0.3644	0.6032 0.3865	Exponential	Exponential	0.6789	0.6290	0.7677	0.1637	1.7882	6.6129
	smoothing	**MLP 5-9-1**	**0.7165 0.2988**	**0.7233 0.3798**	**0.7026 0.3624**	**Logistic**	**Identity**	**0.7705**	**0.7399**	**0.5473**	**0.1167**	**2.2861**	**9.2376**
	SG1D	MLP 5-11-1	0.7406 0.1988	0.6868 0.2678	0.6796 0.2988	Logistic	Identity	0.4405	0.3403	1.1603	0.2474	1.2022	4.3571
	SG2D	MLP 5-7-1	0.7321 0.1999	0.6541 0.3344	0.6223 0.2874	Exponential	Identity	0.5692	0.4962	0.9633	0.2054	1.4781	5.2745
	SNV	MLP 5-11-1	0.7450 0.1855	0.7302 0.2125	0.7246 0.2574	Exponential	Exponential	0.7510	0.7162	0.5655	0.1206	2.1381	8.9775
	MSC	MLP 5-7-1	0.7321 0.1999	0.6541 0.3344	0.6223 0.2874	Exponential	Identity	0.5867	0.5173	0.9629	0.2053	1.4941	5.2722
	smoothing+SNV	MLP 5-11-1	0.7450 0.1855	0.7302 0.2125	0.7246 0.2574	Exponential	Exponential	0.6788	0.6288	0.7499	0.1599	1.5242	6.3739
	smoothing+MSC	MLP 5-7-1	0.6133 0.3111	0.6206 0.3552	0.6266 0.3445	Logistic	Tanh	0.4727	0.3794	0.9289	0.1980	1.1163	4.3740
	SG1D+SNV	MLP 5-7-1	0.8865 0.1888	0.6469 0.3665	0.5936 0.4912	Exponential	Identity	0.5498	0.4727	0.7454	0.1589	1.3418	6.7434
	SG1D+MSC	MLP 5-10-1	0.7855 0.2125	0.7642 0.2478	0.7004 0.2999	Tanh	Tanh	0.7515	0.7168	0.5452	0.1162	2.1160	8.7250
	SG2D+SNV	MLP 5-3-1	0.7477 0.2575	0.7364 0.2322	0.7333 0.2741	Tanh	Identity	0.7397	0.7026	0.6465	0.1378	2.0829	7.4441
	SG2D+MSC	MLP 5-4-1	0.6725 0.2144	0.6938 0.2347	0.6156 0.2777	Exponential	Exponential	0.5332	0.4525	0.6954	0.1483	1.3382	6.6151

Table 99. (*continuing*) Artificial neural network (ANN) models for prediction of number of fungi during the composting process based on the NIR spectra gathered using portable NIR spectrometer (NIR-S-G1, InnoSpectra, Taiwan) (R_{pred}^2=coefficient of determination for prediction; $R_{pred}^2{}_{adj}$=adjusted coefficient of determination for prediction; $RMSEP$=root mean square of prediction; SEP=standard error of prediction; RPD=ratio of prediction to deviation; RER=ratio of the error range). Pretreatment selected as optimal is marked bold

Output variable	NIR spectra pretreatment	Network name	Calibration					Prediction					
			Training perf. Training error	Test perf. Test error	Validation perf. Validation error	Hidden activation	Output activation	R_{pred}^2	$R_{pred}^2{}_{adj}$	RMSEP	SEP	RPD	RER
logCFU$_{fungi}$	raw	MLP 5-4-1	0.6367 0.3616	0.6272 0.3712	0.6062 0.3882	Exponential	Exponential	0.3405	0.2194	0.6805	0.1451	0.9366	4.6591
	smoothing	**MLP 5-9-1**	**0.6112 0.2987**	**0.6035 0.3268**	**0.6009 0.3477**	**Logistic**	**Identity**	**0.7207**	**0.6796**	**0.4449**	**0.0949**	**1.9468**	**9.9802**
	SG1D	MLP 5-11-1	0.8161 0.1899	0.7190 0.2574	0.7063 0.2898	Logistic	Identity	0.5839	0.5139	0.6556	0.1398	1.3500	6.8793
	SG2D	MLP 5-7-1	0.7021 0.2688	0.6941 0.3253	0.6823 0.3869	Exponential	Identity	0.6267	0.5658	0.6913	0.1474	1.4474	6.4227
	SNV	MLP 5-11-1	0.7516 0.1878	0.7345 0.2274	0.7338 0.2873	Exponential	Exponential	0.4761	0.3835	0.5216	0.1112	1.2484	5.8706
	MSC	MLP 5-7-1	0.6999 0.3224	0.6377 0.3541	0.6023 0.3174	Logistic	Tanh	0.6353	0.5762	0.6176	0.1317	1.6073	7.3021
	smoothing+SNV	MLP 5-11-1	0.7421 0.1855	0.7288 0.2125	0.7111 0.2574	Exponential	Exponential	0.7086	0.6649	0.4854	0.1035	1.7601	8.7980
	smoothing+MSC	MLP 5-7-1	0.6533 0.3258	0.6414 0.3745	0.6232 0.3445	Logistic	Tanh	0.5203	0.4370	0.6701	0.1429	1.1888	4.6377
	SG1D+SNV	MLP 5-7-1	0.6355 0.3198	0.6368 0.3874	0.6186 0.4085	Exponential	Identity	0.4948	0.4062	0.2503	0.0534	1.3077	5.5145
	SG1D+MSC	MLP 5-10-1	0.6454 0.3326	0.6179 0.3686	0.6035 0.3748	Tanh	Tanh	0.6329	0.5732	0.4050	0.0863	1.5635	7.6738
	SG2D+SNV	MLP 5-3-1	0.6799 0.3122	0.6722 0.3578	0.6181 0.3587	Tanh	Identity	0.4440	0.2078	0.4402	0.0938	1.9519	7.4285
	SG2D+MSC	MLP 5-4-1	0.6661 0.3131	0.6177 0.3255	0.6083 0.3755	Exponential	Exponential	0.3100	0.2876	0.3194	0.0681	2.6430	7.8100

Table 99. (*continuing*) Artificial neural network (ANN) models for prediction of total number of microorganisms during the composting process based on the NIR spectra gathered using portable NIR spectrometer (NIR-S-G1, InnoSpectra, Taiwan) (R_{pred}^2=coefficient of determination for prediction; $R_{pred}^2{}_{adj}$=adjusted coefficient of determination for prediction; $RMSEP$=root mean square of prediction; SEP=standard error of prediction; RPD=ratio of prediction to deviation; RER=ratio of the error range). Pretreatment selected as optimal is marked bold

Output variable	NIR spectra pretreatment	Network name	Calibration					Prediction					
			Training perf. Training error	Test perf. Test error	Validation perf. Validation error	Hidden activation	Output activation	R_{pred}^2	$R_{pred}^2{}_{adj}$	$RMSEP$	SEP	RPD	RER
logCFU total number of microorganism	raw	MLP 5-4-1	0.7678 0.2987	0.6531 0.3645	0.6187 0.3744	Exponential	Exponential	0.4358	0.3347	1.4697	0.3133	1.2060	4.8803
	smoothing	**MLP 5-9-1**	**0.9156 0.0098**	**0.6803 0.3129**	**0.6681 0.3347**	**Logistic**	**Identity**	**0.7805**	**0.7519**	**0.9640**	**0.2055**	**1.9612**	**9.1320**
	SG1D	MLP 5-11-1	0.7406 0.1988	0.6868 0.2678	0.6796 0.2988	Logistic	Identity	0.6351	0.5760	1.2543	0.2674	1.6101	7.2024
	SG2D	MLP 5-7-1	0.7221 0.2748	0.6955 0.3253	0.6800 0.3869	Exponential	Identity	0.6456	0.5887	1.3352	0.2847	1.6415	6.7378
	SNV	MLP 5-11-1	0.7416 0.1899	0.7445 0.2274	0.7538 0.2873	Exponential	Exponential	0.7377	0.7001	0.8152	0.1738	2.0678	8.7986
	MSC	MLP 5-7-1	0.8797 0.1336	0.8053 0.1654	0.7416 0.2299	Logistic	Tanh	0.6858	0.6374	1.2373	0.2638	1.8112	7.3008
	Smoothing+SNV	MLP 5-11-1	0.7450 0.1855	0.7302 0.2125	0.7246 0.2574	Exponential	Exponential	0.7634	0.7313	1.0318	0.2200	1.7065	8.0133
	Smoothing+MSC	MLP 5-7-1	0.6133 0.3111	0.6206 0.3552	0.6266 0.3445	Logistic	Tanh	0.6171	0.5542	1.0896	0.2323	1.5961	6.0305
	SG1D+SNV	MLP 5-7-1	0.8991 0.0198	0.6785 0.3774	0.5846 0.4985	Exponential	Identity	0.4994	0.4117	0.9161	0.1953	1.2800	6.4782
	SG1D+MSC	MLP 5-10-1	0.8333 0.1223	0.8217 0.1877	0.8176 0.1998	Tanh	Tanh	0.6744	0.6235	0.9367	0.1997	1.7209	7.1614
	SG2D+SNV	MLP 5-3-1	0.9036 0.0098	0.8899 0.1258	0.8017 0.2004	Tanh	Identity	0.7440	0.7078	0.9343	0.1992	2.0817	7.7163
	SG2D+MSC	MLP 5-4-1	0.9886 0.0018	0.8155 0.2141	0.7957 0.2055	Exponential	Exponential	0.4543	0.4202	0.8011	0.1708	2.1447	7.0297

5. DISCUSSION

5.1. Composting processes under different conditions of initial moisture content and air flow rate

In order to investigate the optimal conditions for the initial moisture content of grape skin and the air flow rate for effective composting, nine composting processes under different experimental conditions were carried out in laboratory reactors over the course of 30 days. In this chapter, the changes in the physicochemical properties of compost, the optimization of the composting process, the kinetics of organic matter degradation and microbial growth are discussed. Also, the recorded NIR spectra and developed ANN models for prediction of the composts physicochemical properties based on the NIR spectra will be described.

5.1.1. Physicochemical properties of compost samples and compost extracts during composting

The processes were monitored through important physicochemical variables, such as moisture and dry matter content, organic matter content, ash content, carbon and nitrogen content, C/N ratio, pH, conductivity (S), total dissolved solids (TDS), color change of compost samples and their extracts (ΔE), and microbiological characteristics. The physicochemical variables were monitored every $t = 48$ hours, and the microbiological analysis every $t = 96$ hours. Furthermore, the germination test of the compost was carried out to investigate its maturity. At the end of the processes, the bulk density and porosity of the final composts were determined.

Temperature is considered as a critical variable for the composting process. As explained in the Introduction part, during the composting process, temperature goes through four phases where different communities of microorganisms predominate in each phase. These phases include mesophilic, thermophilic, cooling and maturation phase (Sayara et al., 2020; Waqas et al., 2023). Temperature profiles for the performed composting processes are shown in Figure 13. Only in two composting processes (experiments 3 and 8), the thermophile phase was achieved and the temperature was above $T = 45°C$. In other processes, the temperatures were in the mezophile phase during the 30 days (the temperatures were between $T = 20-34°C$). Similar results were obtained for the composting of grape marc investigated by Paradelo et al. (2013). According to the authors, that does not mean that there was no degradation, because the visual change in the fresh grape skins and composted material was noticed, and also, the other variables can prove the degradation, such as organic matter content and the C/N ratio.

The appearance of grape skin before and after 30 days of composting in laboratory reactors is shown in Figure 14, and there is a visible change, which is also a proof of an effective

composting process. During composting, the substrate gradually turns black due to the degradation of organic matter and the evolution of humic substances (Khan et al., 2009).

The changes in moisture content and dry matter content are shown in Figures 15a and b. Moisture content is an important variable for microbial activity. The initial moisture content of grape skin was between 52.321 ± 0.309 and $64.920 \pm 0.418\%$, which is in accordance with an optimal moisture content for the composting process (Onwosi et al., 2017; Sokač et al., 2022b). During all composting processes, moisture content has increased slightly, and after 30 days, it was between 56.457 ± 0.412 and $70.776 \pm 0.028\%$ due to water release as a result of microbial degradation of organic matter (Azim et al., 2018). Correspondingly, the initial dry matter content was 35.080 ± 0.419 and $47.679 \pm 0.309\%$, and at the end of the processes, it was between 29.226 ± 0.023 and $44.419 \pm 0.237\%$.

Organic matter content and ash content in grape skin were also monitored during the composting process (Figures 15c and d). The initial organic matter content was between 67.964 ± 1.084 and $73.179 \pm 0.576\%$, and at the end of the process, it was between 57.319 ± 0.129 and $67.221 \pm 6.309\%$. Several reactions occur during the composting process, and organic matter is transformed into simpler compounds. Consequently, the organic matter content decreases (Waqas et al., 2018). Also, in the third experiment, which was carried out under an initial moisture content of 65% and an air flow rate of 0.88 L/min and in which the thermophile phase was achieved, the greatest reduction of organic matter was noticed. The initial value was $71.570 \pm 0.219\%$, and at the end of the process, it decreased to $57.319 \pm 0.129\%$. Ash is the inorganic portion of the substrate, comprised of inorganic minerals like magnesium, iron, calcium and sodium, along with other trace metals. In general, organic matter content and ash content are reciprocal, where high organic matter content results in lower ash content (Waqas et al., 2018). The results obtained in this work are in agreement with the literature; the initial grape skin had a higher content of organic matter and lower values of ash content. After 30 days of composting processes, organic matter decreased and the ash content increased.

Carbon is the main constituent of organic waste and in composting processes, it decreases due to the degradation of organic matter and it is lost as carbon dioxide (Onwosi et al., 2017). The carbon content of fresh grape skin was between 47.700 ± 0.004 and $49.600 \pm 0.004\%$, and after the composting process, it decreased to a values between 44.700 ± 0.004 and $48.300 \pm 0.004\%$ (Figure 15e). The initial values of nitrogen content were between 1.270 ± 0.004 and $1.780 \pm 0.004\%$, and a similar values for the grape pomace have been reported by

Perra et al. (2022). At the end of the composting process, the nitrogen content increased to values between 1.570 ± 0.004 and 2.840 ± 0.004%, as shown in Figure 15f, due to the mineralization of organic matter and the production of ammonium and nitrate (Azim et al., 2018).

The C/N ratio is a crucial variable for microbial life, and it is an indicator of the degree of decomposition of organic matter. The initial C/N ratio of grape skin was 27.947 ± 6.210 to 40.074 ± 7.347 (Figure 14g), and similar values for grape pomace were reported by Paradelo et al. (2013). Additionally, the initial values of the C/N ratio were in the optimal range for the composting process, in the range from 25-30:1 (Onwosi et al., 2017; Xie et al., 2023). As shown in Figure 15g, the C/N ratio decreased in all performed experiments, and the final values were between 17.365 ± 2.328 and 27.174 ± 5.729. Although the thermophile phase was not accomplished in most experiments, a significant decrease in the C/N ratio proved that composting processes were successful. Moreover, the greatest drop in the C/N ratio can be noticed in experiment 3, from 40.074 ± 7.347 to 24.673 ± 4.959.

The total color change of compost samples and compost extract samples is shown in Figures 15h and 15l. As shown in Figure 14, there is a significant color change between the compost material at the beginning of the process and after 30 days, confirmed by a notable increase in a total color change (ΔE) . The highest total color change of the compost is observed in reactor 3 (ΔE = 15.302 ± 0.269), and the lowest value is observed in reactor 7 (ΔE = 7.720 ± 1.486). A similar results were reported by Zahrim et al. (2016). A total color change obtained in their work for the tomato residues after 40 days of composting process was ΔE = 15.200.

Furthermore, a significant color change is noticeable between compost extracts at the beginning and end of the process (Figure 14l). The highest total color change of extracts is observed in reactor 6 (ΔE = 5.244 ± 0.045), and the lowest value is observed in reactor 4 (ΔE = 2.347 ± 0.016).

The pH level is an important parameter for the composting process as it affects microbial activity. As explained in the Materials and Methods section, the pH value of fresh grape skin was initially high in an acidic environment, unsuitable for composting. The pH was adjusted with a 10% sodium hydrogencarbonate solution, resulting in values ranging from 5.623 ± 0.006 to 7.683 ± 0.005 (Figure 15i), corresponding to optimal values for the composting process noted by Onwosi et al. (2017) and Azim et al. (2018). pH changes during composting processes were in accordance with the literature: at the beginning of composting, pH decreased due to formic

organic acids (Diaz and Savage, 2007), and as the process progresses, pH started to increase due to the disappearance of easily degradable organic materials and mineralization (Azim et al., 2018). The pH of the final composts ranged from 7.297 ± 0.006 to 9.243 ± 0.021, consistent with literature findings for mature compost (Diaz and Savage, 2007; Hemidat et al., 2018). Finally, before applying the compost to soil, it is important to determine the final pH of the compost (Hemidat et al., 2018).

As shown in Figures 15j and 15k, total dissolved solids and conductivity are two related variables; the greater the concentration of total dissolved solids in compost, the higher the values of conductivity (Hemidat et al., 2018). According to Hemidat et al. (2018), the values of conductivity in compost range from 1 to 10 mS/cm, which corresponds to the results obtained in experiments. During the early stages of the composting process, high microbial activity and the release of mineral salt ions, such as phosphate from the degradation of organic matter, result in an increase in total dissolved solids and conductivity. In the later stages, as temperatures drop, mineral salts are deposited, and microorganisms and ions form stable humus, resulting in a decrease in conductivity (Fan et al., 2023).

Figure 16 presents microbial growth during grape skin composting processes. Bacteria and fungi predominate in all composting processes. Their growth is actually related to the pH value. In the first days of composting, due to the acidic environment, fungi predominate in all reactors. Later, after 10 days of the composting process, when the pH becomes neutral or alkaline, bacteria become predominant. This is in agreement with the literature (Diaz and Savage, 2007).

The changes in germination index are shown in Figure 17. It could be observed that the values of the index increase and decrease during the 30 days of the grape skin composting process, which can be explained by different concentrations of salts and organic acids at different stages of composting (Kong et al., 2022; Wang et al., 2022). At the beginning of the composting process, the germination index ranged from 0 to 56.134%, in accordance with Perra et al. (2022). After 30 days of composting, the germination index ranged from 74.211% to 202.426%. Considering that authors (Hashemi et al., 2019; Gong et al., 2021) reported that a germination index value above 80% indicates compost maturity and non-toxicity for plants, the composts obtained in these experiments are mature. The highest germination index value was achieved in experiment 9 (GI=202.426), which was carried out with an initial moisture content of 57.050% and an air flow rate of 1.060 L/min.

The bulk density is known as the mass of the material in a given volume and affects the mechanical qualities of the material, including strength, porosity, and compaction ease (Agnew and Leonard, 2003). According to Azim et al. (2018) bulk density values for compost often range from 100 to 900 kg/m^3. Higher values imply an increase in mass and a decrease in porosity; conversely, lower values can indicate excessive substrate aeration (Azim et al., 2018). Additionally, Abad et al. (2001) reported that optimal values for compost bulk density should be <400 kg/m^3 to be suitable for use as a growing medium. Figure 18 presents the bulk density and porosity of final composts obtained under different composting conditions. The highest bulk density value was obtained in experiment 9, at 428.804 ± 12.190 kg/m^3, while the lowest values were in experiment 1, with a value of 323.466 ± 0.281 kg/m^3. Comparing the experimental results with the optimal range suggested by Abad et al. (2001), the grape skin composts are suitable for use as a growing medium for plant production. Furthermore, porosity (pore space) depends on the bulk density and moisture content of the samples. Higher values of bulk density result in lower values of porosity (Khater, 2015). The porosity of compost samples ranged from 61.257% to 73.563%, and similar results were obtained by Khater Khater (2015). Additionally, Abad et al. (2001) determined that acceptable porosity of compost substrate should be >85%.

5.1.2. Optimization of the grape skin composting process

In this work, the influence of initial moisture content (X_1) and air flow rate (X_2) on compost organic matter amount at the end of the process (Y) was analyzed. Response surface methodology (RSM) was applied to investigate the effects of independent variables on the responses with the aim of determining optimal conditions for the grape skin composting process.

A second-order polynomial was used to describe the relationship between input variables and the selected output variable. Regression coefficients are shown in Table 11. The obtained results indicate that both variables, initial moisture content (β_1= −8.445) and air flow rate (β_2= −7.466), have a negative effect on compost organic matter amount. This confirms the previously explained higher amounts of moisture content (65-70%), which can result in plugging the pores, impairing oxygen movement, and leading to anaerobic conditions (Diaz and Savage, 2007). On the other hand, higher values of air flow rate can lead to drying of substrate and reducing the microbial activity (Gao et al., 2010; Qasim et al., 2019). Additionally, it is observed from Table 11 that the moisture content and air flow rate interaction (β_{12}= 0.544) have

a positive effect on organic matter amount in compost. Statistical analysis of the model by the F value and analysis of variance showed that the developed model is significant ($p < 0.05$) and can be used for composting process optimization. Also, a lack of fit value showed that model coefficients are significant. The agreement between model experimental data and model predicted data was $R^2 = 0.826$, which indicates the acceptance of the model (Le Man et al., 2010).

Based on the desirability profile derived from the RSM predicted values, composting conditions were optimized. A desirability scale ranging from 0 (undesirable, high organic matter content) to 1 (highly desirable, low organic matter content) was used. The proposed optimal experimental conditions predicted an organic matter content of 65.356% at the end of the composting process (Figure 19). Finally, the optimal conditions obtained using RSM for the grape skin composting process are as follows: initial moisture content of substrate 58.152% and air flow rate of 1.062 L/min.

5.1.3. Kinetics of organic matter degradation and microbial growth

In order to find a useful measure for the loss of organic matter during the composting process, it is necessary to determine the process kinetics using the experimental data obtained under controlled conditions. Organic matter degradation in this work was described by first-order kinetic model.

Table 12 describes the kinetic parameters and the statistical analysis for organic matter degradation. The highest rate of degradation (0.0093 ± 0.0023 1/day) was estimated for experiment 3, followed by experiments 7 and 4. Consequently, in experiment 3, the percentage of degraded organic matter was the highest ($80.401 \pm 2.980\%$). This result can be related to the organic matter content (Figure 14c) for the mentioned experiment, where a significant decrease in organic matter was observed after 30 days of the composting process. In all experiments, the percentage of degraded organic matter was above 70%, confirming the performance of the composting processes.

Due to the significant variability in the composition of composting materials, it is quite difficult to compare the obtained results with available literature. For example, Abu Qdais and Al-Widyan (2016) presented organic matter degradation rates in the range of 0.0015 to 0.0055 % per day in the process of agro-industrial waste, olive milling waste, grain dust, and coffee processing waste mixture composting. Furthermore, Ebrahimzadeh et al. (2017) presented

organic matter degradation rates in the range of 0.011 to 0.013 1/day in the process of kitchen waste, pruned elm tree branches, and sheep manure mixture composting, while Rossetti et al. (2021) presented an organic matter degradation rate of 0.020 1/day in the process of biodegradable polymers composting. According to statistical analysis, the first-order kinetic model is suitable for the description of organic matter degradation (high R^2 and EF, and low RMSE values) during the grape skin composting process and can be used in the analysis of organic matter degradation dynamics.

Table 12 presents the kinetics of microbial growth. Bacterial growth was also described by the first-order model, while fungal growth was described using the logistic model. As can be seen from the table, in experiment 1 the specific bacterial growth rate was the highest (0.019 ± 0.004 1/day), and the lowest was in experiment 8 (0.005 ± 0.001 1/day). Considering the fungal growth, the specific rate was the highest in experiment 6 (0.941 ± 0.018 1/day) and the lowest was in experiment 8 (0.0362 ± 0.005 1/day). Also, the number of bacterial cells was the highest in the experiment 9 (8.593 ± 0.210 logCFU/g_{DM}) and the lowest is in experiment 1 (5.623 ± 0.576 logCFU/g_{DM}).

5.1.4. Basic statistical analysis

The differences in moisture and dry matter content, organic matter content, ash content, carbon and nitrogen content, C/N ratio, pH, TDS, and conductivity between experiments at the beginning (0. day) and end (30. day) of the composting process were statistically analyzed, and the results are shown in Table 13.

It can be observed that there is a significant difference in moisture and dry matter content between experiments 1, 2 and 6 at the beginning and end of the process. Moreover, there is no significant difference in organic matter content and ash content between experiments at the beginning of the process, but significant differences in these variables were observed in experiments 3, 5 and 7 after 30 days of the composting process. Regarding carbon and nitrogen content and C/N ratio, there is no significant difference between experiments at the beginning and end of the process. However, a significant difference in C/N ratio was observed in experiments 3, 4 and 5 at the beginning of the composting process, and in reactor 7 at the end of the process. The pH, TDS, and conductivity values are statistically different between experiments at both the beginning and end of the composting process.

5.1.5. Multivariate analysis

5.1.5.1. Principal Component Analysis (PCA)

The relationship between process variables (initial moisture content, air flow rate and sampling day) and the analyzed physicochemical properties of compost samples (moisture and dry matter content, organic matter and ash content, carbon and nitrogen content, C/N ratio, total color change of compost samples, pH, TDS, conductivity, and total color change of compost extracts) was estimated using the principal component analysis (PCA) and the score plot and loading plot are shown in Figure 19.

The score plot of the principal component analysis (PCA) is shown in Figure 20a. PCA revealed that the five groups were clustered separately based on the total dissolved solids (TDS), with 60.730% of the data variability (PC 1 = 44.180% and PC 2 = 16.550%). The loading plot of principal component analysis (PCA) is shown in Figure 20b, and the relationship between initial moisture content, air flow rate, sampling day and physicochemical properties of compost was investigated. As shown in the figure 20b, the air flow rate, sampling day and initial moisture content were negatively correlated to ash and nitrogen content. Also, the sampling day was positively correlated with organic matter and carbon content. The initial moisture content was positively correlated with C/N ratio, and it was negatively correlated to pH, total dissolved solids, total color change of compost and total color change of extract.

5.1.5.2. Multiple linear regression (MLR) models for the prediction of physicochemical properties of compost

Multiple linear regression models were developed for predicting the physicochemical properties of grape skin compost and compost extracts. In Table 14, the equations with coefficients of multiple linear regression models are presented. The results show that initial moisture content (X_1), air flow rate (X_2) and sampling day (X_3) have a significant influence ($p < 0.05$) on all 12 physicochemical variables (moisture and dry matter content, organic matter and ash content, carbon and nitrogen content, C/N ratio, total color change of compost samples and compost extracts, pH, total dissolved solids and conductivity).

The relationship between experimental data and model-predicted data was estimated based on the determination coefficient (R^2), the ratio of prediction to deviation (*RPD*), and the ratio of the error range (*RER*). According to Henseler et al. (2009), R^2 value of 0.75 is considered acceptable, R^2 value of 0.50 is considered moderate, and R^2 value of 0.26 is

considered weak. Furthermore, the models with *RPD* < 1.4 are considered non- reliable; those with an *RPD* 1.4 - 2 are considered fair; and those with *RPD* > 2 are described as excellent models (Chang et al., 2001). Considering the *RER*, models with the values *RER* > 4 are acceptable for data screening, models with *RER* > 10 can be used for quality control, and models with *RER* > 15 can be used for quantification (Sim et al., 2023).

The comparison between experimental data and MLR models predicted data on physicochemical properties are shown in Figure 21. The best agreement between experimental data and MLR models predicted data was obtained for moisture content (Figure 21a) and dry matter content (Figure 21b) (R_{cal}^2 =0.779, R_{cal}^2 $_{adj}$= 0.777, *RMSE*=2.772, R_{pred}^2 = 0.738, R_{pred}^2 $_{adj}$= 0.738, *RMSEP*=2.781%, *SEP*=0.245, *RPD*=1.948, and *RER*=7.274) followed by organic matter (Figure 21c) (R_{cal}^2 = 0.489, R_{cal}^2 $_{adj}$= 0.484, *RMSE*=4.473, R_{pred}^2 = 0.422, R_{pred}^2 $_{adj}$= 0.408, *RMSEP*=4.735%, *SEP*=0.417, *RPD*=1.314, and *RER*=5.883) and ash content (Figure 21d) (R_{cal}^2 = 0.489, R_{cal}^2 $_{adj}$= 0.484, *RMSE*=4.473, R_{pred}^2 = 0.428, R_{pred}^2 $_{adj}$= 0.415, *RMSEP*=4.648%, *SEP*=0.409, *RPD*=1.321, and *RER*=5.991). The highest scatter between experimental data and model predicted data can be noticed for nitrogen content (Figure 21f) (R_{cal}^2 = 0.158, R_{cal}^2 $_{adj}$= 0.149, *RMSE*=0.424, R_{pred}^2 = 0.123, $R_{pred}^2$$_{adj}$= 0.102, *RMSEP*=0.583%, *SEP*=0.051, *RPD*=0.806, and *RER*=3.789).

Considering the obtained results, it can be concluded that multiple linear regression models developed for the prediction of physicochemical properties of compost samples can be applicable just for the prediction of moisture and dry matter content (R_{cal}^2 > 0.75). Furthermore, due to R_{cal}^2 < 0.75 for the developed models for the other physicochemical properties, these models are not applicable for the prediction.

5.1.5.3. Piecewise linear regression (PLR) models for the prediction of physicochemical properties of compost

The piecewise linear regression models were developed for predicting the physicochemical properties of grape skin compost and compost extracts. In Table 15, the equations with coefficients of piecewise linear regression models are presented. This also indicates that initial moisture content (X_1), air flow rate (X_2), and sampling day (X_3) have a significant influence (p < 0.05) on the 12 physicochemical variables (moisture and dry matter content, organic matter and ash content, carbon and nitrogen content, C/N ratio, total color

change of compost samples and compost extract samples, pH, total dissolved solids, and conductivity).

The comparison between experimental data and PLR model predicted data on physicochemical properties is shown in Figure 22. The best agreement between experimental data and PLR models predicted data was obtained for moisture content (Figure 22a) and dry matter content (Figure 22b) (R_{cal}^2 =0.837, $R_{cal}^2{}_{adj}$= 0.835, *RMSE*=2.501, R_{pred}^2 = 0.834, $R_{pred}^2{}_{adj}$= 0.831, *RMSEP*=2.144%, *SEP*=0.189, *RPD*=2.526, and *RER*=9.433) followed by total color change of compost (Figure 22h) (R_{cal}^2 = 0.781, $R_{cal}^2{}_{adj}$= 0.779, *RMSE*=1.764, R_{pred}^2 = 0.777, $R_{pred}^2{}_{adj}$= 0.772, *RMSEP*=1.925%, *SEP*=0.169, *RPD*=2.159, and *RER*=8.802) and pH (Figure 22j) (R_{cal}^2=0.784, $R_{cal}^2{}_{adj}$=0.782, *RMSE*=0.548, R_{pred}^2=0.766, $R_{pred}^2{}_{adj}$= 0.745, *RMSEP*=0.692%, *SEP*=0.043, *RPD*=2.116, and *RER*=8.611). The highest scatter between experimental data and model predicted data can be noticed for carbon content (Figure 22e) (R_{cal}^2 = 0.644, $R_{cal}^2{}_{adj}$= 0.641, *RMSE*=0.868, R_{pred}^2 = 0.638, $R_{pred}^2{}_{adj}$= 0.636, *RMSEP*=0.890%, *SEP*=0.078, *RPD*=1.709, and *RER*=7.213).

Furthermore, the results obtained by the developed piecewise linear regression (PLR) models for the prediction of the physicochemical properties of compost samples and compost extracts show better accuracy than the multiple linear regression (MLR) models. In other words, the PLR models described the experimental data with higher precision compared to MLR models (for all PLR models, the R_{pred}^2 value is greater than 0.63).

5.1.5.4. Artificial neural network (ANN) models for the prediction of physicochemical properties of compost

The multilayer perceptron (MLP) neural network were developed to improve the prediction of the physicochemical properties of grape skin compost during the composting process. ANN models were developed individually for each of the selected physicochemical properties of compost (moisture and dry matter content, organic matter and ash content, carbon and nitrogen content, C/N ratio, total color change of compost samples and compost extract samples, pH, total dissolved solids, and conductivity), and the results are shown in Table 16 and in Figure 23. ANN modelling ensures better description of experimental data because of the nonlinear functions that are included in the model structure.

The ANN model for the prediction of moisture content shows the best agreement with the experimental data (Figure 23a) (R_{pred}^2 = 0.905, $R_{pred}^2{}_{adj}$= 0.902, *RMSEP*=1.707%,

SEP=0.150, *RPD*=3.172 and *RER*=11.845). The ANN model developed for the prediction of moisture content is MLP 3-6-1, characterized by 3 neurons in the input layer, 6 in the hidden and 1 in the output layer. For hidden activation, the model uses a Tanh function, and for output activation, the model uses an Logistic function (Table 16). The highest scatter between experimental data and model predicted data can be noticed for the C/N ratio (Figure 23g) (R_{pred}^2 = 0.654, $R_{pred}^2{}_{adj}$= 0.648, *RMSEP*=3.609%, *SEP*=0.317, *RPD*=1.989 and *RER*=8.539). The ANN model developed for the prediction of the C/N ratio is MLP 3-10-1, characterized by 3 neurons in the input layer, 10 in the hidden and 1 in the output layer. For hidden activation, the model uses a Tanh function, and for output activation, the model uses an Exponential function.

Considering the R_{pred}^2, only the ANN models for the prediction of moisture content, dry matter content, organic matter content, pH and conductivity (*S*) can be considered acceptable (R_{pred}^2 > 0.75), and the other models are considered as moderate (R_{pred}^2 > 0.65) (Henseler et al., 2009). Taking into account the RPD value, the ANN models for the prediction of moisture and dry matter content, organic matter content, and pH are described as excellent models due to *RPD* > 2. The other ANN models are considered as fair models (1.4 > *RPD* < 2) (Chang et al., 2001).

Hosseinzadeh et al. (2020) also compared the multiple linear regression (MLR) and artificial neural network (ANN) models for the prediction of total nitrogen and total phosphorus from solid waste under different vermicompost treatment. The MLR and ANN models were developed and they were compared by statistical analysis including coefficient of determination (R^2) and root mean square error (*RMSE*). Finally, the developed ANN models provided better prediction for the total nitrogen (R^2=0.998 and *RMSE*=0.013) and total phosphorus (R^2=0.991 and *RMSE*=4.300) comparing to MLR models (the R^2=0.834 and *RMSE*=0.092 were obtained for the prediction of total nitrogen; and R^2=0.729 and *RMSE*=71.490 were obtained for total phosphorus).

The comparison of multiple linear regression (MLR) and artificial neural network (ANN) models was reported by Yildiz and Degirmenci (2015). They investigated the possible use of mentioned models for the oxygen estimation during the windrow composting in three different processes. In general, the correlation values for the developed ANN models were higher (R^2 was between 0.650-0.980) than the ones obtained using the MLR models (R^2 was between 0.330-0.780).

5.1.6. Near-infrared (NIR) spectra of compost samples and compost extract samples

During the composting processes, the NIR spectra were recorded for all compost samples and compost extract samples with different NIR instruments: NIR spectrometer (NIR-128-1.7-USB/6.25/50 μm, Control Development Inc., USA) which records the absorbance in wavelength range from λ = 904 - 1699 nm for and NIR spectrometer (AvaSpec-NIR256-2.5-HSC-EVO, Avantes, USA) which records the absorbance in wavelength range from λ = 1000 - 2500 nm. The different NIR instruments were used due to recording of the NIR spectra in different wavelength ranges and in order to investigate which spectrometer is reliable for the monitoring of the composting processes.

Figure 24 presents the average NIR spectra for compost samples and compost extract samples recorded with the NIR spectrometer NIR-128-1.7-USB/6.25/50 μm. As it can be seen on Figure 24a, the spectra of compost samples for all reactors have the same trend, and the differences between spectra are in the range of wavelength 1350–1550 nm, which indicate O–H bonds, or, in other words, the differences in this spectral range can be correlated with water content in the samples (Valinger et al., 2018). Furthermore, the NIR spectra of compost extract samples (Figure 24b) for all reactors also have the same trend, and the differences can be noticed in a wavelength range of 904–930 and 1350–1699, which indicate changes in the second and third overtone C–H and O–H bonds (Badr Eldin, 2011).

Figure 25 presents the average NIR spectra for compost samples and compost extract samples recorded with the NIR spectrometer AvaSpec-NIR256-2.5-HSC-EVO. The NIR spectra were recorded in a range of wavelengths of 990–2500 nm, and the noises can be observed at wavelengths of 990–2400 nm. The noise represents random fluctuations around the signal that can originate from the instrument or environmental laboratory conditions (Henríquez and Ruz, 2019). From the spectra gathered for compost samples (Figure 25a), it can be noticed that there are two maximums: the first one is between 1350 and 1600 nm, which corresponds to the second overtone H_2O, C–H, and CH_2 bonds, and the second one is between 1900 and 2200 nm, which corresponds to the first overtone H_2O, C–H, and CH_2 bonds (Badr Eldin, 2011). Figure 25b shows the NIR spectra for compost extract samples during the composting processes. It can be noticed that the differences between the obtained spectra are in a range from 1350–1600 nm and from 1800–2100 nm, which correspond to the already mentioned overtones. The NIR spectra of compost extract samples also have noise, and it can be related to a NIR instrument that is more sensitive.

5.1.7. Principal component analysis (PCA) of the preprocessing methods for recorded NIR spectra of compost samples and compost extracts

The preprocessing methods were applied for the NIR spectra of compost samples and compost extracts recorded with the NIR spectrometers NIR-128-1.7-USB/6.25/50 μm and AvaSpec-NIR256-2.5-HSC-EVO. Then the principal component analysis (PCA) was applied and the results are shown in Figures 26-29.

Figure 26 shows the PCA analysis of preprocessed methods of the NIR spectra recorded with the NIR spectrometer NIR-128-1.7-USB/6.25/50 μm for the compost samples, and Figure 27 shows the results for the compost extract samples. Considering the results for compost samples, the PCA analysis for the smoothing as the preprocessing method resulted in the best discrimination of samples (which explained 97.420% of the total variance of the data) (Figure 26b), followed by SG2D+MSC (the second-order Savitzky-Golay derivative followed by multiplicative scatter corrections) (which explained 83.340% of the total variance of the data) (Figure 26l). The highest dissipation can be noticed for the preprocessing method SG2D+SNV (second-order Savitzky-Golay derivative followed by a standard normal variate) (which explained 51.840% of the total variance of the data) (Figure 26k).

Considering the NIR spectra of compost extract samples (Figure 27), the preprocessing method in PCA analysis that resulted in the best discrimination of samples was also smoothing (which explained 95.070% of the total variance of the data) (Figure 27b), followed by MSC (multiplicative scatter corrections) (Figure 27f) and smoothing+MSC (smoothing followed by multiplicative scatter corrections) (Figure 27h) (which explained more than 75% of the total variance of the data). The highest dissipation can be noticed for the preprocessing method SG2D (second-order Savitzky-Golay derivative), with 33.410% of the variability of the data. Also, from Figures 26 and 27 can be noticed that the data was overlapping which indicates the similarities between the samples.

Figure 28 shows the PCA analysis of the NIR spectra recorded with the NIR spectrometer AvaSpec-NIR256-2.5-HSC-EVO for the compost samples, and Figure 29 shows the PCA analysis of the NIR spectra recorded with the same instrument for the compost extract samples. Considering the compost samples (Figure 28), the PCA analysis for the smoothing as the preprocessing method resulted in the best discrimination of samples (which explained 97% of the total variance of the data) (Figure 28b), followed by SG1D (the first-order Savitzky-Golay derivative) (which explained 92% of the total variance of the data) (Figure 28c). The

highest dissipation can be noticed for the preprocessing methods SG2D+SNV (second-order Savitzky-Golay derivative followed by standard normal variate) and SG2D+MSC (second-order Savitzky-Golay derivative followed by multiplicative scatter corrections) (explaining 74% of the total variance of the data) (Figures 28k and l). Considering the results for compost extract samples (Figure 29), the PCA analysis for the smoothing as the preprocessing method resulted in the best discrimination of samples (which explained 97% of the total variance of the data) (Figure 29b), followed by SG1D (the first-order Savitzky-Golay derivative) (which explained 90% of the total variance of the data) (Figure 29c). The highest dissipation can be noticed for the preprocessing method SNV (standard normal variate), with 55% of the variability of the dana (Figure 29e).

5.1.8. Artificial neural network (ANN) models based on the NIR spectra for the prediction of physicochemical properties of compost during the composting process

During the composting processes, the NIR spectra were recorded with different NIR instruments. Then, the different preprocessing methods for NIR spectra were applied, and the principal component analysis (PCA) was applied. Finally, based on obtained PCA factors, the artificial neural network (ANN) models for the prediction of the physicochemical properties of compost during the composting process were developed. The ANN models are shown in Tables 17–42.

The ANN models based on NIR spectra obtained using the NIR spectrometer NIR-128-1.7-USB/6.25/50 μm were developed for each property of the compost samples and compost extracts. The results are shown in Tables 17–29, and the models with the highest values of *RER* are marked in bold. Models with the values *RER* > 4 are acceptable for data screening; models with *RER* > 10 can be used for quality control; and models with *RER* > 15 can be used for quantification (Sim et al., 2023).

As the acceptable pretreatment method of NIR spectra was SNV (standard normal variate), the developed ANN model for the prediction of the day of composting resulted in the highest *RER* value, 4.181. This model is acceptable for data screening. Considering the moisture and dry matter content, organic matter and ash content, and carbon content, the smoothing as a pretreatment method and the developed ANN models resulted in the greatest *RER* values: 44.955, 62.681, 25.333, 28.079, and 5.100, respectively. According to the literature, all models can be used for quantification, except the model for the prediction of carbon content, which is acceptable for data screening.

Furthermore, for the nitrogen content, C/N ratio, and total color change of compost extracts, the smoothing+SNV (smoothing followed by standard normal variate) as a pretreatment method and the developed ANN models resulted in the greatest *RER* values of 10.499, 9.127, and 5.183, and the models can be used for quality control. Next, for the total color change of the compost, the pretreatment method SG2D+MSC (second-order Savitzky-Golay derivative followed by multiplicative scatter corrections) and the developed ANN model for the prediction resulted in an *RER* of 4.834, indicating the model is acceptable for data screening. For pH and TDS, the SNV (standard normal variate) and the developed ANN model resulted in *RER*s of 4.781 and 8.152. Considering the conductivity, the MSC (multiplicative scatter corrections) and the developed model for the prediction of that property resulted in *RER* 5.539. The developed models for pH, TDS, and conductivity are acceptable for data screening.

The ANN models based on NIR spectra obtained using the NIR spectrometer AvaSpec-NIR256-2.5-HSC-EVO were developed for each property of the compost samples and compost extracts. The results are shown in Tables 30-42.

Considering the day of composting, nitrogen content, C/N ratio, and total color change of compost samples, the acceptable pretreatment method was estimated to be SG1D (first-order Savitzky-Golay derivative). The developed ANN models for the prediction of the day of composting, nitrogen content, C/N ratio, and total color change of compost samples resulted in the greatest *RER* values compared to the other pretreatment methods (6.489, 5.194, 6.700, and 5.791). The models are acceptable for data screening. Taking into account moisture content, dry matter content, organic matter and ash content, and organic carbon content, the acceptable pretreatment method SG2D+MSC (second-order Savitzky-Golay derivative followed by multiplicative scatter corrections) and the developed ANN models resulted in an *RER* value of 5.102. For the pH and TDS, the acceptable pretreatment of NIR spectra is SNV (standard normal variate), and the ANN models resulted in *RER* values of 4.686 and 10.598, which means that the model for the prediction of pH is acceptable for data screening, and the model for TDS prediction can be used for quality control. Then, the acceptable pretreatment method of NIR spectra for conductivity was obtained using MSC (multiplicative scatter corrections), and the ANN model for the prediction of conductivity resulted in *RER* 5.816, which means that the model is acceptable for data screening. And the last property is the total color change of the compost extracts. The acceptable pretreatment method was estimated smoothing+SNV (smoothing followed by standard normal variate), and the developed ANN model for the prediction of total color change of the compost extracts resulted in an *RER* value of 5.597.

Lillhonga et al. (2009) also investigated the application of NIR spectroscopy for the monitoring of the composting process. The substrate for composting consisted of food waste, fox manure and yard waste, and the process was carried out in laboratory reactors. The main variables were monitored, and the NIR spectra of samples were recorded. Than, based on the NIR spectra the partial least squares (PLS) regression models were developed and the models resulted with high coefficient of determination for pH, temperature, ammonia concentracion, moisture content and time of composting (the coefficients were from 0.91 to 0.95).

5.1.9. Artificial neural network (ANN) models based on the NIR spectra for the prediction of microbiological properties of compost during the composting process

The ANN models for the prediction of microbiological properties of compost samples during the composting process based on NIR spectra recorded using NIR spectrometer NIR-128-1.7-USB/6.25/50 μm were shown in Tables 43-45. Considering the prediction of number of bacteria, as the acceptable preprocessing method of NIR spectra was smoothing and for the developed ANN model was noticed the highest *RER* value (10.083). Otherwise, taking into account the results for number of fungi and total number of microorganisms, the preprocessing method SG2D+MSC (second-order Savitzky-Golay derivative followed by multiplicative scatter corrections) and the developed ANN model resulted with the highest *RER* values 15.075 and 12.040, respectively.

The similar results were obtained for the preprocessing methods and developed models based on the NIR spectra obtained using the NIR spectrometer AvaSpec-NIR256-2.5-HSC-EVO (Tables 46-48). Considering the prediction of number of bacteria, as the acceptable preprocessing method of NIR spectra was also smoothing and for the developed ANN model was noticed the highest *RER* value (10.083). Furthermore, taking into account the number of fungi, the acceptable preprocessing method was SG2D+SNV (second-order Savitzky-Golay derivative followed by standard normal variate) (*RER* value was 13.292), and the total number of microorganisms resulted with preprocessing method SG2D+MSC (second-order Savitzky-Golay derivative followed by multiplicative scatter corrections) and the developed ANN model resulted with the highest *RER* value 12.040. The obtained *RER* values for the developed ANN models were above 10 which indicates that the models can be used for quality control (Sim et al., 2023)

5.2. Extraction of bioactive molecules from grape skin

In this work, the classical solid-liquid extraction of bioactive molecules from grape skin was performed. Polyphenols are among the biological components in which there is great interest due to their numerous positive and beneficial effects, such as antioxidant, anti-inflammatory, and antibacterial effects. Water was used as the extraction solvent. To ensure optimal conditions for carrying out the extraction procedure, 30 experiments were conducted under different conditions (Table 10). After obtaining the optimal extraction conditions, the bioactive molecules from grape skin were extracted, and the obtained grape skin was used for the composting process in order to compare the efficiency of the composting of grape skin and pretreated (extracted) grape skin.

5.2.1. Physicochemical properties of aqueous grape skin extracts

The physicochemical properties of the prepared grape skin extracts were analyzed, and the results are presented in Tables 49 and 50. As presented in Table 49, it can be seen that the lowest pH (3.690 ± 0.010) occurred in experiment number 26 ($t = 75$ min, $T = 80$ °C, $S/L = 20$ g/L, *rpm* = 750 1/min), and the highest (4.070 ± 0.010) occurred in experiment number 14 ($t = 75$ min, $T = 40$ °C, $S/L = 10$ g/L, *rpm* = 500 1/min). In general, the pH of the extracts did not differ significantly under the various extraction conditions. Similar grape skin pH values, ranging from 3.3 to 3.54, were presented in the work of Yeler and Nas (2021). The lowest values for conductivity and TDS (162.000 ± 1.000 µS/cm and 81.270 ± 0.930 mg/L) can be noticed in experiment 19 ($t = 60$ min, $T = 60$°C, $S/L = 10$ g/L, *rpm* = 500 1/min), and the highest values (379.670 ± 3.210 µS/cm and 191.400 ± 0.260 mg/L) can be noticed in experiment 8 ($t = 75$ min, $T = 60$°C, $S/L = 30$ g/L, *rpm* = 750 1/min); it can be concluded that increases in the solid–liquid ratio and mixing speed contribute to an increase in the percentage of TDS. Moreover, the lowest extraction efficiency (0.135 ± 0.030%) was obtained under the conditions of experiment 5 ($t = 75$ min, $T = 60$°C, $S/L = 10$ g/L, *rpm* = 250 1/min), and the highest extraction efficiency (0.451 ± 0.010%) was obtained under the conditions of experiment 17 ($t = 75$ min, $T = 80$°C, $S/L = 30$ g/L, *rpm* = 500 1/min), again indicating that increases in the solid–liquid ratio and mixing speed contribute to an increase in the extraction efficiency.

The extraction conditions have an influence on the color of the grape skin extracts. The chroma value refers to the vividness or dullness of color; the greater the chroma, the more vivid the color (Hernández et al., 2016). The hue angle correlates with color description and ranges from 0 to 360°, where 0° (or 360°) represents maximum redness, 90° maximum yellowness,

180° maximum greenness, and 270° maximum blueness (Scalisi et al., 2022). The chroma and hue values obtained for extracts under different extraction conditions are presented in Table 50. The lowest chroma value (0.600 ± 0.010) can be noticed in experiment 3 (t = 60 min, T = 80°C, S/L = 20 g/L, *rpm* = 500 1/min) and the highest (1.270 ± 0.010) in the experiment 17 (t = 75 min, T = 80°C, S/L = 30 g/L, *rpm* = 500 1/min). Considering the results, extraction time and solid-liquid ratio significantly affect on the color of the grape skin extract. The hue angle for grape skin extracts is in the range of 77.320 ± 0.700 (experiment 3) to 142.590 ± 0.500 (experiment 25), which corresponds to a yellow-green color.

The total amount of polyphenols and the antioxidant activity using the DPPH and the FRAP method of grape skin extracts were analysed. Table 50 shows that the highest amount of polyphenols (8.240 ± 0.210 mg_{GAE}/g_{DM}) was extracted under the conditions of experiment 17 (t = 75 min, T = 80°C, S/L = 30 g/L, *rpm* = 500 1/min), in which the mass fraction of dry matter was the highest. In contrast, under the conditions of experiment 14 (t = 75 min, T = 40°C, S/L = 10 g/L, *rpm* = 500 1/min), the amount of extracted polyphenols was 7.6 times lower (1.090 ± 0.040 mg_{GAE}/g_{DM}). The above experimental conditions differed in temperature and solid–liquid ratio, and the results show that increasing the temperature and solid–liquid ratio has a positive effect on the concentration of extracted polyphenols (Librán et al., 2013). The extracted polyphenol concentrations obtained in performed experiments were consistent with those found in the available literature. Librán et al. (2013) reported an extraction efficiency of 5 mg_{GAE}/g_{DM} from white grape skins, and Gerardi et al. (2020) reported a polyphenol extraction efficiency of 1.2–3.07 mg_{GAE}/g_{DM}. However, it is worth mentioning that in all the above experiments from the literature, ethanol was used as the extracting solvent. Following the principles of green extraction, in this research the water was used as the extraction solvent (Valinger et al., 2022). The lowest antioxidant activity obtained using the DPPH method (only 0.0003 ± 0.000 $mmol_{TROLOX}/g_{DM}$) came from extracts prepared according to the conditions of experiment 19 (t = 60 min, T = 60°C, S/L = 10 g/L, *rpm* = 500 1/min). Significantly higher DPPH value (0.030 ± 0.001 $mmol_{TROLOX}/g_{DM}$) was obtained in experiment 17 (t = 75 min, T = 80°C, S/L = 30 g/L , *rpm* = 500 1/min). The highest value (0.048 ± 0.001 $mmol_{FeSO4·7H2O}/g_{DM}$) for antioxidant activity determined by FRAP method was obtained in experiment 17, but the lowest (0.003 ± 0.000 $mmol_{FeSO4·7H2O}/g_{DM}$), in contrast to the DPPH method, were observed under the conditions of experiment 14 (t = 75 min, T = 40°C, S/L = 10 g/L, *rpm* = 500 1/min). Finally, the total polyphenol content and antioxidant activity determined by DPPH and FRAP method are

related, which is also obtained in this results (the highest values were obtained in experiment 17). A similar results were reported by Balík et al. (2008).

5.2.2. Principal component analysis (PCA) and optimization of extraction conditions of bioactive molecules from grape skin

The score plot of the principal component analysis (PCA) is shown in Figure 30a. PCA revealed that the three groups were clustered separately based on the extraction temperature with 71.31% of the data variability (PC 1 = 41.130% and PC 2 = 30.180%). The loading plot (Figure 30b) shows the relationship between extraction conditions (extraction time, temperature, solid-liquid ratio and mixing speed) and the physicochemical properties (pH, conductivity, total dissolved solids, extraction yield, Chroma and Hue, total polyphenol content, antioxidant activity determined by DPPH and FRAP method) of grape skin aqueous extracts.

As shown in Figure 30b, there are no significant positive correlations for pH, but the solid-liquid ratio has the greatest negative effect, followed by mixing rate and extraction time. Conductivity and total dissolved solids are positively correlated with temperature, solid-liquid ratio, and mixing speed. In other words, the increase of temperature, solid-liquid ratio and mixing speed will lead to an increase of total dissolved solids and conductivity. Also, it can be noticed that conductivity and total dissolved solids decrease with pH increases. The color variable, chroma, is positively correlated with temperature and solid-liquid ratio, but hue angle is negatively correlated with temperature, mixing speed, extraction time, and solid-liquid ratio. The amount of extracted polyphenol compounds has positive correlations with temperature, extraction time, mixing rate, and solid-liquid ratio (the increase of mentioned variables leads to an increase in extracted polyphenol content). Furthermore, the antioxidant activity measured by the DPPH and the FRAP method has positive correlations with most of the parameters, such as temperature, total dissolved solids, conductivity, temperature, solid-liquid ratio, chroma value, and total polyphenol content. But, in these two methods, there is only a difference in the correlation with mixing speed; there is no significant effect of mixing speed on antioxidant activity determined by the DPPH method, but there is a positive correlation between mixing speed and antioxidant activity determined by the FRAP method.

The aim of using the response surface methodology was to determine the optimal conditions for the solid-liquid extraction of bioactive compounds from white grape skin. The influences of four variables (extraction time (X_1), extraction temperature (X_2), solid-liquid ratio (X_3) and mixing speed (X_4)) on the chemical characteristics (TPC, DPPH, and FRAP) were analyzed. In Table 51, the regression coefficients and analysis of variance for the response

surface models used for TPC, DPPH, and FRAP are presented, and significant coefficients are marked in bold ($p < 0.05$). It can be noticed from Table 51 that all extraction variables and their interactions have an effect on the TPC and antioxidant activity determined by the DPPH and FRAP methods. For the proposed models, high agreement was obtained between predicted and experimental values (R^2 (TPC) =0.801, R^2_{adj}=0.761; R^2 (DPPH)=0.747, R^2_{adj}=0.700 and R^2 (FRAP)=0.950, R^2_{adj}=941). According to Le Man et al. (2010), the model can be applicable if the coefficient of determination exceeds 0.75.

Figure 31 presents the response surfaces of the significant extraction variables, extraction time and solid-liquid ratio, affecting TPC, DPPH, and FRAP. The increase in solid-liquid ratio will result in higher values of TPC, DPPH, and FRAP. Otherwise, the extraction time can have a negative effect on the TPC, DPPH, and FRAP. Prolonging the extraction time could lead to more oxygen exposure and thus increase the chances of oxidation of polyphenolic compounds (Ahmed et al., 2020). In order to obtain a detail understanding of the extraction mechanism, an analysis of the extraction kinetics should be performed via a dynamic experiment.

Based on the desirability profile derived from the RSM predicted values, the extraction conditions were optimized (Figure 32). The optimal conditions obtained using the RSM for the extraction of bioactive molecules from grape skin are as follows: extraction time $t = 67.5$ min; temperature $T = 80$ °C; solid-liquid ratio $S/L = 30$ g/L; and mixing rate $rpm = 750$ 1/min (Figure 32). According to the developed model under specified conditions, extraction ensures the values as follows: TPC=8.2550 mg_{GAE}/g_{DM}, DPPH=0.03232 $mmol_{TROLOX}/g_{DM}$ and FRAP=0.0598 $mmol_{FeSO4 \cdot 7H2O}/g_{DM}$.

5.3. The effect of different pretreatments of grape skin on the efficiency of the composting process

In this research, the effect of different pretreatments on grape skin was investigated. The experiments were as follows: a grape skin without pretreatment; a ground grape skin without pretreatment; a grape skin pretreated to extract bioactive molecules at $T = 40°C$ during $t = 90$ minutes; a ground grape skin pretreated to extract bioactive molecules at $T = 40°C$ during $t = 90$ minutes; and the mixture of grape skin consisted of: grape skin without pretreatment ($w/w = 43.930\%$), ground grape skin without pretreatment ($w/w = 8.110\%$), grape skin pretreated to extract bioactive molecules at $T = 40°C$ during the $t = 90$ minutes ($w/w = 14.250\%$) and ground grape skin pretreated to extract bioactive molecules at $T = 40°C$ during the $t = 90$ minutes ($w/w = 33.660\%$). The processes were monitored during the 30 days through important variables, and the obtained results are presented in this chapter. The kinetics of organic matter degradation and microbial growth are described, and the recorded NIR spectra of compost samples and compost extracts are shown, as well as the developed artificial neural network models for the prediction of physicochemical properties of compost during the composting process.

5.3.1. Physicochemical and microbiological properties of compost samples and their extracts during composting processes

The processes were monitored through important physicochemical variables, such as moisture and dry matter content, organic matter content, ash content, carbon and nitrogen content, C/N ratio, pH, conductivity, total dissolved solids, color change of compost samples and their extracts, and microbiological characteristics. The physicochemical variables were monitored every $t = 48$ hours, and the microbiological analysis every $t = 96$ hours. Furthermore, compost germination test was carried out to investigate its maturity. At the end of the processes, the bulk density and porosity of the final composts were determined.

The results obtained in this set of composting experiments had almost the same trend as the results obtained in the previous composting processes, where the effects of initial moisture content of grape skin and air flow rate were investigated.

Temperature changes for the performed composting processes are shown in Figure 33, and in all performed processes, the temperatures were in the mezophile phase during the 30 days of composting (the temperature did not exceed 45°C). Moreover, that does not mean that there was no degradation (Paradelo et al., 2013). There are other variables that can prove the

degradation during the process, such as organic matter content and the C/N ratio, as well as the visual appearance. The differences between fresh grape skin and compost obtained after 30 days of composting processes are shown in Figure 34.

The changes in moisture content and dry matter content are shown in Figures 35a and b. The moisture content is an important variable for microbial activity. The initial moisture content of grape skin was in a range between $63.186 \pm 1.963\%$ and $69.606 \pm 1.205\%$. During all composting processes, moisture content had increased slightly, and after 30 days, it was between $66.245 \pm 9.171\%$ and $70.774 \pm 1.914\%$ due to water release as a result of microbial degradation (Azim et al., 2018). The initial dry matter content was between $30.394 \pm 1.205\%$ and $36.814 \pm 1.963\%$, and at the end of the process, it was between 28.697 ± 1.344 and $33.754 \pm 9.171\%$.

Organic matter content and ash content in grape skin were monitored during 30 days of the composting processes (Figures 35c and d). The initial organic matter content was in a range from 74.996 ± 0.043 to $91.790 \pm 0.340\%$, and at the end of the process, it was between 65.042 ± 1.415 and $93.765 \pm 0.162\%$. As mentioned before, the organic matter content and the ash content are reciprocal, where high organic matter content results in lower ash content (Waqas et al., 2018). After 30 days of composting processes, organic matter decreased and the ash content increased, which is in accordance with the literature.

Furthermore, the carbon content of fresh grape skin was in the range from 43.498 ± 0.025 to $53.238 \pm 0.197\%$, and after the composting process, it decreased to values between 37.724 ± 0.821 and $54.384 \pm 0.094\%$ (Figure 35e). The initial values of nitrogen content were between $1.710 \pm 0.004\%$ and $1.960 \pm 0.004\%$, which is in accordance with Perra et al. (2022) for the same substrate. At the end of the composting processes, the nitrogen content increased to values between $2.430 \pm 0.004\%$ and $2.700 \pm 0.004\%$, as shown in Figure 35f, due to the mineralization of organic matter and the production of ammonium and nitrate (Azim et al., 2018).

The C/N ratio is an indicator of the degree of decomposition of organic matter. The initial C/N ratio of grape skin was in a range from 25.102 ± 0.004 to 29.380 ± 0.004 (Figure 35g), which was in agreement with the optimal values (25-30:1) in the literature intended for the composting process reported by Onwosi et al. (2017) and Xie et al. (2023). Although the thermophile phase was not reached in five experiments, a significant decrease in the C/N ratio

proved that composting processes were successful. Also, the greatest decrease in the C/N ratio could be noticed in experiment 5, from 28.128 ± 0.004 to 18.555 ± 0.004.

The total color change of compost samples and their extracts is shown in Figures 35h and l. There was a great color change between the compost material at the beginning of the process and after 30 days. Also, the total color change was increasing until the end of the process. It was observed that the highest total color change of the compost is in reactor 3 (ΔE = 15.984 ± 0.142), and the lowest value was obtained in reactor 5 ($\Delta E = 2.087 \pm 0.115$). In general, the substrates during composting gradually turn black due to the degradation of organic matter and the formation of humic substances (Khan et al., 2009).

The pH level is an important variable for the composting process and affects the microbial activity. As explained in the Materials and Methods section, the pH value of fresh grape skin was high in an acidic environment and unsuitable for composting. The pH was adjusted with a 10% sodium hydrogencarbonate solution, and then the values were in a range from 6.123 ± 0.006 to 7.167 ± 0.012 (Figure 35i), which corresponds to the optimal values for the composting process noted by Azim et al. (2018) and Onwosi et al. (2017). In these experiments, the pH decreases and then increases. The pH of the final composts ranged from 8.237 ± 0.023 to 9.506 ± 0.023, which corresponds to literature data for mature compost (Diaz and Savage, 2007; Hemidat et al., 2018). Finally, before applying the compost to a soil, it is important to determine the final pH of the compost (Hemidat et al., 2018).

As shown in Figures 35j and k, total dissolved solids and conductivity are two related variables; the greater the concentration of total dissolved solids in compost, the higher the values of conductivity (Hemidat et al., 2018). According to Hemidat et al. (2018), the values of conductivity of compost range from 1 to 10 mS/cm, which corresponds to the results obtained in experiments. During the early stages of the composting process, due to high microbial activity and the release of mineral salt ions such as phosphate from the degradation of organic matter, there is an increase in total dissolved solids and conductivity. In the later stages, temperature drops, mineral salts are deposited, microorganisms and ions form stable humus, and conductivity decreases (Fan et al., 2023).

Figure 36 presents the microbial growth during the grape skin composting processes. In all composting processes, bacteria and fungi predominate. Actually, their growth is related to their pH value. In the first days of composting, due to the acidic environment, fungi predominate

in all reactors, and later, when the pH is in a neutral or alkali area, bacteria are predominant. This is in agreement with the literature (Diaz and Savage, 2007).

The changes in germination index are shown in Figure 37. It has been observed that the values of the germination index are increasing and decreasing during the 30 days of the grape skin composting process, and this can be explained by different concentrations of salts and organic acids in the different stages of composting (Kong et al., 2022; G. Wang et al., 2022). The germination index after 30 days of the composting process was in the range from 185.135 to 414.960%. Taking into account that the authors (Gong et al., 2021; Hashemi et al., 2019) reported that the value of GI above 80% indicates compost maturity and non-toxicity for plants; the composts obtained in these experiments are non-toxic. The highest value of the germination index was achieved in experiment 4(GI=414.960 ± 3.605), and the lowest value was obtained in experiment 1 (185.135 ± 2.081).

The bulk density is known as the mass of the material in a given volume, and it affects the mechanical qualities of the material, including strength, porosity, and compaction ease (Agnew and Leonard, 2003). According to Azim et al. (2018) the bulk density values for compost are often in the range of 100 to 900 kg/m^3. In Table 46 are shown the values of bulk density of the final composts, and the values are in the range of 292.666 ± 2.396 kg/m^3 (experiment 4) to 448.080 ± 10.941 kg/m^3 (experiment 1). The porosity of compost samples ranged from 68.709 ± 0.764 to 80.536 ± 0.079%, and similar results were obtained by Khater (2015).

5.3.2. Kinetics of organic matter degradation and microbial growth

The kinetics of organic matter degradation in this work were described with a first-order kinetic model. In Table 47, the kinetic parameters for the composting processes with different pretreatments of grape skin are presented. The highest degradation rate (0.0051 ± 0.001 1/day) was estimated for experiment 2, and the lowest rates were estimated for experiments 4 and 5 (0.0001 ± 0.002 1/day). It is difficult to compare the obtained results with the available literature due to the complexity of the composting material. Abu Qdais and Al-Widyan (2016) presented organic matter degradation rates in the range of 0.0015 to 0.0055% per day in the process of agro-industrial waste, olive milling waste, grain dust, and coffee processing waste mixture composting. Also, it can be noticed that the coefficients of determination for this set of composting experiments are very low, which means that the first-order kinetic model is not

suitable for the description of organic matter degradation during the grape skin composting process or that it demands some improvements.

Table 47 presents the kinetics of microbial growth. The bacterial growth was also described by the first-order model, and the fungal growth was described using the logistic model. As it can be seen, in experiment 1, the specific bacterial growth rate is the highest (0.0075 ± 0.0031 1/day), and the lowest is in experiment 4 (0.0028 ± 0.0022 1/day). Taking into account the fungal growth, a specific rate is the highest in experiment 2 (0.0076 ± 0.0019 1/day) and the lowest in experiment 5 (0.0001 ± 0.0001 1/day).

5.3.3. Basic statistical analysis

The results of moisture and dry matter content, organic matter content, ash content, carbon and nitrogen content, C/N ratio, pH, TDS, and conductivity between expariments at the beginning of the composting process and at the end were statistically analyzed, and the results are shown in Table 48.

It has been observed that there are no significant differences in moisture and dry matter content between reactors at the beginning and end of the process. Also, it can be noticed that there is a significant difference in experiment 4 (ground grape skin pretreated to extract bioactive molecules at $T = 40$ °C during the $t = 90$ minutes) considering the values of organic matter content, ash content, and carbon content compared to the other experiments and taking into account the beginning and end of the process. The pH, TDS, and conductivity values are statistically different between experiments at the beginning and at the end of the composting process.

5.3.4. Principal Component Analysis (PCA)

The relationship between composting day and the analyzed physicochemical properties of compost samples (moisture and dry matter content, organic matter and ash content, carbon and nitrogen content, C/N ratio, total color change of compost samples, pH, TDS, conductivity, and total color change of compost extracts) was estimated using the PCA analysis, and the score plot and loading plot are shown in Figure 38.

The score plot of PCA analysis is shown in Figure 38a, and it can be noticed that the first two factors of analysis describe around 50% of the data variability. The loading plot of

PCA is shown in Figure 38b, and the relationship between sampling day and the physicochemical properties of compost was investigated. The moisture content, nitrogen content, total dissolved solids, conductivity, pH, total color change of compost, and total color change of compost extracts are positively correlated with the day of composting. It can be explained that with a further performance of composting process, the increase in mentioned variables will be noticed. Otherwise, the organic matter, carbon content, and C/N ratio are negatively correlated (with a further performance of composting process, the organic matter and carbon content, and C/N ratio will decrease).

5.3.5. NIR spectra of compost samples and compost extracts

In this work, NIR spectroscopy was applied for the monitoring of the composting process. All compost samples and compost extract samples during the 30 days of the composting processes in five reactors have been recorded using different NIR instruments: NIR spectrometer (NIR-128-1.7-USB/6.25/50 μm, Control Development inc., USA) which records the absorbance in wavelength range from $\lambda = 904 - 1699$ nm for all samples; NIR spectrometer (AvaSpec-NIR256-2.5-HSC-EVO, Avantes, USA) which records the absorbance in wavelength range from $\lambda = 1000 - 2500$ nm for all samples; portable NIR spectrometer (NIR-S-G1, InnoSpectra, Taiwan) which records absorbance in wavelength range from $\lambda = 900 - 1700$ nm for compost samples; and portable NIR spectrometer (NIR-M-R2, InnoSpectra, Taiwan) which records absorbance in wavelength range from $\lambda = 900 - 1700$ nm for compost extract samples.

The NIR spectra for all samples were recorded in 5 repetitions. The average values of unprocessed NIR spectra for samples obtained in five reactors and recorded with different NIR instruments are shown in Figures 38–40.

Figure 39 presents the NIR spectra for compost samples and compost extract samples recorded with the NIR spectrometer NIR-128-1.7-USB/6.25/50 μm. As it can be seen in Figure 39a, the spectra of compost samples for all reactors have the same trend, and the differences between spectra are in the wavelength range of 1350–1550 nm, which indicate O–H bonds, or, in other words, the differences in this spectral range can be correlated with water content in the samples (Valinger et al., 2018). Furthermore, the NIR spectra of compost extract samples (Figure 39b) for all reactors also have the same trend, and the differences can be noticed in the wavelength range 904–930 and 1350–1699, which indicate changes in the second and third overtone C–H and O–H bonds (Badr Eldin, 2011).

Figure 40 presents the NIR spectra for compost samples and compost extract samples recorded with the NIR spectrometer AvaSpec-NIR256-2.5-HSC-EVO. The NIR spectra were recorded in the range of wavelength of 990–2500 nm, and the noises can be observed at wavelengths of 990–2400 nm. The noise represents random fluctuations around the signal that can originate from the instrument or environmental laboratory conditions (Henríquez and Ruz, 2019). From the spectra gathered for compost samples (Figure 40a), it can be noticed that there are two maximums: the first one is in the wavelength range between 1350 and 1600 nm, which corresponds to the second overtone H_2O, C–H, and CH_2 bonds, and the second one is between 1900 and 2200 nm, which corresponds to the first overtone H_2O, C–H, and CH_2 bonds (Badr Eldin, 2011). Figure 40b shows the NIR spectra for compost extract samples in five reactors during the composting processes. It can be noticed that the differences between the obtained spectra are in the wavelengths of 1300–1500 nm and 1800–2100 nm, which correspond to the already mentioned overtones. The NIR spectra of compost extract samples also have noise.

Figure 41 shows the NIR spectra gathered with a portable NIR spectrometer. The NIR spectra of compost samples were recorded using the spectrometer NIR-S-G1, which records absorbance in the wavelength range of $\lambda = 900$–1700 nm. From Figure 41a, it can be observed that recorded spectra show the maximum at a wavelength range of 1400–1500 nm, which is correlated to second-overtone H_2O, ROH, RNH_2, CH, CH_2, and CH_3 bonds (Badr Eldin, 2011). The NIR spectra of compost extract samples were recorded using the spectrometer NIR-M-R2, which records absorbance in the wavelength range of $\lambda = 900$–1700 nm. It can be noticed that the differences between the spectra are in the wavelength ranges of 1100–1250 nm, 1300–1500 nm, and 1600–1700 nm, which are related to the first and second overtones (H_2O, C–H, and CH_2 bonds) (Badr Eldin, 2011). Finally, the NIR spectra in Figures 39–41 show the changes in absorbance maximum during the composting processes, which indicates the chemical changes of the grape skin that occurred in the process.

5.3.6. Principal component analysis (PCA) of NIR spectra

Considering the fact that the NIR spectra are complex, often chemometric methods are used to separate the important information about the samples. In this work, principal component analysis was applied for the average NIR spectra of compost samples and compost extract samples. This method is based on the reduction of the dimensionality of a dana set and preserving as much variability as possible. The results of PCA of the NIR spectra are shown in Figures 42–44.

Figure 42 shows the PCA analysis of the NIR spectra of compost samples and compost extract samples in five reactors during the composting process, and the NIR spectra were recorded with the NIR spectrometer NIR-128-1.7-USB/6.25/50 μm. It can be noticed that the first two factors of analysis describe more than 95% of the data variability for the compost samples and more than 97% of the data variability for the compost extract samples. Also, it is observed that the data are overlapping, which indicates the similarities between the samples.

In Figure 43, the results of PCA of the NIR spectra of compost samples and compost extract samples in five reactors during the composting process are shown. The NIR spectra were recorded with the NIR spectrometer AvaSpec-NIR256-2.5-HSC-EVO. On this figure, it can be seen that the first two factors of analysis describe more than 96% of the data variability for the compost samples and more than 94% of the data variability for the compost extract samples. Considering the PCA analysis of compost samples and compost extract samples, it can be noticed that the data are not grouped towards the reactors, the data are overlapping which can be explained by the similarity between the samples.

The results of PCA analysis of the NIR spectra of compost samples and compost extract samples in five reactors during the composting process recorded with a portable NIR spectrometer (NIR-S-G1 for compost samples and NIR-M-R2 for compost extract samples) are shown in Figure 44. The first two factors of analysis describe more than 96% of the data variability for the compost samples and more than 92% of the data variability for the compost extract samples.

5.3.7. Artificial neural network (ANN) models based on the NIR spectra for the prediction of physicochemical properties of compost during the composting process

During the composting processes, the NIR spectra were recorded with different NIR instruments. Then, the different preprocessing methods for NIR spectra were applied, and the artificial neural network (ANN) models for the prediction of the physicochemical properties of compost during the composting process were developed. The ANN models are shown in Tables 55–93.

The ANN models based on NIR spectra obtained using the NIR spectrometer NIR-128-1.7-USB/6.25/50 μm were developed for each property of the compost samples and compost extracts. The results are shown in Tables 55–67, and the models with the highest values of *RER* are marked in bold. Models with the values *RER* > 4 are acceptable for data screening; models

with *RER* > 10 can be used for quality control; and models with *RER* > 15 can be used for quantification (Sim et al., 2023).

As the acceptable pretreatment method of NIR spectra was SNV (standard normal variate), and the developed ANN model for the prediction of the day of composting resulted in the highest *RER* value, 6.027. This model is acceptable for data screening. Considering the results for moisture content, total color change of compost, total dissolved solids and conductivity, the SG2D+MSC (second-order Savitzky-Golay derivative followed by multiplicative scatter corrections) as a pretreatment method and the developed ANN models resulted in the greatest *RER* values: 6.593, 4.894, 6.593, and 6.886, respectively. Considering the results obtained for the dry matter content and organic matter content, the SG2D+SNV (second-order Savitzky-Golay derivative followed by standard normal variate) and the developed ANN models resulted with the greatest *RER* value (5.181). The developed model for the prediction of ash content and preprocessing method smoothing+MSC (smoothing followed by multiplicative scatter corrections) resulted with the *RER* value 4.591. The developed model for the prediction of carbon content and total color change of extract, and preprocessing method smoothing+SNV (smoothing followed by standard normal variate) resulted with the *RER* values 3.780 and 5.630. As the acceptable pretreatment method of NIR spectra was smoothing and the developed ANN model for the prediction of nitrogen content resulted in the highest *RER* value, 4.807. Considering the results obtained for the prediction of C/N ratio and pH, SG1D+MSC (first-order Savitzky-Golay derivative followed by multiplicative scatter corrections) as the preprocessing method and the developed ANN model resulted with a *RER* values 14.457 and 7.673. According to the literature (Sim et al., 2023), the developed models for prediction of carbon content was considered as not acceptable for screanning, and the model developed for the prediction of C/N ratio could be used for quality control. The other developed models for the prediction of physicochemical properties were acceptable for data screening.

The ANN models based on NIR spectra obtained using the NIR spectrometer AvaSpec-NIR256-2.5-HSC-EVO were developed for each property of the compost samples and compost extracts, and the results are shown in Tables 68-80. As the acceptable preprocessing method of NIR spectra was SNV (standard normal variate), and the developed ANN model for the prediction of the day of composting and total dissolved solids resulted in the highest *RER* values, 6.798 and 4.961. The developed model for the prediction of moisture content and preprocessing method smoothing+MSC (smoothing followed by multiplicative scatter corrections) resulted with the *RER* value 6.993. As the acceptable pretreatment method of NIR

spectra was smoothing and the developed ANN model for the prediction of dry matter content, carbon content and total color change of compost resulted with the highest *RER* values, 4.501, 6.232 and 8.393. Furthermore, considering the results obtained for the organic matter content and conductivity, the SG2D (second-order Savitzky-Golay derivative) and the developed ANN models resulted with the greatest *RER* values (5.718 and 6.437). Considering the results obtained for the prediction of ash content and total color change of compost extract samples, SG1D (first-order Savitzky-Golay derivative) as the preprocessing method and the developed ANN model resulted with a *RER* values 6.448 and 6.234. As the acceptable pretreatment method of NIR spectra was SG2D+MSC (second-order Savitzky-Golay derivative followed by multiplicative scatter corrections) and the developed ANN model for the prediction of nitrogen content and C/N ratio, resulted with the highest *RER* values, 4.816 and 7.567. And, considering the results obtained for the prediction of pH, SG2D+SNV(second-order Savitzky-Golay derivative followed by standard normal variate) and the developed ANN model resulted with the greatest *RER* value (4.978). The obtained results indicate that all models for the prediction of physicochemical properties are acceptable for data screening (*RER* > 4).

In this set of composting experiments, the portable NIR spectrometer was used for the recording of NIR spectra, portable NIR spectrometer (NIR-S-G1) for compost samples and portable NIR spectrometer (NIR-M-R2) for compost extracts. The ANN models based on NIR spectra obtained using these NIR spectrometers were developed for each property of the compost samples and compost extracts, and the results are shown in Tables 81-93. As the acceptable preprocessing method of NIR spectra was smoothing+MSC (smoothing followed by multiplicative scatter corrections) and the developed ANN model for the prediction of the day of composting and nitrogen content resulted in the highest *RER* values, 5.614 and 5.470. The developed model for the prediction of moisture content and ash content, and preprocessing method smoothing+SNV (smoothing followed by standard normal variate) resulted with the *RER* values 7.590 and 4.671. Considering the results obtained for the prediction of dry matter content, SG1D+MSC (first-order Savitzky-Golay derivative followed by multiplicative scatter corrections) as the preprocessing method and the developed ANN model resulted with a *RER* value 3.877. As the acceptable pretreatment method of NIR spectra was SNV (standard normal variate), and the developed ANN model for the prediction of the organic matter content resulted in the highest *RER* value, 5.357. As the acceptable pretreatment method of NIR spectra was MSC (multiplicative scatter corrections), and the developed ANN model for the prediction of carbon content and C/N ratio resulted in the highest *RER* values, 5.411 and 7.062. And,

considering the results obtained for the prediction of total color change of compost and pH, SG2D+SNV(second-order Savitzky-Golay derivative followed by standard normal variate) and the developed ANN model resulted with the greatest *RER* values, 5.105 and 5.423. As the acceptable pretreatment method of NIR spectra was smoothing and the developed ANN model for the prediction of total dissolved solids and conductivity resulted with the highest *RER* values, 5.979 and 6.524. And, considering the results obtained for the prediction of total color change of compost extracts, the SG2D (second-order Savitzky-Golay derivative) and the developed ANN models resulted with the greatest *RER* value (5.865). The obtained models are suitable for the dana screening (*RER*>4), except the model for the prediction of dry matter content.

In general, comparing the different NIR instruments, it could be observed that the second NIR instrument (NIR-128-1.7-USB/6.25/50 μm) has the greatest *RER* values for the ANN models for the prediction of properties of compost samples and compost extract samples, which indicates that this instrument is reliable for the analysis of the physicochemical properties (moisture and dry matter content, organic matter and ash content, carbon content, total color change of compost samples and compost extracts, pH, total dissolved solids and conductivity), during the composting process.

5.3.8. Artificial neural network (ANN) models based on the NIR spectra for the prediction of microbiological properties of compost during the composting process

The ANN models for the prediction of microbiological properties of compost samples during the composting process based on NIR spectra recorded using NIR spectrometer NIR-128-1.7-USB/6.25/50 μm were shown in Tables 94-96. Considering the prediction of number of bacteria and the total number of microorganisms, as the acceptable preprocessing method of NIR spectra was SG2D+MSC (second-order Savitzky-Golay derivative followed by multiplicative scatter corrections) and the developed ANN model resulted with the highest *RER* values 10.170 and 11.317, respectively. As the acceptable pretreatment method of NIR spectra was smoothing and the developed ANN model for the prediction of number of fungi resulted with the highest *RER* value 9.478.

Furthermore, the ANN models for the prediction of microbiological properties of compost samples during the composting process based on NIR spectra recorded using NIR spectrometer AvaSpec-NIR256-2.5-HSC-EVO were shown in Tables 97-98. Considering the prediction of number of bacteria and number of fungi as the acceptable preprocessing method of NIR spectra was smoothing, and the developed ANN model resulted with the highest *RER* values 8.813 and 9.521, respectively. As the acceptable pretreatment method of NIR spectra was smoothing and the developed ANN model for the prediction of number of fungi resulted with the highest *RER* value 9.478. Otherwise, taking into account the results for total number of microorganisms, the preprocessing method SG2D+MSC (second-order Savitzky-Golay derivative followed by multiplicative scatter corrections) and the developed ANN model resulted with the highest *RER* value 10.523.

In this set of composting experiments, the portable NIR spectrometer (NIR-S-G1) was used for the recording of NIR spectra. The developed ANN models for the prediction of number of microorganisms are shown in Table 99. Considering the prediction of number of bacteria, number of fungi and total number of microorganisms, as the acceptable preprocessing method of NIR spectra was smoothing, and the developed ANN model resulted with the highest *RER* values 9.237, 9.980 and 9.132.

In general, comparing the different NIR instruments, it could be observed that the first NIR instrument NIR-128-1.7-USB/6.25/50 μm has the greatest *RER* values for the ANN models for the prediction of microbiological properties of compost samples which indicates that this instrument is reliable for the analysis of these properties during the composting process.

6. CONCLUSIONS

In this doctoral research, the potential of NIR spectroscopy coupled with the development of artificial neural network (ANN) models for monitoring the grape skin composting process was investigated. The following specific conclusions were drawn from the thesis:

1. The grape skin composting processes in laboratory reactors were performed under different conditions of initial moisture content and air flow rate. During the process, the main variables were analyzed, and the NIR spectra were recorded with different NIR instruments. Although the thermophile phase was achieved only in two experiments (3 and 8), all composting processes were efficiently performed, which can be proved by the decrease in organic matter content, C/N ratio, and pH value. Also, the obtained values of the germination index indicate the maturity and non-toxicity of the obtained composts for plants (*GI* > 80%).

2. Furthermore, the multiple linear regression (MLP), piecewise linear regression (PLR), and artificial neural network (ANN) models were developed based on the experimental data, and considering the *RER* (ratio of the error range) values, all MLP models are acceptable for screening except the model predicting the nitrogen content. The developed PLR and ANN models can be used for the prediction of the physicochemical properties of grape skin compost during the composting process.

3. The NIR spectra of compost samples and compost extract samples were recorded using different NIR instruments in different wavelength ranges. The spectra for compost samples in different reactors have the same trend, as do the spectra for compost extract samples. Moreover, the spectra of compost samples and compost extract samples showed the changes in absorbance maximum during the composting processes, which indicates the chemical changes of the grape skin that occur during the process.

4. In order to compare the composting process of fresh (not treated) and pretreated grape skin, the extraction of bioactive molecules from grape skin was investigated. The extraction was performed at different conditions of extraction time, temperature, solid-liquid ratio, and mixing speed with water as a solvent. After the extraction, the physicochemical properties (pH, total dissolved solids, conductivity, total polyphenol content, and antioxidant activity determined using DPPH and FRAP method) of the

extracts were determined. Finally, the response surface methodology was applied to optimize the extraction conditions for the total polyphenol content, antioxidant activity determined using DPPH and FRAP method as the output variables, and the results were as follows: extraction time 67.5 min; temperature 80°C; solid-liquid ratio 30 g/L and mixing rate 750 1/min.

5. The composting processes of different pretreated grape skins were performed in laboratory reactors for 30 days at a constant air flow rate of 2 L/min. The experiments were as follows: grape skin without pretreatment; ground grape skin without pretreatment; grape skin pretreated to extract bioactive molecules at 40 °C during the 90 minutes; ground grape skin pretreated to extract bioactive molecules at 40 °C during the 90 minutes; and the mixture of grape skin consisted of: grape skin without pretreatment (w/w = 43.93%), ground grape skin without pretreatment (w/w = 8.11%), grape skin pretreated to extract bioactive molecules at 40 °C during the 90 minutes (w/w = 14.25%), and ground grape skin pretreated to extract bioactive molecules at 40 °C during the 90 minutes (w/w = 33.66%). The efficiency of the composting processes was determined by important variables such as moisture content, organic matter and organic carbon content, C/N ratio, and pH value. All compost samples and compost extract samples have been recorded using different NIR instruments in different wavelength ranges. The NIR spectra show the changes in the absorbance maximum during the composting processes, indicating the chemical changes of the grape skin that occur during the process.

6. The artificial neural network (ANN) models for the prediction of the physicochemical and microbiological properties of grape skin compost were developed based on the preprocessed NIR spectra. The different preprocessed methods were applied. It could be observed that the ANN models developed in the first set of composting experiments (which were carried out under various experimental conditions) had a greater values of *RPD* and *RER*. Finally, the obtained results indicate a significant potential of NIR spectroscopy for the monitoring of the composting process.

7. LIST OF REFERENCES

Abad, M., Noguera, P., Burés, S., 2001. National inventory of organic wastes for use as growing media for ornamental potted plant production: Case study in Spain. Bioresour Technol 77, 197–200. https://doi.org/10.1016/S0960-8524(00)00152-8

Abdi, H., Williams, L.J., 2010. Principal component analysis. Wiley Interdiscip Rev Comput Stat 2, 433–459. https://doi.org/10.1002/wics.101

Abdi, R., Shahgholi, G., Sharabiani, V.R., Fanaei, A.R., Szymanek, M., 2023. Prediction compost criteria of organic wastes with Biochar additive in in-vessel composting machine using ANFIS and ANN methods. Energy Reports 9, 1684–1695. https://doi.org/10.1016/j.egyr.2023.01.001

Abu Qdais, H., Al-Widyan, M., 2016. Evaluating composting and co-composting kinetics of various agro-industrial wastes. Int J Recycl Org Waste Agric 5, 273–280. https://doi.org/10.1007/s40093-016-0137-3

Agnew, J.M., Leonard, J.J., 2003. The physical properties of compost. Compost Sci Util 11, 238–264. https://doi.org/10.1080/1065657X.2003.10702132

Ahmad, B., Yadav, V., Yadav, A., Rahman, M.U., Yuan, W.Z., Li, Z., Wang, X., 2020. Integrated biorefinery approach to valorize winery waste: A review from waste to energy perspectives. Sci Total Environ 719, 137315. https://doi.org/10.1016/j.scitotenv.2020.137315

Ahmed, M.I., Xu, X., Sulieman, A.A., Mahdi, A.A., Na, Y., 2020. Effect of extraction conditions on phenolic compounds and antioxidant properties of koreeb (Dactyloctenium aegyptium) seeds flour. J Food Meas Charact 14, 799–808. https://doi.org/10.1007/s11694-019-00328-9

Albrecht, R., Joffre, R., Gros, R., Le Petit, J., Terrom, G., Périssol, C., 2008. Efficiency of near-infrared reflectance spectroscopy to assess and predict the stage of transformation of organic matter in the composting process. Bioresour Technol 99, 448–455. https://doi.org/10.1016/J.BIORTECH.2006.12.019

Albrecht, R., Le Petit, J., Terrom, G., Périssol, C., 2011. Comparison between UV spectroscopy and nirs to assess humification process during sewage sludge and green wastes co-composting. Bioresour Technol 102, 4495–4500. https://doi.org/10.1016/J.BIORTECH.2010.12.053

Amirvaresi, A., Parastar, H., 2023. Miniaturized NIR spectroscopy and chemometrics: A smart combination to solve food authentication challenges. Front Anal Sci 3, 1–8. https://doi.org/10.3389/frans.2023.1118590

Antonić, B., Jančikova, S., Dordević, D., Tremlova, B., 2020. Grape Pomace Valorization: A Systematic Review and Meta-Analysis. Foods 9, 1627.

Asadu, C.O., Egbuna, S.O., Chime, T.O., Eze, C.N., Kevin, D., Mbah, G.O., Ezema, A.C., 2019. Survey on solid wastes management by composting: Optimization of key process parameters for biofertilizer synthesis from agro wastes using response surface methodology (RSM). Artif Intell Agric 3, 52–61. https://doi.org/10.1016/j.aiia.2019.12.002

Aviezer, Y., Lahav, O., 2022. Determining the kinetic constants leading to mineralization of dilute carbamazepine and estradiol-containing solutions under continuous supercritical water oxidation conditions. J Hazard Mater 422, 126797.

https://doi.org/10.1016/j.jhazmat.2021.126797

Awogbemi, O., Kallon, D.V. Von, 2022. Pretreatment techniques for agricultural waste. Case Stud Chem Environ Eng 6, 100229. https://doi.org/10.1016/j.cscee.2022.100229

Ayilara, M.S., Olanrewaju, O.S., Babalola, O.O., Odeyemi, O., 2020. Waste management through composting: Challenges and potentials. Sustainability 12, 1–23. https://doi.org/10.3390/su12114456

Azim, K., Soudi, B., Boukhari, S., Perissol, C., Roussos, S., Thami Alami, I., 2018. Composting parameters and compost quality: a literature review. Org Agric 8, 141–158. https://doi.org/10.1007/s13165-017-0180-z

Azis, F.A., Rijal, M., Suhaimi, H., Abas, P.E., 2022. Patent Landscape of Composting Technology: A Review. Inventions 7. https://doi.org/10.3390/inventions7020038

Badr Eldin, A.I., 2011. Near-infrared spectroscopy, in: Wide Spectra of Quality Control. p. 11. https://doi.org/10.5772/24208

Balík, J., Kyseláková, M., Vrchotová, N., Tříska, J., Kumšta, M., Veverka, J., Híc, P., Totušek, J., Lefnerová, D., 2008. Relations between polyphenols content and antioxidant activity in vine grapes and leaves. Czech J Food Sci 26, S25–S32. https://doi.org/10.17221/246/2008-cjfs

Benzie, I.F.F., Strain, J.J., 1996. The ferric reducing ability of plasma (FRAP) as a measure of "antioxidant power": The FRAP assay. Anal Biochem 239, 70–76. https://doi.org/10.1006/abio.1996.0292

Beres, C., Costa, G.N.S., Cabezudo, I., da Silva-James, N.K., Teles, A.S.C., Cruz, A.P.G., Mellinger-Silva, C., Tonon, R. V., Cabral, L.M.C., Freitas, S.P., 2017. Towards integral utilization of grape pomace from winemaking process: A review. Waste Manag 68, 581–594. https://doi.org/10.1016/j.wasman.2017.07.017

Blanco, M., Coello, J., Montoliu, I., Romero, M.A., 2001. Orthogonal signal correction in near infrared calibration. Anal Chim Acta 434, 125–132. https://doi.org/10.1016/S0003-2670(01)00820-0

Blanco, M., Villarroya, I., 2002. NIR spectroscopy: A rapid-response analytical tool. TrAC - Trends Anal Chem 21, 240–250. https://doi.org/10.1016/S0165-9936(02)00404-1

Boniecki, P., Dach, J., Pilarski, K., Piekarska-Boniecka, H., 2012. Artificial neural networks for modeling ammonia emissions released from sewage sludge composting. Atmos Environ 57, 49–54. https://doi.org/10.1016/j.atmosenv.2012.04.036

Brand-Williams, W., Cuvelier, M.E., Berset, C., 1995. Use of a free radical method to evaluate antioxidant activity. LWT - Food Sci Technol 28, 25–30. https://doi.org/10.1016/S0023-6438(95)80008-5

Brzezińska, R., Wirkowska-Wojdyła, M., Piasecka, I., Górska, A., 2023. Application of Response Surface Methodology to Optimize the Extraction Process of Bioactive Compounds Obtained from Coffee Silverskin. Appl Sci 13. https://doi.org/10.3390/app13095388

Bucić-Kojić, A., Planinić, M., Tomas, S., Bilić, M., Velić, D., 2007. Study of solid-liquid extraction kinetics of total polyphenols from grape seeds. J Food Eng 81, 236–242. https://doi.org/10.1016/j.jfoodeng.2006.10.027

Buljat, A.M., Jurina, T., Tušek, A.J., Valinger, D., Kljusuric, J.G., Benkovic, M., 2019. Applicability of foam mat drying process for production of instant cocoa powder enriched with lavender extract. Food Technol Biotechnol 57, 159–170. https://doi.org/10.17113/ftb.57.02.19.6064

Carmona-Hernandez, J.C., Taborda-Ocampo, G., González-Correa, C.H., 2021. Folin-Ciocalteu Reaction Alternatives for Higher Polyphenol Quantitation in Colombian Passion Fruits. Int J Food Sci 2021. https://doi.org/10.1155/2021/8871301

Cesaro, A., Belgiorno, V., Guida, M., 2015. Compost from organic solid waste: Quality assessment and European regulations for its sustainable use. Resour Conserv Recycl 94, 72–79. https://doi.org/10.1016/j.resconrec.2014.11.003

Chan, M.T., Selvam, A., Wong, J.W.C., 2016. Reducing nitrogen loss and salinity during "struvite" food waste composting by zeolite amendment. Bioresour Technol 200, 838–844. https://doi.org/10.1016/j.biortech.2015.10.093

Chang, C.-W., Laird, D.A., Mausbach, M.J., Hurburgh, C.R., 2001. Near-Infrared Reflectance Spectroscopy–Principal Components Regression Analyses of Soil Properties. Soil Sci Soc Am J 65, 480–490. https://doi.org/10.2136/sssaj2001.652480x

Chañi-Paucar, L.O., Silva, J.W.L., Maciel, M.I.S., de Lima, V.L.A.G., 2021. Simplified process of extraction of polyphenols from agroindustrial grape waste. Food Sci Technol 41, 723–731. https://doi.org/10.1590/fst.31120

Chowdhary, P., Gupta, A., Gnansounou, E., Pandey, A., Chaturvedi, P., 2021. Current trends and possibilities for exploitation of Grape pomace as a potential source for value addition. Environ Pollut 278, 116796. https://doi.org/10.1016/j.envpol.2021.116796

Ćosić, I., Vuković, M., Gomzi, Z., Briški, F., 2012. Comparison of various kinetic models for batch biodegradation of leachate from tobacco waste composting. Rev Chim 63, 967–971.

Cucina, M., 2023. Integrating anaerobic digestion and composting to boost energy and material recovery from organic wastes in the Circular Economy framework in Europe: A review. Bioresour Technol Reports 24, 101642. https://doi.org/10.1016/j.biteb.2023.101642

Diaz, L.F., Savage, G.M., 2007. Chapter 4: Factors that affect the process, in: Compost Science and Technology. pp. 49–65. https://doi.org/10.1016/S1478-7482(07)80007-8

Diaz, L.F., Savage, G.M., Eggerth, L.L., Chiumenti, A., 2007. Chapter 5 Systems used in composting, in: Compost Science and Technology. pp. 67–87. https://doi.org/10.1016/S1478-7482(07)80008-X

Diaz, M.J., Madejon, E., Lopez, F., Lopez, R., Cabrera, F., 2002. Optimization of the rate vinasse / grape marc for co-composting process. Process Biochem 37, 1143–1150.

Dragoi, E.N., Godini, K., Koolivand, A., 2021. Modeling of oily sludge composting process by using artificial neural networks and differential evolution: Prediction of removal of petroleum hydrocarbons and organic carbon. Environ Technol Innov 21, 101338. https://doi.org/10.1016/j.eti.2020.101338

Ebrahimzadeh, R., Ghazanfari Moghaddam, A., Sarcheshmehpour, M., Mortezapour, H., 2017. A novel kinetic modeling method for the stabilization phase of the composting process for biodegradation of solid wastes. Waste Manag Res 35, 1226–1236.

https://doi.org/10.1177/0734242x17733538

Echarrafi, K., El Harhouri, H., Ben Abbou, M., Rais, Z., El Hassani, I., El Haji, M., 2018. Mixture design formulation for optimized composting with the perspective of using artificial intelligence optimization algorithms. J Appl Sci Environ Stud JASES J Appl Sci Envir Stud 1, 54.

Ezemagu, I.G., Ejimofor, M.I., Menkiti, M.C., Diyoke, C., 2021. Biofertilizer production via composting of digestate obtained from anaerobic digestion of post biocoagulation sludge blended with saw dust: Physiochemical characterization and kinetic study. Environ Challenges 5, 100288. https://doi.org/10.1016/j.envc.2021.100288

Fan, T., Zhang, X., Wan, Y., Deng, R., Zhu, H., Wang, Xihao, Wang, S., Wang, Xingming, 2023. Effect of Different Livestock Manure Ratios on the Decomposition Process of Aerobic Composting of Wheat Straw. Agronomy 13. https://doi.org/10.3390/agronomy13122916

Fearn, T., 2002. Assessing calibrations: SEP,RPD, RER and R2. NIR News 13, 12.

Galvez-Sola, L., Moral, R., Perez-Murcia, M.D., Perez-Espinosa, A., Bustamante, M.A., Martinez-Sabater, E., Paredes, C., 2010a. The potential of near infrared reflectance spectroscopy (NIRS) for the estimation of agroindustrial compost quality. Sci Total Environ 408, 1414–1421. https://doi.org/10.1016/j.scitotenv.2009.11.043

Galvez-Sola, L., Morales, J., Mayoral, A.M., Marhuenda-Egea, F.C., Martinez-Sabater, E., Perez-Murcia, M.D., Bustamante, M.A., Paredes, C., Moral, R., 2010b. Estimation of phosphorus content and dynamics during composting: Use of near infrared spectroscopy. Chemosphere 78, 13–21. https://doi.org/10.1016/j.chemosphere.2009.09.059

Gao, M., Li, B., Yu, A., Liang, F., Yang, L., Sun, Y., 2010. The effect of aeration rate on forced-aeration composting of chicken manure and sawdust. Bioresour Technol 101, 1899–1903. https://doi.org/10.1016/j.biortech.2009.10.027

García-Lomillo, J., González-SanJosé, M.L., 2017. Applications of Wine Pomace in the Food Industry: Approaches and Functions. Compr Rev Food Sci Food Saf 16, 3–22. https://doi.org/10.1111/1541-4337.12238

Gerardi, C., D'amico, L., Migoni, D., Santino, A., Salomone, A., Carluccio, M.A., Giovinazzo, G., 2020. Strategies for Reuse of Skins Separated From Grape Pomace as Ingredient of Functional Beverages. Front Bioeng Biotechnol 8, 1–13. https://doi.org/10.3389/fbioe.2020.00645

Gong, B., Zhong, X., Chen, X., Li, S., Hong, J., Mao, X., Liao, Z., 2021. Manipulation of composting oxygen supply to facilitate dissolved organic matter (DOM) accumulation which can enhance maize growth. Chemosphere 273, 129729. https://doi.org/10.1016/j.chemosphere.2021.129729

Gu, J., Wang, Z., Kuen, J., Ma, L., Shahroudy, A., Shuai, B., Liu, T., Wang, X., Wang, G., Cai, J., Chen, T., 2018. Recent advances in convolutional neural networks. Pattern Recognit 77, 354–377. https://doi.org/10.1016/j.patcog.2017.10.013

Guo, R., Li, G., Jiang, T., Schuchardt, F., Chen, T., Zhao, Y., Shen, Y., 2012. Effect of aeration rate, C/N ratio and moisture content on the stability and maturity of compost. Bioresour Technol 112, 171–178. https://doi.org/10.1016/j.biortech.2012.02.099

Hashemi, S., Boudaghpour, S., Han, M., 2019. Evaluation of different natural additives

effects on the composting process of source separated feces in resource-oriented sanitation systems. Ecotoxicol Environ Saf 185. https://doi.org/10.1016/j.ecoenv.2019.109667

Haynes, R.J., Belyaeva, O.N., Zhou, Y.F., 2015. Particle size fractionation as a method for characterizing the nutrient content of municipal green waste used for composting. Waste Manag 35, 48–54. https://doi.org/10.1016/j.wasman.2014.10.002

Heberger, K., 2008. Chemoinformatics — multivariate mathematical – statistical methods for data evolution, in: Medical Application of Mass Spectrometry. https://doi.org/10.1016/B978-0-444-51980-1.50009-4

Hemidat, S., Jaar, M., Nassour, A., Nelles, M., 2018. Monitoring of Composting Process Parameters: A Case Study in Jordan. Waste and Biomass Valorization 9, 2257–2274. https://doi.org/10.1007/s12649-018-0197-x

Henríquez, P.A., Ruz, G.A., 2019. Noise reduction for near-infrared spectroscopy data using extreme learning machines. Eng Appl Artif Intell 79, 13–22. https://doi.org/10.1016/j.engappai.2018.12.005

Henseler, J., Ringle, C.M., Sinkovics, R.R., 2009. The use of partial least squares path modeling in international marketing. Adv Int Mark 20, 277–319. https://doi.org/10.1108/S1474-7979(2009)0000020014

Hernández, B., Sáenz, C., Alberdi, C., Diñeiro, J.M., 2016. CIELAB color coordinates versus relative proportions of myoglobin redox forms in the description of fresh meat appearance. J Food Sci Technol 53, 4159–4167. https://doi.org/10.1007/s13197-016-2394-6

Hosseinzadeh, A., Baziar, M., Alidadi, H., Zhou, J.L., Altaee, A., Najafpoor, A.A., Jafarpour, S., 2020. Application of artificial neural network and multiple linear regression in modeling nutrient recovery in vermicompost under different conditions. Bioresour Technol 303. https://doi.org/10.1016/j.biortech.2020.122926

Huang, G., Han, L., Yang, Z., Wang, X., 2008. Evaluation of the nutrient metal content in Chinese animal manure compost using near infrared spectroscopy (NIRS). Bioresour Technol 99, 8164–8169. https://doi.org/10.1016/j.biortech.2008.03.025

Huang, Y., Kangas, L.J., Rasco, B.A., 2007. Applications of Artificial Neural Networks (ANNs) in food science. Crit Rev Food Sci Nutr 47, 113–126. https://doi.org/10.1080/10408390600626453

Huang, Y., Sun, X., Liao, K., Han, L., Yang, Z., 2020. Real-time and field monitoring of the key parameters in industrial trough composting process using a handheld near infrared spectrometer. J Near Infrared Spectrosc 28, 334–343. https://doi.org/10.1177/0967033520939323

Iannucci, L., 2021. Chemometrics for Data Interpretation : Application of. IEEE Instrum Meas 24, 42–48.

Ilyas, T., Chowdhary, P., Chaurasia, D., Gnansounou, E., Pandey, A., Chaturvedi, P., 2021. Sustainable green processing of grape pomace for the production of value-added products: An overview. Environ Technol Innov 23, 101592. https://doi.org/10.1016/j.eti.2021.101592

Ioannou, L.A., Michael, C., Vakondios, N., Drosou, K., Xekoukoulotakis, N.P.,

Diamadopoulos, E., Fatta-Kassinos, D., 2013. Winery wastewater purification by reverse osmosis and oxidation of the concentrate by solar photo-Fenton. Sep Purif Technol 118, 659–669. https://doi.org/10.1016/j.seppur.2013.07.049

Iqbal, M.K., Nadeem, A., Sherazi, F., Khan, R.A., 2015. Optimization of process parameters for kitchen waste composting by response surface methodology. Int J Environ Sci Technol 12, 1759–1768. https://doi.org/10.1007/s13762-014-0543-x

Jakubus, M., Spychalski, W., 2022. Evaluation of Agricultural Value of Composts Prepared from Municipal Biowastes in Different Conditions of Composting Process. Agronomy 12. https://doi.org/10.3390/agronomy12061438

Jollife, I.T., Cadima, J., 2016. Principal component analysis: A review and recent developments. Philos Trans R Soc A Math Phys Eng Sci 374. https://doi.org/10.1098/rsta.2015.0202

Jorge, N., Teixeira, A.R., Matos, C.C., Lucas, M.S., Peres, J.A., 2021. Combination of coagulation–flocculation–decantation and ozonation processes for winery wastewater treatment. Int J Environ Res Public Health 18. https://doi.org/10.3390/ijerph18168882

Jurinjak Tušek, A., Benković, M., Valinger, D., Jurina, T., Belščak-Cvitanović, A., Gajdoš Kljusurić, J., 2018. Optimizing bioactive compounds extraction from different medicinal plants and prediction through nonlinear and linear models. Ind Crops Prod 126, 449–458. https://doi.org/10.1016/j.indcrop.2018.10.040

Jurinjak Tušek, A., Jurina, T., Benković, M., Valinger, D., Belščak-Cvitanović, A., Gajdoš Kljusurić, J., 2020. Application of multivariate regression and artificial neural network modelling for prediction of physical and chemical properties of medicinal plants aqueous extracts. J Appl Res Med Aromat Plants 16, 100229. https://doi.org/10.1016/j.jarmap.2019.100229

Kavdir, Y., Ilay, R., Camci Cetin, S., Buyukcan, M.B., Kavdir, I., 2020. Monitoring composting process of olive oil solid waste using FT-NIR spectroscopy. Commun Soil Sci Plant Anal 51, 816–828. https://doi.org/10.1080/00103624.2020.1729375

Khan, M.A.I., Ueno, K., Horimoto, S., Komai, F., Someya, T., Inoue, K., Tanaka, K., Ono, Y., 2009. CIELAB color variables as indicators of compost stability. Waste Manag 29, 2969–2975. https://doi.org/10.1016/j.wasman.2009.06.021

Khater, E.S.G., 2015. Some Physical and Chemical Properties of Compost. Int J Waste Resour 05. https://doi.org/10.4172/2252-5211.1000172

Kong, Y., Wang, G., Chen, W., Yang, Y., Ma, R., Li, D., Shen, Y., Li, G., Yuan, J., 2022. Phytotoxicity of farm livestock manures in facultative heap composting using the seed germination index as indicator. Ecotoxicol Environ Saf 247, 114251. https://doi.org/10.1016/j.ecoenv.2022.114251

Kulcu, R., 2016. New kinetic modelling parameters for composting process. J Mater Cycles Waste Manag 18, 734–741. https://doi.org/10.1007/s10163-015-0376-9

Kumar, K., 2021. Partial Least Square (PLS) Analysis: Most Favorite Tool in Chemometrics to Build a Calibration Model. Resonance 26, 429–442. https://doi.org/10.1007/s12045-021-1140-1

Le Man, H., Behera, S.K., Park, H.S., 2010. Optimization of operational parameters for ethanol production from korean food waste leachate. Int J Environ Sci Technol 7, 157–

164. https://doi.org/10.1007/BF03326127

Li, Z., Lu, H., Ren, L., He, L., 2013. Experimental and modeling approaches for food waste composting: A review. Chemosphere 93, 1247–1257. https://doi.org/10.1016/j.chemosphere.2013.06.064

Liang, C., Das, K.C., Mcclendon, R.W., 2003. Prediction of microbial activity during biosolids composting using artificial neural networks. Am Soc Agric Biol Eng 46, 1713–1719.

Lillhonga, T., Grunwald, J., Geladi, P., 2009. Chemometric monitoring of designed composting processes using laboratory measurements and near infrared spectroscopy. J Near Infrared Spectrosc 17, 275–287. https://doi.org/10.1255/jnirs.852

Lim, L.Y., Bong, C.P.C., Lee, C.T., Klemeš, J.J., Sarmidi, M.R., Lim, J.S., 2017. Review on the current composting practices and the potential of improvement using two-stage composting. Chem Eng Trans 61, 1051–1056. https://doi.org/10.3303/CET1761173

Lin, L., Xu, F., Ge, X., Li, Y., 2019. Biological treatment of organic materials for energy and nutrients production—Anaerobic digestion and composting, 1st ed, Advances in Bioenergy. Elsevier Inc. https://doi.org/10.1016/bs.aibe.2019.04.002

Lofrano, G., Meric, S., 2016. A comprehensive approach to winery wastewater treatment: a review of the state-of the-art. Desalin Water Treat 57, 3011–3028. https://doi.org/10.1080/19443994.2014.982196

Lovreškov, L., Radojčić Redovniković, I., Limić, I., Potočić, N., Seletković, I., Marušić, M., Butorac, L., Jurinjak Tušek, A., Jakovljević, T., 2022. Are Foliar Nutrition Status and Indicators of Oxidative Stress Associated with Tree Defoliation of Four Mediterranean. Plants 11, 3484.

M. Librán, C., Mayor, L., M. Garcia-Castello, E., Vidal-Brotons, D., 2013. Polyphenol extraction from grape wastes: Solvent and pH effect. Agric Sci 04, 56–62. https://doi.org/10.4236/as.2013.49b010

Malamis, D., Moustakas, K., Haralambous, K.J., 2016. Evaluating in-vessel composting in treating sewage sludge and agricultural waste by examining and determining the kinetic reactions of the process. Clean Technol Environ Policy 18, 2493–2502. https://doi.org/10.1007/s10098-016-1230-z

Manyapu, V., Mandpe, A., Kumar, S., 2018. Synergistic effect of fly ash in in-vessel composting of biomass and kitchen waste. Bioresour Technol 251, 114–120. https://doi.org/10.1016/j.biortech.2017.12.039

Martínez Salgado, M.M., Ortega Blu, R., Janssens, M., Fincheira, P., 2019. Grape pomace compost as a source of organic matter: Evolution of quality parameters to evaluate maturity and stability. J Clean Prod 216, 56–63. https://doi.org/10.1016/j.jclepro.2019.01.156

Mason, I.G., 2006. Mathematical modelling of the composting process: A review. Waste Manag 26, 3–21. https://doi.org/10.1016/j.wasman.2005.01.021

Meena, A.L., Karwal, M., KJ, R., Narwal, E., 2021. Aerobic composting versus Anaerobic composting: Comparison and differences. Food Sci Reports 2, 23–26. https://doi.org/10.13140/RG.2.2.21424.69125

Miguel, N., López, A., Jojoa-Sierra, S.D., Fernández, J., Gómez, J., Ormad, M.P., 2022. Physico-Chemical and Microbiological Control of the Composting Process of the Organic Fraction of Municipal Solid Waste: A Pilot-Scale Experience. Int J Environ Res Public Health 19, 15449. https://doi.org/10.3390/ijerph192315449

Mirabella, N., Castellani, V., Sala, S., 2014. Current options for the valorization of food manufacturing waste: A review. J Clean Prod 65, 28–41. https://doi.org/10.1016/j.jclepro.2013.10.051

Mishra, S.K., Yadav, K.D., 2022. Assessment of the effect of particle size and selected physico-chemical and biological parameters on the efficiency and quality of composting of garden waste. Heliyon 10, 107925. https://doi.org/10.1016/j.heliyon.2021.e08415

Montesinos López, O.A., Montesinos López, A., Crossa, J., 2022. Multivariate Statistical Machine Learning Methods for Genomic Prediction, Multivariate Statistical Machine Learning Methods for Genomic Prediction. https://doi.org/10.1007/978-3-030-89010-0

Moreira, F.C., Boaventura, R.A.R., Brillas, E., Vilar, V.J.P., 2015. Remediation of a winery wastewater combining aerobic biological oxidation and electrochemical advanced oxidation processes. Water Res 75, 95–108. https://doi.org/10.1016/j.watres.2015.02.029

Moreno, A.D., Ballesteros, M., Negro, M.J., 2020. Biorefineries for the valorization of food processing waste, The Interaction of Food Industry and Environment. https://doi.org/10.1016/B978-0-12-816449-5.00005-9

Onwosi, C.O., Igbokwe, V.C., Odimba, J.N., Eke, I.E., Nwankwoala, M.O., Iroh, I.N., Ezeogu, L.I., 2017. Composting technology in waste stabilization: On the methods, challenges and future prospects. J Environ Manage 190, 140–157. https://doi.org/10.1016/j.jenvman.2016.12.051

Oviedo-Ocaña, E.R., Abendroth, C., Domínguez, I.C., Sánchez, A., Dornack, C., 2023. Life cycle assessment of biowaste and green waste composting systems: A review of applications and implementation challenges. Waste Manag 171, 350–364. https://doi.org/10.1016/j.wasman.2023.09.004

Ozaki, Y., Huck, C.W., Beć, K.B., 2018. Near-IR Spectroscopy and Its Applications, in: Molecular and Laser Spectroscopy: Advances and Applications. Elsevier Inc., pp. 11–38. https://doi.org/10.1016/B978-0-12-849883-5.00002-4

Papračanin, E., Petric, I., 2017. Mathematical modeling and simulation of the composting process in a pilot reactor. Bull Chem Technol Bosnia Herzegovina 47, no.2, 39–48.

Paradelo, R., Moldes, A.B., Barral, M.T., 2013. Evolution of organic matter during the mesophilic composting of lignocellulosic winery wastes. J Environ Manage 116, 18–26. https://doi.org/10.1016/j.jenvman.2012.12.001

Park, Y.S., Lek, S., 2016. Artificial Neural Networks: Multilayer Perceptron for Ecological Modeling. Dev Environ Model 28, 123–140. https://doi.org/10.1016/B978-0-444-63623-2.00007-4

Perra, M., Cuena-Lombrana, A., Bacchetta, G., Manca, M.L., Manconi, M., Maroun, R.G., Muntoni, A., Tuberoso, C.I.G., Gil, K.A., De Gioannis, G., 2022. Combining different approaches for grape pomace valorization: Polyphenols extraction and composting of the exhausted biomass. Sustainability 14. https://doi.org/10.1016/j.jff.2022.105276

Petric, I., Avdihodžić, E., Ibrić, N., 2015. Numerical simulation of composting process for

mixture of organic fraction of municipal solid waste and poultry manure. Ecol Eng 75, 242–249. https://doi.org/10.1016/j.ecoleng.2014.12.003

Petric, I., Helić, A., Avdić, E.A., 2012. Evolution of process parameters and determination of kinetics for co-composting of organic fraction of municipal solid waste with poultry manure. Bioresour Technol 117, 107–116. https://doi.org/10.1016/j.biortech.2012.04.046

Petric, I., Selimbašić, V., 2008. Development and validation of mathematical model for aerobic composting process. Chem Eng J 139, 304–317. https://doi.org/10.1016/J.CEJ.2007.08.017

Pinto, R., Correia, C., Mourão, I., Moura, L., Brito, L.M., 2023. Composting Waste from the White Wine Industry. Sustainability 15. https://doi.org/10.3390/su15043454

Qasim, W., Moon, B.E., Okyere, F.G., Khan, F., Nafees, M., Kim, H.T., 2019. Influence of aeration rate and reactor shape on the composting of poultry manure and sawdust. J Air Waste Manag Assoc 69, 633–645. https://doi.org/10.1080/10962247.2019.1569570

Rasapoor, M., Nasrabadi, T., Kamali, M., Hoveidi, H., 2009. The effects of aeration rate on generated compost quality, using aerated static pile method. Waste Manag 29, 570–573. https://doi.org/10.1016/j.wasman.2008.04.012

Raypah, M.E., Faris, A.N., Azlan, M.M., Yusof, N.Y., Suhailin, F.H., Shueb, R.H., Ismail, I., Mustafa, F.H., 2022. Near-Infrared Spectroscopy as a Potential COVID-19 Early Detection Method: A Review and Future Perspective. Sensors 22. https://doi.org/10.3390/s22124391

Reich, G., 2005. Near-infrared spectroscopy and imaging: Basic principles and pharmaceutical applications. Adv Drug Deliv Rev 57, 1109–1143. https://doi.org/10.1016/j.addr.2005.01.020

Robles-Morales, D.L., Reyes Cervantes, A., Díaz-Godínez, R., Tovar-Jiménez, X., Medina-Moreno, S.A., Jiménez-González, A., 2021. Design and Performance Evaluation of a Fungi-Bacteria Consortium to Biodegrade Organic Matter at High Concentration on Synthetic Slaughterhouse Wastewater. Water Air Soil Pollut 232. https://doi.org/10.1007/s11270-021-05177-1

Rodrigues, R.P., Gando-Ferreira, L.M., Quina, M.J., 2022. Increasing Value of Winery Residues through Integrated Biorefinery Processes: A Review. Molecules 27. https://doi.org/10.3390/molecules27154709

Rossetti, I., Conte, F., Ramis, G., 2021. Kinetic Modelling of Biodegradability Data of Commercial Polymers Obtained under Aerobic Composting Conditions. Eng 2, 54–68. https://doi.org/10.3390/eng2010005

Rueda, M.P., Comino, F., Aranda, V., José Ayora-Cañada, M., Domínguez-Vidal, A., 2023. Understanding the compositional changes of organic matter in torrefied olive mill pomace compost using infrared spectroscopy and chemometrics. Spectrochim Acta - Part A Mol Biomol Spectrosc 293. https://doi.org/10.1016/j.saa.2023.122450

Sandak, J., Sandak, A., Meder, R., 2016. Assessing trees, wood and derived products with near infrared spectroscopy: Hints and tips. J Near Infrared Spectrosc 24, 485–505. https://doi.org/10.1255/jnirs.1255

Sangamithirai, K.M., Jayapriya, J., Hema, J., Manoj, R., 2015. Evaluation of in-vessel co-composting of yard waste and development of kinetic models for co-composting. Int J

Recycl Org Waste Agric 4, 157–165. https://doi.org/10.1007/s40093-015-0095-1

Sarker, I.H., 2021. Deep Learning: A Comprehensive Overview on Techniques, Taxonomy, Applications and Research Directions. SN Comput Sci 2, 1–20. https://doi.org/10.1007/s42979-021-00815-1

Sayara, T., Basheer-Salimia, R., Hawamde, F., Sánchez, A., 2020. Recycling of organic wastes through composting: Process performance and compost application in agriculture. Agronomy 10. https://doi.org/10.3390/agronomy10111838

Scalisi, A., O'connell, M.G., Islam, M.S., Goodwin, I., 2022. A Fruit Colour Development Index (CDI) to Support Harvest Time Decisions in Peach and Nectarine Orchards. Horticulturae 8. https://doi.org/10.3390/horticulturae8050459

Seng, B., Kaneko, H., Hirayama, K., Katayama-Hirayama, K., 2012. Development of water movement model as a module of moisture content simulation in static pile composting. Environ Technol 33, 1685–1694. https://doi.org/10.1080/09593330.2011.642897

Shah, G.M., Tufail, N., Bakhat, H.F., Imran, M., Murtaza, B., Farooq, A.B.U., Saeed, F., Waqar, A., Rashid, M.I., 2017. Anaerobic degradation of municipal organic waste among others composting techniques improves N cycling through waste-soil-plant continuum. J Soil Sci Plant Nutr 17, 529–542. https://doi.org/10.4067/S0718-95162017005000038

Sharma, D., Pandey, A.K., Yadav, K.D., Kumar, S., 2021. Response surface methodology and artificial neural network modelling for enhancing maturity parameters during vermicomposting of floral waste. Bioresour Technol 324, 124672. https://doi.org/10.1016/j.biortech.2021.124672

Sharma, D., Yadav, K.D., Kumar, S., 2018. Biotransformation of flower waste composting: Optimization of waste combinations using response surface methodology. Bioresour Technol 270, 198–207. https://doi.org/10.1016/j.biortech.2018.09.036

Shen, G., Chen, Y., Zhang, J., Wu, Y., Yi, Y., Li, S., Yin, S., 2023. Quantitative analysis of index factors in agricultural compost by infrared spectroscopy. Heliyon 9. https://doi.org/10.1016/j.heliyon.2023.e14010

Siles-Castellano, A.B., López, M.J., López-González, J.A., Suárez-Estrella, F., Jurado, M.M., Estrella-González, M.J., Moreno, J., 2020. Comparative analysis of phytotoxicity and compost quality in industrial composting facilities processing different organic wastes. J Clean Prod 252. https://doi.org/10.1016/j.jclepro.2019.119820

Sim, J., McGoverin, C., Oey, I., Frew, R., Kebede, B., 2023. Near-infrared reflectance spectroscopy accurately predicted isotope and elemental compositions for origin traceability of coffee. Food Chem 427, 136695. https://doi.org/10.1016/j.foodchem.2023.136695

Sokač Cvetnić, T., Krog, K., Benković, M., Jurina, T., Valinger, D., Radojčić Redovniković, I., Gajdoš Kljusurić, J., Jurinjak Tušek, A., 2023. Application of Near-Infrared Spectroscopy for Monitoring and/or Control of Composting Processes. Appl Sci 13. https://doi.org/10.3390/app13116419

Sokač Cvetnić, T., Krog, K., Lisak Jakopović, K., Valinger, D., Gajdoš Kljusurić, J., Benković, M., Jurina, T., Jakovljević, T., Radojčić Redovniković, I., Jurinjak Tušek, A., 2024. Grape Skin Composting Process to Recycle Food Waste : Kinetics and
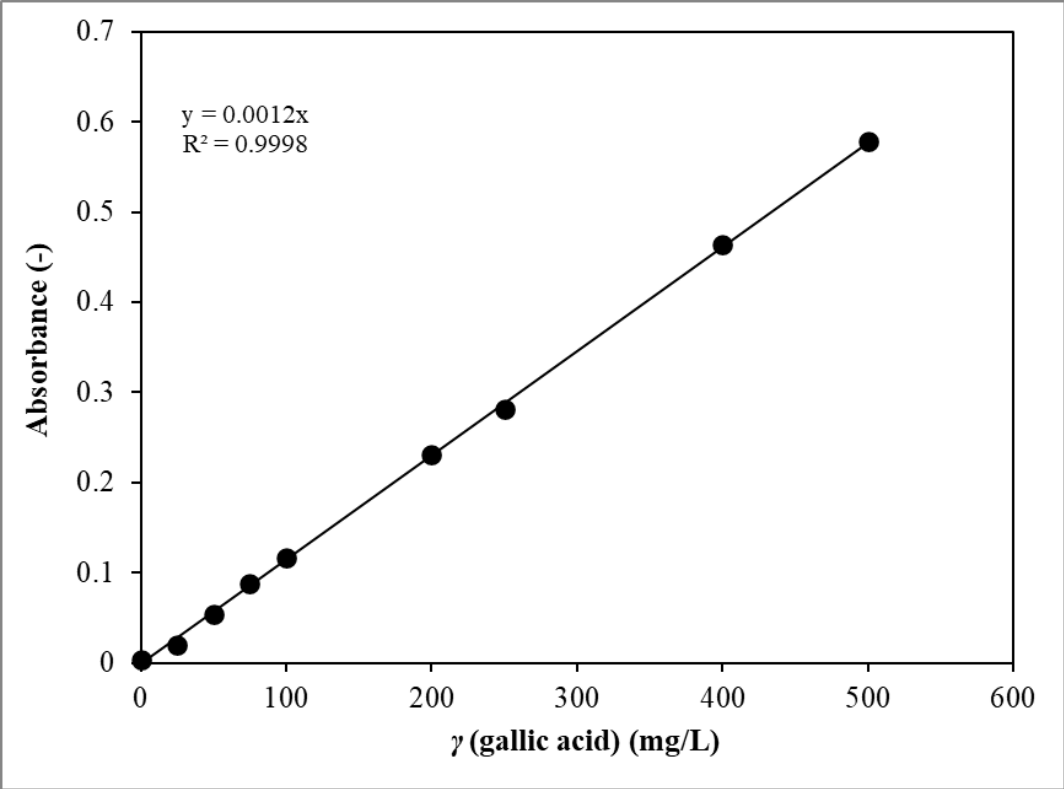
Optimization. Foods 13, 21.

Sokač, T., Gunjević, V., Pušek, A., Jurinjak Tušek, A., Dujmić, F., Brnčić, M., Kovačević Ganić, K., Jakovljević, T., Uher, D., Mitrić, G., Radojčić Redovniković, I., 2022a. Comparison of Drying Methods and Their Effect on the Stability of Graševina Grape Pomace Biologically. Foods 11.

Sokač, T., Šalić, A., Kučić Grgić, D., Šabić Runjavec, M., Vidaković, M., Jurinjak Tušek, A., Horvat, Đ., Juras Krnjak, J., Vuković Domanovac, M., Zelić, B., 2022b. An enhanced composting process with bioaugmentation: Mathematical modelling and process optimization. Waste Manag Res 40, 745–753. https://doi.org/10.1177/0734242X211033712

Sokač, T., Valinger, D., Benković, M., Jurina, T., Gajdoš Kljusurić, J., Radojčić Redovniković, I., Jurinjak Tušek, A., 2022c. Application of Optimization and Modeling for the Enhancement of Composting Processes. Processes 10. https://doi.org/10.3390/pr10020229

Soriano-Disla, J.M., Gómez, I., Guerrero, C., Navarro-Pedreño, J., García-Orenes, F., 2010. The potential of NIR spectroscopy to predict stability parameters in sewage sludge and derived compost. Geoderma 158, 93–100. https://doi.org/10.1016/J.GEODERMA.2009.12.022

Soto-Paz, J., Alfonso-Morales, W., Caicedo-Bravo, E., Oviedo-Ocaña, E.R., Torres-Lozada, P., Manyoma, P.C., Sanchez, A., Komilis, D., 2020. A New Approach for the Optimization of Biowaste Composting Using Artificial Neural Networks and Particle Swarm Optimization. Waste and Biomass Valorization 11, 3937–3951. https://doi.org/10.1007/s12649-019-00716-8

Spinei, M., Oroian, M., 2021. The potential of grape pomace varieties as a dietary source of pectic substances. Foods 10. https://doi.org/10.3390/foods10040867

Toledo, M., Gutiérrez, M.C., Siles, J.A., García-Olmo, J., Martín, M.A., 2017. Chemometric analysis and NIR spectroscopy to evaluate odorous impact during the composting of different raw materials. J Clean Prod 167, 154–162. https://doi.org/10.1016/j.jclepro.2017.08.163

Turan, N.G., 2008. The effects of natural zeolite on salinity level of poultry litter compost. Bioresour Technol 99, 2097–2101. https://doi.org/10.1016/j.biortech.2007.11.061

Ugak, M.A.M., Aji, N.A.S., Yaser, A.Z., Lamaming, J., Rajin, M., Saalah, S., 2022. Food waste-dry leaves composting: Mixture formulation, turning frequency and kinetic analysis. Borneo Sci | J Sci Technol 43. https://doi.org/10.51200/bsj.v43i1.4404

Valinger, D., Kušen, M., Benković, M., Jurina, T., Panić, M., Redovniković, I.R., Kljusurić, J.G., Tušek, A.J., 2022. Enhancement of the Green Extraction of Bioactive Molecules from Olea europaea Leaves. Separations 9, 1–17. https://doi.org/10.3390/separations9020033

Valinger, D., Kušen, M., Jurinjak Tušek, A., Panić, M., Jurina, T., Benković, M., Radojčić Redovniković, I., Gajdoš Kljusurić, J., 2018. Development of near infrared spectroscopy models for quantitative prediction of the content of bioactive compounds in olive leaves. Chem Biochem Eng Q 32, 535–543. https://doi.org/10.15255/CABEQ.2018.1396

Vergnoux, A., Guiliano, M., Le Dréau, Y., Kister, J., Dupuy, N., Doumenq, P., 2009.

Monitoring of the evolution of an industrial compost and prediction of some compost properties by NIR spectroscopy. Sci Total Environ 407, 2390–2403. https://doi.org/10.1016/j.scitotenv.2008.12.033

Vidriales-Escobar, G., Rentería-Tamayo, R., Alatriste-Mondragón, F., González-Ortega, O., 2017. Mathematical modeling of a composting process in a small-scale tubular bioreactor. Chem Eng Res Des 120, 360–371. https://doi.org/10.1016/j.cherd.2017.02.006

Vigneswaran, S., Kandasamy, J., Johir, M.A.H., 2016. Sustainable Operation of Composting in Solid Waste Management. Procedia Environ Sci 35, 408–415. https://doi.org/10.1016/j.proenv.2016.07.022

Wang, G., Kong, Y., Liu, Y., Li, D., Zhang, X., Yuan, J., Li, G., 2020. Evolution of phytotoxicity during the active phase of co-composting of chicken manure, tobacco powder and mushroom substrate. Waste Manag 114, 25–32. https://doi.org/10.1016/j.wasman.2020.06.034

Wang, G., Yang, Y., Kong, Y., Ma, R., Yuan, J., Li, G., 2022. Key factors affecting seed germination in phytotoxicity tests during sheep manure composting with carbon additives. J Hazard Mater 421, 126809. https://doi.org/10.1016/j.jhazmat.2021.126809

Wang, M., An, H., Cai, W., Shao, X., 2023. Wavelet Transform Makes Water an Outstanding Near-Infrared Spectroscopic Probe. Chemosensors 11, 1–15. https://doi.org/10.3390/chemosensors11010037

Wang, S., Di, J., Wang, D., Dai, X., Hua, Y., Gao, X., Zheng, A., Gao, J., 2022. State-of-the-Art Review of Artificial Neural Networks to Predict, Characterize and Optimize Pharmaceutical Formulation. Pharmaceutics 14. https://doi.org/10.3390/pharmaceutics14010183

Waqas, M., Hashim, S., Humphries, U.W., Ahmad, S., Noor, R., Shoaib, M., Naseem, A., Hlaing, P.T., Lin, H.A., 2023. Composting Processes for Agricultural Waste Management: A Comprehensive Review. Processes 11, 731. https://doi.org/10.3390/pr11030731

Waqas, M., Nizami, A.S., Aburiazaiza, A.S., Barakat, M.A., Ismail, I.M.I., Rashid, M.I., 2018. Optimization of food waste compost with the use of biochar. J Environ Manage 216, 70–81. https://doi.org/10.1016/j.jenvman.2017.06.015

Watanabe, L.S., Bovolenta, Y.R., Junior, V.R.A., Barbin, D.F., Madeira, T.B., Nixdorf, S.L., 2018. Investigation of NIR spectra pre-processing methods combined with multivariate regression for determination of moisture in powdered industrial egg. Acta Sci - Technol 40. https://doi.org/10.4025/actascitechnol.v40i1.30133

Wu, D., Wei, Z., Mohamed, T.A., Zheng, G., Qu, F., Wang, F., Zhao, Y., Song, C., 2022. Lignocellulose biomass bioconversion during composting: Mechanism of action of lignocellulase, pretreatment methods and future perspectives. Chemosphere 286. https://doi.org/10.1016/j.chemosphere.2021.131635

Xie, S., Tran, H.T., Pu, M., Zhang, T., 2023. Transformation characteristics of organic matter and phosphorus in composting processes of agricultural organic waste: Research trends. Mater Sci Energy Technol 6, 331–342. https://doi.org/10.1016/j.mset.2023.02.006

Xu, A., Chang, H., Xu, Y., Li, R., Li, X., Zhao, Y., 2021. Applying artificial neural networks

(ANNs) to solve solid waste-related issues: A critical review. Waste Manag 124, 385–402. https://doi.org/10.1016/j.wasman.2021.02.029

Xu, P., Shu, L., Li, Y., Zhou, S., Zhang, G., Wu, Y., Yang, Z., 2023. Pretreatment and composting technology of agricultural organic waste for sustainable agricultural development. Heliyon 9, e16311. https://doi.org/10.1016/j.heliyon.2023.e16311

Yang, Z., Muhayodin, F., Larsen, O.C., Miao, H., Xue, B., Rotter, V.S., 2021. A Review of Composting Process Models of Organic Solid Waste with a Focus on the Fates of C , N , P , and K. Processes 9, 1–18.

Yeler, H.B., Nas, S., 2021. Optimization of extraction time and temperature for natural antioxidants of öküzgözü grape pomace using various solvent ratios. Food Sci Technol 41, 127–135. https://doi.org/10.1590/fst.38119

Yildiz, S., Degirmenci, M., 2015. Estimation of oxygen exchange during treatment sludge composting through multiple regression and artificial neural networks (estimation of oxygen exchange during composting). Int J Environ Res 9, 1173–1182.

Yu, H., Huang, G.H., 2009. Effects of sodium acetate as a pH control amendment on the composting of food waste. Bioresour Technol 100, 2005–2011. https://doi.org/10.1016/j.biortech.2008.10.007

Zahrim, A.Y., Leong, P.S., Ayisah, S.R., Janaun, J., Chong, K.P., Cooke, F.M., Haywood, S.K., 2016. Composting paper and grass clippings with anaerobically treated palm oil mill effluent. Int J Recycl Org Waste Agric 5, 221–230. https://doi.org/10.1007/s40093-016-0131-9

Zareef, M., Chen, Q., Hassan, M.M., Arslan, M., Hashim, M.M., Ahmad, W., Kutsanedzie, F.Y.H., Agyekum, A.A., 2020. An Overview on the Applications of Typical Non-linear Algorithms Coupled With NIR Spectroscopy in Food Analysis. Food Eng Rev 12, 173–190. https://doi.org/10.1007/s12393-020-09210-7

Zeaiter, M., Rutledge, D., 2009. Preprocessing Methods. Compr Chemom 3, 121–231. https://doi.org/10.1016/B978-044452701-1.00074-0

Zieliński, M., Kazimierowicz, J., Dębowski, M., 2023. Advantages and Limitations of Anaerobic Wastewater Treatment—Technological Basics, Development Directions, and Technological Innovations. Energies 16. https://doi.org/10.3390/en16010083
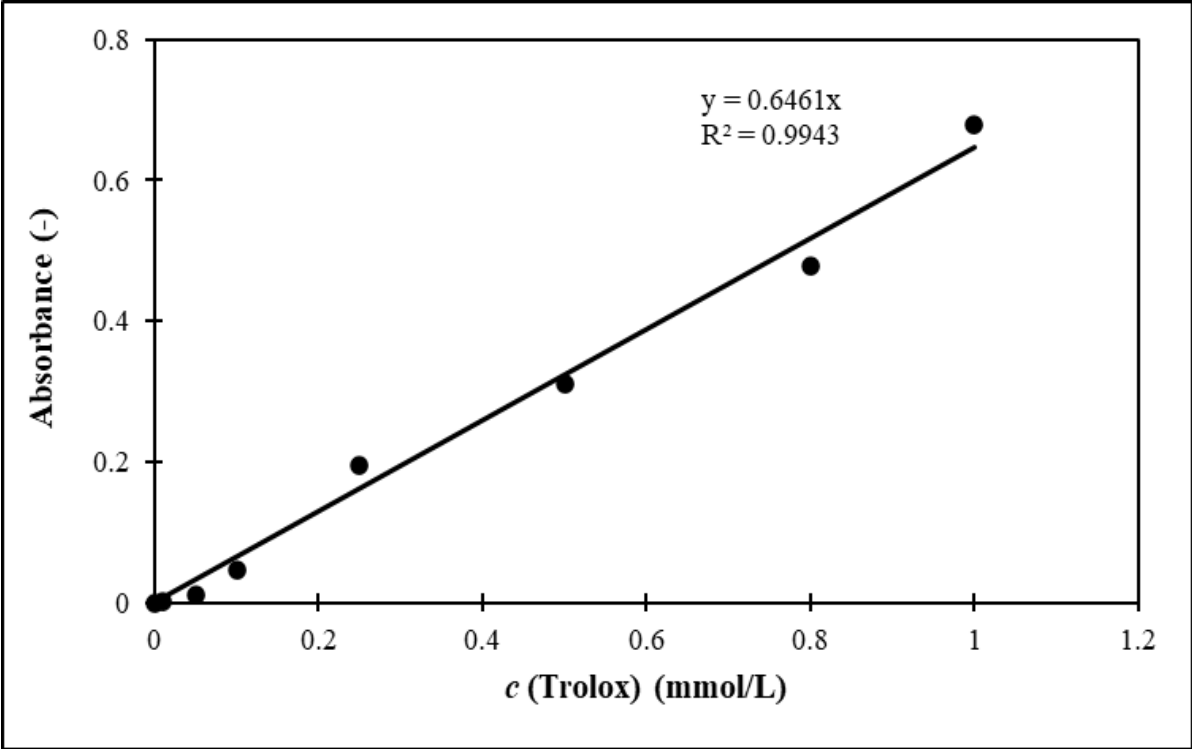
8. SUPPLEMENTARY

8.1. Calibration curve for TPC determination

8.2. Calibration curve for determination of antioxidant activity using DPPH method

The plot shows Absorbance (-) on the y-axis (0 to 0.8) versus c (Trolox) (mmol/L) on the x-axis (0 to 1.2). The regression line is labeled:

$$y = 0.6461x$$
$$R^2 = 0.9943$$

8.3. Calibration curve for determination of antioxidant activity using FRAP method

Plot of Absorbance (-) versus c (FeSO$_4$·7H$_2$O) (mmol/L) with regression equation $y = 0.6738x$ and $R^2 = 0.9803$.
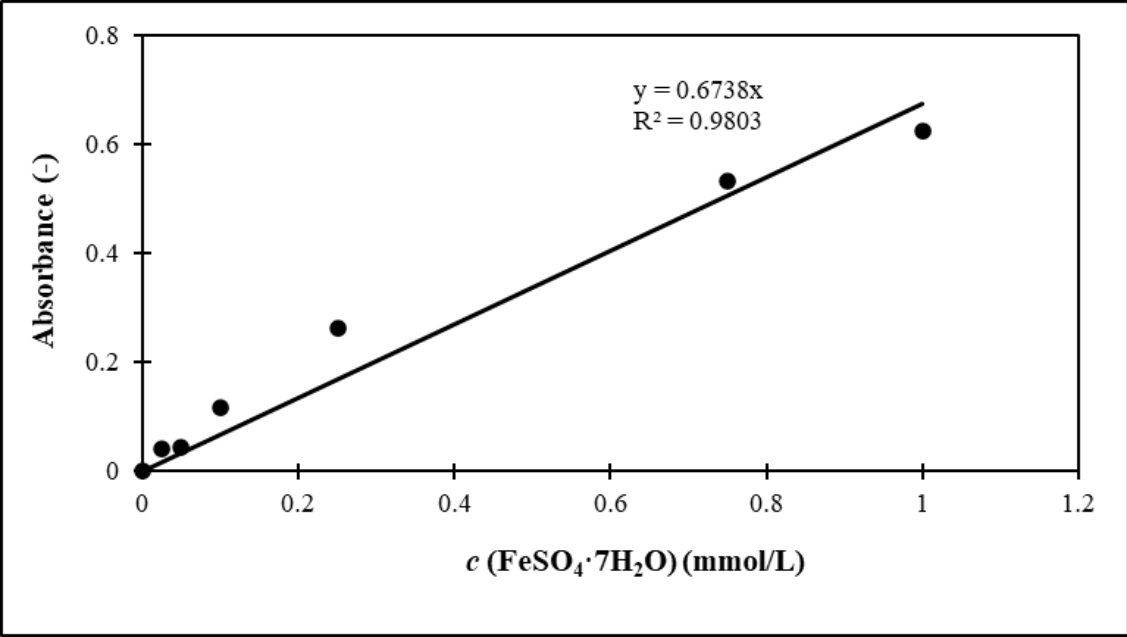
8.4. List of symbols and abbreviations

AC	ash content (%)
CC	carbon content (%)
DM	dry matter content (%)
GI	germination index (%)
MC	moisture content (%)
NC	nitrogen content (%)
OM	organic matter content (%)
S	conductivity (μS/cm)
TDS	total dissolved solids (mg/L)
TPC	total phenolic content (mg_{GAE}/g_{DM})

Autobiography

Tea Sokač Cvetnić was born on 28th of September in 1992 in Zagreb. She graduated Environmental Engineering at Faculty of Chemical Engineering and Technology, University of Zagreb in 2017 with a thesis entitled „Mathematical model of enzymatic synthesis of 6-cyano-4-hexaonic acid". In 2018 she worked as associate in a production of products from medicinal herbs in a small company, Darvitalis d.o.o. In 2019 she worked as assistant on a project „Development of Tehnix plant for bioreactor composting of biodegradable municipal waste" at Faculty of Chemical Engineering and Technology. Since 2021, she has been employed as assistant on a project „Sustainable waste management of winery by-products" at Faculty of Food Technology and Biotechnology. In the same year, she started the postgraduate study in Biotechnology and Bioprocess Engineering, Food Technology and Nutrition. Until now, she has co-authored 12 scientific papers in journals indexed in Web of Science. She participated in many international and national conferences where she presented her research results in the form of oral or poster presentations.

List of authors publications

Original scientific papers indexed in Web of Science (Current Contents Connect):

1. Sokač Cvetnić, Tea; Krog, Korina; Valinger, Davor; Gajdoš Kljusurić, Jasenka; Benković, Maja; Jurina, Tamara; Jakovljević, Tamara; Radojčić Redovniković, Ivana; Jurinjak Tušek, Ana (2024) Application of Multivariate Regression and Artificial Neural Network Modelling for the prediction of Physicochemical Properties of Grape Skin Compost. *Bioengineering*, 11 (3), 285

2. Sokač Cvetnić, Tea; Krog, Korina; Lisak Jakopović, Katarina; Valinger, Davor; Gajdoš Kljusurić, Jasenka; Benković, Maja; Jurina, Tamara; Jakovljević, Tamara; Radojčić Redovniković, Ivana; Jurinjak Tušek, Ana (2024) Grape Skin Composting Process to Recycle Food Waste: Kinetics and Optimization. *Foods*, 13 (6), 824. doi: 10.3390/foods13060824

3. Sokač Cvetnić, Tea; Krog, Korina; Benković, Maja; Jurina, Tamara; Valinger, Davor; Gajdoš Kljusurić, Jasenka; Radojčić Redovniković, Ivana; Jurinjak Tušek, Ana (2023) Solid–Liquid Extraction of Bioactive Molecules from White Grape Skin: Optimization and Near-Infrared Spectroscopy. *Separations*, 10 (8); 1-17. doi: 10.3390/separations10080452

4. Sokač Cvetnić, Tea; Gunjević, Veronika; Damjanović, Anja; Pušek, Anita; Jurinjak Tušek, Ana; Jakovljević, Tamara; Radojčić Redovniković, Ivana; Uher, Darko (2023) Monitoring of Chemical and Fermentative Characteristics during Different Treatments of Grape Pomace Silage. *Agriculture*, 13 (12); 1-12. doi: 10.3390/agriculture13122264

5. Benković, Maja; Jurinjak Tušek, Ana; Sokač Cvetnić, Tea; Jurina, Tamara; Valinger, Davor; Gajdoš Kljusurić, Jasenka (2023) An Overview of Ingredients Used for Plan-Based Meat Analogue Production and Their Influence on Structural and Textural Properties of Final Compost. *Gels* 9(12), 921. doi: 10.3390/gels9120921

6. Božinović, Marko; Sokač, Tea; Šalić, Anita; Dukarić, Ana-Marija; Tišma, Marina; Planinić, Mirela; Zelić, Bruno (2023) Standardization of 3,5-dinitrosalicylic acid (DNS) assay for measuring xylanase activity: detecting and solving problems. *Croatian journal of food science and technology*. 15 (2); 151-162. doi: 10.17508/CJFST.2023.15.2.03

7. Sokač Cvetnić, Tea; Krog, Korina; Benković, Maja; Jurina, Tamara; Valinger, Davor; Radojčić Redovniković, Ivana; Gajdoš Kljusurić, Jasenka; Jurinjak Tušek, Ana (2023) Application of Near-Infrared Spectroscopy for Monitoring and/or Control of Composting Processes. *Processes*, 13(11), 6419. doi: 10.3390/app13116419

8. Sirovec, Sara; Benković, Maja; Valinger, Davor; Sokač Cvetnić, Tea; Gajdoš Kljusurić, Jasenka; Jurinjak Tušek, Ana; Jurina, Tamara (2023) Development of ANN Models for Prediction of Physical and Chemical Characteristics of Oil-in-Aqueous Plant Extract Emulsions Using Near-Infrared Spectroscopy. *Chemosensors*, 11 (5); 278, 20. doi: 10.3390/chemosensors11050278

9. Sirovec, Sara; Jurinjak Tušek, Ana; Benković, Maja; Valinger, Davor; Sokač Cvetnić, Tea; Gajdoš Kljusurić, Jasenka; Jurina, Tamara (2022) Emulsification of Rosemary and Oregano Aqueous Extracts and Their In Vitro Bioavailability. *Plants*, 11(23); 3372, 22. doi: 10.3390/plants11233372

10. Sokač, Tea; Gunjević, Veronika; Pušek, Anita; Jurinjak Tušek, Ana, Dujmić, Filip; Brnčić, Mladen; Kovačević Ganić, Karin; Jakovljević, Tamara; Uher, Darko; Mitrić, Grozdana; Radojčić Redovniković, Ivana (2022) Comparison of Drying Methods and Their Effect on the Stability of Graševina Grape Pomace Biologically Active Compounds. *Foods*, 11(1), 112. doi: 10.3390/foods11010112.

11. Sokač, Tea; Šalić, Anita; Kučić Grgić, Dajana; Šabić Runjavec, Monika; Vidaković, Marijana; Jurinjak Tušek, Ana; Horvat, Đuro; Juras Krnjak, Jasmina; Vuković Domanovac, Marija; Zelić, Bruno (2022) An enhanced composting process with bioaugmentation: Mathematical modelling and process optimization. *Waste management & research*, 40 (6); 745-753.doi:10.1177/0734242X211033712

12. Šibalić, Darijo; Šalić, Anita; Jurinjak Tušek, Ana; Sokač, Tea; Brekalo, Karla; Zelić, Bruno; Tran, Nghiep Nam; Hessel, Volker; Tišma, Marina (2020) Sustainable production of lipase from Thermomyces lanuginosus: process optimization and enzyme characterization, *Industrial & engineering chemistry research*, 59 (48); 21144-21154. doi: 10.1021/acs.iecr.0c04329

13. Sokač, Tea; Gojun, Martin; Jurinjak Tušek, Ana; Šalić, Anita; Zelić, Bruno (2020) Purification of biodiesel produced by lipase catalyzed transesterification by ultrafiltration: Selection of membranes and analysis of membrane blocking mechanisms. *Renewable energy*, 159, 642-651. doi: 10.1016/j.renene.2020.05.132

Abstracts in Book of Abstracts:

1. Sokač Cvetnić, Tea; Krog, Korina; Valinger, Davor; Gajdoš Kljusurić, Jasenka; Jurina, Tamara; Benković, Maja; Radojčić Redovniković, Ivana; Jurinjak Tušek, Ana (2023) Potential of portable near-infrared spectrometer for evaluation of grape skin composting process // 6TH ISEKI-Food E-conference "Food production based on food safety, sustainable development and circular economy" Book of Abstracts. Timisoara, Rumunjska: Editura Universităţii „Lucian Blaga" din Sibiu, str. 113-114

2. Sokač Cvetnić, Tea; Krog, Korina; Benković, Maja; Valinger, Davor; Jurina, Tamara; Gajdoš Kljusurić, Jasenka; Radojčić Redovniković, Ivana; Jurinjak Tušek, Ana (2023) COMPOSTING – AN OPPORTUNITY TO PREVENT THE CLIMATE CHANGE // Book of abstracts of 2nd international conference "Food and Climate Change". Koprivnica: Sveučilište Sjever, str. 84-84

3. Marjanović, Blaženko; Sokač Cvetnić, Tea; Valinger, Davor; Gajdoš Kljusurić, Jasenka; Jurina, Tamara; Benković, Maja; Jurinjak Tušek, Ana (2023) Optimization of ultrasound-assisted extraction of proteins from Spirulina platensis // 6TH ISEKI-Food E-conference "Food production based on food safety, sustainable development and circular economy" Book of Abstracts. Timisoara, Rumunjska: Editura Universităţii „Lucian Blaga" din Sibiu, 2023. str. 118-119

4. Gojun, Martin ; Sokač, Tea ; Jurinjak Tušek, Ana ; Valinger, Davor ; Šalić, Anita ; Zelić, Bruno (2021) Biokatalitička razgradnja onečišćivala u mikrosustavima // Proceedings book (International Conference "The Holistic Approach to Environment") / Štrkalj, Anita ; Glavaš, Zoran (ur.). 2021. str. 157-166

5. Sokač Cvetnić, Tea ; Valinger, Davor ; Cigić, Filip ; Jurinjak Tušek, Ana ; Jurina, Tamara ; Gajdoš Kljusurić, Jasenka ; Radojčić Redovniković, Ivana ; Benković, Maja (2023) Applicability of near-infrared spectroscopy in the analysis of macronutrient contents of grape pomace and grape pomace mixtures // Book of Abatracts 58th Croatian & 18th International Symposium on Agriculture | / Carović-Stanko, Klaudija ; Širić, Ivan (ur.). Zagreb: Agronomski fakultet Sveučilišta u Zagrebu, str. 213-213

6. Benković, Maja ; Cigić, Filip ; Valinger, Davor ; Jurinjak Tušek, Ana ; Jurina, Tamara ; Sokač Cvetnić, Tea ; Gajdoš Kljusurić, Jasenka ; Radojčić Redovniković, Ivana (2023) The use of grape pomace in food products - an overview // Book of Abstracts 58th Croatian & 18th

International Symposium on Agriculture / Carović-Stanko, Klaudija ; Širić, Ivan (ur.). Zagreb: Agronomski fakultet Sveučilišta u Zagrebu, str. 194-194

7. Valinger, Davor; Sokač Cvetnić, Tea; Gajdoš Kljusurić, Jasenka; Jurina, Tamara; Benković, Maja; Tušek, Kristina (2023) EFFECT OF MIXTURE COMPOSITION OF HONEY AND OAT BASED COCOA POWDERS ON POLYPHENOL BIOAVAILABILITY // 6TH ISEKI-Food E-conference "Food production based on food safety, sustainable development and circular economy" Book of Abstracts. Timisoara, Rumunjska: Editura Universităţii „Lucian Blaga" din Sibiu, str. 22-23

8. Sokač Cvetnić, Tea ; Benković, Maja ; Valinger, Davor ; Jurina, Tamara ; Gajdoš Kljusurić, Jasenka ; Radojčić Redovniković, Ivana ; Jurinjak Tušek, Ana (2023) In-vessel composting of grape pomace // Book of Abstracts 58th Croatian & 18th International Symposium on Agriculture / Carović-Stanko, Klaudija ; Širić, Ivan (ur.). Zagreb: Agronomski fakultet Sveučilišta u Zagrebu, str. 39-39

9. Sokač, Tea ; Benković Maja ; Valinger, Davor ; Gajdoš Kljusurić, Jasenka ; Jurina, Tamara ; Jurinjak Tušek, Ana (2022) NON-STATIONARY PARAMETER SENSITIVITY ANALYSIS OF A MODIFIED ACTIVATED SLUDGE MODEL No. 3 // Book of Abstracts WATER FOR ALL 2022 / Habuda-Stanić, Mirna ; Lauš, Ivana ; Šuvak-Pirić, Ivana (ur.). Osijek: Prehrambeno tehnološki fakultet Sveučilišta Josipa Jurja Strossmayera u Osijeku, str. 84-84

10. Benković, Maja ; Jurina, Tamara ; Gregov, Marija ; Ćurko, Josip ; Matošić, Marin ; Jurinjak Tušek, Ana ; Sokač, Tea ; Gajdoš Kljusurić, Jasenka ; Valinger, Davor (2022) Application of near infrared spectroscopy for distinction of drinking water quality based on different treatments // Book of Abstracts WATER FOR ALL 2022 / Habuda-Stanić, Mirna ; Lauš, Ivana ; Šuvak-Pirić, Ivana (ur.). Osijek, str. 105-105

11. Klara Pavić ; Valentina Rožić ; Anja Damjanović ; Anita Pušek ; Tea Sokač ; Manuela Panić ; Ivana Radojčić Redovniković (2022) Application of green technologies for sustainable use of grape pomace // KNJIGA SAŽETAKA 2. međunarodna studentska GREEN konferencija. str. 172-172

12. Šalić, Anita ; Gojun, Martin ; Sokač, Tea ; Zelić, Bruno (2021) Biodiesel production and composting – sustainable solutions for food waste management // Book of abstracts of 1st

international conference FOOD & CLIMATE CHANGES / Šamec, Dunja ; Šarkanj, Bojan ; Sviličić Petrić, Ines (ur.). Koprivnica: Sveučilište Sjever, str. 26-26

13. Gojun, Martin ; Sokač, Tea ; Ljubić, Anabela ; Šalić, Anita ; Valinger, Davor ; Zelić, Bruno (2022) On-line monitoring of biodiesel production by near-infrared spectroscopy // International Conference 18th Ružička days "TODAY SCIENCE – TOMORROW INDUSTRY" / Jukić, Ante (ur.). Zagreb : Osijek: Hrvatsko društvo kemijskih inženjera i tehnologa (HDKI), str. 67-67

14. Šibalić, Darijo ; Šalić, Anita ; Jurinjak Tušek, Ana ; Sokač, Tea ; Brekalo, Klara ; Zelić, Bruno; Tišma, Marina (2020) Production, purification and characterization of lipase from Thermomyces lanuginosus // Book of abstracts 18th Ružička days "TODAY SCIENCE – TOMORROW INDUSTRY" / Jukić, Ante (ur.). Zagreb : Osijek: Hrvatsko društvo kemijskih inženjera i tehnologa (HDKI) ; Prehrambeno tehnološki fakultet Sveučilišta Josipa Jurja Strossmayera u Osijeku, str. 88-88

15. Gojun, Martin ; Sokač, Tea ; Šalić, Anita (2020) Primjena ultrafiltracijskih membrana za pročišćavanje biodizela // XIII. Susret mladih kemijskih inženjera-Knjiga sažetaka / Dejanović, Igor ; Vrsaljko, Domagoj ; Žižek, Krunoslav (ur.). Zagreb: Hrvatsko društvo kemijskih inženjera i tehnologa (HDKI), str. 116-116